

การวิเคราะห์ลำดับดีเอ็นเอโดยอาศัยพีเอ็นเอโพรบและมัลติ-ทอปแอสสเปกโทเมตรี



นางสาว นุญจิรา นุญทา

วิทยานิพนธ์นี้เป็นส่วนหนึ่งของการศึกษาตามหลักสูตรปริญญาวิทยาศาสตรดุษฎีบัณฑิต

สาขาเคมี ภาควิชาเคมี

คณะวิทยาศาสตร์ จุฬาลงกรณ์มหาวิทยาลัย

ปีการศึกษา 2552

ลิขสิทธิ์ของจุฬาลงกรณ์มหาวิทยาลัย

**DNA SEQUENCE ANALYSIS USING PNA PROBE  
AND MALDI-TOF MASS SPECTROMETRY**



**Miss Boonjira Boontha**

**A Dissertation Submitted in Partial Fulfillment of the Requirements  
for the Degree of Doctor of Philosophy Program in Chemistry**

**Department of Chemistry**

**Faculty of Science**

**Chulalongkorn University**


**Academic Year 2009**

**Copyright of Chulalongkorn University**


Thesis Title            DNA SEQUENCE ANALYSIS USING PNA PROBE AND  
MALDI-TOF MASS SPECTROMETRY  
By                        Miss Boonjira Boontha  
Field of Study        Chemistry  
Thesis Advisor       Associate Professor Tirayut Vilaivan, D. Phil.

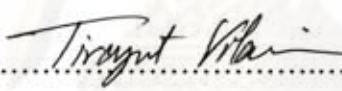
---

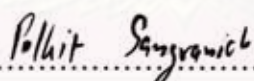
Accepted by the Faculty of Science, Chulalongkorn University in Partial  
Fulfillment of the Requirements for Doctoral Degree


  
..... Dean of the Faculty of Science  
(Professor Supot Hannongbua, Dr.rer.nat.)

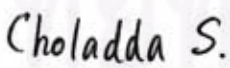
THESIS COMMITTEE

  
..... Chairman  
(Associate Professor Mongkol Sukwattanasinitt, Ph.D.)

  
..... Thesis Advisor  
(Associate Professor Tirayut Vilaivan, D. Phil.)

  
..... Examiner  
(Associate Professor Polkit Sangvanich, Ph.D.)

  
..... Examiner  
(Assistant Professor Piyasak Chaumpluk, Ph.D.)

  
..... Examiner  
(Choladda Srisuwannaket, Ph. D.)

  
..... External Member  
(Associate Professor Palangpon Kongsaree, Ph.D.)

บุญจิรา บุญทา : การวิเคราะห์ลำดับดีเอ็นเอโดยอาศัยพีเอ็นเอโพรบและมัลติ-ทอพแมสสเปกโตรเมตรี: (DNA SEQUENCE ANALYSIS USING PNA PROBE AND MALDI-TOF MASS SPECTROMETRY) : อ.ที่ปรึกษาวิทยานิพนธ์หลัก : รองศาสตราจารย์ ดร. ธีรยุทธ วิไลวัลย์, 183 หน้า.

งานวิจัยนี้มุ่งเน้นถึงการพัฒนาเทคนิคใหม่โดยนำเอาเทคนิคแมสสเปกโตรเมตรีมาใช้ในการวิเคราะห์ลำดับเบสของดีเอ็นเอโดยการนำมาใช้ร่วมกับพีเอ็นเอใหม่ชนิดเบต้า-พิโรลิโคนิลพีเอ็นเอที่เรียกว่า *acpcPNA* และตัวคู้ดจับชนิดแลกเปลี่ยน ไอออนเทคนิคนี้อาศัยหลักการคู้ดจับอย่างจำเพาะเจาะจงของพีเอ็นเอ-ดีเอ็นเอ ไฮบริดซึ่งมีประจุลบบนตัวคู้ดจับซึ่งมีประจุบวกซึ่งเทคนิคดังกล่าวจะเกี่ยวข้องกับการเอาพีเอ็นเอผสมกับดีเอ็นเอตัวอย่างในสารละลายบัฟเฟอร์แล้วตามด้วยการเติมตัวคู้ดจับชนิดแลกเปลี่ยน ไอออนลงไป ในสารละลายผสมของพีเอ็นเอและดีเอ็นเอตัวอย่าง หลังจากนั้นจึงแยกพีเอ็นเอ-ดีเอ็นเอ ไฮบริดที่อยู่บนตัวคู้ดจับออกจากพีเอ็นเอที่ไม่เกิดไฮบริดโดยการล้างและจากนั้นนำตัวคู้ดจับดังกล่าวไปวิเคราะห์โดยเทคนิคมัลติทอพแมสสเปกโตรเมตรีซึ่งลำดับเบสของดีเอ็นเอตัวอย่างสามารถตรวจสอบได้จากมวลโมเลกุลของพีเอ็นเอที่ถูกคู้ดจับบนผิวของตัวคู้ดจับได้ ทั้งนี้เนื่องจากพีเอ็นเอเป็น โมเลกุลที่เป็นกลางจึงทำให้พีเอ็นเอไม่ถูกคู้ดจับโดยตัวแลกเปลี่ยนแอนไอออน นอกจากจะเกิดไฮบริดกับดีเอ็นเอที่มีลำดับเบสคู่สมกัน จึงทำให้การปรากฏของพีเอ็นเอบนผิวของตัวคู้ดจับถือว่าการเกิดไฮบริดระหว่างพีเอ็นเอ-ดีเอ็นเอขึ้น ซึ่งกล่าวได้ว่าลำดับเบสของพีเอ็นเอมีลำดับเบสที่เป็นคู่สมกับดีเอ็นเอตัวอย่าง จุดเด่นของเทคนิคนี้คือไม่ยุ่งยาก, รวดเร็ว, ราคาไม่แพงเนื่องจากไม่จำเป็นต้องใช้พีเอ็นเอหรือดีเอ็นเอตัวอย่างที่ติดฉลาก ด้วยความสามารถในการจับคู่กับดีเอ็นเอได้อย่างแข็งแรง และมีความจำเพาะเจาะจงสูงของพีเอ็นเอระบบนี้จึงทำให้สามารถตรวจสอบดีเอ็นเอความยาว 9-15 เบสที่มีลำดับแตกต่างกันเพียง 1 ตำแหน่งได้ จากผลการทดลองทั้งหมดซึ่งรวมไปถึงการวิเคราะห์ดีเอ็นเอตัวอย่างด้วยเทคนิคนี้สามารถบอกความแตกต่างระหว่างดีเอ็นเอที่มีลำดับเบสคู่สมและที่มีเบสแตกต่างกันเพียง 1 ตำแหน่งได้อย่างชัดเจนจึงทำให้วิธีนี้สามารถนำมาประยุกต์ใช้ตรวจสอบซิงเกิลนิวคลีโอไทด์โพลิมอร์ฟิซึม (SNP) โดยเฉพาะในรูปแบบของมัลติเพล็กซ์ (multiplex) ได้อย่างมีประสิทธิภาพ

ภาควิชา.....เคมี.....ลายมือชื่อนิติ.....บุญจิรา บุญทา  
สาขาวิชา.....เคมี.....ลายมือชื่อ อ. ที่ปรึกษาวิทยานิพนธ์หลัก.....  
ปีการศึกษา.....2552.....

# #487 38247 23: MAJOR CHEMISTRY

KEYWORDS : PEPTIDE NUCLEIC ACID / PNA / SNP/ GENOTYPING

BOONJIRA BOONTHA: DNA SEQUENCE ANALYSIS USING PNA PROBE AND MALDI-TOF MASS SPECTROMETRY. THESIS ADVISOR: ASSOC. PROF. TIRAYUT VILAIVAN, D.Phil. 183 pp.

This research emphasizes on the development of a novel mass spectrometric technique for DNA sequence analysis by combining a new beta-pyrrolidinyl peptide nucleic acid called *acpcPNA* and an anion exchange solid support. This method relies on the selective absorption of negatively charged PNA·DNA hybrids onto a positively charged ion exchange support. The procedure involves mixing the PNA probe and the DNA sample in a buffer followed by addition of the anion exchange support. The solid support-bound PNA·DNA hybrid was then washed and directly analyzed by MALDI-TOF. The sequence of the DNA sample was determined by the detected molecular masses of the absorbed PNA probe. Since the neutral PNA could not be not adsorbed by the anion exchanger unless it hybridized with the complementary DNA, the presence of PNA on the support suggested a successful formation of the PNA·DNA hybrid, implying that the sequence of the PNA and the DNA were complementary. The technique was simple, rapid, cost-effective and required no labelling of the DNA samples. Because of an exceptional high specificity of this new PNA probe, the method is capable of detecting a single mismatched base out of 9–15 base DNA sequences. In all cases tested – including real DNA samples analysis – a clear-cut differentiation between complementary and single base mismatch DNA targets was achieved. Potential applications of this technique in genotyping of Single Nucleotide Polymorphisms (SNP), especially in multiplex format, have also been demonstrated.

Department :.....Chemistry.....Student's signature.....*Boonjira Boontha*  
 Field of study :.....Chemistry.....Advisor's signature.....*Tirayut Vilaivan*  
 Academic year :.....2009.....

## ACKNOWLEDGMENT

I would like to express my sincere appreciation to my advisor Associate Professor Dr. Tirayut Vilaivan for his guidance and encouragement throughout my education at Chulalongkorn University. I would also like to thank the members of my committee, Assoc. Prof. Dr. Mongkol Sukwattanasinitt, Dr. Choladda Srisuwannaket, Assist. Prof. Dr. Piyasak Chaumpluk, Associate Professor Dr. Polkit Sangvanich and Associate Professor Dr. Palangpon Kongsaree for their valuable comments and suggestions. My appreciation also extended to Thailand-Japan Technology Transfer Project (TJTTP), Center for Petroleum, Petrochemicals, and Advanced Materials, Organic Synthesis Research Unit; Department of Chemistry, Chulalongkorn University for the use of facilities, equipment, glassware, and chemicals. Special thanks go to Dr. Nattiya Hirankarn and Mr. Jeerawat Nakkuntod from Department of Microbiology, Faculty of Medicine and Dr. Piyasak Chaumpluk, Department of Botany, Faculty of Science, Chulalongkorn University for kindly support the human and meat DNA samples; Dr. Choladda Srisuwannaket, Miss Cheeraporn Ananthanawat, Miss Rojarek Karnjanavarut, Miss Patchayaporn Korkeaw and Dr. Chaturong Suparpprom for synthesis of some intermediate compounds and PNA oligomers; Mr. Nuttawut Yothapan for NMR experiments. I am also grateful to Dr. Metha Rutnakornpituk and Dr. Uthai Wichai form Naresuan University for their valuable suggestion to improve in my dissertation. Much thank is also extended to all members of TV & WB group for their friendship, advice and their helpful throughout my graduate career. My warmest appreciation is extended to Nasesuan University for financial support during my study. Finally, I would like to especially thank my father, mother and brother for their love and inspiration throughout my study period.

## CONTENTS

	Pages
Abstract in Thai.....	iv
Abstract in English.....	v
Acknowledgements.....	vi
Contents.....	vii
List of Tables .....	xi
List of Figures .....	xii
List of Abbreviations.....	xxiv
CHAPTER I : INTRODUCTION.....	1
1.1 Peptide nucleic acid as DNA analogue .....	1
1.2 Modification of PNA oligomer .....	5
1.3 Applications of peptide nucleic acid (PNA).....	11
1.3.1 PNA as a potential antisense and antigene drugs.....	11
1.3.2 PNA as a molecular-biological device.....	13
1.3.3 PNA as probe for diagnosis and nucleic acid biosensor...	14
1.4 The objective of this Research .....	29
CHAPTER II : EXPERIMENTAL.....	30
2.1 General procedure.....	30
2.1.1 Equipments .....	30
2.1.2 Materials .....	31
2.2 Synthesis of PNA monomers.....	32
2.3 Synthesis of positive charge labeling group.....	32
2.4 Synthesis of PNA .....	33
2.4.1 Preparation of the reaction pipette and apparatus for solid phase synthesis .....	33
2.4.2 PNA oligomers synthesis .....	34
2.5 Purification of crude PNA oligomers .....	41

	Pages
2.5.1 Reverse-phase HPLC .....	41
2.5.2 Anion exchange solid support capture method .....	42
2.6 Characterization of PNA oligomers .....	42
2.7 PNA synthesis .....	43
2.7.1 Synthesis of Ac- TTTTTTTTT-Lys-NH <sub>2</sub> ( <b>P1</b> ).....	43
2.7.2 Synthesis of Ac- GTAGATCACT-Ser-NH <sub>2</sub> ( <b>P2</b> ).....	44
2.7.3 Synthesis of Ac-Arg-AAAATCCCATT-Ser-NH <sub>2</sub> ( <b>P7</b> ).....	45
2.7.4 Synthesis of Ac-Arg-AAAATTCATT -Ser-NH <sub>2</sub> ( <b>P8</b> ).....	46
2.7.5 Synthesis of P-TTCCCCCTCCCAA -Ser-NH <sub>2</sub> ( <b>P9</b> ).....	48
2.7.6 Synthesis of P-TTCCCCCTCCCAA -Ser-NH <sub>2</sub> ( <b>P10</b> ).....	49
2.7.7 Synthesis of P- ATGTAACATCTCT -Ser-NH <sub>2</sub> ( <b>P11</b> ).....	51
2.7.8 Synthesis of P- ATGTAATATCTCT-Ser-NH <sub>2</sub> ( <b>P12</b> ).....	52
2.7.9 Synthesis of P- GCCTGTACTGTAG -Ser-NH <sub>2</sub> ( <b>P13</b> ).....	54
2.7.6 Synthesis of P- GCCTGTCCTGTAG -Ser-NH <sub>2</sub> ( <b>P14</b> ).....	55
2.8 UV Melting Experiments .....	57
2.9 PNA hybridization and ion exchange capture experiments.....	57
2.9.1 Hybridization between PNA probe and single stranded (synthetic) DNA .....	57
2.9.2 Hybridization between PNA probe and double stranded DNA (synthetic and PCR samples) .....	58
<b>CHAPTER III : RESULTS AND DISCUSSION.....</b>	<b>60</b>
3.1 Synthesis of pyrrolidine nucleobase monomers .....	61
3.2 Synthesis of (1 <i>S</i> ,2 <i>S</i> )-2-aminocyclopentanecarboxylic acid ( <i>ssACPC</i> ) spacer .....	64
3.3 Synthesis of carboxybutyltriphenylphosphonium bromide <i>N</i> - hydroxysuccinimidyl ester .....	65
3.4 Synthesis of PNA oligomers .....	68
3.4.1 Solid phase synthesis of <i>acpcPNA</i> using standard conditions	68
3.4.2 Purification and characterization of PNA oligomer .....	73
3.5 Hybridization Properties of PNA.....	80
3.6 Ion-exchange capture technique for DNA sequence analysis.....	84



	Pages
3.6.1 The principle.....	84
3.6.2 Validation of the concept.....	85
3.6.3 The ability of formamide-containing buffer to reduce non-specific absorption of PNA in DNA sequence determination.....	91
3.6.4 Investigation of alternative solid supports to eliminate non-specific absorption.....	102
3.6.5 The effectiveness of the Q-sepharose based method in detection of PNA-DNA hybridization.....	109
3.6.6 Applications in SNP analysis: Validation of present method with synthetic single stranded DNA.....	115
3.6.7 Applications in SNP analysis: Validation of present method with synthetic double stranded DNA.....	120
3.6.8 Investigation of the effect of positively charged labeling groups on PNA to enhance the sensitivity of the detecting DNA sequence .....	125
3.7 Investigation of the applicability of this method in real DNA samples derived from PCR amplification.....	128
3.7.1 Identification of meat products in feedstuff.....	128
3.7.2 Genotyping of single nucleotide polymorphism (SNP) in human gene.....	135
CHAPTER IV : CONCLUSIONS.....	151
REFERENCES.....	153
APPENDICES.....	164
VITAE.....	183

## LIST OF TABLES

Tables	Pages
Table 2.1 Sequences of PNA oligomers used in this work.....	34
Table 3.1 An average coupling efficiency/step and overall coupling efficiency in the synthesis of PNA sequences used in this study.....	70
Table 3.2 An average coupling efficiency/step and overall coupling efficiency in the synthesis of PNA sequences used in this study.....	72
Table 3.3 Characterization data of all PNA sequences.....	80
Table 3.4 $T_m$ data of all PNA oligomers used in this study.....	82
Table 3.5 Type and ionic capacity of each of solid anion exchanger support.....	106
Table 3.6 Effect of acetonitrile on $T_m$ of 1:1 <b>P2·D2A</b> Condition: ratio of PNA:DNA = 1:1, [PNA] = 1 $\mu$ M, heating rate 1.0 $^{\circ}$ C/min.....	114
Table 3.7 PNA probes and DNA targets were employed in these experiments.....	116
Table 3.8 Analysis results of DNA samples obtained from meat products.	134
Table 3.9 Sequence polymorphism of PCR product and corresponding PNA probe.....	136
Table 3.10 Analysis results of <i>IL-10</i> SNP from 10 human DNA samples obtained from meat products of different origins.....	147
Table 3.11 Comparison of $T_m$ between Nielsen's <i>aeg</i> PNA and Vilaivan's <i>acpc</i> PNA .....	150

ศูนย์วิทยทรัพยากร

จุฬาลงกรณ์มหาวิทยาลัย

## LIST OF FIGURES

Figures	Pages
Figure 1.1	1
Figure 1.2	2
Figure 1.3	3
Figure 1.4	4
Figure 1.5	6
Figure 1.6	7
Figure 1.7	9
Figure 1.8	10
Figure 1.9	11
Figure 1.10	13
Figure 1.11	16
Figure 1.12	16
Figure 1.13	17

Figures	Pages	
Figure 1.14	(A) In FIT probes, an intercalator dye such as TO serves as the base surrogate that responds to perturbations of the duplex structure. (B) The fluorescence of noncomplexed TO is low owing to the rapid depletion of the excited state by torsional motions.....	18
Figure 1.15	Schematic representation for the use of a cationic polymer (CCP) with specific PNA-C* optical reporter probe to detect a complementary.....	19
Figure 1.16	Amplification of a PNA (black)_ssDNA-C* (red) solid-state sensor by polyelectrolytic deposition of the CCP (orange).....	19
Figure 1.17	dsDNA detection using a cationic conjugated polymer (CCP) and a specific PNA-C* optical reporter probe.....	20
Figure 1.18	Schematics of the procedure for hybridization of molecular beacons to dsDNA.....	21
Figure 1.19	Strategy for SNP detection using the combination of PNA beacon and nuclease S1.....	21
Figure 1.20	(a). Schematic of the principle of the SiNW array biosensor for DNA.(b). Schematic of PNA immobilization and PNA-DNA hybridization on oxide-etched SiNW surface.....	22
Figure 1.21	PNA modified magnetic bead-based assay for the specific detection of hybridization in connection with an intercalator, Meldola's blue (MDB).....	23
Figure 1.22	Affinity capture assay for DNA. The detected molecular weight of the PNA probe indicates the DNA sample.....	25
Figure 1.23	Schematic representation of the processes for SNP detection by exonuclease III/nuclease S1/PNA systems.....	25
Figure 1.24	Concept of multiplexed oligonucleotide by positively charge-tagged PNA detected by MALDI-TOF MS.....	27
Figure 1.25	Schematic representation of the processes genotyping by MALDI-TOF monitored nuclease selections.....	28

Figures	Pages	
Figure 1.26	Schematics representation for DNA sequence analysis using PNA as probe and ion exchange method and MALDI-TOF mass spectrometry.....	29
Figure 2.1	The first strategy for solid phase synthesis of PNA ( <b>P1–P8</b> ).....	36
Figure 2.2	The second strategy for solid phase synthesis of PNA ( <b>P9–P14</b> ).....	38
Figure 3.1	Structure of <i>aeg</i> PNA ( <b>3</b> ) and <i>ss</i> ACPC-PNA ( <b>4</b> ).....	60
Figure 3.2	The synthetic scheme of all four pyrrolidine monomers ( <b>11</b> ), ( <b>12</b> ), ( <b>16</b> ) and ( <b>17</b> ) according to Vilaivan <i>et al.</i> .....	61
Figure 3.3	The schematic of synthesized ( <i>N</i> -Fluoren-9-ylmethoxycarbonylamino)- <i>cis</i> -4-( <i>N</i> <sup>2</sup> -isobutyrylguanin-9-yl)-D-proline pentafluorophenyl ester ( <b>10</b> ).....	62
Figure 3.4	Synthesis of (1 <i>S</i> ,2 <i>S</i> )-2-aminocyclopentane pentafluorophenyl ester ( <b>27</b> ).....	64
Figure 3.5	The synthetic mechanism to formation of carboxybutyl triphenylphosphonium bromide <i>N</i> -hydroxysuccinimidyl ester.....	65
Figure 3.6	(a) <sup>1</sup> H NMR (400 MHz, CDCl <sub>3</sub> ) and (b) <sup>13</sup> C NMR (100 MHz, CDCl <sub>3</sub> ) spectra of carboxybutyl triphenylphosphonium bromide <i>N</i> -hydroxysuccinimidyl ester ( <b>2</b> ).....	67
Figure 3.7	TentaGel S RAM Fmoc resin.....	69
Figure 3.8	Mechanism for coupling of Fmoc-Arg(Mtr)-OH <i>via</i> HATU activator.....	71
Figure 3.9	(a) HPLC chromatogram of i) crude and ii) purified PNA ( <b>P10</b> ) and (b) MALDI-TOF MS of purified PNA ( <b>P10</b> ).....	74
Figure 3.10	MALDI-TOF MS of PNA P8: (a) Before and after hybridization between PNA and DNA-bound support and (b) After elute with several aqueous acetonitrile system and heat in boiling water.....	75
Figure 3.11	(a) HPLC chromatogram of PNA P8 and (b) MALDI-TOF MS of PNA P8 after purify by anion exchange capture.....	77
Figure 3.12	MALDI-TOF MS of PNA <b>P14</b> before and after purify by HPLC technique.....	78
Figure 3.13	MALDI-TOF MS of PNA <b>P14</b> after washing with aqueous MeCN and heating in boiling water.....	78

Figures	Pages
Figure 3.14	MALDI-TOF MS of PNA <b>P14</b> after purify by anion exchange solid support capture..... 79
Figure 3.15	The changing of UV absorbance in the thermal denaturation experiment of DNA duplex..... 81
Figure 3.16	The first derivative plot obtained from a typical thermal denaturation experiment of a DNA duplex..... 81
Figure 3.17	The concept of DNA sequence determination by employing a solid anion exchanger support to selectively capture complementary PNA·DNA hybrids followed by subsequent MALDI-TOF analysis..... 85
Figure 3.18	Structure of quaternary ammonium modified silica (trimethylaminopropyl)..... 86
Figure 3.19	MALDI-TOF analysis of a mixture of two PNA probes, <b>P3</b> and <b>P4</b> , after hybridization with the DNA targets ( <b>D3</b> or <b>D4</b> ) using anion exchanger (SAX) as solid support. Experiments from top to bottom: no DNA (solution), no DNA (solution), + <b>D3</b> (solid), + <b>D4</b> (solid)..... 87
Figure 3.20	The effect of three different hybridization medium to non-specificity background. Experiments from top to bottom: no DNA (solution), no DNA (solid), + <b>D3</b> (solid), + <b>D4</b> (solid). All spectra were recorded in reflectron mode..... 89
Figure 3.21	MALDI-TOF analysis of the effect of including formamide in the hybridization medium to non-specificity background. All spectra were operated in reflectron mode..... 91
Figure 3.22	Discrimination between complementary and non-complementary DNA targets ( <b>D1</b> and <b>D2a</b> ) by the PNA probes <b>P1</b> and <b>P2</b> . Experiments from top to bottom: no DNA (solution), no DNA (solid), + <b>D1</b> (solid), + <b>D2a</b> (solid)..... 92

Figures	Pages	
Figure 3.23	Discrimination between complementary and non-complementary DNA targets ( <b>D3</b> and <b>D4</b> ) by the PNA probes <b>P3</b> and <b>P4</b> . Experiments from top to bottom: no DNA (solution), no DNA (solid), <b>+D3</b> (solid), <b>+D4</b> (solid). All spectra were acquired in reflectron mode.....	93
Figure 3.24	Estimation of the optimum quantity of PNA probes by MALDI-TOF analysis employing <b>P3</b> and <b>P4</b> . All spectra were obtained in reflectron mode.....	95
Figure 3.25	Discrimination between complementary and various types of single mismatch DNA targets by PNA probe <b>P2</b> . Experiments from top to bottom: no DNA (solution), no DNA (solid), <b>+D2a</b> (solid), <b>+D2b</b> (solid), <b>+D2c</b> (solid), <b>+D2d</b> (solid). All spectra were acquired in reflectron mode.....	96
Figure 3.26	Discrimination between complementary and single mismatched DNA targets using 15mer mixed base PNA <b>P5</b> probes. Experiments from top to bottom: no DNA (solution), no DNA (solid), <b>+D5a</b> (solid), <b>+D5d</b> (solid). All spectra were obtained in linear mode.....	98
Figure 3.27	MALDI-TOF analysis revealing the effect of formamide in the hybridization medium to eliminate non-specificity background. All spectra were obtained in linear mode.....	99
Figure 3.28	Discrimination between complementary and various types of single mismatch DNA targets by PNA <b>P5</b> probe. Experiments from top to bottom: no DNA (solution), no DNA (solid), <b>+D5a</b> (solid), <b>+D5b</b> (solid), <b>+D5c</b> (solid), <b>+D5d</b> (solid), <b>+D6a</b> (solid), <b>+D6b</b> (solid). All spectra were obtained in linear mode.....	100
Figure 3.29	Structures of anion exchange supports used in this study.....	102
Figure 3.30	MALDI-TOF analysis of study of hydrophobic interaction between PNA probe and various solid supports in the absence of DNA targets and formamide. For other conditions see text.....	103

Figures	Pages
Figure 3.31 (a) MALDI-TOF analysis of solid support after hybridization with the DNA target <b>D1</b> or <b>D2A</b> (b) MALDI-TOF analysis of a mixture of two PNA probes, <b>P1</b> and <b>P2</b> , after hybridization with the DNA target <b>D1</b> or <b>D2A</b> .....	105
Figure 3.32 Determination of the limit of detection for PNA probe <b>P1</b> with DNA <b>D1</b> target (fixing the amount DNA target at 100 pmol/ 30 $\mu$ L hybridization reaction).....	107
Figure 3.33 Determination of the limit of detection for DNA target using PNA probe <b>P1</b> (fixing the amount PNA probe at 10 pmol/ 30 $\mu$ L hybridization reaction).....	108
Figure 3.34 Discrimination between complementary and various types of single mismatch DNA targets by using homothymine nonamer PNA probe <b>P1</b> .....	110
Figure 3.35 Discrimination between complementary and various types of single mismatch DNA targets by using mixed base 10mer PNA probe <b>P2</b> .....	111
Figure 3.36 Discrimination between complementary and various types of single mismatch DNA targets by using mixed base 15mer PNA probe <b>P5</b> .....	112
Figure 3.37 $T_m$ curves of <b>P2</b> · <b>D2A</b> hybrid in the presence of various hybridization buffer: Condition PNA: DNA = 1:1, [PNA] = 1 $\mu$ M, heating rate 1.0 $^{\circ}$ C/min.....	113
Figure 3.38 MALDI-TOF analysis of the effect of including acetonitrile in the washing medium to eliminate non-specificity background.....	115
Figure 3.39 Discrimination between complementary and fully mismatched DNA targets using a combination of two PNA probes <b>P1</b> and <b>P2</b> . Hybridization conditions: PNA 10 pmol each and DNA 10 pmol in 30 $\mu$ L binding buffer at 30 $^{\circ}$ C. Experiments from top to bottom: no DNA target (solution, positive control), no DNA target (solid, negative control), + <b>D1</b> (complementary to <b>P1</b> , single mismatch to <b>P2</b> ), + <b>D2A</b> (complementary to <b>P2</b> , single mismatch to <b>P1</b> ).....	117



Figures	Pages	
Figure 3.40	Discrimination between complementary and fully mismatched DNA targets using a combination of two PNA probes <b>P3</b> and <b>P4</b> . Hybridization conditions: PNA 10 pmol each and DNA 10 pmol in 30 $\mu$ L binding buffer at 30 $^{\circ}$ C. Experiments from top to bottom: no DNA target (solution, positive control), no DNA target (solid, negative control), + <b>D3</b> (complementary to <b>P3</b> , single mismatch to <b>P4</b> ), + <b>D4</b> (complementary to <b>P4</b> , single mismatch to <b>P3</b> ).....	118
Figure 3.41	Discrimination between complementary and fully mismatched DNA targets using a combination of two PNA probes <b>P5</b> and <b>P6</b> . Hybridization conditions: PNA 10 pmol each and DNA 10 pmol in 30 $\mu$ L binding buffer at 30 $^{\circ}$ C. Experiments from top to bottom: no DNA target (solution, positive control), no DNA target (solid, negative control), + <b>D5A</b> (complementary to <b>P5</b> , single mismatch to <b>P6</b> ), + <b>D6A</b> (complementary to <b>P6</b> , single mismatch to <b>P5</b> ).....	119
Figure 3.42	Determination of the effect of salt concentration to the hybridization between PNA and synthetic double strand DNA.....	121
Figure 3.43	Discrimination between complementary and single mismatch in double stranded DNA targets by the 15mer PNA probe <b>P5</b> . Hybridization conditions: PNA 10 pmol, DNA 5 pmol, 10 mM sodium phosphate buffer pH 7.0 (30 $\mu$ L) at 30 $^{\circ}$ C. Experiments from top to bottom: no DNA target (solution, positive control), no DNA target (solid, negative control), +ds <b>D5A/D5A'</b> (complementary, double-stranded), + <b>D5A</b> (complementary, single-stranded), +ds <b>D5C/D5C'</b> (C·T single mismatch, double-stranded).+ <b>D5C</b> (C·T single mismatch, single-stranded).....	123
Figure 3.44	Comparison the efficacy of PNA·DNA hybridization under usual condition and new condition with additional heating step.....	124

Figures	Pages
Figure 3.45 Structure of (a) arginine and (b) carboxybutyl triphenyl phosphonium group.....	126
Figure 3.46 Determination of the limit of detection of (a) unmodified PNA (PNA (Ac)) (b) PNA with N-terminal arginine group (PNA (Arg)) (c) PNA with N-terminal carboxybutyltriphenylphosphonium group (PNA (P)).....	127
Figure 3.47 (a) Sequence of PNA <b>P7</b> and PNA <b>P8</b> (b) Target cytochrome b sequence used for identification of meat samples.....	129
Figure 3.48 Identification of bovine and porcine DNA in meat products by the 11mer PNA probes <b>P7</b> and <b>P8</b> . Hybridization conditions: PNA 10 pmol each, DNA 10 pmol, 10 mM sodium phosphate buffer pH 7.0 (30 $\mu$ L) at 30 $^{\circ}$ C. Experiments from top to bottom: no DNA target (solution, positive control), no DNA target (solid, negative control), + <b>D7</b> (complementary to <b>P7</b> ), + <b>D8</b> (complementary to <b>P8</b> ).....	130
Figure 3.49 Identification of bovine and porcine DNA in meat products by using the PNA probes <b>P7</b> and <b>P8</b> .....	132
Figure 3.50 <i>IL-10</i> promoter gene sequence.....	135
Figure 3.51 Discrimination between complementary and single mismatched DNA targets using a combination of two PNA probes <b>P9</b> and <b>P10</b> . Hybridization conditions: PNA 1 pmol each and DNA 5 pmol in 30 $\mu$ L binding buffer at 30 $^{\circ}$ C. Experiments from top to bottom: no DNA target (solution, positive control), no DNA target (solid, negative control), + <b>D9</b> (complementary to <b>P9</b> , single mismatch to <b>P10</b> ), + <b>D10</b> (complementary to <b>P10</b> , single mismatch to <b>P9</b> ).....	137

Figures	Page	
Figure 3.52	Discrimination between complementary and single mismatched DNA targets using a combination of two PNA probes <b>P11</b> and <b>P12</b> . Hybridization conditions: PNA 1 pmol each and DNA 5 pmol in 30 $\mu$ L binding buffer at 30 $^{\circ}$ C. Experiments from top to bottom: no DNA target (solution, positive control), no DNA target (solid, negative control), + <b>D11</b> (complementary to <b>P11</b> , single mismatch to <b>P10</b> ), + <b>D12</b> (complementary to <b>P12</b> , single mismatch to <b>P11</b> ).....	138
Figure 3.53	Singleplex SNP typing of the -1082 position of the human <i>IL-10</i> gene using a two PNA probes <b>P9</b> (-1082G probe) and <b>P10</b> (-1082A probe).....	140
Figure 3.54	Singleplex SNP typing of the -819 position of the human <i>IL-10</i> gene using two PNA probes <b>P11</b> (-819C probe) and <b>P12</b> (-819T probe).....	140
Figure 3.55	Duplex SNP typing in the synthetic DNA using four PNA probes ( <b>P9</b> , <b>P10</b> , <b>P11</b> and <b>P12</b> ). Hybridization conditions: PNA 1 pmol each and DNA 5 pmol in 30 $\mu$ L binding buffer at 30 $^{\circ}$ C. Experiments from top to bottom: no DNA target (solution, positive control), no DNA target (solid, negative control), + <b>D17a</b> (complementary to <b>P9</b> and <b>P11</b> , single mismatch to <b>P10</b> and <b>P12</b> ), + <b>D17b</b> (complementary to <b>P10</b> and <b>P12</b> , single mismatch to <b>P9</b> and <b>P11</b> ).....	142
Figure 3.56	Duplex SNP genotyping of the -819 position and -1082 position of the human <i>IL-10</i> gene using four PNA probes <b>P9</b> (-1082G probe), <b>P10</b> (-1082A probe), <b>P11</b> (-819T probe) and <b>P12</b> (-819C probe). Hybridization conditions: PNA 1 pmol each, DNA sample (from PCR) 5 pmol, 10 mM sodium phosphate buffer pH 7.0 (30 $\mu$ L) at 30 $^{\circ}$ C. Experiments from top to bottom: no DNA target (solution, positive control), no DNA target (solid, negative control), + <b>D17a</b> (positive control), + <b>D17b</b> (positive control), +DNA sample S64 (-819C/C and -1082G/G homozygous), +DNA sample.....	143

Figures	Page	
Figure 3.57	Simultaneous multiplex typing of the human <i>IL-10</i> gene promoter at SNP positions –1082, –819 and –592 using a combination of six PNA probes <b>P9</b> (–1082G probe), <b>P10</b> (–1082A probe), <b>P11</b> (–819T probe), <b>P12</b> (–819C probe), <b>P13</b> (–592C probe) and <b>P14</b> (–592A probe).....	144
Figure 3.58	Simultaneous multiplex typing of the human <i>IL-10</i> gene promoter of unknown samples using a combination of six PNA probes ( <b>P9–P14</b> ).....	146
Figure 3.59	Comparison of specificity between Nielsen’s PNA and Vilaivan’s pyrrolidinyl PNA.....	149
Figure A.1	<sup>1</sup> H NMR spectrum of ( <i>N</i> -Fluoren-9-ylmethoxycarbonyl)- <i>cis</i> -4-(thymine-1-yl)-D-proline pentafluorophenyl ester ( <b>11</b> ).....	165
Figure A.2	<sup>1</sup> H NMR spectrum of ( <i>N</i> -Fluoren-9-ylmethoxycarbonylamino)- <i>cis</i> -4-( <i>N</i> <sup>2</sup> -isobutrylguanin-9-yl)-D-proline pentafluorophenyl ester ( <b>12</b> ).....	165
Figure A.3	<sup>1</sup> H NMR spectrum of ( <i>N</i> -Fluoren-9-ylmethoxycarbonyl)- <i>cis</i> -4-( <i>N</i> <sup>6</sup> -benzoyladenine-9-yl)-D-proline pentafluorophenyl ester ( <b>16</b> ).....	166
Figure A.4	<sup>1</sup> H NMR spectrum of ( <i>N</i> -Fluoren-9-ylmethoxycarbonyl)- <i>cis</i> -4-( <i>N</i> <sup>4</sup> -benzoylcytosine-1-yl)-D-proline pentafluorophenyl ester ( <b>17</b> ).....	166
Figure A.5	<sup>1</sup> H NMR spectrum of ethyl (1 <i>S</i> ,2 <i>S</i> )-2-[(1' <i>S</i> )-phenylethyl]-aminocyclopentane carboxylate ( <b>23</b> ).....	167
Figure A.6	<sup>1</sup> H NMR spectrum of (1 <i>S</i> ,2 <i>S</i> )-2-Aminocyclopentane carboxylic acid hydrochloride ( <b>24</b> ).....	167
Figure A.7	<sup>1</sup> H NMR spectrum of (1 <i>S</i> ,2 <i>S</i> )-2-( <i>N</i> -Fluoren-9-ylmethoxycarbonyl)-aminocyclopentanecarboxylic acid ( <b>26</b> ).....	168
Figure A.8	<sup>1</sup> H NMR spectrum of (1 <i>S</i> ,2 <i>S</i> )-2-( <i>N</i> -fluoren-9-ylmethoxycarbonyl)-aminocyclopentane pentafluorophenyl ester ( <b>27</b> ).....	168
Figure A.9	<sup>1</sup> H NMR spectrum of carboxybutyltriphenylphosphonium bromide <i>N</i> -hydroxysuccinimidyl ester ( <b>2</b> ).....	169
Figure A.10	<sup>13</sup> C NMR spectrum of carboxybutyltriphenylphosphonium bromide <i>N</i> -hydroxysuccinimidyl ester ( <b>2</b> ).....	169

Figures	Page
Figure A.11 HPLC chromatogram of Ac-T <sub>9</sub> -Lys-NH <sub>2</sub> ( <b>P1</b> ).....	170
Figure A.12 HPLC chromatogram of Ac-GTAGATCACT-Ser-NH <sub>2</sub> ( <b>P2</b> ).....	170
Figure A.13 HPLC chromatogram of Ac-TGTACGTCACAACATA-Lys-NH <sub>2</sub> ( <b>P5</b> ).....	171
Figure A.14 HPLC chromatogram of Ac-TGTACGTAACAACATA-Lys-NH <sub>2</sub> ( <b>P6</b> ).....	171
Figure A.15 HPLC chromatogram of Ac-Arg-AAAATCCCATT-Ser-NH <sub>2</sub> ( <b>P7</b> )..	172
Figure A.16 HPLC chromatogram of Ac-Arg-AAAATTCCATT-Ser-NH <sub>2</sub> ( <b>P8</b> ).....	172
Figure A.17 HPLC chromatogram of P-TTCCCCCTCCCAA-Ser-NH <sub>2</sub> ( <b>P9</b> ).....	173
Figure A.18 HPLC chromatogram of P-TTCCCCCTCCCAA-Ser-NH <sub>2</sub> ( <b>P10</b> ).....	173
Figure A.19 HPLC chromatogram of P-ATGTAACATCTCT-Ser-NH <sub>2</sub> ( <b>P11</b> ).....	174
Figure A.20 HPLC chromatogram of P-ATGTAATATCTCT-Ser-NH <sub>2</sub> ( <b>P12</b> ).....	174
Figure A.21 HPLC chromatogram of P-GCCTGTACTGTAG-Ser-NH <sub>2</sub> ( <b>P13</b> ).....	175
Figure A.22 HPLC chromatogram of P-GCCTGTCCTGTAG-Ser-NH <sub>2</sub> ( <b>P14</b> ).....	175
Figure A.23 MALDI-TOF mass spectrum of Ac-TTTTTTTTT-LysNH <sub>2</sub> ( <b>P1</b> ).....	176
Figure A.24 MALDI-TOF mass spectrum of Ac-GTAGATCACT-Ser-NH <sub>2</sub> ( <b>P2</b> ).....	176
Figure A.25 MALDI-TOF mass spectrum of Ac-TGTACGTAACAACATA-Lys-NH <sub>2</sub> ( <b>P5</b> ).....	177
Figure A.26 MALDI-TOF mass spectrum of Ac-TGTACGTCACAACATA-Lys-NH <sub>2</sub> ( <b>P6</b> ).....	177
Figure A.27 MALDI-TOF mass spectrum of Ac-Arg-AAAATCCCATT-Ser-NH <sub>2</sub> ( <b>P7</b> ).....	178

Figures	Pages
Figure A.28 MALDI-TOF mass spectrum of Ac-Arg-AAA ATTCCATT-Ser-NH <sub>2</sub> ( <b>P8</b> ).....	178
Figure A.29 MALDI-TOF mass spectrum of P-TTCCCCCTCCCAA-Ser-NH <sub>2</sub> ( <b>P9</b> ).....	179
Figure A.30 MALDI-TOF mass spectrum of P-TTCCCCCTCCCAA-Ser-NH <sub>2</sub> ( <b>P10</b> ).....	179
Figure A.31 MALDI-TOF mass spectrum of P-ATGTAACATCTCT-Ser-NH <sub>2</sub> ( <b>P11</b> ).....	180
Figure A.32 MALDI-TOF mass spectrum of P-ATGTAATATCTCT-Ser-NH <sub>2</sub> ( <b>P12</b> ).....	180
Figure A.33 MALDI-TOF mass spectrum of P-GCCTGTACTGTAG-Ser-NH <sub>2</sub> ( <b>P13</b> ).....	181
Figure A.34 MALDI-TOF mass spectrum of P-GCCTGTCCTGTAG-Ser-NH <sub>2</sub> ( <b>P14</b> ).....	181
Figure A.35 The melting curves of PNA <b>P1</b> with DNA <b>D1</b> . The $T_m$ were measured at a ratio of PNA:DNA = 1:1, [PNA] = 1 $\mu$ M, 10 mM sodium phosphate buffer, pH 7.0, heating rate 1.0 $^{\circ}$ C/min.....	182
Figure A.36 The melting curves of PNA <b>P2</b> with DNA <b>D2a</b> . The $T_m$ were measured at a ratio of PNA: DNA = 1: 1, [PNA] = 1 $\mu$ M, 10 mM sodium phosphate buffer, pH 7.0, heating rate 1.0 $^{\circ}$ C/min.....	182

ศูนย์วิทยทรัพยากร

จุฬาลงกรณ์มหาวิทยาลัย

## LIST OF ABBREVIATIONS

$\delta$	chemical shift
$\mu\text{L}$	microliter
$\mu\text{mol}$	micromole
$[\alpha]_{\text{D}}$	specific rotation
A	adenine
A <sup>Bz</sup>	N <sup>4</sup> -benzoyladenine
Ac	acetyl
Ac <sub>2</sub> O	acetic anhydride
AcOH	acetic acid
Ar	aryl
Arg	arginine
aq	aqueous
Boc	<i>tert</i> -butoxycarbonyl
br	broad
BSA	bovine serum albumin
Bz	benzoyl
c	concentration
C	cytosine
calcd	calculated
C <sup>Bz</sup>	N <sup>4</sup> -benzoylcytosine
CCA	$\alpha$ -cyano-4-hydroxy cinnamic acid
CDCl <sub>3</sub>	deuterated chloroform
d	doublet
DABCO	1,4-diazabicyclo[2.2.2]octane
DBU	1,8-Diaza-bicyclo-[5,4,0]-undec-7-en or Diazabicycloundecen
D <sub>2</sub> O	deuterium oxide
DCC	dicyclohexyl carbodiimide
DCM	dichloromethane
DCU	dicyclohexylurea
DEAE	Diethylaminoethyl sepharose

Dhbt	3,4-dihydro-4-oxo-1,2,3-benzotriazin-3-yl
DIAD	diisopropylazodicarboxylate
DIEA	Diisopropylethylamine
DMF	<i>N,N'</i> -dimethylformamide
DMSO- <i>d</i> <sub>6</sub>	deuterated dimethylsulfoxide
DNA	deoxyribonucleic acid
Dpm	diphenylmethyl
ds	double strand
EA	elemental analysis
equiv	equivalent (s)
Fmoc	9-fluorenylmethoxycarbonyl
FmocCl	9-fluorenylmethyl chloroformate
FmocOSu	9-fluorenylsuccinimidyl carbonate
Fmol	femtomole
FRET	fluorescence resonance energy transfer
g	gram
G	guanine
G <sup>Ibu</sup>	<i>N</i> <sup>2</sup> -isobutyrylgaunine
G <sup>Ibu</sup> (ONpe)	<i>N</i> <sup>2</sup> -isobutyrylgaunine 2-(4-nitrophenyl)ethyl
h	hour
HATU	<i>O</i> -(7-azabenzotriazol-1-yl)- <i>N,N,N',N'</i> -tetramethyluronium hexafluorophosphate
HOAt	1-hydroxy-7-azabenzotriazole
HPLC	high performance liquid chromatography
Ibu	isobutyryl
<i>IL-10</i>	interleukin-10
<i>J</i>	coupling constant
Lys	lysine
m	multiplet
MALDI-TOF	matrix-assisted laser desorption/ionization-time of flight
MeCN	acetonitrile
MeOH	methanol
MeOTs	methyl tosylate
mg	milligram



MHz	megahertz
min	minute
mL	milliliter
mM	millimolar
mmol	millimole
mRNA	messenger ribonucleic acid
MS	mass spectrometry
Mtr	methoxy - 2,3,6 – trimethylbenzenesulfonyl
<i>m/z</i>	mass to charge ratio
nm	nanometer
NMR	nuclear magnetic resonance
Npe	2-(4-nitrophenyl)ethyl
°C	degree celcius
OD <sub>xxx</sub>	optical density at xxx nm (= A <sub>xxx</sub> )
P	carboxybutyl triphenyl phosphonium
PCR	polymerase chain reaction
Pfp	pentafluorophenyl
PfpOTfa	pentafluorophenyl trifluoroacetic acid
PG	an unspecified protecting group
Ph	phenyl
PNA	peptide nucleic acid or polyamide nucleic acid
ppm	part per million
pmol	picomole
PSA	ethylenediamine-N-propyl silica
Q sepharose	Quaternary ammonium sepharose
R <sub>f</sub>	retention factor
RNA	ribonucleic acid
s	singlet
Ser	serine
SNP	single nucleotide polymorphism
S/N	signal to noise ratio
ss	single strand
t	triplet
T	thymine

T <sup>Bz</sup>	<i>N</i> <sup>3</sup> -benzoylthymine
TEA	triethylamine
TFA	trifluoroacetic acid
THF	tetrahydrofuran
TLC	thin layer chromatography
<i>T</i> <sub>m</sub>	melting temperature
<i>t</i> <sub>R</sub>	retention time
Ts	<i>p</i> -toluenesulfonyl (=tosyl)
UV	ultraviolet



ศูนย์วิทยทรัพยากร  
จุฬาลงกรณ์มหาวิทยาลัย

# CHAPTER I

## INTRODUCTION

### 1.1 Peptide nucleic acid as DNA analogue

The function of deoxyribonucleic acid (DNA) is to store genetic information and transfer genetic codes from one generation to another in every living species. In addition, DNA also acts as a structural scaffold for the arrangement of multiprotein complexes in cell [1]. DNA structure is composed of repeating nucleotide subunits. Each nucleotide subunit contains three components: i) a heterocyclic base (purine or pyrimidine) ii) a phosphate group, and iii) a sugar (deoxyribose). These repeating units are linked together through the reaction between 5'-hydroxy ends of phosphate groups and 3'-hydroxy terminal of other molecules to form phosphodiester linkages. Since Watson and Crick's elucidation of DNA structure, the DNA double helix has been accepted that the central features of DNA structure. According to this model, the two anionic sugar-phosphate backbones winds around the outside of a cylindrical helix and the neutral nucleobases occupy the center as to avoid water. The paired bases are roughly perpendicular to the helical axis and further stabilized by  $\pi$ - $\pi$  interaction and hydrophobic interaction, the so called base stacking [1]. The stability of DNA duplex relies on the specific order of the four nucleobases: Adenine (A) pairs with thymine (T), forming two hydrogen bonds, whereas cytosine (C) pairs with guanine (G), forming three hydrogen bonds (**Figure 1.1**). The specific pairing between A and T, C and G are as known as Watson-Crick base pairing rules [2].

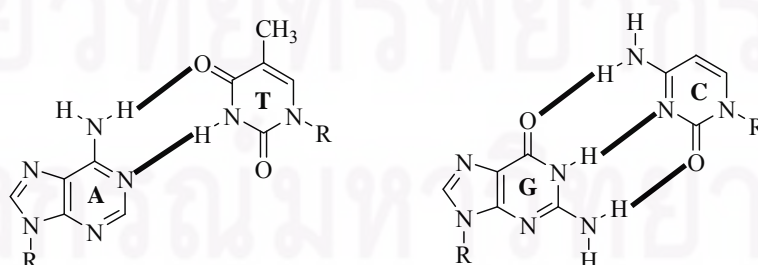


**Figure 1.1** Hydrogen bonding *via* Watson-Crick base pairing rules.

The most important molecular recognition event in nature is the base-pairing of nucleic acids to form double helical hybrid, which guarantee the storage and expression of genetic information in living systems. In normal cells, the expression of genetic information consists of two processes namely transcription and translation. In transcription process, a DNA strand serves as the template for the synthesis of another strand of ribonucleic acid, with a complementary sequence. In translation process, the RNA's base sequence determines the order of amino acid that will be joined together by ribosomes. This generates proteins with specific structure and function. Inhibition of gene expression can be achieved by binding of an oligonucleotide to RNA with a portion of its complementary sequence (the so-called antisense inhibition). This will result in interference of the normal translation process. In a similar concept, an antigene oligonucleotide can be targeted to the complementary DNA sequence to inhibit the transcription. The concepts are illustrated in **Figure 1.2**.

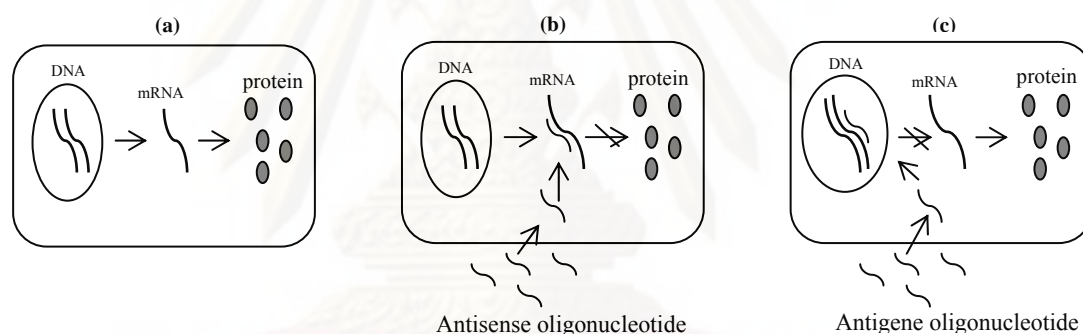


**Figure 1.2** Schematic illustration of gene expression; (a) normal gene expression (b) antisense inhibition and (c) antigene inhibition.

The highly specific recognition through the pairing of the four nucleobase has become increasingly important for the development of DNA diagnostics and for oligonucleotide therapeutics in the form of antisense and antigene oligonucleotide [3]. Natural oligonucleotides have been shown to exhibit both antisense and antigene properties *in vitro*. However, DNA is rapidly degraded by nucleases *in vivo* [4]. This stimulates several developments of novel oligonucleotide mimics to overcome this serious obstacle. In addition, modification can improve some properties such as binding-affinity to complementary nucleic acid and membrane permeability. A large number of oligonucleotide analogues has been constructed during the last two decades that related to the modification of the phosphate group or the ribose or the nucleobase

[4]. One of the most interesting concept is the total replcaement of the sugar phosphate backbone with a peptide like structure as in peptide nucleic acid or poly amide nucleic acid (PNA). The structure of PNA represents a dramatic deviation from conventional oligonucleotide chemistry.

The first PNA has been synthesized in 1991 by Nielsen and coworkers first synthesized a new compound having analogous structure to DNA [5]. A major difference between DNA and PNA it that PNA is comprised of 2-aminoethyl glycine units instead of deoxyribose phosphate groups of DNA backbone, resulting in an achiral and uncharged DNA mimic. A methylene carbonyl linker connects natural nucleobase to this backbone at the amino nitrogen [6] as shown in **Figure 1.3**.

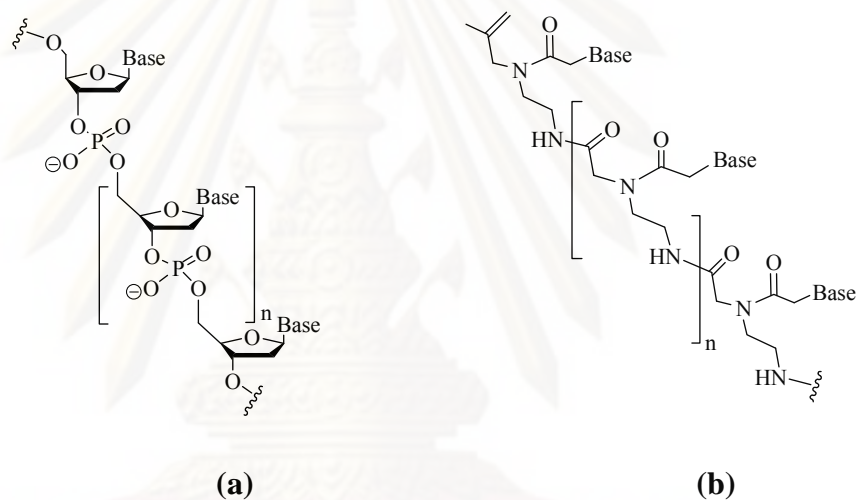


**Figure 1.3** The structure of a DNA molecule (a) and an aegPNA molecule (b)

Interestingly, this structural difference does not inhibit the base-base recognition of between DNA and PNA. Base pairing between PNA and DNA essentially follows the Watson-Crick base pairing rules [3]. More importantly, these PNA·DNA hybrids are even more stable than the corresponding DNA·DNA hybrids due to the absence of electrostatic repulsion between the uncharged PNA backbone and the negatively charged sugar-phosphate backbone of DNA/RNA. The thermal stability follows the order PNA·PNA > PNA·RNA > PNA·DNA (> RNA·DNA > DNA·DNA) [7].

In contrast to DNA, PNA can bind in both parallel and antiparallel formation however; antiparallel PNA·DNA hybrids are considerably more stable than the

corresponding DNA·DNA hybrids. Another remarkable properties of PNAs is their ability to recognize sequences with in duplex DNA to form triple helices either by triple helix formation or a unique strand invasion mechanism which results in displacement of one of the DNA strand to form the so-called D-loop or P-loop structures (**Figure 1.4a**) [8,9]. According to X-ray crystallographic studies of PNA·DNA·PNA triple helices, it was demonstrated that the first strand of PNA hybridized to DNA by a Watson-Crick base pairing, while the second strand of PNA hybridized to the same DNA by Hoogsteen base-pairing (**Figure 1.4b**) [10]. The second sequence of PNA also shows specific interactions (H-bonding) between each amide N-H of the backbone of the Hoogsteen PNA strand and the phosphate oxygen of the DNA backbone, which also contributes to the high stability of such triplexes.

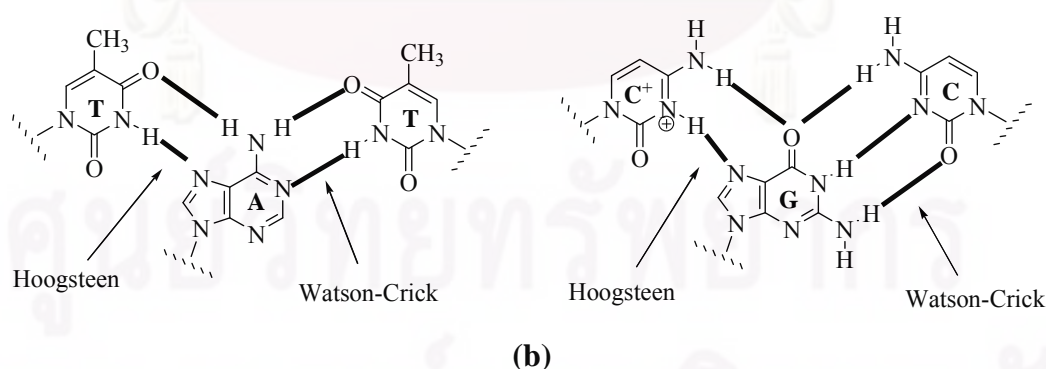
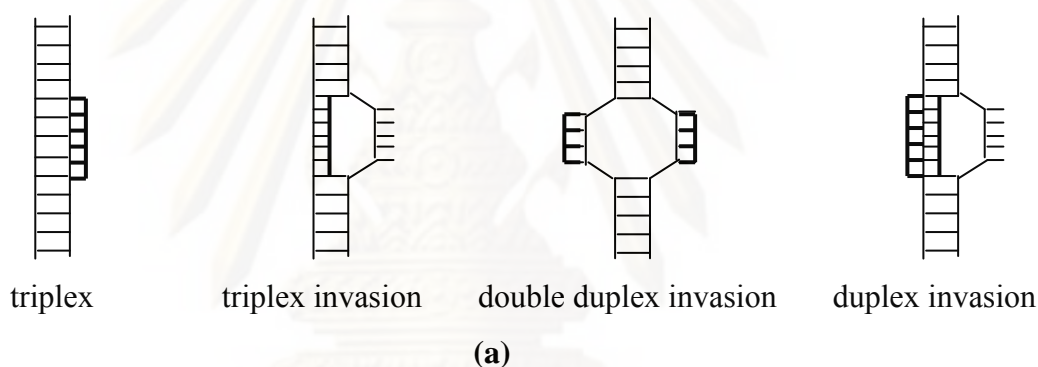


**Figure 1.4** (a) Schematic of *aeg*PNA binding mode for double stranded DNA  
 (b) Hydrogen bonding *via* Watson-Crick and Hoogsteen base pairing

## 1.2 Modification of PNA oligomer

Since Nielsen *et. al.* reported its discovery in 1991 [5], PNA became a popular research topic due to its many special features. For instance, PNA can bind with complementary DNA to form double or triple helix hybrids. The hybrid showed surprisingly high stability compared to the natural DNA. In addition, PNA exhibited a better binding specificity when compared to DNA as indicated by a more decrease in stability of the PNA·DNA compared to the corresponding DNA·DNA hybrids when one or more base mismatch(es) exist. Furthermore, PNA is stable against enzymes including nucleases and proteases, which suggests the potential use of PNA under physiological conditions. Because of these advantages, PNA is a potentially useful oligonucleotide analogue to be used in antisense/antigene therapeutics. However, the original PNA has a number of limitations such as low water solubility, similar stability between parallel and anti-parallel hybrids, and the inability to penetrate through cell wall unless a carrier is attached to its structure. Therefore, extensive works have been focused on structural modification of Nielsen's PNA to overcome these drawbacks. PNA oligomers containing residue extended in the either the backbone or in the linker to the nucleobases had been synthesized and their hybridization properties examined [11, 12]. Unfortunately, incorporation of the modified structure into the standard PNA oligomers lead to substantial reduction in the stability of the resulting PNA·DNA and PNA·RNA hybrids ( $\Delta T_m$  of  $-0.7$  to  $-22$  °C compared to the unmodified PNA) [7,13].

Because of the conformational limitation of PNA and DNA complexation, the hybridization of PNA to its complementary oligonucleotide resulted in a large enthalpy gain, by hydrogen-bonding and base-stacking interactions, and significant entropy loss by the formation of a highly ordered and rigid duplex structure from two oligonucleotide strands. In order to reduce the entropy loss, modification of PNA oligomers by the insertion of a rigid structure especially cyclic moiety in the PNA strands have been made to enhance the rigidity of PNA structure. In addition, the presence of chiral residue can have beneficial effect to orientation selectivity in the complementary DNA/RNA binding [7, 14]. For these reasons, many works have focused on designing new conformationally constrained PNA.

As an example, incorporation of a methylene group to link between the aminoethylglycyl backbone and the methylene carbonyl side chain of *aeg*PNA might be a method of choice to obtain a variety of five- or six- membered nitrogen heterocyclic analogues [7,15]. These modified PNA bind to DNA/RNA targets with varying affinities. For example, in 4-aminopropyl PNA (**Figure 1.5a**), a methylene linkage was inserted between the C-2 atom of the glycine part and the C-5 atom of the aminoethyl part of the *aeg*PNA to give a rigid pyrrolidine ring with two stereogenic centers. The presence of two stereogenic centers in the structure resulted in PNAs with more than one stereoisomers and each isomer showed unique specific pairing affinity [7]. In another example, the effect of insertion of *cis*-(1*S*,2*R*/1*R*,2*S*) cyclohexyl moieties on the aminoethyl segment of aminoethylglycyl PNA has been evaluated (**Figure 1.5b**). It was proposed that the *cis*-diaminocyclohexyl moiety may allow the restriction of the torsion angle in the ethylenediamine segment. The experimental results showed that the PNA with (1*S*,2*R*)-cyclohexyl stereochemistry increases the affinity to RNA over DNA as compared to the control *aeg*PNA and the same cyclohexyl PNA with (1*R*,2*S*) isomer [16]. In another example, a new chiral prolylgylycyl PNA [17–19] was constructed by incorporating a methylene bridge between the C-2 atom of the glycine unit and the C-2' atom of the nucleobase linker of the *aeg*PNA (**Figure 1.5c**). These PNA systems were synthesized in both in *cis*- and *trans*-stereochemistry of nucleobase at C-4 position against the carbonyl group of proline. It was observed that the homothymine decamer of *cis*-D, *cis*-L and *trans*-D isomer showed a good binding affinity with both DNA and RNA and with apparent 1:1 stoichiometry for *cis*-D-isomer. Unfortunately, this modified PNA has poor solubility in aqueous media, which can have serious implication for biological studies [20].

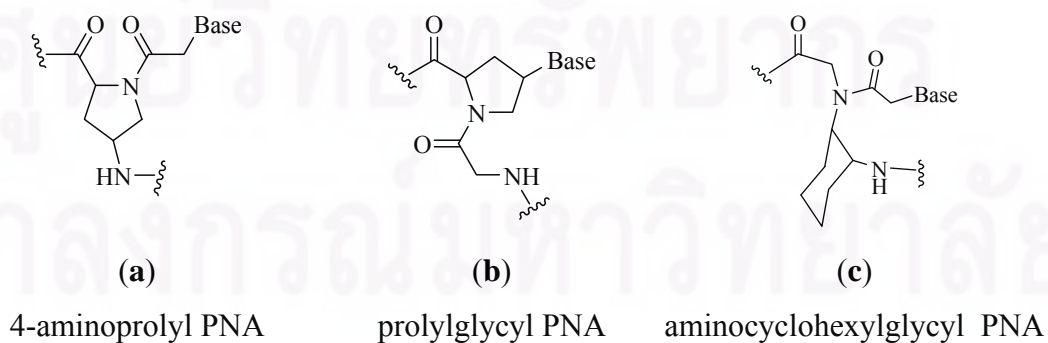


**Figure 1.5** Structure of modified PNA backbone



One of the most interesting design is the so-called aminoethylpropyl (aep) PNA developed independently by Kumar [21] and Vilaivan [22]. In this PNA, the flexibility of the aminoethyl segment of *aeg*PNA is retained whereas the glycine and the side chain are constrained via a methylene bridge. This flexibility should allow the *aep*PNA to adopt a wider range of conformations than the prolylglycyl PNA. Moreover, the presence of the positive charge and the tertiary pyrrolidine ring nitrogen should attract the negatively charged phosphate group of DNA, providing further stabilization of the hybrid formed with natural DNA. The resulting homothymine oligomer of *aep*PNA showed a strong and specific binding property toward target DNA/RNA sequence [20]. In many other related works, the pyrrolidine ring had been widely used as a rigid component in the PNA structure as shown in **Figure 1.6** [21].

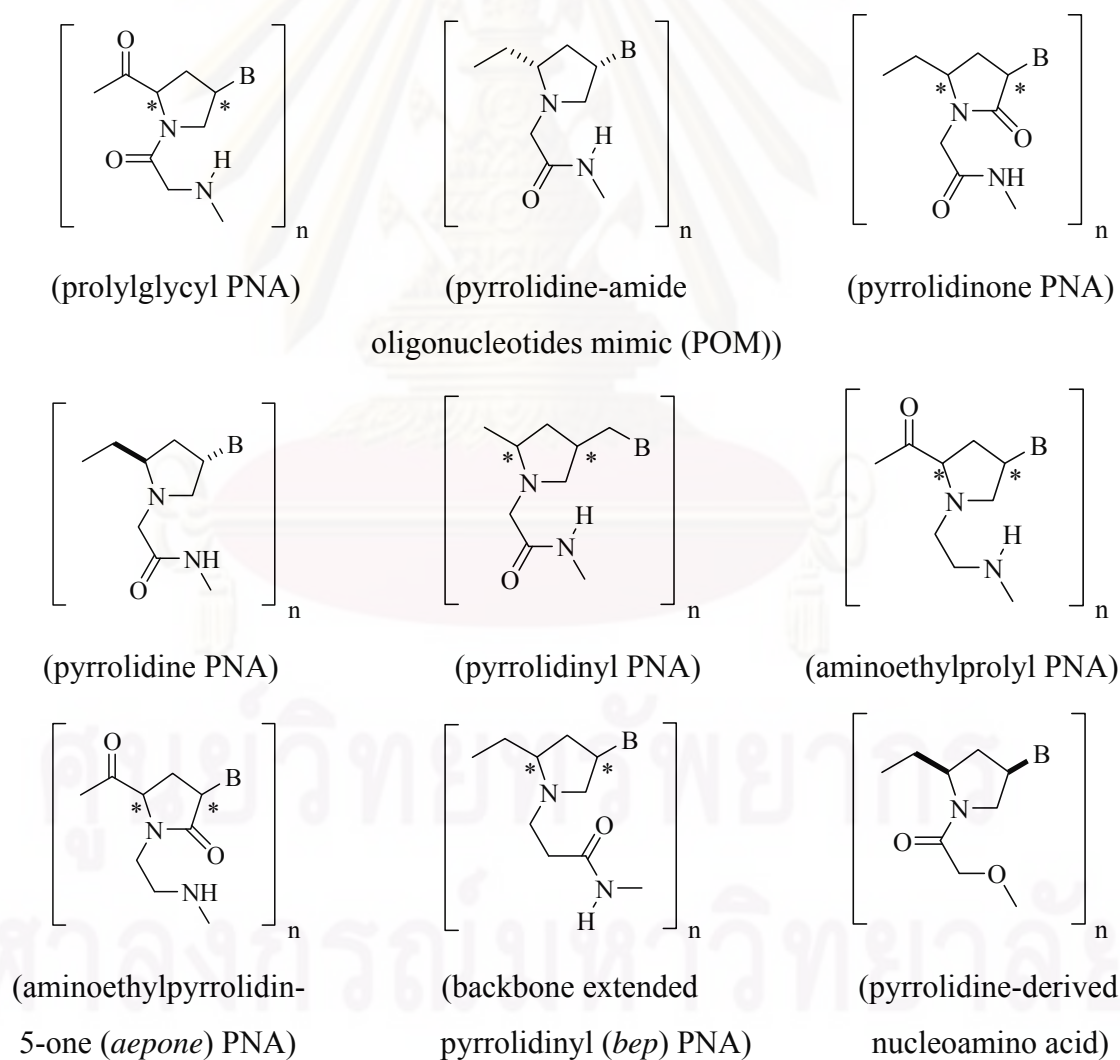


**Figure 1.6** Structure of modified pyrrolidine PNA

Unfortunately, in most of the research, usually only a few modified pyrrolidinyll subunits were inserted into the core structure of *aeg*PNA at various positions to form chimeric backbones. The hybridization results of these chimeric PNA with DNA/RNA are not easily interpreted in these cases since the effect on  $T_m$  is not only dependent on the structure modification but also to the number and position of the modified residues in the original PNA strand. Only a few systems have been studied with non-chimeric backbones. For example, Micklefield and co-workers described the synthesis of pyrrolidine-amide oligonucleotide mimics (POMs) using Fmoc-peptide chemistry in 2007. The Fmoc-protected nucleobase monomers were prepared and thyminyll and adeninyll POM pentamers were synthesized. These pentamers showed to hybridize strongly with both DNA and RNA [23]. In addition, in the same year, they also reported the synthesis of a mixed sequence POM by using Boc-Z-protected thyminyll, adeninyll and cytosinyll POM monomers and the resulting POM oligomer exhibited a strong binding with sequence selectivity to both complementary parallel and antiparallel RNA and DNA strands [24].

During the last decade, the term of foldamer was introduced by Gellman *et. al* [25]. to describe oligomers, particularly of  $\beta$ -amino acids, with a strong tendency to adopt a specific secondary or tertiary structures. They reported that the conformationally rigid  $\beta$ -peptides can form stable helical structure in solid state. For example, short oligo(*trans*-2-aminocyclohexane carboxylic acid) and oligo(*trans*-2-aminocyclopentane carboxylic acid) (**Figure 1.7**) can form 14-helix and 12-helix *via* intramolecular H-bonding between backbone amide nitrogens and carbonyl groups. These features suggested that  $\beta$ -amino acid can be potentially useful to pre-organize PNA oligomer.

ศูนย์วิทยทรัพยากร

จุฬาลงกรณ์มหาวิทยาลัย

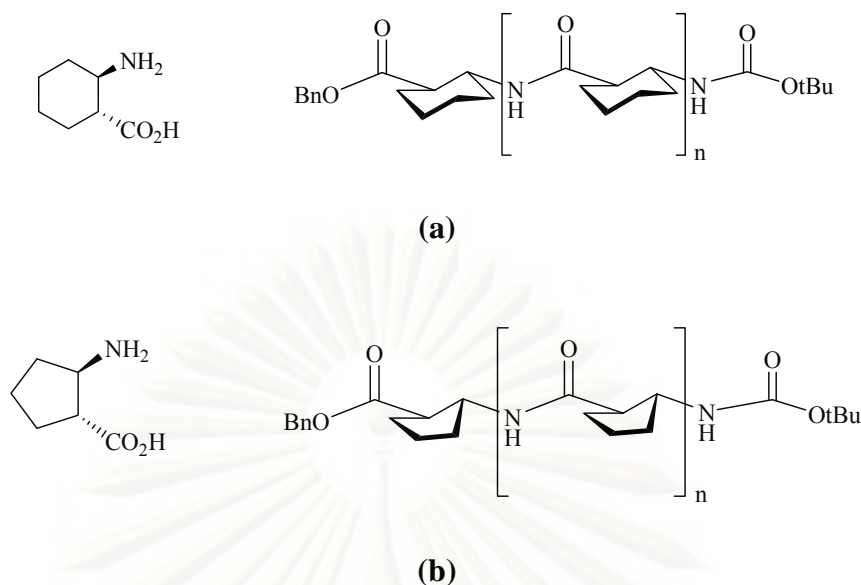


**Figure 1.7** Structure of *trans*-ACHC (a) and *trans*-ACPC (b)

Vilaivan *et al.* has recently investigated pyrrolidiny PNA carrying β-amino acid spacers. To study the effect of the structure and positive charge on the β-amino acid spacer, many new pyrrolidiny PNA carrying various acyclic and cyclic β-amino acid in the backbone have been designed and evaluated for their DNA binding properties (**Figure 1.8**) [26,27,28]. For instance, a new pyrrolidiny PNA having a flexible spacer such as β-alanine and *N*-amino-*N*-methylglycine spacers failed to show binding to DNA and RNA [26]. This reduced the binding affinity with DNA target can be explained by the higher entropy loss upon binding. To minimize such entropy loss, the pyrrolidiny PNA bearing cyclic β-amino acid spacers such as (*S,S*)-*trans*-2-amino cyclopentane carboxylic had been developed [29].

It was evident that the stereochemistry of the spacer is important for successful binding. For example, a pyrrolidiny PNA having 1-aminopyrrolidine-(2*R*)-carboxylic acid (D-Apc) (*dapc*PNA), but not the enantiomeric 1-aminopyrrolidine-(2*S*)-carboxylic acid (L-Apc), spacer showed a strong hybrid with its complementary DNA. Furthermore, the pyrrolidiny PNA shows preference for binding to DNA over RNA, [26, 28] a property that had never been reported in other PNA systems. From the stoichiometry study by UV and CD spectroscopy, it was observed that only 1:1 PNA·DNA hybrid was formed, following the Watson-crick base pairing rules [28]. In 2005, Vilaivan and co-worker designed another novel β-pyrrolidiny PNA having 2-aminocyclopentane carboxylic acid (ACPC) as spacer. It was observed that the PNA

consisting of D-proline and (1*S*, 2*S*) ACPC (*acpcPNA*) showed a strong binding affinity and high sequence specificity with its complementary DNA target and only form 1:1 hybrid similar to *dapcPNA*. The melting temperature ( $T_m$ ) value of a hybrid between the PNA homothymine decamer and its complementary DNA is extremely high ( $> 85$  °C). This indicates that the hybrid is far more stable than natural DNA·DNA and other PNA·DNA hybridss including the original PNA and D-Apc PNA with the same sequence [29, 30]. It was possible that the absence of favorable contribution from electrostatic interaction in *dapcPNA* is compensated by the more structurally rigid *ssACPC* backbone. Recently, mixed-base *acpcPNA* consisting all four nucleobases have been successfully synthesized and studies of its binding affinity and sequence specificity towards DNA and RNA investigated. It was found that the mixed-base *acpcPNA* hybridized strongly and selectively to its complementary DNA in an antiparallel formation following the Watson-Crick base pairing rules. Furthermore, it also showed preference for binding to DNA over RNA similar to *dapcPNA* [30]. As a result, both *dapcPNA* and *acpcPNA* appears to be apotential candidate for DNA-based diagnostic and therapeutic applications.

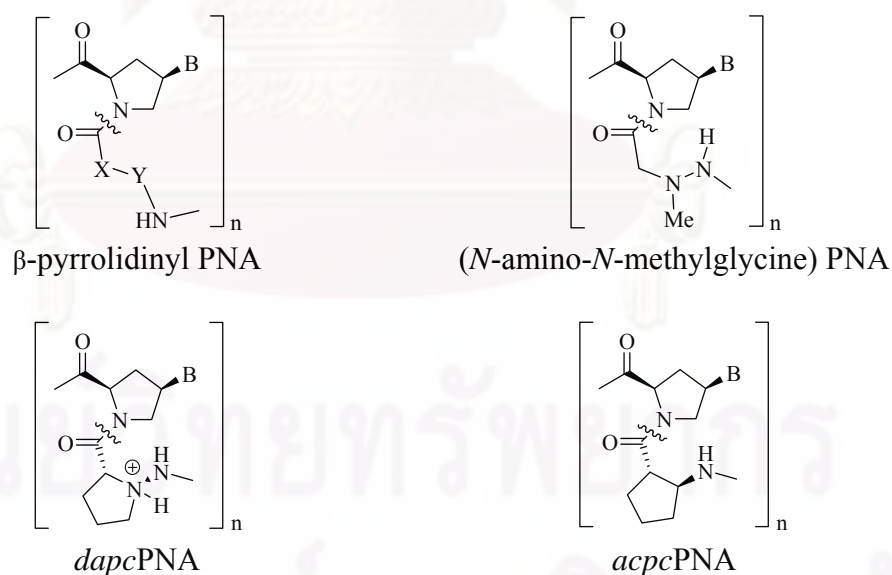


**Figure 1.8** Structures of modified PNA bearing various  $\beta$ -amino acid spacers

### 1.3 Applications of peptide nucleic acid (PNA)

Because of the special features of PNA mentioned above in combination with its excellent resistance to enzyme nuclease and protease, PNA is now widely applied in biotechnological and medical applications. For many purposes, it can be used in place of natural oligonucleotide or modified oligonucleotide [31]. Most of applications of PNA involve the use of the original Nielsen's *aeg*PNA system since it is the only one that is presently commercially available. In the present day, there are three or four major groups of application for this PNA including antisense-antigene therapy, molecular probe as biosensor, biomolecular device and architecture technology [4, 6].

#### 1.3.1 PNA as a potential antisense and antigene drugs

The stronger binding properties and biological stability of PNA implies that a small amount of PNA can be effective in interfering of transcription or translation processes. The sequence-specific inhibition of transcription and translation by PNA could potentially be exploited for therapeutic application [3]. The concept underlying antisense - antigene technology is relatively straightforward. For inhibition of translation (antisense strategy) oligonucleotides or their analogs are designed, complementary by virtue of Watson-Crick base pairing rule, to a specific mRNA can inhibit its expression and then induce a blockade in the transfer of genetic information from DNA to protein [32]. On the other hand, in the inhibition of transcription (antigene strategy), a nucleic acid analogue is designed to recognize and hybridize to the complementary sequences in a particular gene of interest, whereby they should interfere with the transcription of the particular gene (**Figure 1.9**) [3].

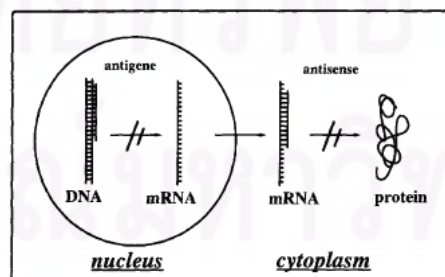


**Figure 1.9** Principle in antisense and antigene strategies

On the basis of mechanism of antisense action, two classes of antisense oligonucleotides can be distinguished. The first one is RNaseH-dependent antisense oligonucleotides, which induce the degradation of mRNA upon binding. The second one is steric-blocker oligonucleotides, which physically inhibit the progression of the translational mechanism. A majority of antisense drugs investigated in the clinical phase operates on RNaseH-dependent mechanism. RNaseH is a ubiquitous enzyme that hydrolyzes the RNA strand of an RNA·DNA duplex whereas PNA·RNA duplexes are not substrates for RNaseH. Therefore, PNA should inhibit protein expression by steric blockage mechanism. Many examples of antisense effect by PNA have been reported. For example, PNA can inhibit intron excision, lead to the lack of expression of a mature protein. An inhibition in the translation of PML/RAR $\alpha$ , promyelocytic leukemia/retinoic acid receptor- $\alpha$ , was achieved with a PNA pentadecamer [33]. Moreover, PNA can inhibit the SV40-T-antigen expression and the mechanism of inhibition was very probably steric blocking and not a RNaseH-mediated mRNA degradation whereas the expression of the  $\beta$ -gal was not affected under this condition [32]. Lewis and co-workers reported a novel antisense peptide-PNA conjugate that is designed for targeting *B-cell lymphoma/leukemia-2 (bcl-2)* expression. This peptide-PNA conjugate was able to bind to immobilized bcl-2 mRNA with high specificity comparable to antisense DNA [34]. In case of the antigene strategy or transcription inhibition by PNA can obtain either by triple-helix formation, or by a strand invasion or strand displacement mechanism. PNA targeted against the promoter region of a gene can form stable PNA·DNA hybrid that limit the DNA access of the polymerase, while PNA binding in a region far from the promoter can block the polymerases progression and lead to the production of shortened RNA transcripts [35]. In 2001, Murphy and co-worker introduced the phosphonium-PNA conjugate into mitochondria. The results showed that the phosphonium-PNA selectively inhibited the *in vitro* replication of DNA containing the mutant point that causes a human mtDNA disease but not the wild-type sequence [1]. Triplex invasion by PNA shows a good potential in antigene therapy. There have been many experimental data that shows good antigene effects of PNA both *in vitro* and *in vivo* [31]. In one example, Nielsen *et al.* have reported that a PNA octamer can efficiently block transcriptional elongation by (PNA)<sub>2</sub>·DNA triplex formation that influence to blocking phage T3 polymerase activity [35]. Moreover, in 2006 Zhilina *et al.*

developed a novel antigene PNA by using the mono- and bis-pyrimidine-rich PNAs that were conjugated to nitrogen mustard at either the amino or carboxy terminus in order to improve the efficiency of binding between PNAs and HER-2/neu promoter that is known to be associated with human cancer. The result demonstrated that the PNA-nitrogen mustard conjugates suppressed HER-2/neu expression by up to 80% [36]. However, one of the major drawbacks to applying PNA as an antigene drugs is that the formation of strand displacement or strand invasion is rather slow at physiological salt concentrations [6]. Another problem is the poor cell and nuclear membrane-permeability of unmodified PNA. In general, conjugation with a peptide carrier is necessary [37].

### 1.3.2 PNA as a molecular-biological device

In addition, to the application for PNAs in the antisense-antigene technology already explained, they can also be employed as tools in molecular biology and functional genomics research. For instance, the high stability and sequence specificity of PNA-DNA hybridization have been exploited in the analysis of single base pair mutations in DNA during amplification by polymerase chain reaction in a so-called PNA directed PCR clamping [3, 4, 35].

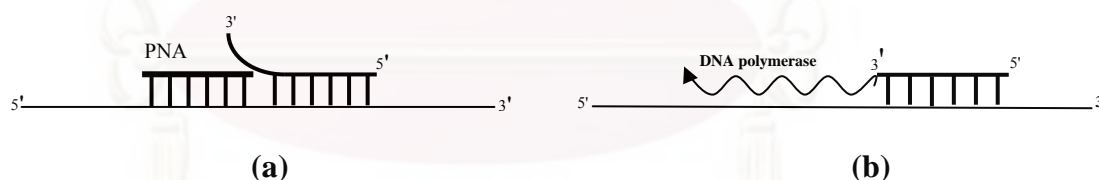


**Figure 1.10** Diagram of the “PCR clamping” technique.

- Blockage of the PCR reaction by PNA probe to the wild-type gene
- Positive PCR caused by weaker PNA binding to the mutated gene.

The PCR clamping method for the detection of point mutations relied on the ability of PNAs to bind more strongly to complementary nucleic acids target than oligonucleotides, conjunction with their inability to function as primers in the polymerase chain reaction (PCR). Targeting of the PNA oligomer, even partially, against the primer binding site can block the formation of the PCR product. The

procedure is powerful and has been used successfully to detect and screen for single-base pair genetic variation [38]. Using this approach, Thiede *et al* [39] able to discrimination of point mutations in the K-ras gene detect a codon 12 K-ras mutation. A concentration of 2.84  $\mu\text{M}$  PNA complementary to wild-type K-ras DNA was found sufficient to inhibit amplification of the wild-type gene, relative to the mutated gene, to which it binds with lower affinity

In addition, PNA oligomer was also extensively employed combination with the PCR technique for various molecular genetic applications including the amplification of variable number of tandem repeat (VNTR) loci for the purpose of genetic typing. In the process, small PNA oligomers are used to block the template, and the latter becomes unavailable for intra- and inter-strand interaction during reassociation. On the other hand, the primer extension is not blocked; during this extension, the polymerase displaces the PNA molecules from the template and the primer is extended toward completion of reaction. This technique is so powerful that it is possible to obtain a specific signal from a single mutation oncogene in the presence of a 1,000–10,000 fold excess of the non-mutated wild type normal gene [40–41]. Moreover, this approach indicates the potential of PNA application for PCR amplification where fragments of different sizes are more accurately and evenly amplified [3].

A new automated real-time PCR has recently been developed employing PNAs - the so called Q-PNA PCR. This technique relies on the hybridization between a generic quencher labeled PNA (Q-PNA) and fluorescent labeled DNA primer in order to quench the fluorescence of the primer. During PCR amplification, the Q-PNA is displaced by integration of the primer into amplicons, thus enhancing the fluorescence of the labeling group [35,42]. Furthermore, PNA in conjunction with the enzyme nuclease S1 has been used as artificial restriction enzyme [4]. In an example, after a PNA binds to DNA duplex with a strand displacement, the displaced DNA strand can be selectively cleaved by nuclease S1. Hence the combination of PNA and nuclease S1 can be employed as artificial restriction enzymes that cleave DNA strands at the position determined by the PNA sequence employed [3, 31].



### 1.3.3 PNA as probe for diagnosis and nucleic acid biosensor

The development of PNA-based biosensors has increased tremendously over the past few years as demonstrated by the large number of scientific publication [43]. PNAs offer some advantages over DNA such as higher specificity, sensitivity and accuracy in the detection of target sequence. PNAs have been incorporated into expanding variety of applications in many fields ranging from DNA diagnostics, gene analysis, forensic and detection of biological agents. In addition, detection of genetic mutations at the molecular level opens up the possibility of performing reliable diagnostics even before any symptom of a disease appears [43–44]. A large number of example of using PNA as a probe to detect DNA base sequence has been demonstrated, most of which rely on the use of Nielsen's PNA in conjunction with different characterizing techniques. For instance, Zare *et al.* presented a colorimetric method in conjunction with PNA to screen for genetic mutation by employing a cyanine dye. This method based on the color change of dye from blue to purple upon binding to PNA-DNA duplexes. The color changing that is used to visualize formation/dissociation of the hybrid duplex [45]. In 2003, Komiyama and co-workers has reported a combination of PNA and S1 nuclease can differentiate single-base alteration in DNA target with a remarkable specificity. The mixture after the enzymatic digestion was stained by cationic dye namely 3, 3'-diethylthiadicardocyanine which showed different color upon binding to single stranded PNA and its hybrid with DNA. When a mismatch is present in the DNA strand, the resulting mismatched PNA·DNA duplexes are hydrolyzed by S1 while the perfectly-matching hybrids remain intact. After the digestion, a cationic dye was added. When the DNA sample is complementary with PNA probe, a purple color is generated, whereas in the presence of single base mismatch DNA, the color of solution remains blue as shown in **Figure 1.11** [44, 46].

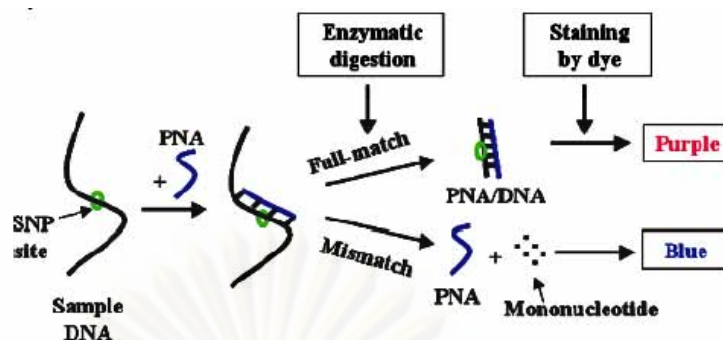


**Figure 1.11** Strategy for SNP detection by the PNA/Nuclease/Dye system [46].

Another example of colorimetric detection for DNA sequence analysis was reported by Appella and Zhang in 2007 [47]. They applied a colorimetric sandwich-hybridization strategy to detect anthrax DNA samples. A cyclopentane-modified PNA was used in the form of surface-bound probe. In this method, one PNA probe is employed as a capture probe ( $\text{PNA}\alpha$ ) to immobilize the DNA target to the surface and another probe, that is labeled with biotin ( $\text{PNA}\beta$ ), is used as a detection probe (**Figure 1.12a**). The hybridization results in immobilization of the biotin labelled  $\text{PNA}\beta$ , which could be detected by treatment with avidin-horseradish peroxidase conjugate (HRP-avidin) and tetramethylbenzidine (TMB). The perfectly matched DNA gives a color change visible to the naked eye as indicated in **Figure 1.12b**.

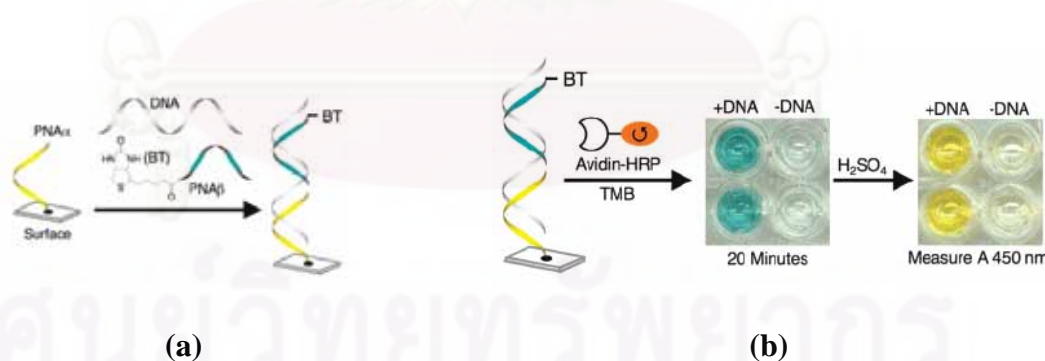


**Figure 1.12** (a) PNA-based sandwich-hybridization assay.  $\text{PNA}\alpha$  is the capture probe, and  $\text{PNA}\beta$  is the detection probe [47].  
 (b) Signal amplification from PNA-based sandwich-hybridization. The blue color results from initial oxidation of 1-Step Turbo TMB, and the yellow color is produced once the enzymatic reaction is stopped [47].

In the present day, DNA sequence determination using a combination of PNA and fluorescence techniques had been widely used. In most of these works, a fluorescent labeling group is attached on to the PNA probe to detection of DNA sequence. For example, Svanvik and co-workers reported a light-up PNA probe for nucleic acid detection by attachment of an asymmetric cyanine dye thiazole orange onto the PNA probe for DNA sequence analysis [48]. This method relies on the fluorescence enhancement of TO upon binding to complementary DNA. When the PNA hybridizes to DNA target, a strong fluorescent is generated whereas the unhybridized probe showed a low fluorescent signal as illustrated in **Figure 1.13**.

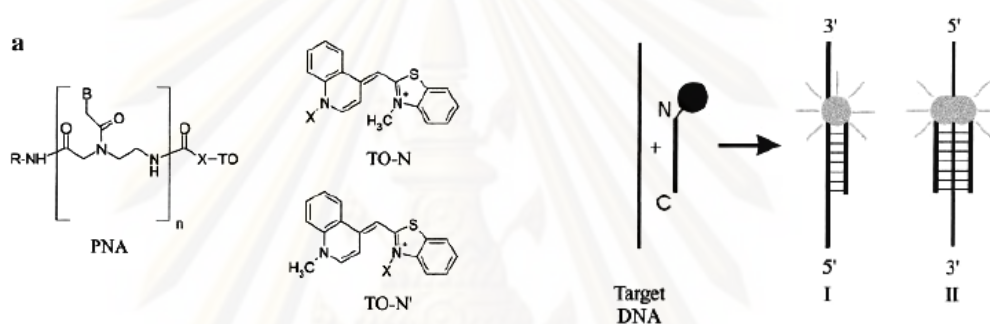


**Figure 1.13** Strategy for nucleic acid detection *via* light-up probe [48].

Moreover, Sosher *et al.* recently described a new fluorescent-based PNA·DNA hybridization assay using a forced intercalation (FIT) PNA probe in which one base is replaced by a thiazole orange (TO) molecule [49]. If the FIT-PNA probe is complementary to the DNA sample, the TO dye will exhibit a strong fluorescent signal due to the stacking in the duplexes enforces a coplanar arrangement even in the excited state. In the presence of the one-mismatch DNA target, the fluorescent signal of TO dye is dramatically decrease because of the TO dye has undergo torsional motions that lead to rapid depletion of the excited state as shown in **Figure 1.14**.

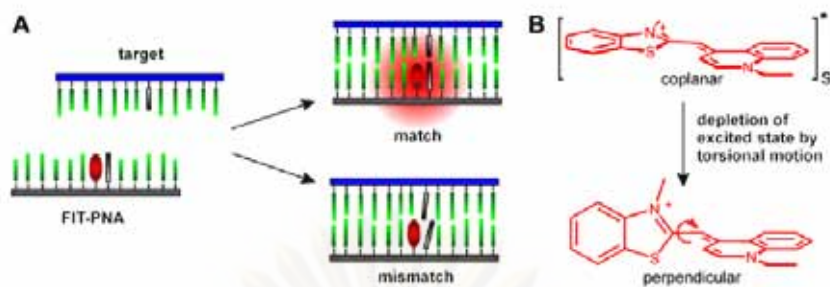


**Figure 1.14** (A) In FIT probes, an intercalator dye such as TO serves as the base surrogate that responds to perturbations of the duplex structure. (B) The fluorescence of noncomplexed TO is low owing to the rapid depletion of the excited state by torsional motions [49].

In addition, biosensor based on fluorescence resonance energy transfer (FRET) utilizing dye-labeled PNA probe has been widely employed for hybridization assay. In 2002, Gaylord and co-workers [50] reported the method for detecting PNA·DNA interactions based on FRET using a cationic conjugated polymer (CCP), (poly[(9,9-bis(6-*N,N,N*-trimethylammoniumhexylbromide)fluorene)-co-phenylene]) donor and a PNA labeled with a chromophore dye ( $C^*$ ) acceptor. The light-harvesting properties of cationic polymer are used to sensitize the emission of chromophore on the PNA probe. This method relies on the electrostatic interaction between positively charged polymer and negatively charged PNA·DNA hybrid. This interaction brings the cationic polymer and hybrid complex within distances required for FRET. If the PNA- $C^*$  hybridizes to the complementary DNA target, the donor (CCP) and acceptor ( $C^*$ ) will be sufficiently close that excitation of the results in FRET and emission from  $C^*$  is observed. On the other hand, if the target is not complementary to the PNA- $C^*$  probe, the polymer to  $C^*$  distance is large and no FRET take place, therefore no  $C^*$  emission can be observed. This method can be detected the DNA target at concentrations down to 10 pM using a standard spectrofluorometer. The overall scheme is shown in **Figure 1.15**.

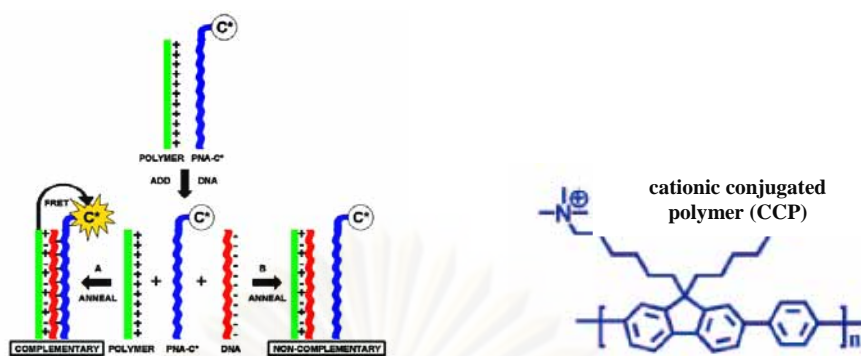


**Figure 1.15** Schematic representation for the use of a cationic polymer (CCP) with specific PNA-C\* optical reporter probe to detect a complementary [50].

In 2005, Liu *et al.* [51] constructed a specific DNA biosensor by using a cationic conjugated polymer and a surface-bound PNA. The transduction mechanism operates by taking advantage of the net increase in negative charge at the PNA upon hybridization with DNA. The resulting PNA-DNA complexes cause the cationic polymer to bind selectively to the surface with electrostatic interaction. The scheme of this method is illustrated in **Figure 1.16**.

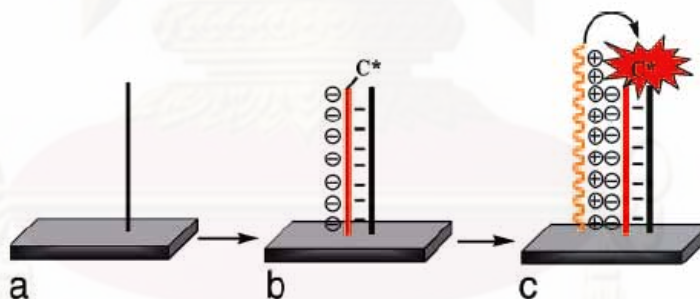


**Figure 1.16** Amplification of a PNA (black)-ssDNA-C\* (red) solid-state sensor by polyelectrolytic deposition of the CCP (orange) [51].

Furthermore, Baker and co-workers [52] developed biosensor for the detection of sequence-specific dsDNA. The method based on fluorescence resonance energy transfer (FRET) process by using a water-soluble cationic conjugated polymer (CCP) as the donor and a dye-labeled PNA as the acceptor (**Figure 1.17**). In this assays, the emission of the donor or acceptor would signify the absence or presence of the target, respectively. If the dsDNA target hybridizes to a complementary PNA-C\* probe

making the donor (CCP) and acceptor (PNA-C\*) are close enough that excitation of the CCP results in FRET and emission from C\*. On the other hand, if the dsDNA target is not complementary to the PNA probe, the polymer to C\* distance is large, and no C\* emission is observed. The types of complexes between a PNA strand and dsDNA structures were determined by using gel electrophoresis, and ion mobility mass spectrometry.

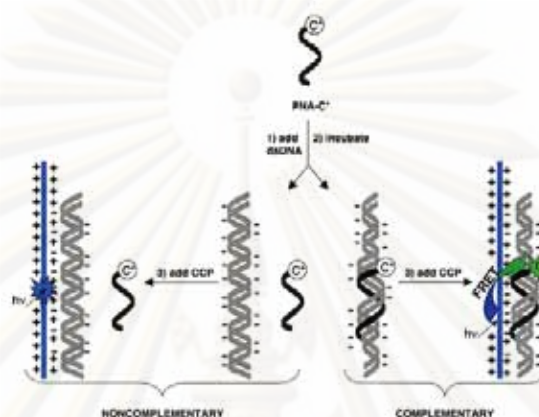


**Figure 1.17** dsDNA detection using a cationic conjugated polymer (CCP) and a specific PNA-C\* optical reporter probe

PNA can also be used as, or in combination with, molecular beacons (MBs). Traditional MBs are doubly end-labeled PNA probe carrying a fluorophore and a quencher [53–54]. In the absence of the DNA target or when not hybridized with the target, the beacon form a closed structure that brings these labels in juxtaposition, resulting in quenching of the fluorescence from a dye bound to one end of the PNA probe by the second dye bound to another end. In the presence of a complementary DNA target, duplex structure forms, this spatially separated the two dyes, and thus the beacon become fluorescent [55]. A variety of applications to DNA sequence detection have been proposed using molecular beacon in combination with PNA probe. For instance, Kuhn *et. al.* in 2002 [54] reported the use of PNA openers in combination with MBs for the detection of a selected target sequence directly in dsDNA. The use of stemless PNA beacon improves specificity of the detection against the single mismatch target. The scheme of this procedure is shown in **Figure 1.18**.

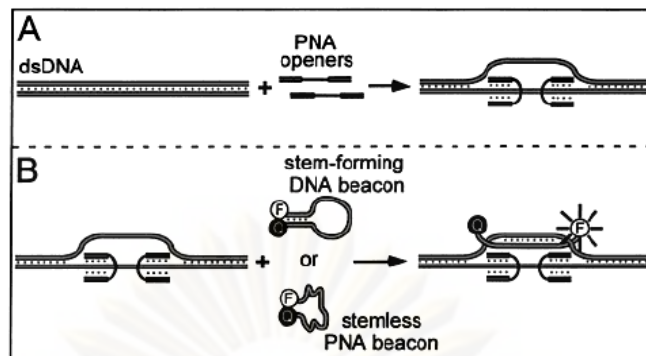


**Figure 1.18** Schematics of the procedure for hybridization of molecular beacons to dsDNA [54].

Recently, Komiyama and co-workers has proposed [55] the use of a PNA based molecular beacon in combination with nuclease S1 to do SNP genotyping in genomic DNA. The PNA molecular beacon contains fluorescein at the *C*-terminal and dabcyI group at the *N*-terminal. Nuclease S1 stringently recognizes and digests the DNA component in the mismatched PNA·DNA duplexes. The strategy of this genotyping method is illustrated in **Figure 1.19**.

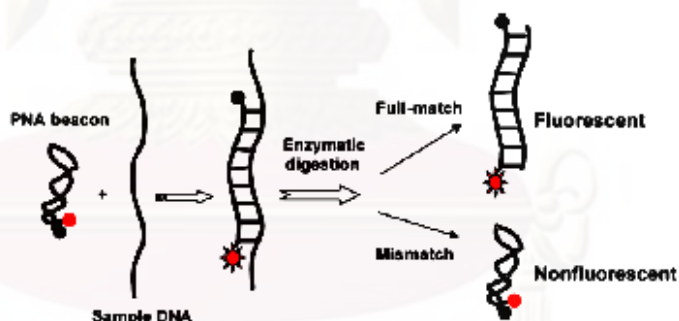


**Figure 1.19** Strategy for SNP detection using the combination of PNA beacon and nuclease S1 [55].

In 2005, Appella and coworkers reported a quencher-free molecular beacon strategy employing a PNA that was modified with a 9-fluorene group that use as the fluorophore at the *N*-terminus as a probe for DNA sequence detection [56]. The fluorescent intensity of the fluorophore-PNA probe will increases upon binding to perfectly complementary because of the separation of the fluorophore and the nucleobase which acted as quencher. Moreover, in 2008, Totsingan *et. al.* [57]

employed PNA beacon and ion-exchange HPLC for the label-free detection of DNA sequence. This technique can be used to directly visualize the PNA-DNA hybridization since the duplex showed retention time different from those of PNA and single stranded or double stranded DNA.

Apart from uses of PNA in conjunction with molecular beacon, PNA was also used in with semiconductor to form PNA sensor chips [58–60]. For example, Gao and co workers [59] constructed silicon nanowires (SiNW) that was fabricated using complementary metal-oxide semiconductor (CMOS) compatible technology and their surface was functionalized with PNA probes. The PNA–DNA hybridization was detected by electrical measurement that related to resistance change of the silicon chip before and after hybridization. The resistance of the silicon chip is enhanced upon addition of negative charges. The principle is illustrated in **Figure 1.20a**. In the following year, Zhang and co-workers [60] have established a novel oxide-etched silicon nanowire biosensor with the aim to improve the sensitivity of the silicon chip. This SiNWs was functionalized with a densely packed organic monolayer, which was subsequently immobilized with PNA as indicated in **Figure 1.20b**.

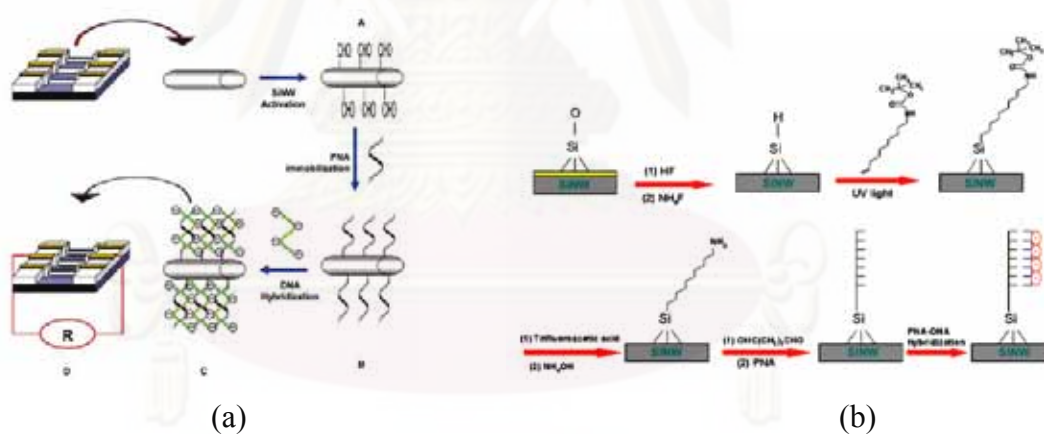


**Figure 1.20** (a). Schematic of the principle of the SiNW array biosensor for DNA [59].

(b). Schematic of PNA immobilization and PNA-DNA hybridization on oxide-etched SiNW surface [60].

In addition, a novel method for solid-phase SNP genotyping that combining allele-specific hybridization, PNA probe and microsphere-based flow cytometric detection was introduced by Rockenbauer and co-workers [61]. In this method, the PNA–DNA interaction was analyzed by flow cytometry.



Most of the PNA-based assays for DNA sequence analysis described above relies on color, fluorescence or resistance change. No separation of hybridized and unhybridized probe is required. However, this advantage can also be a drawback since non-specific background signals may be generated from the unhybridized probe. In 2004, Kerman and co-workers [62] reported the use of biotinylated PNA probes with streptavidine coated magnetic beads in conjunction with a redox-active intercalator Meldola's blue (MDB). The PNA·DNA hybrid was separated from the unbound PNA by labeling of the DNA samples with biotin. The PNA-DNA hybridization was followed by the voltammetric signal of MDB. The strategy is indicated in **Figure 1.21**.

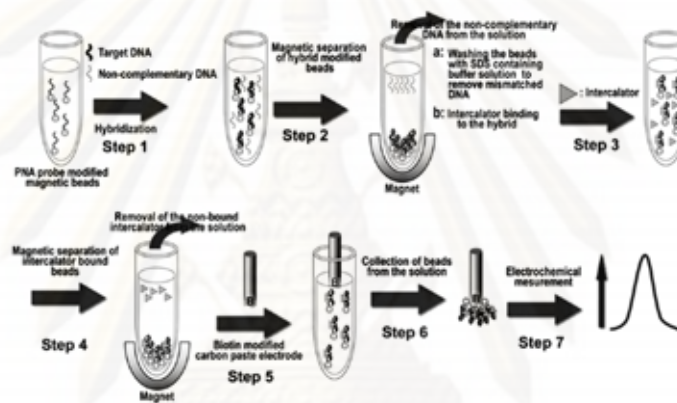


**Figure 1.21** PNA modified magnetic bead-based assay for the specific detection of hybridization in connection with an intercalator, Meldola's blue (MDB) [62].

From the variety of methods for DNA sequence analysis by using PNA as probe as explained above, it was apparent that some techniques showed some drawbacks such as in case of enzymatic digestion method for detecting nucleic acid, it is difficult to control the condition of the reaction, especially for large-scale testing [63]. In addition, some method required labeled PNA probes or DNA samples that are quite complicated and expensive, yet providing only indirect information of DNA sequence [64]. Furthermore some methods require complicated analysis techniques and prepare preparations. A number of attempts for further improvements are being made in many laboratories [65–67]. The major requirements for the DNA sequence detection strategy are simple setup, inexpensive, using small quantity sample or probe,

high sensitivity and flexibility of the procedure. Furthermore, the method should be straightforwardly automated and scalable as well [61, 68]. In this regard, MALDI-TOF mass spectrometry appeared to be a potential technique for the detection of nucleic acid sequences. It is a very powerful mean of analysis for a variety of compounds, protein, nucleic acid and peptide compound, and possesses the capacity to rapidly, high accurately and can distinguish individual component of complex mixture on the basis of the intrinsic physical property of mass-to-charge ( $m/z$ ) ratio. In contrast to other DNA sequence analysis technique, MALDI-TOF mass spectrometry based on the direct mass determination of compounds rather than on an indirect analysis [69–70]. Moreover, it also allows the detection of nucleic acids in seconds without requirement for labels. The formation of predominantly singly charged molecular ion makes the analysis of complex mixtures by MALDI-TOF mass spectrometry even more attractive for complex biological molecules. From these advantages, MALDI-TOF MS shows a great potential for high-throughput nucleic acid detection applications [71–72].

PNAs are very compatible with MALDI-TOF mass spectrometric analysis. Unlike DNA molecule, it has a neutral backbone, and thus less prone to fragmentation during the MALDI process. In addition, it do not tend to form cation adducts, which can result in reduced sensitivity and signal resolution in DNA analysis [69, 71, 73]. Furthermore, PNA possesses strong binding affinity and a high sequence specificity to binding with DNA under low ionic strength conditions [71]. These unique characteristics make PNA an attractive probe candidate to be used in combination with MALDL-TOF mass spectrometric technique for detection of DNA sequence. There are a few reports on the use of Nielsen's PNA in combination with MALDI-TOF MS to analyze DNA sequence [74–75]. The DNA sample was first tagged with biotin and captured onto streptavidin magnetic beads. The captured DNA sample was then hybridized with a PNA probe. After stringent washing of the PNA·DNA–bead conjugate to remove the unhybridized PNA probe, the beads were directly analyzed by MALDI-TOF MS. The presence of  $m/z$  of PNA indicates that the sequences of the DNA and the PNA are complementary. It should be noted that only molecular mass of PNA was observed because it is a peptide molecule which easily ionizes as compared to DNA. The schematic outline of PNA based MALDI-TOF mass spectrometry experiment is shown in **Figure 1.22**.

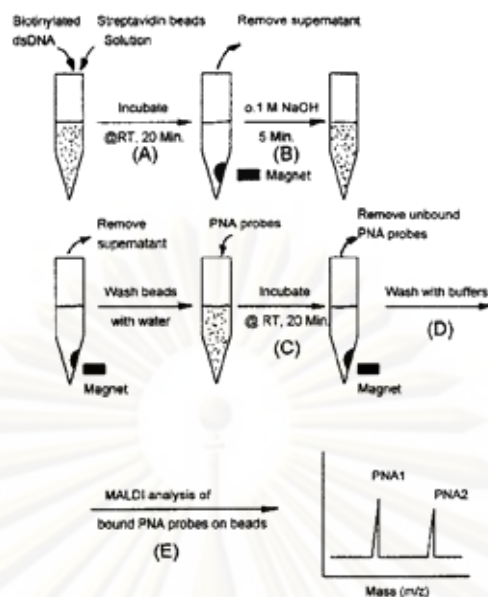


**Figure 1.22** Affinity capture assay for DNA. The detected molecular weight of the PNA probe indicates the DNA sample [75].

In 2004, Ren and co-worker [76] reported a related method which straightforwardly genotypes SNPs in double-stranded DNA (dsDNA) using PNA as a probe and MALDI-TOF mass spectrometric detection. In this method, the dsDNA sample was first treated with exonuclease III and then with nuclease S1 in the presence of PNA. This PNA probe protects designated segments of the DNA from enzymatic digestion. In these one-pot-reactions, the single-stranded DNA fragments including the SNP sites were obtained and then analyzed by MALDI-TOF MS and only molecular mass of PNA was observed. The principle of this method is presented in **Figure 1.23**.

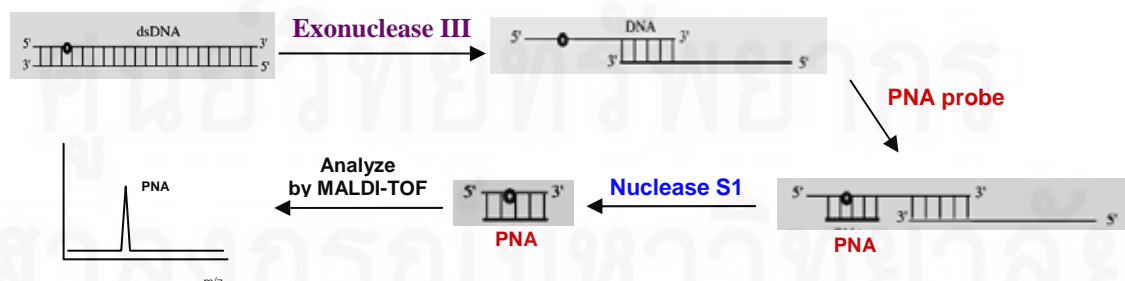


**Figure 1.23** Schematic representation of the processes for SNP detection by exonuclease III/nuclease S1/PNA systems [76].

In addition, Griffin and co-workers [77] reported the method of detection of multiple, single base polymorphisms in polymerase chain reaction (PCR) amplified human DNA by coupling solid phase affinity chemistry and PNA as allele-specific hybridization probes with MALDI-TOF MS. This method was applied to analyze 182bp exon 4 polymorphism of human tyrosinase gene. In this assay, the double-stranded biotinylated DNA target was first immobilized on the streptavidin-coated magnetic beads and then the non-biotinylated strand was removed. Subsequently, biotinylated DNA-bound magnetic beads were hybridized with PNA probe. After washing of the PNA·DNA–bead conjugate to remove the one-base mismatched PNA probe, the beads were directly analyzed by MALDI-TOF MS. The resulting mass showed peaks of distinct masses corresponding to the PNA probe that complementary with the DNA sample, resulting in a mass spectral “fingerprint” for each DNA sample.

Furthermore, Schatz and co-workers [78] reported the method for complex analysis of DNA methylation by employing peptide nucleic acid (PNA) library probe hybridization in combination with MALDI-TOF MS in 2006. In such process, biotinylated PCR-amplificates were prepared and immobilized in streptavidin coated plates and a PNA-library hybridization containing 100 nM of each PNA was subsequently performed. After removing unspecifically bound probes, PNAs were then analyzed with MALDI and the methylation level was estimated by dividing the signal intensity of a probe specific to the methylated allele by the sum of signal intensities of both probes. This method is rapid and allows simultaneous detection of DNA methylation markers in a single reaction only small amounts of DNA samples and enables the parallel analysis of several methylation positions.

Another example of MALDI-TOF detection for DNA sequence analysis was reported by Seitz and Mattes [79]. They developed method for the multiplex detection of DNA single nucleotide polymorphisms by using PNA probe based on ligation reaction, a technique for constructing an amide-bond from two or more unprotected peptides. The ligation displayed remarkable sequence selectivity: the single-mismatch template was ineffective in accelerating the formation of PNA- dipeptide hybrid. A highly sequence-selective ligation was monitored by MALDI-TOF MS. This method was applied to using a multiplexed ligation assay about detection of three potential mutations in the pig-ras gene segment in a single experiment.

Moreover, Bauer and co-workers [80] have developed a method for DNA sequence analysis by using multiplexed hybridizations of positive charged tag PNA probe and analyzed by MALDI-TOF MS. The introduction of quaternary ammonium as charge-tags on PNA probe was shown a high resolution and sensitivity including considerably increase the detectability of small DNA oligonucleotides by MALDI-TOF MS. In this method, the different charge-tagged PNA probes (667 nM each) were simultaneously hybridized in solution of PCR-amplified cDNA and genomic DNA clones. Following purification with magnetic bead system and only those PNA probes that hybridize to the target DNA were directly analyzed by MALDI-TOF MS. Thereby, DNA-specific hybridization profiles are generated that are characteristic for each clone as shown in the **Figure 1.24**.

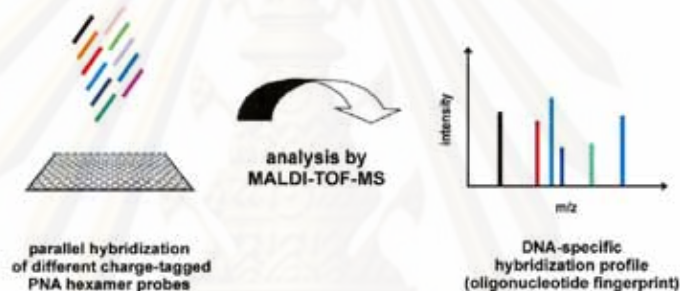


**Figure 1.24** Concept of multiplexed oligonucleotide by positively charge-tagged PNA detected by MALDI-TOF MS. [80]

Apart from employing PNA as probe in DNA sequence analysis, there are a few technique employing DNA probe in conjunction with MALDI-TOF MS for detection of DNA sequence. For example, Stoerker *et. al.* [81] reported the method by using MALDI-TOF-monitored nuclease selections for genotyping by employing library DNA probes containing DNA probes that known genotypes (complementary probe) and DNA probe that are not complementary with the DNA target. In this process (**Figure 1.25**), the library probes were annealed to the DNA target, followed by treatment with the single strand specific nuclease. The reaction solution was monitored by MALDI-TOF MS, the target-bound, complementary probe was resistant to nuclease digestion making its peak remains in mass spectra. Whereas, the non-

complementary probe was digested by nuclease making peaks of the digested probes disappear from the mass region of interest.

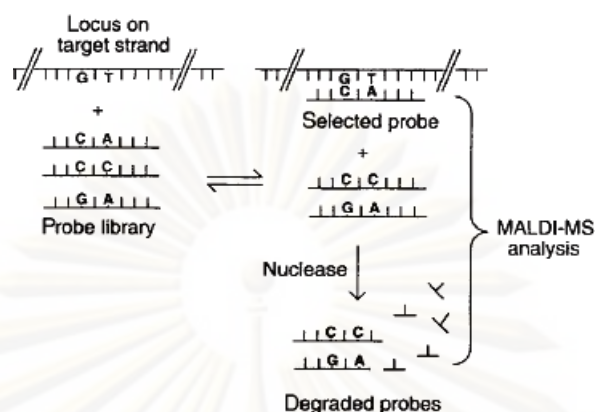


**Figure 1.25** Schematic representation of the processes genotyping by MALDI-TOF-monitored nuclease selections [81].

Additionally, Mengel-Jørgensen *et al.*, [82] presented the protocol for typing of multiple SNPs in a single reaction in order to detection of single base extension primers (SBE) by MALDI-TOF. In the procedure, the SBE reactions were prepared with biotin-labeled ddNTPs and then solid-phase capture on monomeric avidin beads. The biotin-labeled DNA was eluted by placing triethylamine directly on the beads and the resulting biotin-labeled DNA product was directly analyzed by the MALDI-TOF process. The biotin-ddNTPs containing linkers with different masses were used in order to ensure a clear separation of the alleles even for SBE primers. This method was applied to an analysis of a multiplex SBE reaction targeting 17 Y-chromosome SNPs.

Form above researches, there are many methods have been published for the detection of DNA sequence. However, the most frequently used assays are limited such as some method required biotin label on the DNA samples, which added the cost of the labeling groups and sample preparation. In addition, some method is not capable of multiplex analysis because it was limited by the variable thermal stabilities of PNA·DNA duplexes having different base sequence. Therefore, the procedure conditions must be optimized for each hybridization probe separately, which might not be appropriated for high throughput application [69].

## 1.4 The objective of this Research

The aim of this work is to develop a new PNA-MALDI-TOF based technique for DNA sequence analysis that should be very simple, rapid, cost-effective and not require labeling of the PNA probe or the DNA samples. The idea is to immobilize the DNA samples (or its hybrid with PNA) on a solid anion exchange support instead of biotin-streptavidin interaction. The immobilized DNA can then hybridized with PNA, resulting in absorption of the PNA probe onto the solid support, which cannot take place in the absence of the DNA since PNA is electrostatically neutral. The support-bound PNA·DNA hybrid is then removed from the unhybridized PNA by thorough washing and subsequently analyzed for the presence of the PNA probe by MALDI-TOF mass spectrometry. The presence of the  $m/z$  signal of the PNA suggests that the DNA and PNA sequences are complementary (**Figure 1.26**).

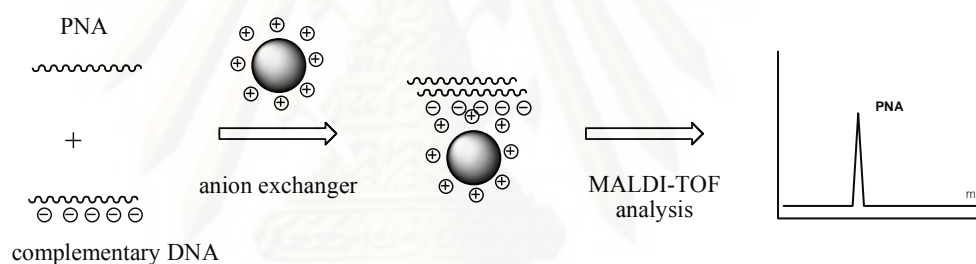


**Figure 1.26** Schematics representation for DNA sequence analysis using PNA as probe and ion exchange method and MALDI-TOF mass spectrometry.

The PNA used in this research is a new conformationally rigid beta pyrrolidinylyl *acpc*PNA which was recently reported by Vilaivan and co-workers. This PNA showed a very strong binding affinity and high sequence specificity towards complementary DNA target. Several anion exchange materials including functionalized silica, sepharose, chitosan and its derivatives are evaluated for the ability to immobilize the PNA·DNA hybrid and detection of DNA sequence. In addition, application of the new technique to detect DNA sequences in real DNA samples, with the aim to identify single base mutation such as SNP analysis will be explored.

## CHAPTER II

### EXPERIMENTAL SECTION

#### 2.1 General Procedure

##### 2.1.1 Equipments

Unless otherwise stated, all reaction glasswares were oven dried. The progress of reaction was followed by thin layer chromatography (TLC) using Merck D.C. silica gel 60 F<sub>254</sub> 0.2 mm-pre-coated aluminium plates. Visualization of TLC plates was accomplished using either UV light (254 nm), iodine, or ninhydrin. Evaporation of solvent was performed on Büchi Rotavapor R-200 with a water aspirator model B-490 or a Refco Vacubrand pumps. The weight of all chemical substances was determined on Metler Toledo electrical balance. Column chromatography was performed on silica gel having 70-230 mesh for column chromatography.

Proton (<sup>1</sup>H) and carbon (<sup>13</sup>C) NMR spectra were recorded on a Varian Mercury-400 plus NMR spectrometer operating at 400 MHz for <sup>1</sup>H NMR and 100 MHz for <sup>13</sup>C NMR in appropriate deuterated solvents. Chemical shifts ( $\delta$ ) are reported in part per million (ppm) relative to tetramethylsilane (TMS) or using the residual protonated solvent signal as a reference. Optical rotations were measured using sodium light (D line, 589.3 nm) at ambient temperature on a Jasco P-1010 Polarimeter. Elemental analysis results were analyzed on CHNS/O Analyzer (Perkin Elmer PE2400 Series II) at Scientific and Technological Research Equipment Center, Chulalongkorn University.

The PNA were purified using Reverse phase HPLC on a Water 600<sup>TM</sup> controller system equipped with gradient pump and Water 996<sup>TM</sup> photodiode array detector. A Varian<sup>TM</sup> C<sub>18</sub> HPLC column 3  $\mu$ m particle size 4.6  $\times$  50 mm was used for the purification of PNA oligomers. Peak monitoring and data processing were performed on the base Empower software. The fractions were collected manually and assisted by real-time HPLC chromatogram monitoring. The combined pure PNA fractions were concentrated *in vacuo* and Freeze Drying (Freezone 77520, Benchtop Labconco). MALDI-TOF mass spectra were measured in positive ion mode with a



static accelerating voltage of +20 kV on a Bruker Daltonics Microflex MALDI-TOF mass spectrometer.

### 2.1.2 Materials

All commercially available chemical were purchased from Fluka, Merck, Lab Scan or Aldrich Chemical Co., Ltd., and used without purification. Commercial grade solvents for column chromatography were distilled prior to use. Solvents for reactions were AR grade used without purification. Tetrahydrofuran and 1,4-dioxane were distilled from fresh thin-cut sodium metal and benzophenone under N<sub>2</sub>. HPLC grade acetonitrile and methanol for HPLC experiments, obtained from Fluka and Lab Scan, were filtered through Nylon membrane (13 mm diameter, 0.45 μm pore size) before use. Each sample was filtered through a millex-HV syringe filter unit prior to injection on to the chromatograph. MilliQ water was obtained from ultrapure water system with Millipak<sup>®</sup> 40 filter unit 0.22 μm, Millipore (USA). High purify nitrogen, hydrogen and helium (99.5% purity) were obtained from Thai Industrial Gas (TIG).

For solid phase peptide synthesis, anhydrous *N,N*-dimethylformamide (H<sub>2</sub>O ≤ 0.01%, dried over activated 3Å molecular sieves) using as solvent was purchased from Merck and Lab Scan. TentaGel S RAM Fmoc resin used as solid support was purchased from Fluka. The protected amino acids and chemical substances were obtained from commercial source and used without purification namely Fmoc-L-Lys(Boc)-OPfp) and Fmoc-Arg(Mtr)-OH were obtained from Novabiochem. Fmoc-Ser(tBu)-ODhbt, carboxybutyltriphenyl phosphonium and *N*-hydroxysuccinimide, trifluoroacetic acid (98%) were purchased from Fluka. All oligonucleotides were purchased from Bioservice Unit, National Science and Technology Development Agency (Thailand).

The ion exchange materials, quaternary ammonium modified silica (trimethylaminopropyl) (SAX), ethylenediamine-*N*-propyl (PSA) were obtained from Varian, Inc. diethylaminoethyl cellulose (DEAE cellulose) was purchased from Fluka. Diethylaminoethyl sepharose (DEAE sepharose) and quaternary ammonium sepharose (Q sepharose) were purchased from GE Healthcare.

*N*<sup>3</sup>-benzoylthymine, *N*<sup>6</sup>-benzoyladenine, *N*<sup>4</sup>-benzoylcytosine were synthesized by Miss Cheeraporn Ananthanawat and Dr. Chaturong Suparpprom. Human and meat

DNA samples were kindly supplied by Dr. Nattiya Hirankarn and Mr. Jeerawat Nakkuntod from Department of Microbiology, Faculty of Medicine, and by Dr. Piyasak Chaumpluk, Department of Botany, Faculty of Science, Chulalongkorn University.

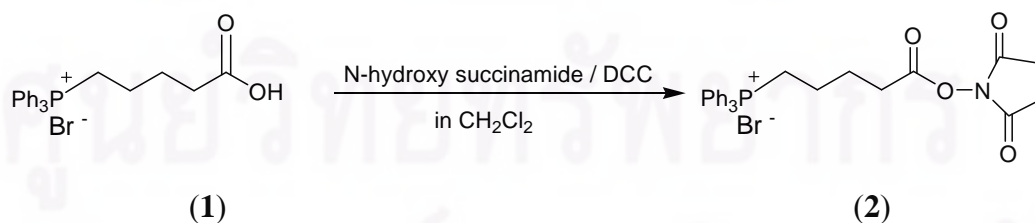
## 2.2 Synthesis of PNA monomers

PNA monomers consist of two parts. The first one is activated pyrrolidinyl PNA monomers namely (*N*-Fluoren-9-ylmethoxycarbonyl)-*cis*-4-(thymine-1-yl)-D-proline pentafluorophenyl ester (**11**), (*N*-Fluoren-9-ylmethoxycarbonylamino)-*cis*-4-(*N*<sup>2</sup>-isobutyrylguanin-9-yl)-D-proline pentafluorophenyl ester (**12**), (*N*-Fluoren-9-ylmethoxycarbonyl)-*cis*-4-(*N*<sup>4</sup>-benzoyladenine-9-yl)-D-proline pentafluorophenyl ester (**16**) and (*N*-Fluoren-9-ylmethoxycarbonyl)-*cis*-4-(*N*<sup>4</sup>-benzoylcytosine)-D-proline pentafluorophenyl ester (**17**). All compounds were synthesized and purified according to Vilaivan and co-workers [83–86].

The second part is activated ACPC spacer namely (1*S*,2*S*)-2-(*N*-Fluoren-9-ylmethoxycarbonyl)-aminocyclopentane carboxylic acid pentafluorophenyl ester (**27**). It was synthesized and characterized according to the literature [85–87].

## 2.3 Synthesis of positive charge labeling group

### Carboxybutyl triphenylphosphonium bromide *N*-hydroxysuccinimidyl ester (**2**)



To a suspension of carboxybutyltriphenyl phosphonium bromide (0.886 g, 2 mmol) in dichloromethane (20 mL) was added *N*-hydroxysuccinimide (0.28 g, 2.4 mmol) and DCC (0.50 g, 2.4 mmol) followed by stirring at room temperature for 8 h. After completion of reaction (TLC), DCU was obtained as by product which was

filtered off by suction filtration. The filtrate was concentrated by rotary evaporation and the resulting crude product was diluted with dichloromethane and extracted three times with water. The combined aqueous layer was extracted again with dichloromethane and the organic phase was concentrated to afford the desired product as colorless oil (**2**) (0.859 g, 85%)

$^1\text{H}$  NMR (400 MHz;  $\text{CDCl}_3$ ):  $\delta$  7.77-7.60 (m, 15H, ArH), 3.68 (t,  $J=14.9$  Hz, 1H, PCHH CH<sub>2</sub>), 3.51 (t,  $J=14.9$  Hz, 1H, PCHHCH<sub>2</sub>), 2.78 (s, 2H, COCH<sub>2</sub> CH<sub>2</sub>), 2.67 (t,  $J=6$  Hz, COCHHCH<sub>2</sub>), 2.58 (s, 2H, COCH<sub>2</sub>CHH), 2.47 (t,  $J=6$  Hz, 1H, COCHHCH<sub>2</sub>), 2.08 (t,  $J=6.4$  Hz, 1H, CH<sub>2</sub>CHHCH<sub>2</sub>), 1.85 (t,  $J=6.6$  Hz, CH<sub>2</sub>CHHCH<sub>2</sub>), 1.80-1.60 (m, 2H, CH<sub>2</sub>CH<sub>2</sub>CH<sub>2</sub>).  $^{13}\text{C}$  NMR (100 MHz;  $\text{CDCl}_3$ ):  $\delta_{\text{C}}$  21.5 [ $^1J_{\text{CP}}=46$  Hz, Ph<sub>3</sub>P-CH<sub>2</sub>CH<sub>2</sub>] 25.4 and 25.7 [COCH<sub>2</sub>CH<sub>2</sub>CO], 21.2 [ $^2J_{\text{CP}}=31$  Hz, Ph<sub>3</sub>P-CH<sub>2</sub>CH<sub>2</sub>], 21.8 [ $^3J_{\text{CP}}=25$  Hz, Ph<sub>3</sub>P-CH<sub>2</sub>CH<sub>2</sub>CH<sub>2</sub>], 130.4, 130.6, 130.7 [ $^1J_{\text{CP}}=46$  Hz,  $^1J_{\text{CP}}=76$  Hz,  $^1J_{\text{CP}}=46$  Hz, Ph<sub>3</sub>P-CAr], 117.5, 118.3, 133.5, 133.7, 135.1 [CHArPPh<sub>3</sub>], 172.7, 175.1 [CO succidimidyl ester], 169.4 [CH<sub>2</sub>CO]. Anal Calcd. for C<sub>27</sub>H<sub>27</sub>O<sub>4</sub>NP requires C, 56.14%; H, 5.88%; N, 3.04%; Found C, 56.16%; H, 5.85%, N, 3.04%.

## 2.4 Synthesis of PNA

### 2.4.1 Preparation of the reaction pipette and apparatus for solid phase synthesis

All PNA oligomers were synthesized manually using a custom-built peptide synthesis column which has been previously developed in this laboratory described [85–86]. The weighed accurately resin was downloaded into the column and first swelled in the required solvent for 1 h before starting the synthesis cycle. In each step, the reagents were directly sucked in, driven out or held on with manual control over period of time indicated. Occasional agitation may be performed using this apparatus under manual control.

### 2.4.2 PNA oligomers synthesis

All *acpc*PNA oligomers were synthesized from the respective four (A,T,G,C) monomers (11),(12),(16),(17) and *ssACPC* spacer (27) using standard Fmoc solid-phase synthesis protocol. The sequences of all PNA oligomers used in this study are shown in **Table 2.1**

**Table 2.1** Sequences of PNA oligomers used in this work

Code of PNA	Base Sequence (N-terminus to C-terminus)
<b>P1</b>	Ac-TTTTTTTTT-Lys-NH <sub>2</sub>
<b>P2</b>	Ac-GTAGATCACT-Ser-NH <sub>2</sub>
<b>P3</b>	Ac-TTTTATTTT-Lys-NH <sub>2</sub>
<b>P4</b>	Ac-TTTTGTTTT-Lys-NH <sub>2</sub>
<b>P5</b>	Ac-TGTACGTCACAATA-Lys-NH <sub>2</sub>
<b>P6</b>	Ac-TGTACGTAACAATA-Lys-NH <sub>2</sub>
<b>P7</b>	Ac-Arg-AAAATCCCATT-Ser-NH <sub>2</sub>
<b>P8</b>	Ac-Arg-AAA ATTCCATT-Ser-NH <sub>2</sub>
<b>P9</b>	P-TTCCCCCTCCCAA-Ser-NH <sub>2</sub>
<b>P10</b>	P-TTCCCCCTCCCAA-Ser-NH <sub>2</sub>
<b>P11</b>	P-ATGTAACATCTCT-Ser-NH <sub>2</sub>
<b>P12</b>	P-ATGTAATATCTCT-Ser-NH <sub>2</sub>
<b>P13</b>	P-GCCTGTACTGTAG-Ser-NH <sub>2</sub>
<b>P14</b>	P-GCCTGTCCTGTAG-Ser-NH <sub>2</sub>

P = carboxybutyl triphenyl phosphonium

**P3** and **P4** were synthesized by Dr. Choladda Srisuwanaket

**P5** and **P6** were synthesized by Miss Cheeraporn Ananthanawat

Solid phase synthesis of PNA oligomers consists of three major steps as follows:

- i) Removal of the *N*-terminal Fmoc group from the growing PNA oligomers
- ii) Coupling of the activated monomers onto the *N*-terminus of the growing PNA chain
- iii) Capping of the unreacted amino group

Each of the individual steps in the synthesis cycle has been previously optimized for the preparation of PNA oligomers [85]. After coupling of the last monomer, the resin-bound PNA was cleaved from the resin by the appropriate reagent. Two different protocols are used in this study.

The first protocol was previously developed in our laboratory by Dr.Choladda Srisuwannaket and Dr. Chaturong Suparpprom [85–86]. The PNA **P1–P8** were synthesized on 1.0  $\mu\text{mol}$  scale using this strategy. The protocol is shown in **Figure 2.1**.

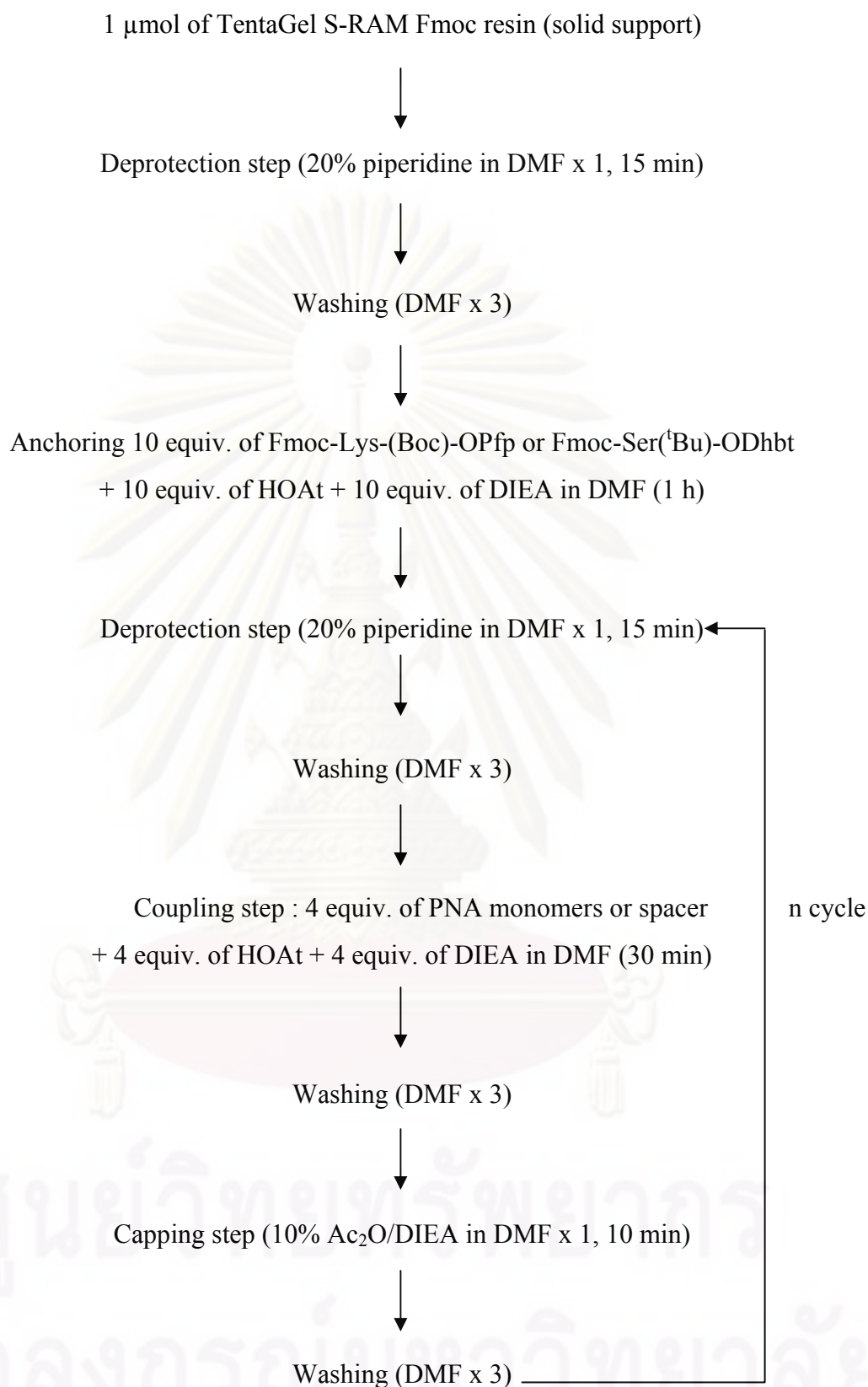


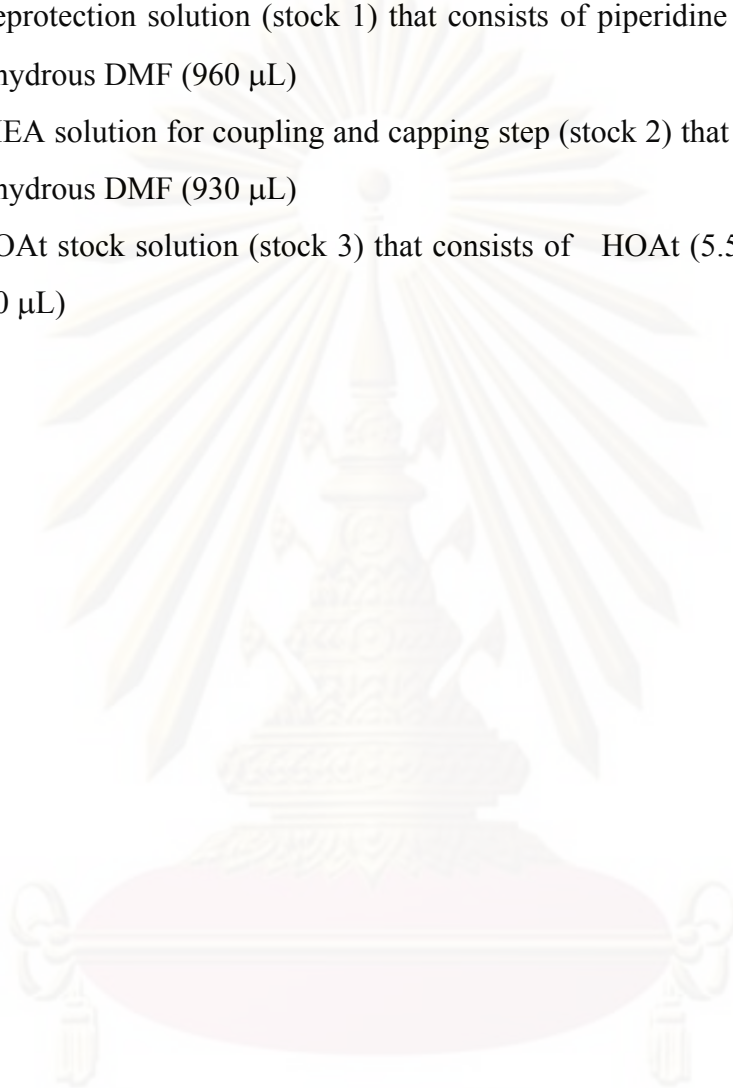
**Figure 2.1** The first strategy for solid phase synthesis of PNA (**P1–P8**)

The second protocol which was slightly adapted from the first one was used to prepare the remaining PNA oligomer as shown in **Table 2.1**. All of PNA oligomers synthesis was carried out on 1.5  $\mu\text{mol}$  scale. The procedure is summarized in **Figure 2.2**. Firstly, three stock solutions were prepared as follows:

Deprotection solution (stock 1) that consists of piperidine (20  $\mu\text{L}$ ), DBU (20  $\mu\text{L}$ ) in anhydrous DMF (960  $\mu\text{L}$ )

DIEA solution for coupling and capping step (stock 2) that contains DIEA (70  $\mu\text{L}$ ) in anhydrous DMF (930  $\mu\text{L}$ )

HOAt stock solution (stock 3) that consists of HOAt (5.5 mg) in anhydrous DMF (100  $\mu\text{L}$ )



ศูนย์วิทยทรัพยากร  
จุฬาลงกรณ์มหาวิทยาลัย

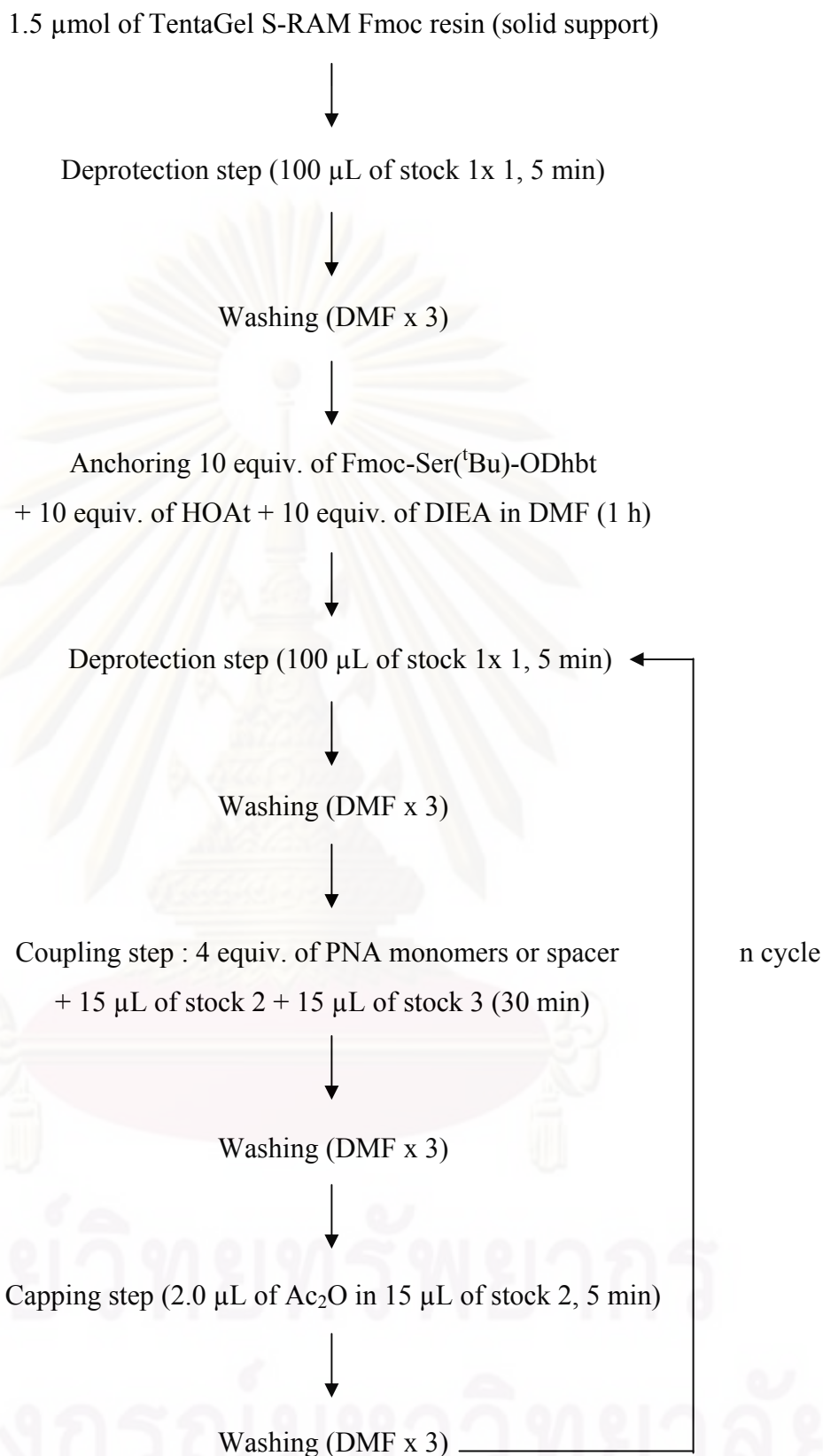


**Figure 2.2** The second strategy for solid phase synthesis of PNA (**P9–P14**)



Each step of this strategy was described as following

**i. Removal of N-terminal Fmoc protecting group of solid support**

TentaGel S RAM Fmoc resin (6.3 mg, 1.5  $\mu\text{mol}$ ) was loaded into the pipette column and swelled in anhydrous DMF for 1 h before use. To remove the Fmoc group, the prepared solid support was treated with 100  $\mu\text{L}$  of stock 1 at room temperature (30  $^{\circ}\text{C}$ ) for 5 min with occasional agitation. After 5 min, the resin was extensively washed with anhydrous DMF.

**ii. Coupling with the first amino acid (serine) residue**

Fmoc-Ser(<sup>t</sup>Bu)-ODhbt (7.9 mg, 15  $\mu\text{mol}$ ) was activated by treatment with HOAt (2.1 mg, 15  $\mu\text{mol}$ ) and DIEA (2.6  $\mu\text{L}$ , 20  $\mu\text{mol}$ ) in anhydrous DMF (30  $\mu\text{L}$ ) to give a yellow solution. The prepared resin was treated with this solution under occasional agitation at 30  $^{\circ}\text{C}$  for 1 h. After the specified period of time, the reagent was removed and the resin was washed with DMF.

**iii. Capping step**

After each of coupling step, the capping step was required to avoid formation of deletion sequences. This could simplify purification of the full length PNA oligomers. This step was carried out after the coupling step by treatment with a mixture of acetic anhydride (2.0  $\mu\text{L}$ ) and DIEA stock 2 (30  $\mu\text{L}$ ) with occasional agitation. After 5 minutes, the reagent was squeezed off and the reaction column was then washed with anhydrous DMF.

**iv. Deprotection of the Fmoc protecting group at N-terminus**

After the coupling and capping were completed, the deprotection of the *N*-terminal Fmoc group from the growing peptide chain was performed as described in step **i**. To determine the effectiveness of the previous coupling step the deprotection solution containing dibenzofulvene-piperidine adduct was measured for UV

absorbance at 264 nm. The first UV-absorbance of the deprotection solution, obtained from the first loading of Fmoc-Ser(<sup>t</sup>Bu)-ODhbt-resin, was assumed to be 100%. The efficiency should be up to 95 % for each step in order to give acceptable yield and purify of the final 10-15mer PNA.

**v. Coupling with PNA monomers**

a. pyrrolidinyll nucleobase monomer

After removing the Fmoc group, the free amino group at the *N*-terminus was subsequently coupled with the nucleobase monomer. This was carried out by treating the resin with a mixture of the activated nucleobase monomers, DIEA stock 2 (15  $\mu$ L) and HOAt stock 3 (15  $\mu$ L) at room temperature with occasional agitation. After 30 min of coupling, the reagent was squeezed off and the reaction column was then washed with anhydrous DMF.

b. ACPC spacer

After coupling of the nucleobase monomer, capping and Fmoc group removed were completed. The resin was treated with a solution of (**27**) (3.1 mg, 6  $\mu$ mol), DIEA stock 2 (15  $\mu$ L) and HOAt stock 3 (15  $\mu$ L) with occasional agitation for 30 min. After 30 min of coupling, the reagent was squeezed off and the reaction column was then washed with anhydrous DMF.

**vi. Deprotection of nucleobase protecting groups**

For PNA oligomers bearing adenine, cytosine or guanine bases in the sequence, the nucleobase protecting groups (Bz for A and C, Ibu for G) must be removed before the PNA was cleaved from resin by treating the resin with aqueous ammonia/dioxane 1:1 in a sealed test tube at 60 °C. After approximately 6 h of deprotection, the reagent was squeezed off and the reaction column was then washed with methanol.

**vii. Attachment of carboxybutyltriphenyl phosphonium charge label**

Coupling of the carboxybutyl triphenyl phosphonium labeling group at the *N*-termini of the PNA oligomers was carried out after removal of the exocyclic amino protecting groups by ammonia treatment (step vi). The washed resin was re-swollen in DMF and treated with a mixture of (2) (6.90 mg, 15  $\mu$ mol) and DIEA (5.2  $\mu$ L, 15  $\mu$ mol) in anhydrous DMF (30  $\mu$ L). After coupling was allowed to proceed for 1 h, the reagent was squeezed off and the reaction column was then washed with anhydrous DMF.

**viii. Cleavage of PNA oligomer from the resin**

The cleavage of the PNA from the resin was accomplished by treatment with trifluoroacetic acid (TFA). The resin bound PNA was treated with trifluoroacetic acid (0.5 mL) at room temperature with occasional agitation. The resin became red during this time. After approximately 2 h of cleavage, the trifluoroacetic acid was removed under a stream of nitrogen to give a sticky brown residue. The resulting residue was resuspended in diethyl ether. The suspension was centrifuged and the ether was decanted to yield the crude PNA as a white solid. The crude PNA was repeatedly washed with diethyl ether (3 times). After the ether wash, the crude PNA was air-dried and stored at  $-20$  °C until further used.

**2.5 Purification of crude PNA oligomers****2.5.1 Reverse-phase HPLC**

PNA oligomers were purified on reverse-phase HPLC with UV detection at 260 nm. The solution of PNA in deionized water was filtered throughout a nylon membrane filter (0.45  $\mu$ m). A Varian Polaris<sup>TM</sup> C<sub>18</sub> (3  $\mu$ m particle size 4.6  $\times$  50 mm) analytical HPLC column was used for both analytical and preparative purpose.. The eluents were 0.1% TFA in acetonitrile (solvent A) and 0.1% TFA in milliQ water (solvent B). The gradient system was first A:B (20:80) for 5 min then linear gradient to A:B (80:20) over a period of 65 min then hold for 10 min before revert back to A:B

(20:80) in a period of 10 min at flow rate 0.5 mL/min. The desired product was collected and characterized by MALDI-TOF mass spectrometry.

### **2.5.2 Anion exchange solid support capture method**

The anion-exchange support (~0.2 mL) was packed in a peptide synthesis column and pre-equilibrated with phosphate buffer (pH 7, 10 mM) for 15 min. The DNA was dissolved in 10 mM phosphate buffer (pH 7) (0.5 mL), then loaded onto the prepared anion-exchanger column and incubated with occasional agitation for 15 min at room temperature. After washing with water, the DNA bound solid supports were then treated with the crude PNA solution and was incubated with occasional agitation for another 20 min at room temperature. To estimate the efficiency of the ion exchange capture, 1  $\mu$ L of the remaining PNA solution was mixed with 10  $\mu$ L of CCA matrix solution. One  $\mu$ L of this PNA solution/matrix mixture was spotted onto the target, and allowed to dry at room temperature. The sample target was then subjected to MALDI-TOF mass spectrometry analysis. After the absorption of PNA on the DNA-bound ion exchange support was complete, the resulting PNA: DNA-bound beads were then washed with several aliquots of deionized water or aqueous acetonitrile to remove any nonspecifically absorbed PNA probe. After washing, the desorption of PNA was performed by treatment of the PNA·DNA-bound support with 0.5 mL of boiling water for 5-10 min. The process was repeated to ensure complete desorption of the PNA. The progress of the desorption was monitored by MALDI-TOF analysis.

### **2.6 Characterization of PNA oligomers**

After purification by either HPLC or DNA capture method, the PNA were characterized by MALDI-TOF mass spectrometry using  $\alpha$ -cyano-4-hydroxy cinnamic acid (CCA) as matrix. Mass spectra of all the studies were obtained on Microflex MALDI-TOF mass spectrometry (Bruker Daltonics) and recorded in the positive ion linear time-of-flight mode with accelerating voltage of +20 kV. The sample (1  $\mu$ L each) was mixed with matrix solution (10  $\mu$ L) containing a saturated solution of CCA in 0.1% trifluoroacetic acid in acetonitrile:water (1:2) solution. One  $\mu$ L of this PNA

solution/matrix mixture was spotted onto the target, and allowed to dry at room temperature. The sample target was then subjected to MALDI-TOF mass spectrometry analysis. All spectra were processed by averaging between 20 and 30 individual laser shots. External mass calibration was performed using PNAs of known molecular weight (1850.0, 3558.8, 5208.6 Da.)

## 2.7 PNA synthesis

### 2.7.1 Synthesis of Ac- TTTTTTTTTT-Lys-NH<sub>2</sub> (P1)

This PNA oligomer was synthesized according to first protocol using TentaGel S RAM Fmoc resin (4.2 mg, 1.0  $\mu$ mol). The coupling efficiency of each monomer is shown in the table below.

Cycle	Monomers	A <sub>264</sub>	Coupling efficiency
1	Fmoc-Lys- OPfp	0.832	100.0
2	Fmoc-T-OPfp	0.793	95.3
3	Fmoc-ACPC -OPfp	0.782	98.6
4	Fmoc-T-OPfp	0.743	95.0
5	Fmoc-ACPC -OPfp	0.694	93.4
6	Fmoc-T-OPfp	0.707	101.9
7	Fmoc-ACPC -OPfp	0.739	104.5
8	Fmoc-T -OPfp	0.726	98.2
9	Fmoc-ACPC -OPfp	0.736	101.4
10	Fmoc-T-OPfp	0.716	97.3
11	Fmoc-ACPC -OPfp	0.706	98.6
12	Fmoc-T-OPfp	0.685	97.1
13	Fmoc-ACPC -OPfp	0.690	100.7
14	Fmoc-T-OPfp	0.655	94.9
15	Fmoc-ACPC -OPfp	0.631	96.3
16	Fmoc-T-OPfp	0.571	90.5

Cycle	Monomers	A <sub>264</sub>	Coupling efficiency
17	Fmoc-ACPC -OPfp	0.597	104.5
18	Fmoc-T-OPfp	0.568	95.1
19	Fmoc-ACPC -OPfp	0.736	98.6
	average		96.9

After final Fmocdeprotection and acetylation at the *N*-terminus, the PNA was cleaved from the resin. The crude PNA was then purified by reverse phase HPLC. In the chromatogram, the PNA (**P1**) appeared at  $t_R = 20.1$  min. MALDI-TOF mass spectrum showed  $m/z$  at 3179.7 ( $M \cdot H^+_{\text{calcd}} = 3179.4$ )

### 2.7.2 Synthesis of Ac- GTAGATCACT-Ser-NH<sub>2</sub> (P2)

This PNA was synthesized as described for the **PNA P1** on TentaGel S RAM Fmoc resin (4.3 mg, 1.0  $\mu\text{mol}$ ). The coupling efficiency of each monomer is shown in the table below.

Cycle	Monomers	A <sub>264</sub>	Coupling efficiency
1	Fmoc-Ser( <sup>t</sup> Bu)-ODhbt	0.842	100.0
2	Fmoc-T-OPfp	0.836	99.2
3	Fmoc-ACPC -OPfp	0.833	99.6
4	Fmoc-C <sup>Bz</sup> -OPfp	0.756	90.4
5	Fmoc-ACPC -OPfp	0.788	104.2
6	Fmoc-A <sup>Bz</sup> -OPfp	0.743	94.3
7	Fmoc-ACPC -OPfp	0.769	103.4
8	Fmoc-C <sup>Bz</sup> -OPfp	0.725	94.2
9	Fmoc-ACPC -OPfp	0.739	101.9
10	Fmoc-T-OPfp	0.720	97.4
11	Fmoc-ACPC -OPfp	0.740	102.8
12	Fmoc-A <sup>Bz</sup> -OPfp	0.718	97.2
13	Fmoc-ACPC -OPfp	0.754	105.0
14	Fmoc-G <sup>ibu</sup> -OPfp	0.752	99.7

Cycle	Monomers	A <sub>264</sub>	Coupling efficiency
15	Fmoc-ACPC -OPfp	0.720	95.8
16	Fmoc-A <sup>Bz</sup> -OPfp	0.690	95.8
17	Fmoc-ACPC -OPfp	0.704	102.0
18	Fmoc-T-OPfp	0.680	96.6
19	Fmoc-ACPC -OPfp	0.675	99.2
20	Fmoc-G <sup>tBu</sup> -OPfp	0.638	94.5
21	Fmoc-ACPC -OPfp	0.596	93.4
	average		98.3

After acetylation, the nucleobase protecting group was removed prior to cleavage from resin as described in step **vi**. After final Fmocdeprotection and acetylation at the *N*-terminus, the PNA was cleaved from the resin. The crude PNA was then purified by reverse phase HPLC. In the chromatogram, the PNA (**P2**) appeared at  $t_R = 21.7$  min. MALDI-TOF mass spectrum showed  $m/z$  at 3517.6 ( $M \cdot H^+_{\text{calcd}} = 3517.8$ )

### 2.7.3 Synthesis of Ac-Arg-AAAATCCCATT-Ser-NH<sub>2</sub> (P7)

This PNA was established according to first strategy as revealed for PNA P1 using TentaGel S RAM Fmoc resin (6.3 mg, 1.5  $\mu\text{mol}$ ). The coupling efficiency of each monomer is revealed in table below.

Cycle	Monomers	A <sub>264</sub>	Coupling efficiency
1	Fmoc-Ser( <sup>t</sup> Bu)-ODhbt	1.028	100.0
2	Fmoc-T-OPfp	1.064	103.5
3	Fmoc-ACPC -OPfp	1.039	97.6
4	Fmoc-T-OPfp	1.057	101.7
5	Fmoc-ACPC -OPfp	1.056	99.9
6	Fmoc-A <sup>Bz</sup> -OPfp	0.972	92.0
7	Fmoc-ACPC -OPfp	0.967	99.4
8	Fmoc-C <sup>Bz</sup> -OPfp	0.981	101.4

Cycle	Monomers	A <sub>264</sub>	Coupling efficiency
9	Fmoc-ACPC -OPfp	1.029	104.9
10	Fmoc-C <sup>Bz</sup> -OPfp	0.955	92.8
11	Fmoc-ACPC -OPfp	0.913	95.6
12	Fmoc-C <sup>Bz</sup> -OPfp	0.509	111.5
13	Fmoc-ACPC -OPfp	0.500	98.2
14	Fmoc-T-OPfp	0.452	90.4
15	Fmoc-ACPC -OPfp	0.426	94.2
16	Fmoc-A <sup>Bz</sup> -OPfp	0.432	101.4
17	Fmoc-ACPC -OPfp	0.402	93.0
18	Fmoc-A <sup>Bz</sup> -OPfp	0.381	94.8
19	Fmoc-ACPC -OPfp	0.409	107.3
20	Fmoc-A <sup>Bz</sup> -OPfp	0.389	95.1
21	Fmoc-ACPC -OPfp	0.345	88.7
22	Fmoc-A <sup>Bz</sup> -OPfp	0.322	93.3
23	Fmoc-ACPC -OPfp	0.314	97.5
24	Fmoc-Arg (Mtr)-OH	0.289	92.0
	average		97.8

<sup>a</sup> Cycle 1-11: A<sub>264</sub> and Coupling efficiency at 1.5  $\mu$ mole of resin. Cycle 12-24: A<sub>264</sub> and Coupling efficiency at 0.75  $\mu$ mole of resin (split in to 2 reactions)

After final Fmoc deprotection and acetylation at the *N*-terminus, the PNA was cleaved from the resin. The crude PNA was then purified by reverse phase HPLC. In the chromatogram, the PNA (**P7**) appeared at  $t_R = 23.2$  min. MALDI-TOF mass spectrum showed  $m/z$  at 3961.5 ( $M \cdot H^+_{calcd} = 3961.2$ )

#### 2.7.4 Synthesis of Ac-Arg-AAAATTCCATT-Ser-NH<sub>2</sub> (P8)

This PNA was constructed according to first protocol using TentaGel S RAM Fmoc resin (6.3 mg, 1.5  $\mu$ mol). The coupling efficiency of each monomer is revealed in table below.



Cycle	Monomers	A <sub>264</sub>	Coupling efficiency
1	Fmoc-Ser( <sup>t</sup> Bu)-ODhbt	1.028	100.0
2	Fmoc-T-OPfp	1.064	103.5
3	Fmoc-ACPC -OPfp	1.039	97.6
4	Fmoc-T-OPfp	1.057	101.7
5	Fmoc-ACPC -OPfp	1.056	99.9
6	Fmoc-A <sup>Bz</sup> -OPfp	0.972	92.0
7	Fmoc-ACPC -OPfp	0.967	99.4
8	Fmoc-C <sup>Bz</sup> -OPfp	0.981	101.4
9	Fmoc-ACPC -OPfp	1.029	104.9
10	Fmoc-C <sup>Bz</sup> -OPfp	0.955	92.8
11	Fmoc-ACPC -OPfp	0.913	95.6
12	Fmoc-T-OPfp	0.502	109.6
13	Fmoc-ACPC -OPfp	0.549	109.3
14	Fmoc-T-OPfp	0.579	105.5
15	Fmoc-ACPC -OPfp	0.547	94.4
16	Fmoc-A <sup>Bz</sup> -OPfp	0.499	91.2
17	Fmoc-ACPC -OPfp	0.512	102.6
18	Fmoc-A <sup>Bz</sup> -OPfp	0.474	92.6
19	Fmoc-ACPC -OPfp	0.501	105.6
20	Fmoc-A <sup>Bz</sup> -OPfp	0.474	94.6
21	Fmoc-ACPC -OPfp	0.463	97.7
22	Fmoc-A <sup>Bz</sup> -OPfp	0.417	90.1
23	Fmoc-ACPC -OPfp	0.407	97.6
24	Fmoc-Arg (Mtr)-OH	0.313	76.9
	average		98.9

<sup>a</sup> Cycle 1-11: A<sub>264</sub> and Coupling efficiency at 1.5 μmole of resin. Cycle 12-24: A<sub>264</sub> and coupling efficiency at 0.75 μmole of resin (split in to 2 reactions)

After removing the final Fmoc group, the resulting free amino group was capped with acetyl group and the nucleobase protecting group was subsequently removed prior to cleavage from resin as described in step **viii**. The crude PNA was purified by anion exchange capture. The purity of **P8** was confirmed by HPLC ( $t_R = 23.8$  min). MALDI-TOF mass spectrum showed  $m/z$  at 3976.4 ( $M \cdot H^+_{\text{calcd}} = 3976.2$ )

### 2.7.5 Synthesis of P-TTCCCCCTCCCAA -Ser-NH<sub>2</sub> (P9)

This sequence was prepared according to second protocol using TentaGel S RAM Fmoc resin (6.3 mg, 1.5  $\mu\text{mol}$ ). The coupling efficiency of each monomer is revealed in table below.

Cycle	Monomers	A <sub>264</sub>	Coupling efficiency
1	Fmoc-Ser( <sup>t</sup> Bu)-ODhbt	0.826	100.0
2	Fmoc-A <sup>Bz</sup> -OPfp	0.789	95.5
3	Fmoc-ACPC -OPfp	0.748	94.8
4	Fmoc-A <sup>Bz</sup> -OPfp	0.772	103.2
5	Fmoc-ACPC -OPfp	0.712	92.2
6	Fmoc-C <sup>Bz</sup> -OPfp	0.736	103.4
7	Fmoc-ACPC -OPfp	0.721	97.9
8	Fmoc-C <sup>Bz</sup> -OPfp	0.712	98.7
9	Fmoc-ACPC -OPfp	0.703	98.7
10	Fmoc-C <sup>Bz</sup> -OPfp	0.694	98.7
11	Fmoc-ACPC -OPfp	0.675	97.3
12	Fmoc-T-OPfp	0.658	97.5
13	Fmoc-ACPC -OPfp	0.664	100.9
14	Fmoc-C <sup>Bz</sup> -OPfp	0.314	94.6
15	Fmoc-ACPC -OPfp	0.317	100.9
16	Fmoc-C <sup>Bz</sup> -OPfp	0.304	95.9
17	Fmoc-ACPC -OPfp	0.307	101.0
18	Fmoc-C <sup>Bz</sup> -OPfp	0.296	96.4
19	Fmoc-ACPC -OPfp	0.307	103.7

Cycle	Monomers	A <sub>264</sub>	Coupling efficiency
20	Fmoc-C <sup>Bz</sup> -OPfp	0.308	100.3
21	Fmoc-ACPC -OPfp	0.290	94.2
22	Fmoc-C <sup>Bz</sup> -OPfp	0.298	102.8
23	Fmoc-ACPC -OPfp	0.293	98.3
24	Fmoc-T-OPfp	0.285	97.3
25	Fmoc-ACPC -OPfp	0.275	96.5
26	Fmoc-T-OPfp	0.249	90.5
27	Fmoc-ACPC -OPfp	0.239	95.9
	average		97.9

<sup>a</sup> Cycle 1-13: A<sub>264</sub> and coupling efficiency at 1.5  $\mu$ mole of resin. Cycle 14-27: A<sub>264</sub> and coupling efficiency at 0.75  $\mu$ mole of resin (split in to 2 reactions)

After removing the final Fmoc group, the nucleobase protecting group was subsequently removed as described in step **vi**. The free amino group at the N-terminus was subsequently coupled with the carboxybutyl triphenyl phosphonium labeling group (step **vii**) prior to cleavage from resin. The crude PNA was then purified by reverse phase HPLC. In the chromatogram, the PNA (**P9**) appeared at  $t_R = 20.9$  min. MALDI-TOF mass spectrum showed  $m/z$  at 4668.0 ( $M^+_{\text{calcd}} = 4667.8$ )

### 2.7.6 Synthesis of P-TTCCCCTTCCCAA -Ser-NH<sub>2</sub> (P10)

This sequence was prepared in the same way as described for the PNA P9 using TentaGel S RAM Fmoc resin (6.3 mg, 1.5  $\mu$ mol). The coupling efficiency of each monomer is revealed in table below.

Cycle	Monomers	A <sub>264</sub>	Coupling efficiency
1	Fmoc-Ser( <sup>t</sup> Bu)-ODhbt	0.826	100.0
2	Fmoc-A <sup>Bz</sup> -OPfp	0.789	95.5
3	Fmoc-ACPC -OPfp	0.748	94.8
4	Fmoc-A <sup>Bz</sup> -OPfp	0.772	103.2
5	Fmoc-ACPC -OPfp	0.712	92.2

Cycle	Monomers	A <sub>264</sub>	Coupling efficiency
6	Fmoc-C <sup>Bz</sup> -OPfp	0.736	103.4
7	Fmoc-ACPC -OPfp	0.721	97.9
8	Fmoc-C <sup>Bz</sup> -OPfp	0.712	98.7
9	Fmoc-ACPC -OPfp	0.703	98.7
10	Fmoc-C <sup>Bz</sup> -OPfp	0.694	98.7
11	Fmoc-ACPC -OPfp	0.675	97.3
12	Fmoc-T-OPfp	0.658	97.5
13	Fmoc-ACPC -OPfp	0.664	100.9
14	Fmoc-T-OPfp	0.339	102.1
15	Fmoc-ACPC -OPfp	0.328	96.8
16	Fmoc-C <sup>Bz</sup> -OPfp	0.333	101.5
17	Fmoc-ACPC -OPfp	0.317	95.2
18	Fmoc-C <sup>Bz</sup> -OPfp	0.314	99.0
19	Fmoc-ACPC -OPfp	0.304	96.8
20	Fmoc-C <sup>Bz</sup> -OPfp	0.314	103.3
21	Fmoc-ACPC -OPfp	0.309	98.4
22	Fmoc-C <sup>Bz</sup> -OPfp	0.296	95.8
23	Fmoc-ACPC -OPfp	0.290	97.9
24	Fmoc-T-OPfp	0.269	92.8
25	Fmoc-ACPC -OPfp	0.266	98.8
26	Fmoc-T-OPfp	0.247	92.9
27	Fmoc-ACPC -OPfp	0.248	100.4
	average		98.0

<sup>a</sup> Cycle 1-13: A<sub>264</sub> and coupling efficiency at 1.5  $\mu$ mole of resin. Cycle 14-27: A<sub>264</sub> and coupling efficiency at 0.75  $\mu$ mole of resin (split in to 2 reactions)

After removing the final Fmoc group, the nucleobase protecting group was subsequently removed as described in step **vi**. The free amino group at the N-terminus was subsequently coupled with the carboxybutyl triphenyl phosphonium labeling group (step **vii**) prior to cleavage from resin. The crude PNA was then purified by reverse phase HPLC. In the chromatogram, the PNA (**P10**) appeared at  $t_R = 20.6$  min. MALDI-TOF mass spectrum showed  $m/z$  at 4683.3 ( $M^+_{\text{calcd}} = 4682.8$ )

### 2.7.7 Synthesis of P- ATGTAACATCTCT -Ser-NH<sub>2</sub> (P11)

This sequence was prepared according to the second strategy as described above using TentaGel S RAM Fmoc resin (6.4 mg, 1.5  $\mu$ mol). The coupling efficiency of each monomer is revealed in table below.

Cycle	Monomers	A <sub>264</sub>	Coupling efficiency
1	Fmoc-Ser( <sup>t</sup> Bu)-ODhbt	1.109	100.0
2	Fmoc-T-OPfp	1.030	92.9
3	Fmoc-ACPC -OPfp	1.068	103.7
4	Fmoc-C <sup>Bz</sup> -OPfp	1.021	95.6
5	Fmoc-ACPC -OPfp	0.996	97.6
6	Fmoc-T-OPfp	1.003	100.7
7	Fmoc-ACPC -OPfp	1.089	108.5
8	Fmoc-C <sup>Bz</sup> -OPfp	0.919	84.4
9	Fmoc-ACPC -OPfp	0.812	88.4
10	Fmoc-T-OPfp	0.796	98.0
11	Fmoc-ACPC -OPfp	0.806	101.2
12	Fmoc-A <sup>Bz</sup> -OPfp	0.844	104.7
13	Fmoc-ACPC -OPfp	0.886	105.3
14	Fmoc-C <sup>Bz</sup> -OPfp	0.447	100.9
15	Fmoc-ACPC -OPfp	0.454	101.5
16	Fmoc-A <sup>Bz</sup> -OPfp	0.433	95.4
17	Fmoc-ACPC -OPfp	0.421	97.2
18	Fmoc-A <sup>Bz</sup> -OPfp	0.404	95.9
19	Fmoc-ACPC -OPfp	0.413	102.2
20	Fmoc-T-OPfp	0.399	96.6
21	Fmoc-ACPC -OPfp	0.390	97.7
22	Fmoc-G <sup>ibu</sup> -OPfp	0.407	104.3
23	Fmoc-ACPC -OPfp	0.364	89.4
24	Fmoc-T-OPfp	0.348	95.6
25	Fmoc-ACPC -OPfp	0.338	97.1

Cycle	Monomers	A <sub>264</sub>	Coupling efficiency
26	Fmoc-A <sup>Bz</sup> -OPfp	0.358	105.9
27	Fmoc-ACPC -OPfp	0.305	85.2
	average		98.3

<sup>a</sup> Cycle 1-13: A<sub>264</sub> and coupling efficiency at 1.5  $\mu$ mole of resin. Cycle 14-27: A<sub>264</sub> and coupling efficiency at 0.75  $\mu$ mole of resin (split in to 2 reactions)

After removing the final Fmoc group, the nucleobase protecting group was subsequently removed as described in step **vi** followed by resulting free amino group at the N-terminus was subsequently coupled with the carboxybutyl triphenyl phosphonium labeling group (step **vii**) prior to cleavage from resin. The crude PNA was then purified by reverse phase HPLC. In the chromatogram, the PNA (**P11**) appeared at  $t_R = 21.0$  min. MALDI-TOF mass spectrum showed  $m/z$  at 4785.8 ( $M^+_{calcd} = 4785.9$ )

### 2.7.8 Synthesis of P- ATGTAATATCTCT-Ser-NH<sub>2</sub> (P12)

This sequence was synthesized according to the second protocol as earlier revealed above using TentaGel S RAM Fmoc resin (6.3 mg, 1.5  $\mu$ mol). The coupling efficiency of each monomer is revealed in table below.

Cycle	Monomers	A <sub>264</sub>	Coupling efficiency
1	Fmoc-Ser( <sup>t</sup> Bu)-ODhbt	1.109	100.0
2	Fmoc-T-OPfp	1.030	92.9
3	Fmoc-ACPC -OPfp	1.068	103.7
4	Fmoc-C <sup>Bz</sup> -OPfp	1.021	95.6
5	Fmoc-ACPC -OPfp	0.996	97.6
6	Fmoc-T-OPfp	1.003	100.7
7	Fmoc-ACPC -OPfp	1.089	108.5
8	Fmoc-C <sup>Bz</sup> -OPfp	0.919	84.4
9	Fmoc-ACPC -OPfp	0.812	88.4
10	Fmoc-T-OPfp	0.796	98.0

Cycle	Monomers	A <sub>264</sub>	Coupling efficiency
11	Fmoc-ACPC -OPfp	0.806	101.2
12	Fmoc-A <sup>Bz</sup> -OPfp	0.844	104.7
13	Fmoc-ACPC -OPfp	0.886	105.3
14	Fmoc-T-OPfp	0.436	98.4
15	Fmoc-ACPC -OPfp	0.450	103.2
16	Fmoc-A <sup>Bz</sup> -OPfp	0.441	98.0
17	Fmoc-ACPC -OPfp	0.409	92.7
18	Fmoc-A <sup>Bz</sup> -OPfp	0.416	101.7
19	Fmoc-ACPC -OPfp	0.430	103.3
20	Fmoc-T-OPfp	0.407	94.7
21	Fmoc-ACPC -OPfp	0.427	104.9
22	Fmoc-G <sup>ibu</sup> -OPfp	0.416	97.4
23	Fmoc-ACPC -OPfp	0.384	92.3
24	Fmoc-T-OPfp	0.364	94.8
25	Fmoc-ACPC -OPfp	0.345	94.7
26	Fmoc-A <sup>Bz</sup> -OPfp	0.328	95.1
27	Fmoc-ACPC -OPfp	0.290	88.4
	average		98.0

<sup>a</sup> Cycle 1-13: A<sub>264</sub> and coupling efficiency at 1.5 μmole of resin. Cycle 14-27: A<sub>264</sub> and coupling efficiency at 0.75 μmole of resin (split in to 2 reactions)

After removing the final Fmoc group, the nucleobase protecting group was subsequently removed as described in step **vi**. The free amino group at the N-terminus was subsequently coupled with the carboxybutyl triphenyl phosphonium labeling group (step **vii**) prior to cleavage from resin. The crude PNA was then purified by reverse phase HPLC. In the chromatogram, the PNA (**P12**) appeared at  $t_R = 20.0$  min. MALDI-TOF mass spectrum showed  $m/z$  at 4801.4 ( $M^+_{\text{calcd}} = 4800.9$ )

### 2.7.9 Synthesis of P- GCCTGTACTGTAG -Ser-NH<sub>2</sub> (P13)

This sequence was synthesized according to the second protocol as earlier revealed above using TentaGel S RAM Fmoc resin (6.3 mg, 1.5  $\mu$ mol). The coupling efficiency of each monomer is revealed in table below.

Cycle	Monomers	A <sub>264</sub>	Coupling efficiency
1	Fmoc-Ser( <sup>t</sup> Bu)-ODhbt	0.875	100.0
2	Fmoc-G <sup>ibu</sup> -OPfp	0.855	97.7
3	Fmoc-ACPC -OPfp	0.808	94.5
4	Fmoc-A <sup>Bz</sup> -OPfp	0.878	108.6
5	Fmoc-ACPC -OPfp	0.851	96.9
6	Fmoc-T-OPfp	0.817	96.0
7	Fmoc-ACPC -OPfp	0.821	100.4
8	Fmoc-G <sup>ibu</sup> -OPfp	0.808	98.4
9	Fmoc-ACPC -OPfp	0.795	98.4
10	Fmoc-T-OPfp	0.789	99.2
11	Fmoc-ACPC -OPfp	0.778	98.6
12	Fmoc-C <sup>Bz</sup> -OPfp	0.781	100.4
13	Fmoc-ACPC -OPfp	0.779	99.7
14	Fmoc-A <sup>Bz</sup> -OPfp	0.301	77.3
15	Fmoc-ACPC -OPfp	0.299	99.3
16	Fmoc-T-OPfp	0.294	98.3
17	Fmoc-ACPC -OPfp	0.301	102.4
18	Fmoc-G <sup>ibu</sup> -OPfp	0.281	93.4
19	Fmoc-ACPC -OPfp	0.277	98.6
20	Fmoc-T-OPfp	0.280	101.1
21	Fmoc-ACPC -OPfp	0.256	91.4
22	Fmoc-C <sup>Bz</sup> -OPfp	0.268	104.7
23	Fmoc-ACPC -OPfp	0.251	93.6
24	Fmoc-C <sup>Bz</sup> -OPfp	0.250	99.6
25	Fmoc-ACPC -OPfp	0.231	92.4



Cycle	Monomers	A <sub>264</sub>	Coupling efficiency
26	Fmoc-G <sup>ibu</sup> -OPfp	0.244	105.6
27	Fmoc-ACPC -OPfp	0.229	93.8
	average		97.5

<sup>a</sup> Cycle 1-13: A<sub>264</sub> and coupling efficiency at 1.5  $\mu$ mole of resin. Cycle 14-27: A<sub>264</sub> and coupling efficiency at 0.75  $\mu$ mole of resin (split in to 2 reactions)

After removing the final Fmoc group, the nucleobase protecting group was subsequently removed as described in step **vi**. The free amino group at the N-terminus was subsequently coupled with the carboxybutyl triphenyl phosphonium labeling group (step **vii**) prior to cleavage from resin. The crude PNA was then purified by reverse phase HPLC. In the chromatogram, the PNA (**P13**) appeared at  $t_R = 20.1$  min. MALDI-TOF mass spectrum showed  $m/z$  at 4818.6 ( $M^+_{\text{calcd}} = 4818.9$ )

#### 2.7.10 Synthesis of P- GCCTGTCCTGTAG -Ser-NH<sub>2</sub> (P14)

This sequence was synthesized according to the second protocol as earlier revealed above using TentaGel S RAM Fmoc resin (6.3 mg, 1.5  $\mu$ mol). The coupling efficiency of each monomer is revealed in table below.

Cycle	Monomers	A <sub>264</sub>	Coupling efficiency
1	Fmoc-Ser( <sup>t</sup> Bu)-ODhbt	0.875	100.0
2	Fmoc-G <sup>ibu</sup> -OPfp	0.855	97.7
3	Fmoc-ACPC -OPfp	0.808	94.5
4	Fmoc-A <sup>Bz</sup> -OPfp	0.878	108.6
5	Fmoc-ACPC -OPfp	0.851	96.9
6	Fmoc-T-OPfp	0.817	96.0
7	Fmoc-ACPC -OPfp	0.821	100.4
8	Fmoc-G <sup>ibu</sup> -OPfp	0.808	98.4
9	Fmoc-ACPC -OPfp	0.795	98.4
10	Fmoc-T-OPfp	0.789	99.2
11	Fmoc-ACPC -OPfp	0.778	98.6

Cycle	Monomers	A <sub>264</sub>	Coupling efficiency
12	Fmoc-C <sup>Bz</sup> -OPfp	0.781	100.4
13	Fmoc-ACPC -OPfp	0.779	99.7
14	Fmoc-C <sup>Bz</sup> -OPfp	0.283	72.8
15	Fmoc-ACPC -OPfp	0.266	93.9
16	Fmoc-T-OPfp	0.257	96.6
17	Fmoc-ACPC -OPfp	0.277	107.7
18	Fmoc-G <sup>ibu</sup> -OPfp	0.269	97.1
19	Fmoc-ACPC -OPfp	0.254	94.4
20	Fmoc-T-OPfp	0.268	105.5
21	Fmoc-ACPC -OPfp	0.237	88.4
22	Fmoc-C <sup>Bz</sup> -OPfp	0.242	102.1
23	Fmoc-ACPC -OPfp	0.228	94.2
24	Fmoc-C <sup>Bz</sup> -OPfp	0.235	103.1
25	Fmoc-ACPC -OPfp	0.211	89.8
26	Fmoc-G <sup>ibu</sup> -OPfp	0.201	95.3
27	Fmoc-ACPC -OPfp	0.206	102.5
	average		97.1

<sup>a</sup> Cycle 1-13: A<sub>264</sub> and coupling efficiency at 1.5  $\mu$ mole of resin. Cycle 14-27: A<sub>264</sub> and coupling efficiency at 0.75  $\mu$ mole of resin (split in to 2 reactions)

After removing the final Fmoc group, the nucleobase protecting group was subsequently removed as described in step **vi**. The free amino group at the N-terminus was subsequently coupled with the carboxybutyl triphenyl phosphonium labeling group (step **vii**) prior to cleavage from resin. The crude PNA was then purified by reverse phase HPLC. In the chromatogram, the PNA (**P14**) appeared at  $t_R = 21.0$  min. MALDI-TOF mass spectrum showed  $m/z$  at 4843.0 ( $M^+_{calcd} = 4842.9$ )

## 2.8 UV Melting Experiments

UV melting was used to study binding property and sequence specificity of all PNA oligomers. Thermal denaturation profiles of the hybrids were measured at 260 nm with a CARY 100 Bio UV–Visible spectrophotometer (Varian Ltd.) equipped with a thermal melt system. The DNA·PNA sample (1:1) were prepared in 10 mM sodium phosphate (pH 7.0) at a total volume of 1000  $\mu$ L in a 10 mm quartz cell with a Teflon stopper and equilibrated at the starting temperature for 10 min. The  $A_{260}$  was recorded in steps heating from 20–90  $^{\circ}$ C, cooling 90–20  $^{\circ}$ C and reheating 20–90  $^{\circ}$ C (block temperature) with a temperature ramp of 1  $^{\circ}$ C /min. The temperature recorded was the block temperature and was corrected using the temperature read-out obtained from a built-in temperature probe. The equation for determining the corrected temp was obtained by measuring the actual temp in the cuvette using a temperature probe and plotting against the set temperature ( $T_{\text{block}}$ ) from 20–90  $^{\circ}$ C. The linear equation and relationship were obtained with  $Y = 0.9696X - 0.8396$  and  $r^2 > 0.99$ . In addition, the result taken from the last heating cycle was used and was normalized by dividing the absorbance at each temperature by the initial absorbance.

Correct temperature and normalized absorbance are defined as follows.

$$\begin{aligned} \text{Correct. Temp.} &= (0.9696 \times T_{\text{block}}) - 0.8396 \\ \text{Normalized Abs.} &= \text{Abs}_{\text{obs}} / \text{Abs}_{\text{init}} \end{aligned}$$

The melting temperature ( $T_m$ ) was determined from the maximum of the first derivative after smoothing using KaliedaGraph 3.6 (Synergy Software). Data analysis was performed on a PC compatible computer using Microsoft Excel XP (Microsoft Corp.).  $T_m$  values obtained from independent experiments were accurate within  $\pm 0.5$   $^{\circ}$ C.

## **2.9 PNA hybridization and ion exchange capture experiments**

### **2.9.1 Hybridization between PNA probe and single stranded (synthetic) DNA**

The strong anion exchanger was washed once with deionized water and twice with binding buffer (10 mM sodium phosphate, pH 7.0) and resuspended in the same binding buffer. Equimolar amounts of the PNA probe (or probe mixture) and DNA sample (1 – 100 pmol each) were mixed in 10 mM sodium phosphate buffer pH 7.0 and incubated at room temperature for 20 min. The prepared anion exchanger (3  $\mu$ L, ~3 mg) was added to this PNA·DNA hybrid solution and left for another 20 min at room temperature. After the period of time indicated, the support-bound PNA·DNA hybrid was washed with several aliquots of deionized water or aqueous acetonitrile (3 – 15%) to remove unhybridized PNA probes. One  $\mu$ L of the resulting support-bound PNA·DNA hybrid was suspended in 10  $\mu$ L of matrix solution (a saturated solution of CCA in 0.1% trifluoroacetic acid in 1:2 acetonitrile:water). One  $\mu$ L of the support/matrix mixture was placed on the target, and allowed to dry at room temperature. The sample on the target was then subject to MALDI-TOF mass spectrometry analysis.

### **2.9.2 Hybridization between PNA probe and double stranded DNA (synthetic and PCR samples)**

The anion exchanger was pre-equilibrated in 10 mM sodium phosphate buffer pH 7.0 as explained above. The double-stranded DNA (1 – 10 pmol for synthetic DNA or 5  $\mu$ L for PCR samples) in 30  $\mu$ L of 10 mM sodium phosphate buffer pH 7.0 was first denatured in a boiling water bath for about 5 – 10 min. The mixture was rapidly cooled down at 0 °C and then the pre-equilibrated solid support (3  $\mu$ L, ~3 mg) was immediately added and incubated for 15 – 20 min at room temperature to immobilize the single-stranded DNA. After the period of time indicated, the solid support was then washed with 10 mM sodium phosphate buffer (pH 4) and re-suspended in 30  $\mu$ L of the hybridization buffer (10 mM sodium phosphate buffer pH 7.0). For hybridization, a mixture containing equimolar quantity of each PNA probe was added to the support-bound DNA suspended in the binding buffer. The

hybridization mixture was incubated at room temperature for 15 – 20 min. The support-bound PNA-DNA hybrid was then washed with deionized water ( $3 \times 100 \mu\text{L}$ ) or aqueous acetonitrile (3 – 15%). Finally, 1  $\mu\text{L}$  of the resulting solid support was taken out for analysis by MALDI-TOF mass spectrometry as described above.



ศูนย์วิจัยทรัพยากร  
จุฬาลงกรณ์มหาวิทยาลัย

## CHAPTER III

### RESULTS AND DISCUSSION

In this research, a new conformationally rigid pyrrolidinyl PNA oligomers *ssACPC*-PNA (4) is employed as the sensor probe. The new PNA system consists of C-4 nucleobase-modified proline with *cis*-D configuration and a  $\beta$ -amino acid spacer (1*S*,2*S*)-2-aminocyclopentanecarboxylic acid (ACPC) backbone instead of an aminoethyl glycine segment of *aeg*PNA (Figure 3.1).

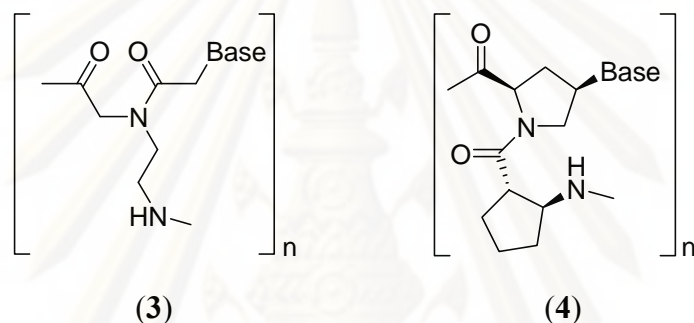
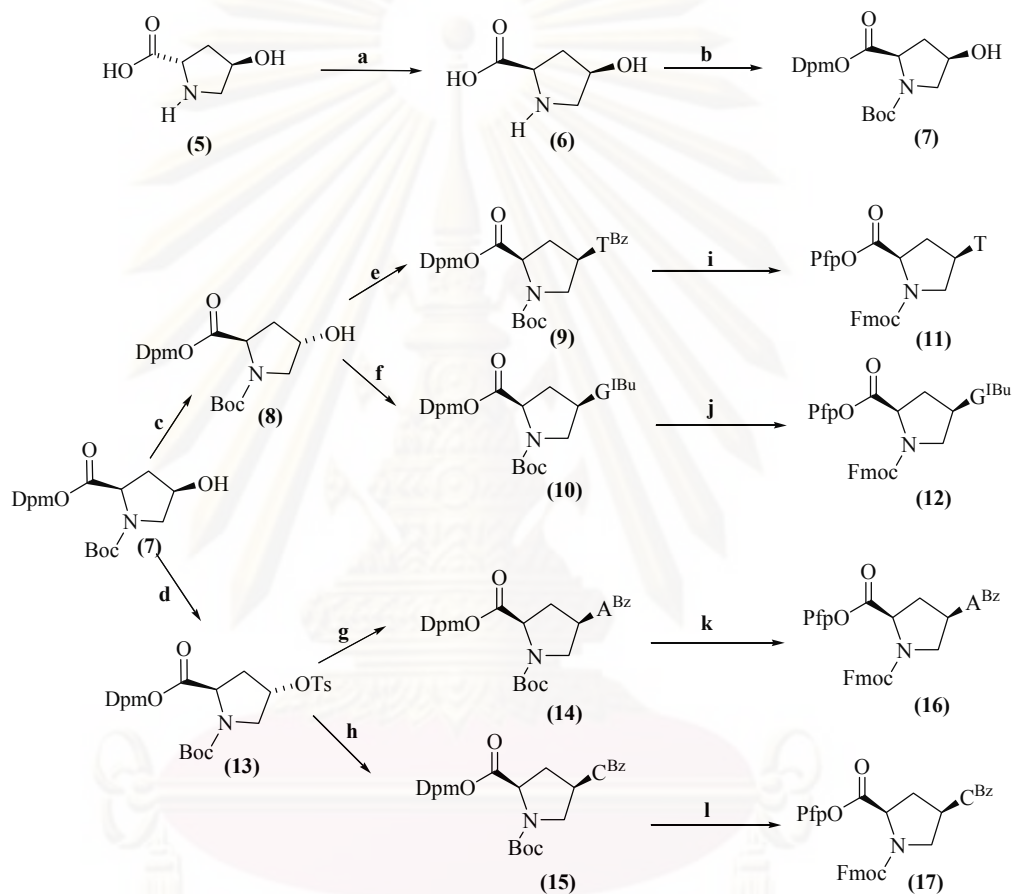


**Figure 3.1** Structure of *aeg*PNA (3) and *ssACPC*-PNA (4)

The synthesis of PNA oligomer was separated into two parts. The first part involves synthesis of the pyrrolidinyl nucleobase monomers and  $\beta$ -amino acid spacer. The identity of each compound was confirmed by comparison of NMR spectra with reference materials previously synthesized in this laboratory. In the second part, the resulting monomer and spacer units were used as monomers for the synthesis of the PNA oligomer *via* solid phase peptide synthesis. Details of each step will be described in the next section.

### 3.1 Synthesis of pyrrolidine nucleobase monomers

The synthetic strategy of all the pyrrolidine monomers has been reported by Vilaivan and co-workers [17–18]. All pyrrolidine nucleobase monomers were constructed from the same starting material - *trans*-4-hydroxy-L-proline. The procedure and the conditions are illustrated in **Figure 3.2**.



**Reagents and conditions:** **a)** i. Ac<sub>2</sub>O, heat 90 °C 16 h; ii. 2 M HCl, reflux 5 h; iii. propylene oxide, MeOH; **b)** i. Boc<sub>2</sub>O, <sup>t</sup>BuOH, NaOH (aq), 8 h; ii. Ph<sub>2</sub>CN<sub>2</sub>, EtOAc, 8 h; **c)** i. HCO<sub>2</sub>H, Ph<sub>3</sub>P, DIAD, THF, 8 h; ii. NH<sub>3</sub>, MeOH, 2 h; **d)** MeOTs, Ph<sub>3</sub>P, DIAD, THF, 8 h.; **e)** *N*<sup>3</sup>-BzT, Ph<sub>3</sub>P, DIAD, THF, 8 h; ii. NH<sub>3</sub>, MeOH, 2 h; **f)** i. *N*<sup>2</sup>-IbuG(ONpe), Ph<sub>3</sub>P, DIAD, dioxane, 8 h; ii. DBU, pyridine 2 h; **g)** *N*<sup>6</sup>-BzA, K<sub>2</sub>CO<sub>3</sub>, DMF, 90 °C 6 h; **h)** *N*<sup>4</sup>-BzC, K<sub>2</sub>CO<sub>3</sub>, DMF, 90 °C 6 h. **i-l)** i. TFA/anisole, 8 h; ii. Fmoc-OSu, NaHCO<sub>3</sub>, MeCN:H<sub>2</sub>O (1:1); iii. Pfp-OTfa. DIEA, CH<sub>2</sub>Cl<sub>2</sub>

**Figure 3.2** The synthetic scheme of all four pyrrolidine monomers (11), (12), (16) and (17) according to Vilaivan *et al.* [17–18, 30]

From the above protocol, the commercially available *trans*-4-hydroxy-L-proline (**5**) was used as the starting material. A diphenylmethyl (Dpm) ester was employed as the carboxyl protecting group in combination with *N*-Boc protection as described in the literature [17]. The *cis*-D pyrrolidinyll monomers consisting of thymine (**9**) and guanine (**10**) were synthesized through Boc/Dpm protected *trans*-4-hydroxy-D-proline intermediate (**8**) by using Mitsunobu reaction. On the other hand, synthesis of the adenine (**14**) and cytosine (**15**) pyrrolidinyll monomers *via* S<sub>N</sub><sup>2</sup> reaction required a *trans*-D tosylate (**13**) intermediate as the substrate. Synthesis of the guanine monomer (**10**) was inefficient due to poor solubility of *N*<sup>2</sup>-IbuG(ONpe) (**21**) under Mitsunobu conditions. To overcome this problem, a new method was also developed starting from 2-amino-6-chloropurine using a procedure described for a different PNA monomer [88] that is shown in the **Figure 3.3**.

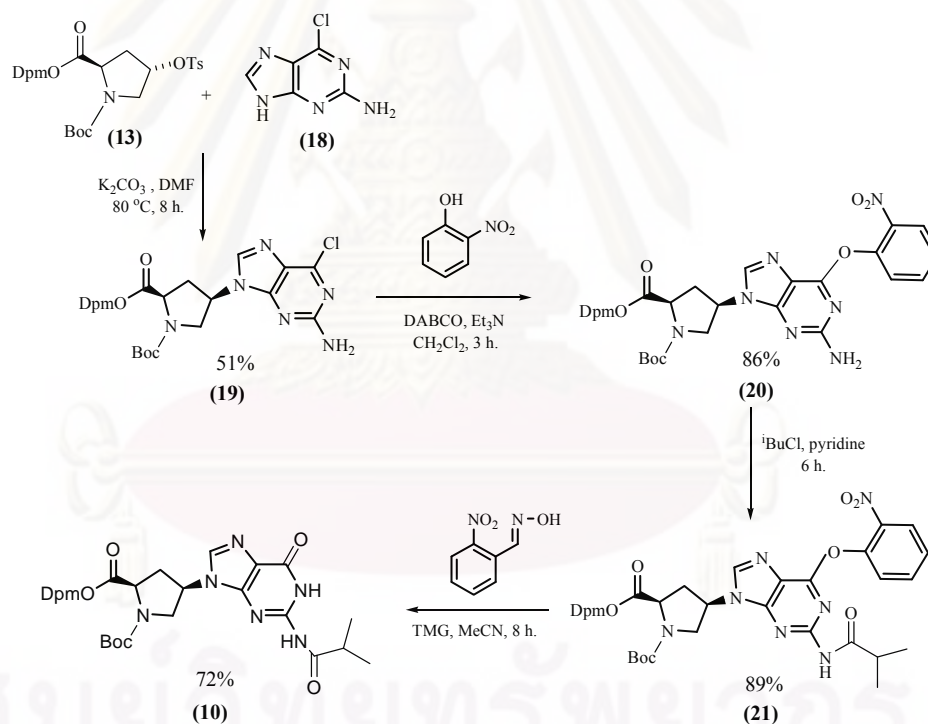


**Figure 3.3** The schematic of synthesized (*N*-Fluoren-9-ylmethoxycarbonylamino)-*cis*-4-(*N*<sup>2</sup>-isobutyrylguanin-9-yl)-D-proline pentafluorophenyl ester (**10**)



From the above figure, the substitution of the *trans*-D tosylate (**13**) with 2-amino-6-chloropurine proceeded smoothly to give the *N*<sup>9</sup>-substitution product (**19**) in 51% yield. A literature method [88] was employed to convert the 2-amino-6-chloropurine monomer to the corresponding *N*<sup>2</sup>-isobutyrylguanine monomer. First, the chlorine was displaced with 2-nitrophenol in the presence of Et<sub>3</sub>N/DABCO to give the *O*-(2-nitrophenylether) (**20**) in 86% yield. The exocyclic amino group was then protected with IbuCl/pyridine to obtain the Ibu-protected derivative (**21**) in 89% yield. Finally the 2-nitrophenyl ether was removed by treatment with 2-nitrobenzaldoxime/*N,N,N',N'*-tetramethylguanidine to afford the Boc/Ibu/Dpm protected guanine monomer (**10**) in 72% yield. The overall yield of the protected intermediate (**10**) starting from the *trans*-D tosylate (**13**) was 28 % yield. The product was identical by TLC and <sup>1</sup>H NMR to the material obtained from the previous method.

After all four Boc/Dpm protected nucleobase pyrrolidinyl monomers (**9**), (**10**), (**14**) and (**15**) were obtained, these compounds were converted into the Fmoc-protected form in order to be used in solid-phase synthesis of PNA oligomer. The Fmoc chemistry was selected to use in the PNA synthesis because of a number of advantages over Boc chemistry.[19] Most importantly, the Fmoc protecting group could be removed under milder conditions (20% piperidine) as compared to the Boc group (50% TFA) [89–90]. Under such a mild deprotection condition, the Fmoc group can be removed without affecting the more stable acyl protecting groups of nucleobase. [91–92] In these PNA monomers, the terminal carboxylic function must be activated to allow condensation reaction between the carboxylic function and the amino group during the solid phase synthesis. Previous work in this group suggested that pentafluorophenyl (Pfp) ester was a suitable activating group because it still provided stable crystalline products [93]. Nevertheless, the reactivity of the Pfp esters may be increased by addition of a nucleophilic catalyst such as hydroxybenzotriazole (HOBt) or its derivatives [94]. Therefore, the target molecules were Fmoc-protected pentafluorophenyl (Pfp) activated nucleobase monomers (**11**), (**12**), (**16**) and (**17**). The structures and yields of the pyrrolidine intermediate and monomers synthesized in this work are shown in **Figures 3.2–3.3**.

The identity of all compounds was confirmed by comparison of NMR spectra with reference materials previously prepared in our laboratory.

### 3.2 Synthesis of (1*S*,2*S*)-2-aminocyclopentanecarboxylic acid (*ss*ACPC) spacer

The (1*S*,2*S*)-2-aminocyclopentanecarboxylic acid spacer was synthesized according to Gellman's protocol [87], with some slight modifications [85–86]. The procedure is summarized as shown in the **Figure 3.4**.

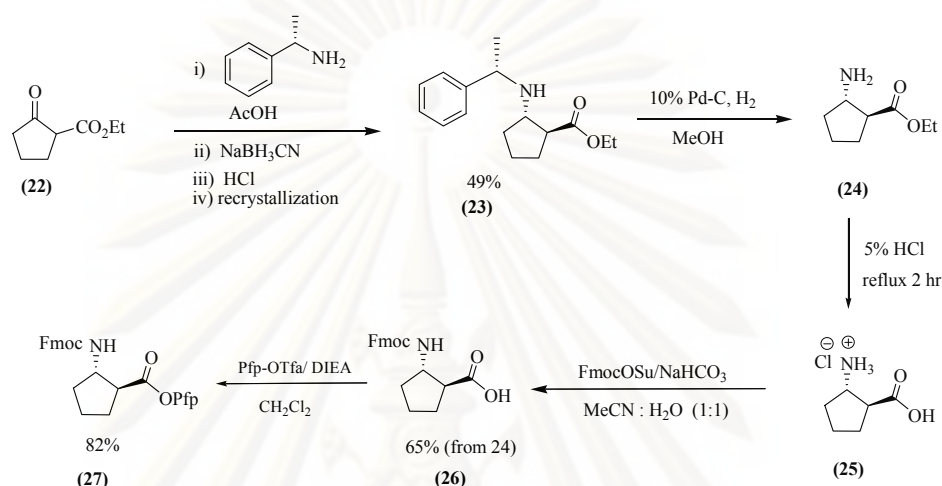


**Figure 3.4** Synthesis of (1*S*,2*S*)-2-aminocyclopentane pentafluorophenyl ester (27)

According to the above strategy, the desired (*S,S*)-*trans* isomer (23) could be obtained as a single diastereomer in the form of crystalline HCl salt (49% yield) by precipitation with 4 N HCl in dioxane followed by recrystallization from ethanol. Hydrogenation over a palladium hydroxide on charcoal catalyst was then performed to remove the *S*-methylbenzylamine chiral auxiliary. This was followed by acid hydrolysis to give the free amino acid as its hydrochloride salt (25). The free amino group was further protected with Fmoc to give the Fmoc(1*S*,2*S*)-2-aminocyclopentanecarboxylic acid (26) as the desired product in 65 % yield (from compound (24)) without the need for chromatography. The correct stereoisomer was confirmed by optical rotation. In order to use *ss*ACPC spacer in condensation reaction between carboxylic acid and an amine to form amide bond, the Fmoc protected acid (26) was also activated with Pfp group similar to the pyrrolidine nucleobase monomers. The Fmoc/Pfp *ss*ACPC monomer (27) was obtained as a white solid in 82% yield. The structures and stereochemistry of compounds (26) and (27) were

ascertained by comparison of the NMR spectra and optical rotation values with reference materials.

### 3.3 Synthesis of carboxybutyltriphenylphosphonium bromide *N*-hydroxysuccinimidyl ester

According to the literature, it had been suggested that a labeling group carrying the positive charge might enhance the sensitivity of MALDI-TOF mass spectrometry which operated in positive-ion mode [73, 95]. Since all PNA oligomers were analyzed in positive-ion mode in this work, it was proposed that incorporating of a positive charge tag to the PNA would increase the sensitivity of the detection. In this study, a permanent charge tag – carboxybutyltriphenylphosphonium – was attached to the N-terminus of the PNA *via* an amide bond. This required activation of the carboxyl group of the commercially available charge tag to form an active ester. Succinimidyl ester was chosen because this group acted as a good leaving group and could enhance the efficiency of condensation reaction between the tag and the PNA. Carboxyl activation was performed by reaction of the corresponding carboxylic acid (as a bromide salt) (1) and *N*-hydroxysuccinimide in the presence of *N,N'*-dicyclohexylcarbodiimide (DCC) in dichloromethane. The mechanism of this reaction is shown in **Figure 3.5**

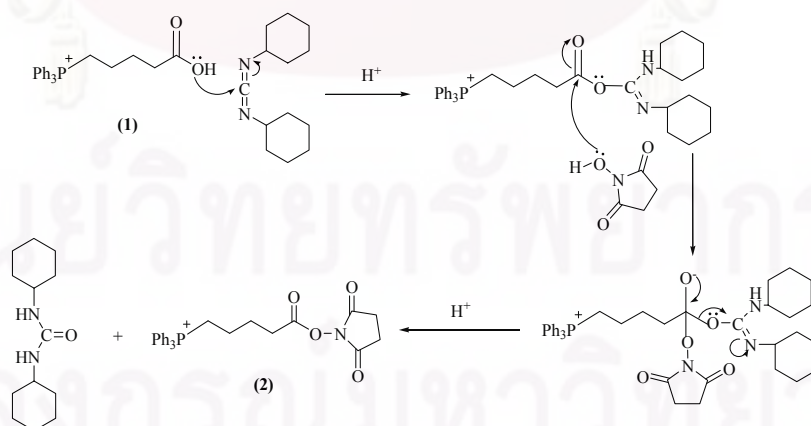
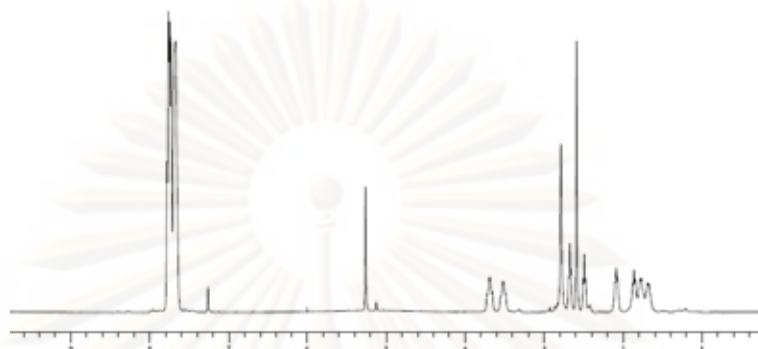
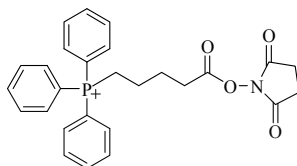


**Figure 3.5** The synthetic mechanism to formation of carboxybutyl triphenylphosphonium bromide *N*-hydroxysuccinimidyl ester (2)

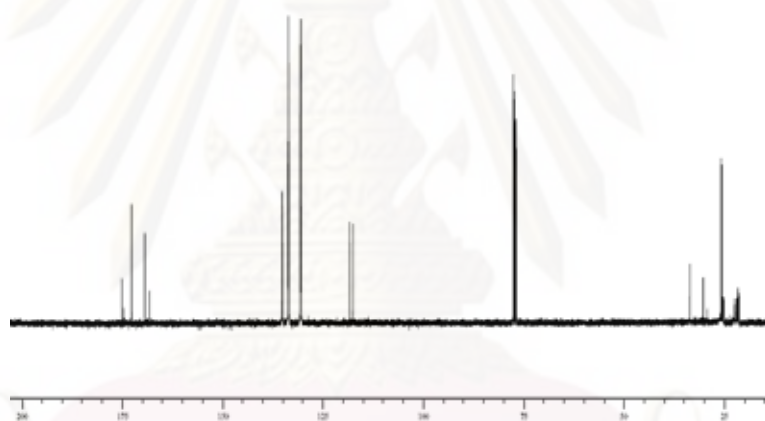
According to the mechanism, the carboxylate ion added to the electrophilic carbon of the diimide, giving an activated acyl derivative (*O*-acylisourea). This activated derivative reacted readily with the *N*-hydroxysuccinimide to give the desired active ester. In this step, *N,N'*-dicyclohexylurea (DCU) serves as an excellent leaving group.[96] The DCU precipitated as a white solid which could be easily removed by filtration. The product (**2**), being appreciably soluble in DCM and H<sub>2</sub>O, was isolated from the remaining DCU by extraction. The purified succinimidyl ester (**2**) was obtained as a colorless oil in a simple one-pot reaction in high yield (85 %) and acceptable purity. The structure of the desired product was confirmed by <sup>1</sup>H NMR and <sup>13</sup>C NMR spectra which are shown in the **Figure 3.6**.



ศูนย์วิจัยทรัพยากร  
จุฬาลงกรณ์มหาวิทยาลัย



(a)



(b)

**Figure 3.6** (a)  $^1\text{H}$  NMR (400 MHz,  $\text{CDCl}_3$ ) and (b)  $^{13}\text{C}$  NMR (100 MHz,  $\text{CDCl}_3$ ) spectra of carboxybutyl triphenylphosphonium bromide *N*-hydroxysuccinimidyl ester (**2**).

From the **Figure 3.6**, the  $^1\text{H}$  NMR spectrum of compound (**2**) showed the following important signals:  $\delta$  7.77–7.60 (m, 15H, ArH), 3.68 (t,  $J=14.9$  Hz, 1H, PCHH CH<sub>2</sub>), 3.51 (t,  $J=14.9$  Hz, 1H, PCHHCH<sub>2</sub>), 2.78 (s, 2H, COCH<sub>2</sub> CH<sub>2</sub>), 2.67 (t,  $J=6$  Hz, COCHHCH<sub>2</sub>), 2.58 (s, 2H, COCH<sub>2</sub>CHH), 2.47 (t,  $J=6$  Hz, 1H, COCHHCH<sub>2</sub>), 2.08 (t,  $J=6.4$  Hz, 1H, CH<sub>2</sub>CHHCH<sub>2</sub>), 1.85 (t,  $J=6.6$  Hz, CH<sub>2</sub>CHHCH<sub>2</sub>), 1.80–1.60 (m, 2H, CH<sub>2</sub>CH<sub>2</sub>CH<sub>2</sub>).  $^{13}\text{C}$  NMR spectrum of compound (**2**) revealed the following important signals:  $\delta_{\text{C}}$  21.5 [ $^1J_{\text{CP}} = 46$  Hz, Ph<sub>3</sub>P-CH<sub>2</sub>CH<sub>2</sub>] 25.4 and 25.7

[COCH<sub>2</sub>CH<sub>2</sub>CO], 21.2 [<sup>2</sup>J<sub>CP</sub> =31 Hz, Ph<sub>3</sub>P-CH<sub>2</sub>CH<sub>2</sub>], 21.8 [<sup>3</sup>J<sub>CP</sub> =25 Hz, Ph<sub>3</sub>P-CH<sub>2</sub>CH<sub>2</sub>CH<sub>2</sub>], 130.4, 130.6, 130.7 [<sup>1</sup>J<sub>CP</sub> =46 Hz, <sup>1</sup>J<sub>CP</sub> =76 Hz, <sup>1</sup>J<sub>CP</sub> =46 Hz, Ph<sub>3</sub>P-C<sub>Ar</sub>], 117.5, 118.3, 133.5, 133.7, 135.1 [CH<sub>Ar</sub>PPh<sub>3</sub>], 172.7, 175.1 [CO succidimidyl ester], 169.4 [CH<sub>2</sub>CO]. The values are fully consistent with the expected structures, indicating that the reactions were successful.

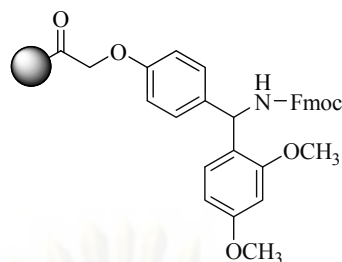
Since this compound is new, the identity of the compounds was further confirmed by the elemental analysis (EA) and the experimental values were in good agreement with the calculated number. From <sup>1</sup>H, <sup>13</sup>C NMR and EA data, it can be concluded that the expected product (**2**) had been successfully synthesized in good purity suitable for PNA labelling in the next step.

### 3.4 Synthesis of PNA oligomers

#### 3.4.1 Solid phase synthesis of *acpc*PNA using standard conditions

In this research, Fmoc-based solid phase peptide synthesis [97] was employed to construct the *ss*ACPC-PNA. The desired PNA sequence was obtained by alternately coupling of the Fmoc-protected PNA monomers and spacer onto a solid support according to the previously developed protocol. [85]

The PNA synthesis was carried out manually at 1–2 micromoles scale in a custom-made peptide synthesis column as described in experimental section. A commercially available polystyrene-based Tentagel resin [98] bearing a PEG graft and a moderately acid labile Rink amide (RAM) linker (**Figure 3.7**) [99] was employed as the solid support. This linker was designed to release peptide acids or amides upon treatment under acid condition (95% TFA) and stable under basic conditions, which makes it compatible with Fmoc chemistry.



 = PEG grafted on polystyrene solid support

**Figure 3.7** TentaGel S RAM Fmoc resin

In general, the solid phase peptide synthesis of PNA oligomers consists of three major steps: deprotection, coupling and capping. The deprotection step involves removal of Fmoc protecting group from the terminal amino group of the growing PNA oligomers. This step is usually achieved under basic conditions. The coupling step involves reacting the activated PNA monomer with the *N*-terminus of the resin-bound PNA oligomer. The final capping step is required to inactivate the resin-bound amino group that had not been successfully coupled during the previous step. The three-step cycles are repeated until the desired PNA oligomer was obtained. After coupling the last monomer, the PNA-bound resin was cleaved from the resin using TFA. Synthesis of PNA oligomers were carried out using two different protocols as described next.

In the first protocol, the PNA synthesis was performed according to a previously developed method in this laboratory [85-86]. In details, after swelling the resin (~ 1 h) in anhydrous DMF, removal of the *N*-terminal Fmoc group was first performed by treatment with 20% piperidine in anhydrous DMF for 15 min to obtain free amino *N*-terminus. After the deprotection, a hydrophilic amino acid such as Fmoc-Lys(Boc)-OPfp or Fmoc-Ser(tBu)-ODhbt was then coupled to the resin as the first residue to enhance the solubility of PNA oligomer. After the anchoring of the first amino acid residue, the Fmoc deprotection step was repeated to expose the free amino group at the *N*-terminus. The resin was then alternately coupled with the activated pyrrolidine monomers and spacer. Similar to lysine or serine loading, coupling of the pyrrolidine monomers and spacers were generally carried out using excess (4 equivalents) in conjunction with 4 equivalents of HOAt and DIEA in

anhydrous DMF for 30 min. Washing with DMF was performed in each step to remove the excess reagents. After the coupling step, any unreacted amino groups were capped by treatment of the resin with 10 % Ac<sub>2</sub>O/DIEA in DMF (10 min) in order to stop the formation of deletion sequence. The coupling efficiency in each step was determined by measurement of the absorbance of dibenzofulvene-piperidine adduct released upon removal of Fmoc group at 264 nm and was calculated from UV-absorption. Subsequently, the next cycle (deprotection, coupling and capping) were repeated with the same procedure until the growing peptide chain was extended to the desired sequence.

The PNA **P1–P2** and **P7–P8** were synthesized in this way. The PNA **P3–P6** was a generous gift from Dr. Choladda Srisuwanaket and Miss Cheeraporn Anantanawat. The percent coupling efficiency (overall and average) during the synthesis of the PNA **P1**, **P2**, **P7** and **P8** as measured from UV absorbance at 264 nm of the deprotection solution is reported in **Table 3.1**.

**Table 3.1** An average coupling efficiency/step and overall coupling efficiency in the synthesis of PNA sequences used in this study.

Sequence	Scale ( $\mu$ mole)	Coupling efficiency (%)	
		average	overall
H-TTTTTTTTTT-Lys-NH <sub>2</sub> ( <b>P1</b> )	1.0 $\mu$ mole of resin	96.9	79.4
H-GTAGATCACT-Ser-NH <sub>2</sub> ( <b>P2</b> )		98.3	70.8
H-AAAATCCCATT-Ser-NH <sub>2</sub> ( <b>P7</b> )	2.0 $\mu$ mole (split in to 2 reactions)	97.8	61.1
H-AAAATTCCA TT-Ser-NH <sub>2</sub> ( <b>P8</b> )		98.9	79.2

From the data above, an average coupling efficiency of >95% per step was achieved, which translated into >60% overall coupling efficiency. The exact figures depend on length and sequence of the PNA.

After the coupling of final monomer, the *N*-terminal Fmoc group was then removed to obtain the free amino group. In case of the PNA **P1** and **P2**, the resulting free amino was subsequently acetylated using 10% Ac<sub>2</sub>O/DIEA in anhydrous DMF in



order to enhance the stability of PNA oligomer. In the cases of PNA **P7** and **P8**, their free amino N-termini were modified with arginine using Fmoc-Arg (Mtr)-OH in the presence of HATU/DIEA. The mechanism of the coupling reaction is revealed in **Figure 3.8**. Next, the *N*-Fmoc group of arginine was removed and the free amino group was capped by acetylation similarly to the PNA **P1** and **P2**. In case of PNA oligomers having adenine, cytosine and guanine bases, the nucleobase protecting groups (Bz for A and C, Ibu for G) must be removed prior to the cleavage from the resin (*vide infra*) by treatment with 1:1 aqueous ammonia/dioxane at 60 °C [28].

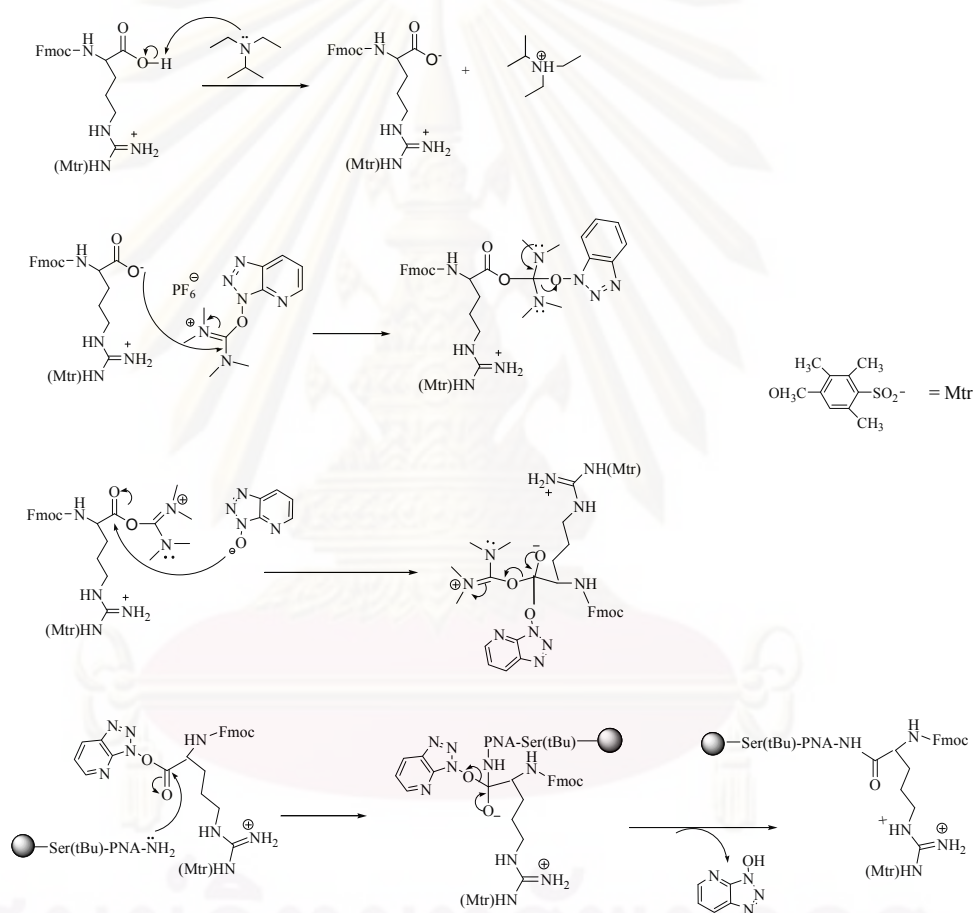


**Figure 3.8** Mechanism for coupling of Fmoc-Arg(Mtr)-OH via HATU activator

In the second protocol, a slight modification of the first protocol was made to shorten the synthesis time without compromising the synthesis efficiency. To reduce the time required in the deprotection step, a mixture of a strong base 2% DBU and 2% piperidine (to trap the electrophilic dibenzofulvene released upon Fmoc deprotection) in DMF was employed in the deprotection step in place of 20% piperidine previously

employed and the deprotection time was decreased to 5 min. Furthermore, all coupling reagents were prepared as stock solutions as follows: DIEA stock solution (7% DIEA in anhydrous DMF) and HOAt stock solution (5.5 mg HOAt in 100  $\mu$ L anhydrous DMF). In the coupling step, the activated nucleobase monomers or spacer was first mixed with 15  $\mu$ L of DIEA stock solution and 15  $\mu$ L of HOAt solution and then the resin was treated with activated monomer solution for 30 min. In the capping step, the capping reagent was also prepared from the mixture of acetic anhydride (2.0  $\mu$ L) and DIEA stock solution (30  $\mu$ L) and the capping time was reduced to 5 min. The coupling efficiency was monitored and calculated similar to the first strategy.

Six PNA sequences, **P9–P14**, were synthesized *via* the second protocol at 1.5  $\mu$ mol scale. The percent coupling efficiency (overall and average) of PNA **P9–P14** was reported in **Table 3.2**.

**Table 3.2** An average coupling efficiency/step and overall coupling efficiency in the synthesis of **PNA** sequences used in this study.

Sequence	Scale ( $\mu$ mole)	Coupling efficiency (%)	
		average	overall
H-TTCCCCCTCCCAA-Ser-NH <sub>2</sub> ( <b>P9</b> )	0.75 $\mu$ mole of resin (split in to 2 reactions)	97.9	57.8
H-TTCCCCTTCCCAA-Ser-NH <sub>2</sub> ( <b>P10</b> )		98.0	59.8
H-ATGTAACATCTCT-Ser-NH <sub>2</sub> ( <b>P11</b> )		98.3	64.6
H-ATGTAATATCTCT-Ser-NH <sub>2</sub> ( <b>P12</b> )		98.0	59.2
H-GCCTGTAAGTAG-Ser-NH <sub>2</sub> ( <b>P13</b> )		97.5	52.3
H-GCCTGTCCTGTAG-Ser-NH <sub>2</sub> ( <b>P14</b> )		97.1	47.2

From the above table, high average coupling efficiency (97–98%) was usually achieved which translated into overall coupling efficiency over 50%, depending on the length and sequence of the PNA.

Prior to the final cleavage from the resin, the *N*-termini of the PNA **P9–P14** were further modified with the carboxybutyltriphenylphosphonium group in order to increase the sensitivity of detection by mass spectrometry. First, the Fmoc group was

removed by treatment with the deprotection solution. Next the nucleobase exocyclic amino protecting groups (benzoyl group and isobutyryl group) were removed by treatment with hot ammonia solution as described earlier. The resulting on-resin PNA oligomer carrying *N*-terminal amino group was then reacted with a mixture of carboxybutyltriphenylphosphonium bromide *N*-hydroxysuccinimidyl ester (**2**) (10 equiv.) and DIEA (10 equiv) in DMF. The reaction was completed within 1 h as monitored by MALDI-TOF mass spectrometry.

It should be pointed out that the deprotection of nucleobase protecting groups was carried out prior to coupling with the phosphonium label because the carboxybutyltriphenyl phosphonium is unlikely to be stable under strongly basic conditions required for such deprotection. [96] After the coupling was complete, the PNA oligomers were released from the resin by treatment with 95 % trifluoroacetic acid followed by precipitation with diethyl ether. The resulting crude PNA was then purified by reverse-phase HPLC or anion exchange solid support capture method (*vide infra*) and characterized by MALDI-TOF mass spectrometry. The carboxybutyltriphenylphosphonium group enhanced the hydrophobic property of the modified PNA oligomers, making separation of the desired PNA from acetyl-capped deletion products by reverse phase HPLC straightforward.

### 3.4.2 Purification and characterization of PNA oligomer

The PNA **P1**, **P2**, **P9–P14** were purified by C-18 reverse-phase HPLC with UV detection at 260 nm. Fractions containing the pure PNA were combined and freeze-dried. The residues were re-dissolved in 150  $\mu$ L of water and the concentration of the PNA was determined by spectrophotometrically. The identity of the PNA was confirmed by MALDI-TOF mass spectrometry which showed the expected mass of the molecular ion  $[M+H]^+$  or  $[M]^+$ . Typical examples of HPLC chromatogram and mass spectrum of PNA **P10** are illustrated in **Figure 3.9**.

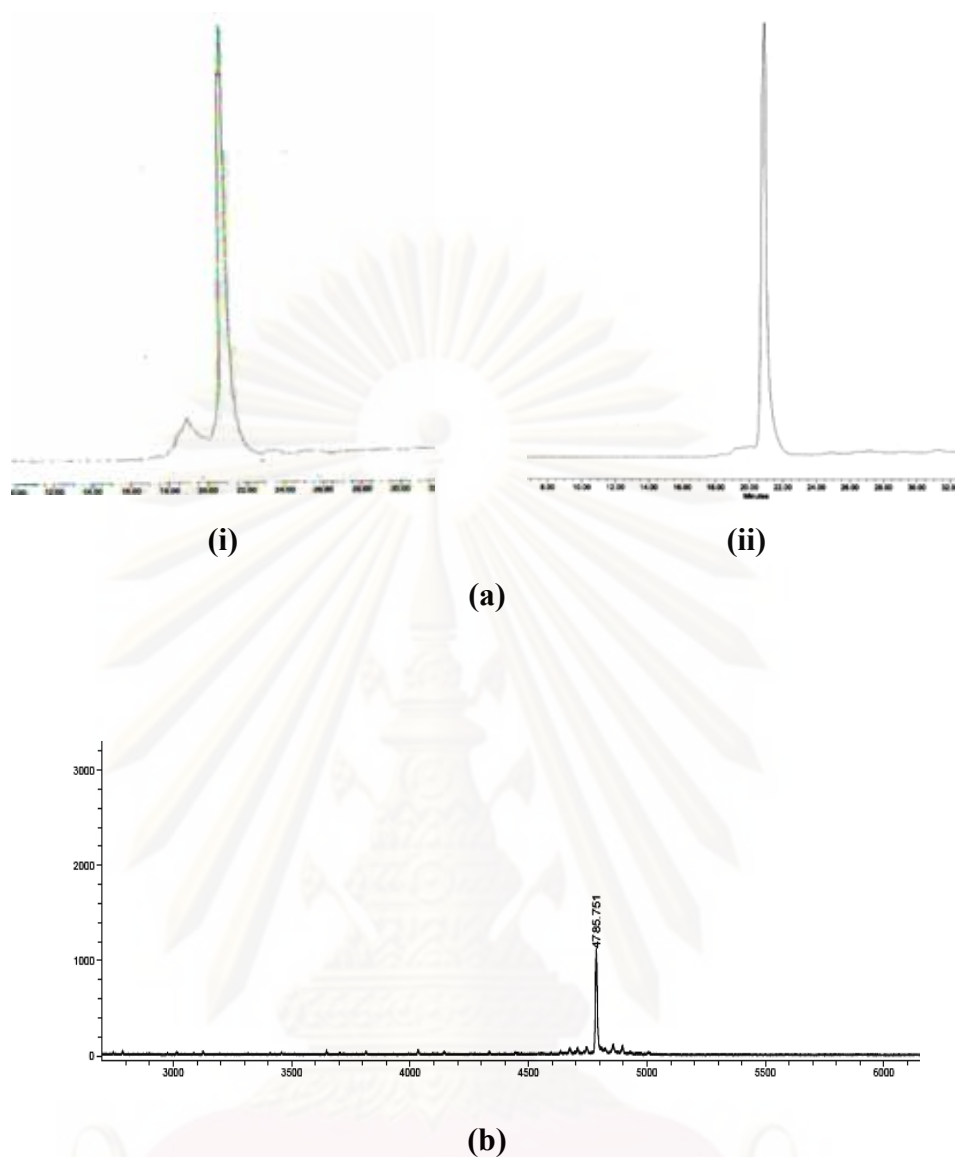


**Figure 3.9** (a) HPLC chromatogram of i) crude and ii) purified PNA (**P10**) and (b) MALDI-TOF MS of purified PNA (**P10**)

HPLC purification of some PNA sequences was problematic especially those carrying *N*-terminal arginine (**P7** and **P8**). It was difficult to separate the complete PNA from acetyl-capped truncated sequences due to the similar polarities of the complete and truncated sequences. In order to solve this problem, an anion exchange capture technique was used to purify the PNA **P7** and **P8** in stead of HPLC. This method relied on the ionic interaction between complete PNA and its complementary DNA-bound support. After hybridization between the PNA and its complementary DNA electrostatically bound to the support, the PNA·DNA-bound support was then

washed with aqueous buffers to eliminate the non-specific PNA probe or incomplete sequences. The existence of the desired PNA in the solid support was analyzed by MALDI-TOF mass spectrometry. After washing, the complete PNA sequence was separated from the DNA-bound support by heating. The desired PNA were then eluted into the solution, which could be monitored by MALDI-TOF mass spectrometry. The typical example mass spectra of PNA **P8** before and after purify are illustrated in **Figure 3.10**.

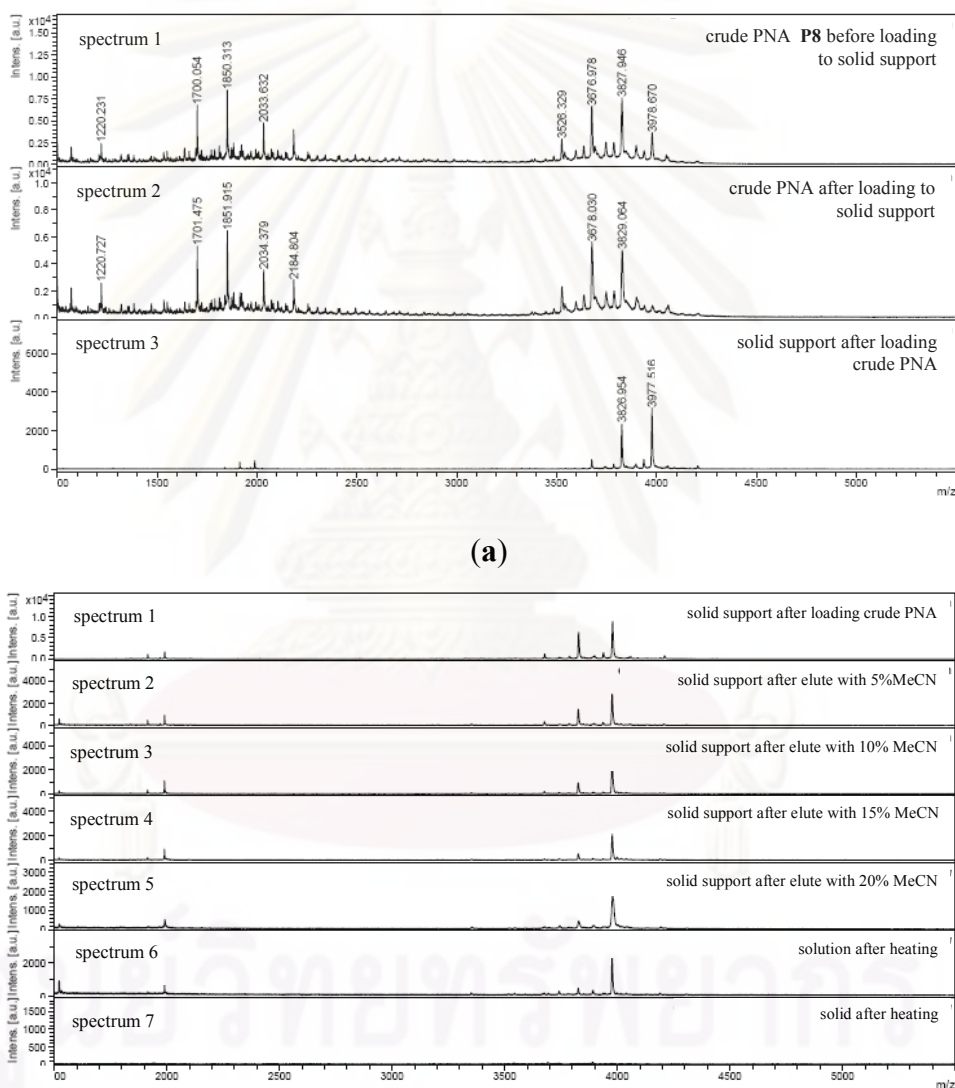


**Figure 3.10** MALDI-TOF MS of PNA **P8**: (a) Before and after hybridization between PNA and DNA-bound support and (b) After elute with several aqueous acetonitrile system and heat in boiling water.

From the above figure, after absorption of the crude PNA solution on the DNA-bound support, the solid support was analyzed by MALDI-TOF mass spectrometry. It was found that the required PNA **P8** ( $m/z = 3978.6$ ) and an unidentified incorrect sequence ( $m/z = 3827.9$ ) were able to hybridize with the DNA-bound support (spectrum 3a). No mass signal of the correct PNA could be found in the crude PNA solution (spectrum 2a). The results indicated that all of the correct PNA completely hybridized with the complementary DNA bound onto the solid support. To remove the absorbed non-specific PNA probe at  $m/z = 3827.9$ , the PNA-DNA bound onto the solid support was washed with various percentage of MeCN in water. After washing, the support was then analyzed by MALDI-TOF (spectra 2b–5b). The percentage of MeCN in water was varied in ranging 5–20% and the result showed that 20% acetonitrile in water could completely eliminate practically all undesired PNA signals (spectrum 6b). The desired PNA oligomer was then released from the DNA-bound support by heating in boiling water. The existence of the expected PNA in the eluent was confirmed by MALDI-TOF mass spectrometry (spectrum 6b). No PNA signal was observed on the solid support after heating (spectrum 7b).

Thereafter, the combined eluted fractions were freeze-dried. The residue was redissolved in 100  $\mu\text{L}$  of water and the concentration of the PNA was determined spectrophotometrically. The purity and identity of the purified PNA was ascertained by HPLC and MALDI-TOF MS as shown in **Figure 3.11**.



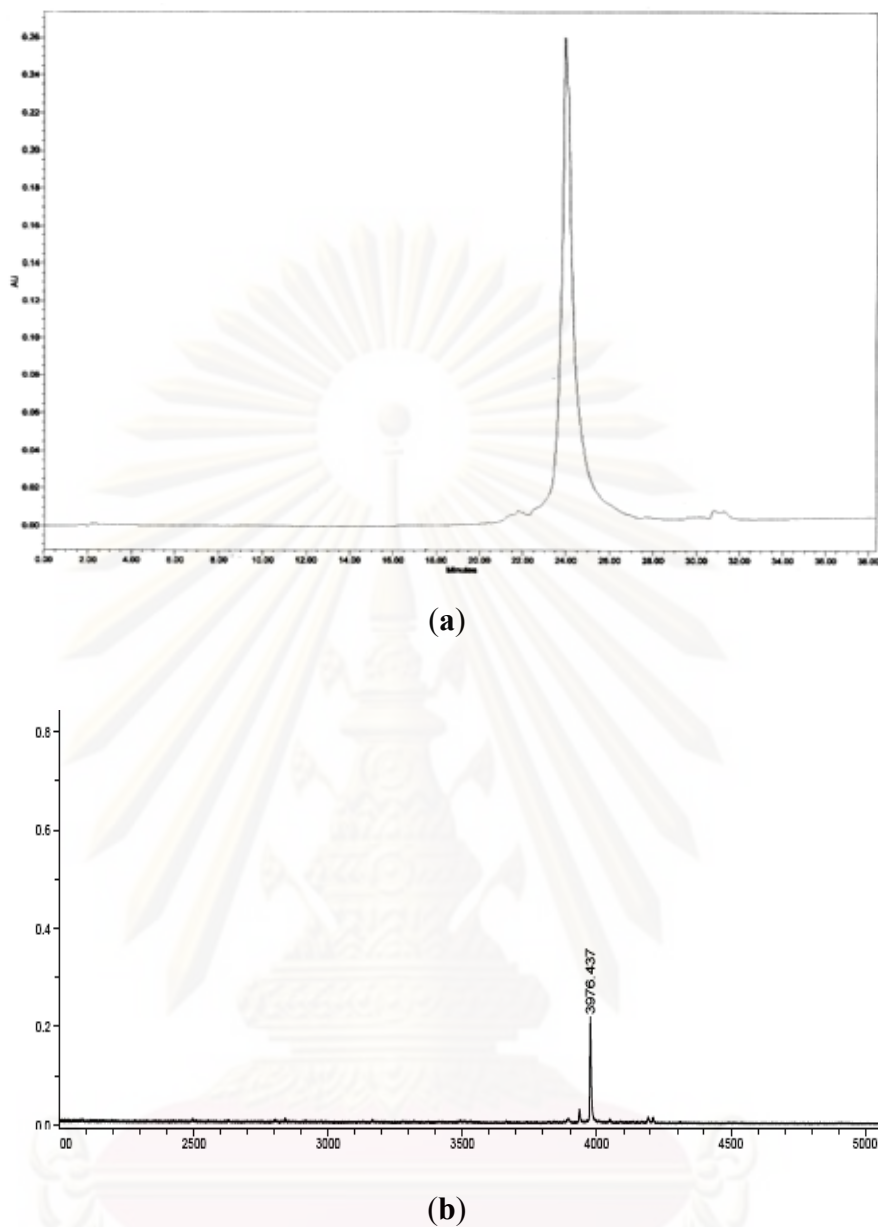


**Figure 3.11** (a) HPLC chromatogram of PNA **P8** and (b) MALDI-TOF MS of PNA **P8** after purify by anion exchange capture

In cases of the PNA **P13** and **P14**, after HPLC purification, some impurities was still present which were difficult to separate from the complete PNA. For example, despite the single peak HPLC chromatogram of the PNA **P14**, a number of unexpected mass peaks were detected in addition of the expected mass of PNA **P14** at  $m/z = 4842.1$  (**Figure 3.12**).

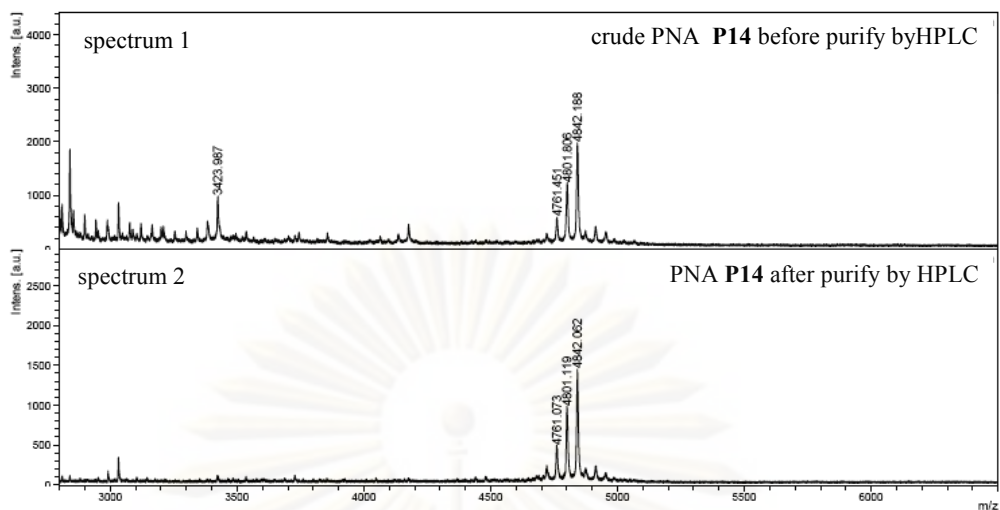


**Figure 3.12** MALDI-TOF MS of PNA **P14** before and after purify by HPLC technique

Consequently, the anion exchange capture technique was again used to purify the PNA oligomers **P13** and **P14** after the unsuccessful HPLC separation. The purification was performed in the same way as described for PNA **P8**, except that the capture DNA sequences were changed so that they are complementary to the PNA to be captured. The results are shown in **Figure 3.13**.

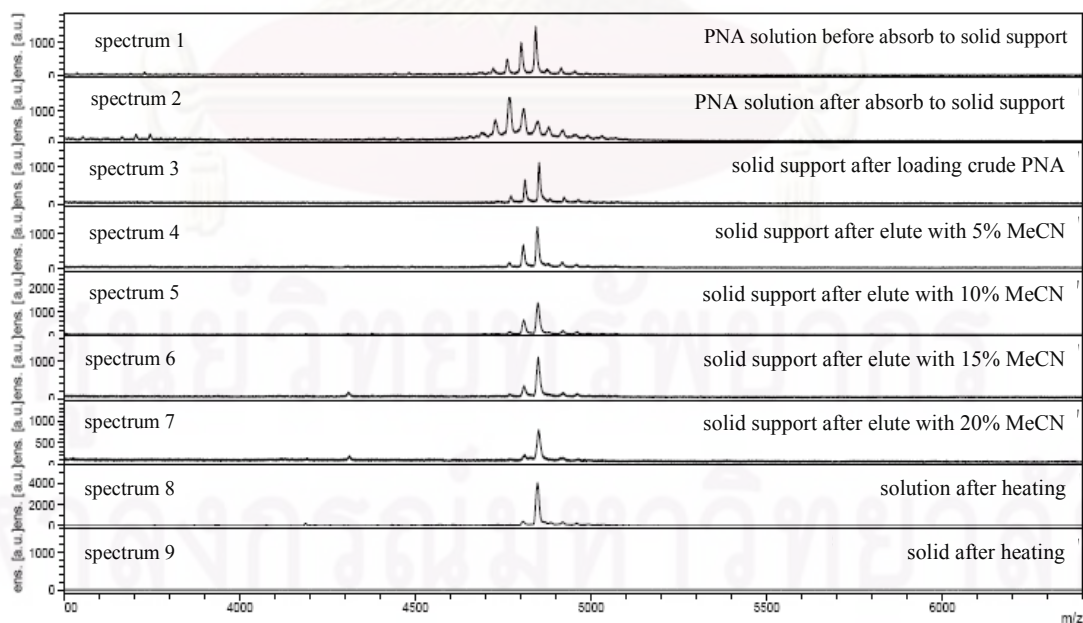


**Figure 3.13** MALDI-TOF MS of PNA **P14** after washing with aqueous MeCN and heating in boiling water.



From **Figure 3.13** after absorption of PNA solution into its complementary DNA-bound support, both the mass peaks of the desired PNA ( $m/z = 4842.1$ ) and non-specific sequences ( $m/z = 4801.1$ ) appeared on the solid support (spectrum 3) whereas the amount of the desired PNA in the remaining solution decreased (spectrum 2). After washing of the solid support with 20% aqueous acetonitrile, only the molecular weight of the desired PNA sequence was observed on the solid support as revealed in spectrum 7. The expected PNA oligomer was then recovered from the solid support as described above. The identity of the PNA was ascertained by MALDI-TOF MS as shown in **Figure 3.14**.

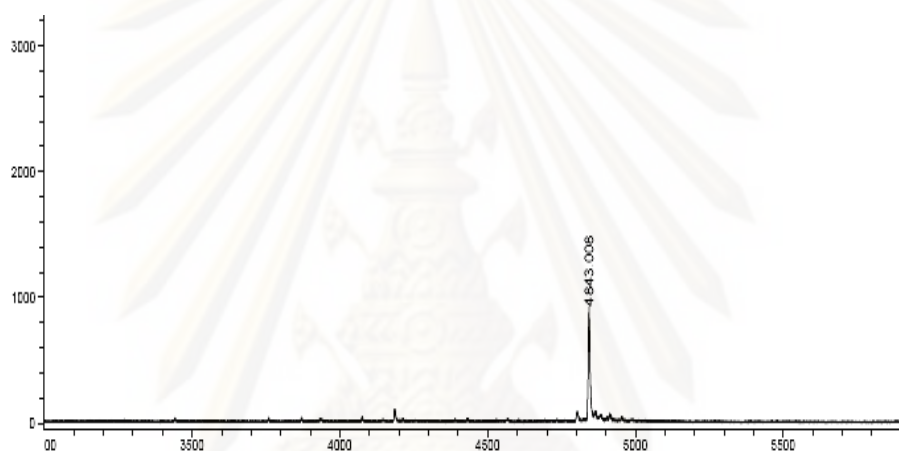


**Figure 3.14** MALDI-TOF MS of PNA P14 after purify by anion exchange solid support capture

After purification with HPLC technique and/or anion exchange capture, all PNA oligomers were obtained in pure form having observed molecular weights in good agreement with the calculated values. The data are shown in **Table 3.3**.

**Table 3.3** Characterization data of all PNA sequences

	PNA <sup>a</sup>	<i>t</i> <sub>R</sub> (min)	<i>m/z</i> (calcd) <sup>b</sup>	<i>m/z</i> (found)
<b>P1</b>	Ac-TTTTTTTTTT-Lys-NH <sub>2</sub>	20.1	3179.4	3179.7
<b>P2</b>	Ac-GTAGATCACT-Ser-NH <sub>2</sub>	21.7	3517.8	3517.6
<b>P7</b>	Ac-Arg-AAAATCCCATT-Ser-NH <sub>2</sub>	23.2	3961.2	3961.5
<b>P8</b>	Ac-Arg-AAA ATTCCATT-Ser-NH <sub>2</sub>	23.8	3976.2	3976.4
<b>P9</b>	P- TTCCCCCTCCCAA -Ser-NH <sub>2</sub>	20.9	4667.8	4668.0
<b>P10</b>	P- TTCCCCTTCCCAA -Ser-NH <sub>2</sub>	20.6	4682.8	4683.3
<b>P11</b>	P-ATGTAACATCTCT-Ser-NH <sub>2</sub>	21.0	4785.9	4785.8
<b>P12</b>	P-ATGTAATATCTCT-Ser-NH <sub>2</sub>	20.0	4800.9	4801.4
<b>P13</b>	P-GCCTGTAAGTAG-Ser-NH <sub>2</sub>	20.1	4818.9	4818.6
<b>P14</b>	P-GCCTGTCCTGTAG-Ser-NH <sub>2</sub>	21.0	4842.9	4843.0

<sup>a</sup>P = carboxybutyl triphenyl phosphonium

<sup>b</sup>average mass: M·H<sup>+</sup> for **P1**, **P2**, **P7**, **P8**, M<sup>+</sup> for **P10–P14**

**P3**, **P4** were synthesized, purified and characterized by Dr. Choladda Srisuwanaket

**P5**, **P6** were synthesized, purified and characterized by Miss Cheeraporn Anantanawat

### 3.5 Hybridization Properties of PNA

UV melting technique was used to study the binding property and sequence specificity of all PNA oligomers. DNA·DNA or PNA·DNA duplexes are formed as a result of hydrogen bonding between complementary bases following the Watson-crick base pairing rules [95, 100–101] and are further stabilized by additional hydrophobic,  $\pi$ - $\pi$  and dipole-dipole interactions between the stacked base pairs. In principle, base-base stacking decreases the molar extinction coefficient ( $\epsilon$ ) value of the pairing DNA strands (hypochromism). Separation of the duplex into single stranded oligonucleotides, e.g. by heating, resulted in unstacking of the DNA or PNA bases, which was accompanied by a slight increase in the extinction coefficient (~ 10–20%) (hyperchromism). The hyperchromicity is conveniently monitored at 260 nm, the wavelength at which all four nucleobases strongly absorb. The resulting plot is known as “melting curve” which is S-shaped (**Figure 3.15**). The temperature at the midpoint of the melting curve is known as melting temperature ( $T_m$ ) which corresponds to a temperature at which 50% of duplex has been dissociated. The cooperativity between base-base interactions required that the melting process occurs

within a relatively narrow temperature range (ca 10–20 °C). Once the input energy is sufficient to break the first hydrogen-bonded base pair, the dissociation continues until the two strands completely separate without detectable intermediate structures. The melting temperature can provide information about the stability of the duplex structure. As an approximation, stable duplexes melt at a higher temperature (have higher  $T_m$ ) than less stable ones when measured under identical conditions (concentration, pH, ionic strength).

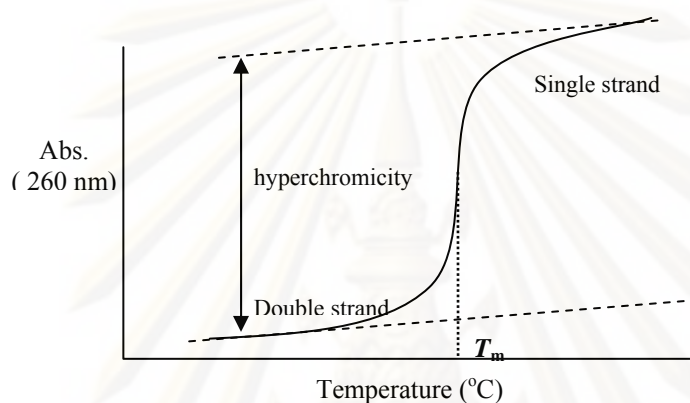


**Figure 3.15** The changing of UV absorbance in the thermal denaturation experiment of DNA duplex.

From the melting curve, the accurate melting temperature ( $T_m$ ) could be determined from the maxima of the first derivative plot ( $dA/dT$ ) against temperature (Figure 3.16).

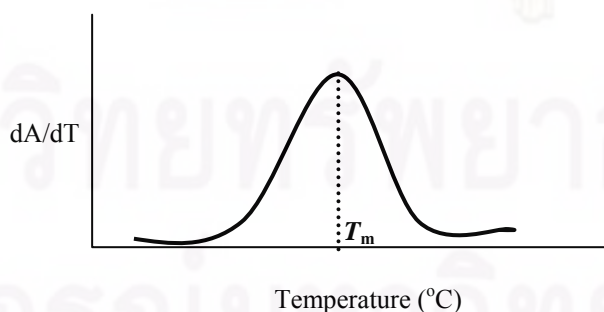


**Figure 3.16** The first derivative plot obtained from a typical thermal denaturation experiment of a DNA duplex.

The results of  $T_m$  experiments of all PNA sequences and their complementary and single mismatched DNA targets are summarized in **Table 3.4**.

**Table 3.4**  $T_m$  data of all PNA oligomers used in this study

PNA <sup>a</sup>	DNA sequence (5'→3')	note	Corrected $T_m$ (°C) <sup>b</sup>	$\Delta T_m$ (°C) <sup>c</sup>
P1	(D1) AAAAAAAAAA	perfect match	74.9	–
P2	(D2a) AGTGATCTAC	perfect match	54.8	–
P3	(D3) AAAA <u>T</u> AAAA	perfect match	67.0	–
	AAAA <u>C</u> AAAA	single mismatch	34.0	–33.0
P4	(D4) AAAA <u>C</u> AAAA	perfect match	64.0	–
	AAAA <u>T</u> AAAA	single mismatch	39.0	–25.0
P5	(D5a) TAGTTGT <u>G</u> ACGTACA	perfect match	78.6	–
	TAGTTGT <u>T</u> ACGTACA	single mismatch	61.1	–17.5
P6	(D6a) TAGTTGT <u>T</u> ACGTACA	perfect match	78.9	–
	TAGTTGT <u>G</u> ACGTACA	single mismatch	60.5	–18.4
P7	(D7) AATGG <u>G</u> ATTTT	perfect match	63.1	–
	AATGG <u>A</u> ATTTT	single mismatch	38.7	–24.4
P8	(D8) AATGG <u>A</u> ATTTT	perfect match	65.9	–
	AATGG <u>G</u> ATTTT	single mismatch	37.8	–28.1
P9	(D9) TTGGG <u>A</u> GGGGAA	perfect match	63.8	–
	TTGGG <u>A</u> GGGGAA	single mismatch	32.4	–31.4

PNA <sup>a</sup>	DNA sequence (5'→3')	note	Corrected $T_m$ (°C) <sup>b</sup>	$\Delta T_m$ (°C) <sup>c</sup>
<b>P10</b>	( <b>D10</b> ) TTGGGA <u>A</u> GGGGAA	perfect match	67.9	–
	TTGGGA <u>G</u> GGGGAA	single mismatch	32.8	–35.1
<b>P11</b>	( <b>D11</b> ) AGAGAT <u>G</u> TTACAT	perfect match	72.6	–
	AGAGAT <u>A</u> TTACAT	single mismatch	52.8	–19.8
<b>P12</b>	( <b>D12</b> ) AGAGAT <u>A</u> TTACAT	perfect match	75.8	–
	AGAGAT <u>G</u> TTACAT	single mismatch	43.9	–31.9
<b>P13</b>	( <b>D13</b> ) CTACAG <u>T</u> ACAGGC	perfect match	75.6	–
	CTACAG <u>G</u> ACAGGC	single mismatch	44.5	–31.1
<b>P14</b>	( <b>D14</b> ) CTACAG <u>G</u> ACAGGC	perfect match	67.7	–
	CTACAG <u>T</u> ACAGGC	single mismatch	51.5	–16.2

<sup>a</sup> The  $T_m$  data of PNA **P3** and **P4** was obtained from Dr. Choladda Srisuwanaket dissertation .[85]

<sup>b</sup>  $T_m$  were measured at [DNA] = [PNA] = 1  $\mu$ M, 10 mM sodium phosphate buffer, pH 7.0, heating rate 1.0 °C/min. Corrected values, as described in section 2.6

<sup>c</sup>  $\Delta T_m = T_m(\text{complementary}) - T_m(\text{mismatched})$  (same PNA, different DNA)

The data in **Tables 3.4** demonstrated that each PNA oligomer can hybridize with its complementary DNA target with a strong affinity. The homothymine nonamers **P1** and its complementary DNA **D1** gave the highest  $T_m$  (74.9 °C) compared to other PNA nonamer. In all cases, the melting temperature of single base mismatch hybrid was significantly lower than that of the perfect match hybrid. When purine base is present in the DNA and/or PNA sequence, a high  $\Delta T_m$  was observed such as PNA **P3** and DNA **D4** (33.0 °C) compared with PNA **P4** and DNA **D3** (25.0 °C). For decamers, the  $T_m$  of PNA **P2** and its complementary DNA **D2a** was 54.8 °C. For pentadecamers, the PNA **P5** and **P6** bind to complementary DNA targets with a high  $T_m$  (78.6 °C and 78.9 °C respectively). A single mismatch at the central positions

in the DNA strands caused a drop in  $T_m$  of 17.5 and 18.4 °C. From the results it was concluded that both short and longer sequences of PNA can form hybrid with complementary DNA in a highly sequence-specific manner, which is in good agreement with the literature [85–86].

The PNA **P7–P14** were designed based on the sequence of DNA to be detected (**P7** and **P8**: bovine and porcine; **P9–P14**: human *IL-10* promoter) in the PCR product. The results in **Table 3.6** indicated that the hybrids of 11mer PNA oligomers (**P7** and **P8**) and their complementary DNA targets provided the highest  $T_m$  values of 63.1 °C and 65.9 °C for the pairs **P7/D7** and **P8/D8** respectively. The presence of single mismatch at the central positions in the DNA strands caused a drop in  $T_m$  (24.4 °C for **P7/D8** and 28.1 °C for **P8/D7**). For 13mers PNA **P9–P14**, the  $T_m$  values of perfect match hybrids were higher than the 11mer PNA **P7** and **P8** (63.8 °C for **P9/D9**, 67.9 °C for **P10/D10**, 72.9 °C for **P11/D11**, 75.8 °C for **P12/D12**, 75.6 °C for **P13/D13** and 67.7 °C for **P14/D13**). In all cases the  $T_m$  values of single mismatched hybrids were ~16–35 °C lower than that of the perfect match hybrids. This high decrease in  $T_m$  confirmed the high affinity and sequence specificity of the new *acpc*PNA. Therefore, the PNA should be suitable to use as a probe for DNA sequence analysis.

### 3.6 Ion-exchange capture technique for DNA sequence analysis

#### 3.6.1 The principle

This research focused on the development of a new technique for DNA sequence analysis by using *ssACPC* PNA probes. The present method relies on a selective adsorption of a negatively charged PNA·DNA hybrid over unhybridized PNA by an anion exchanger. PNA is an electrostatically neutral molecule, therefore it cannot be immobilized onto the anion exchanger unless it is first hybridized with a negatively-charged complementary DNA target to form a negatively charged PNA·DNA hybrid. After hybridization, the negatively-charged hybrids can then be absorbed onto the solid support. The support bound PNA·DNA hybrid was isolated from the unhybridized PNA by simple washing. The presence of the PNA·DNA hybrid on the support can be detected by various means such as MALDI-TOF mass

spectrometry. PNA is very suitable for analysis with MALDI-TOF technique because it is less prone to fragmentation during the MALDI process. Furthermore, due to the much better ionization of PNA than DNA under the MALDI-TOF analysis conditions, interference by the mass signal of DNA is expected to be minimal. [74] The principle of the present method is illustrated in **Figure 3.17**.

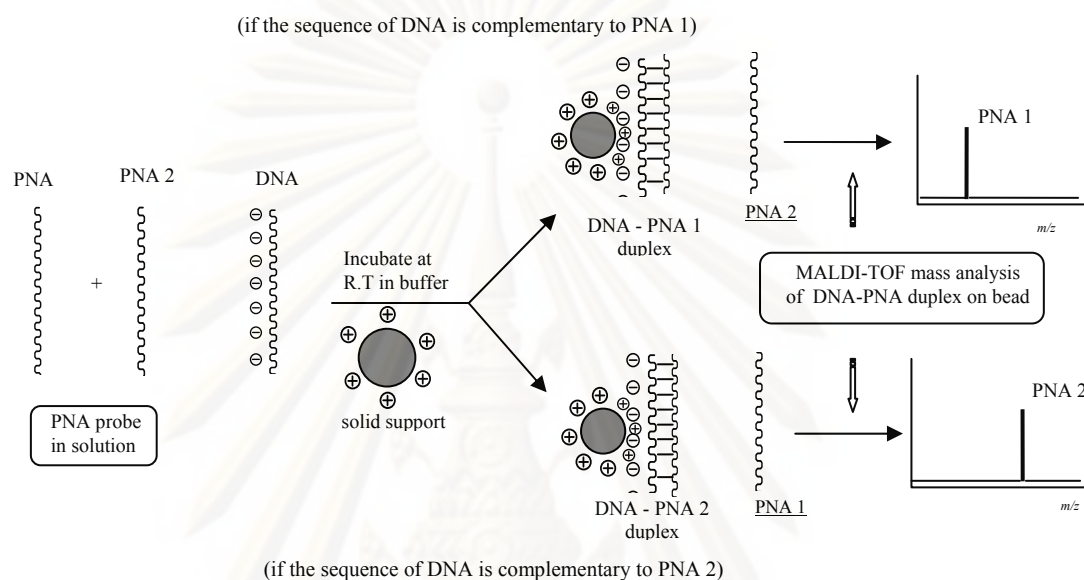


**Figure 3.17** The concept of DNA sequence determination by employing a solid anion exchanger support to selectively capture complementary PNA·DNA hybrids followed by subsequent MALDI-TOF analysis.

### 3.6.2 Validation of the concept

To validate the ion-exchange capture concept explained above, a preliminary experiment was first investigated by using quaternary ammonium (trimethylaminopropyl) modified silica (SAX, Varian) as the anion exchange support.

Its structure of which is shown in **Figure 3.18**.

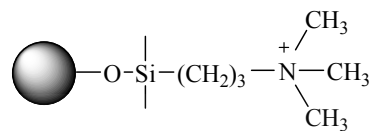


**Figure 3.18** Structure of quaternary ammonium modified silica (trimethylaminopropyl)

The ability of this anion exchanger to absorb PNA and PNA·DNA hybrids was first determined. Two PNA probes containing single base mismatch to each other namely Ac-TTTTATTTT-Lys-NH<sub>2</sub> (**P3**,  $m/z = 3186.48$ ) and Ac-TTTTGTTTT-Lys-NH<sub>2</sub> (**P4**,  $m/z = 3202.47$ ) were selected as models. Two DNA targets: dAAAATAAAA (**D3**) that is complementary with PNA (**P3**) and dAAAACAAAA (**D4**) that is complementary with PNA (**P4**) were also chosen as models. In the experiment, a mixture of the two PNA probes (100 pmol each) in 30  $\mu$ L of 10 mM phosphate buffer pH 7.0 as binding buffer was hybridized with each DNA target (200 pmol). The hybridization mixture was incubated at room temperature for 15 min. Subsequently, the anion exchange support (SAX) was added to the PNA·DNA hybrid solution and incubated at room temperature for another 15 min. The support bound PNA·DNA duplex was extensively washed with Milli Q water and then analyzed for the presence of PNA by MALDI-TOF mass spectrometry. The results are shown in **Figure 3.19**.

ศูนย์วิทยทรัพยากร

จุฬาลงกรณ์มหาวิทยาลัย



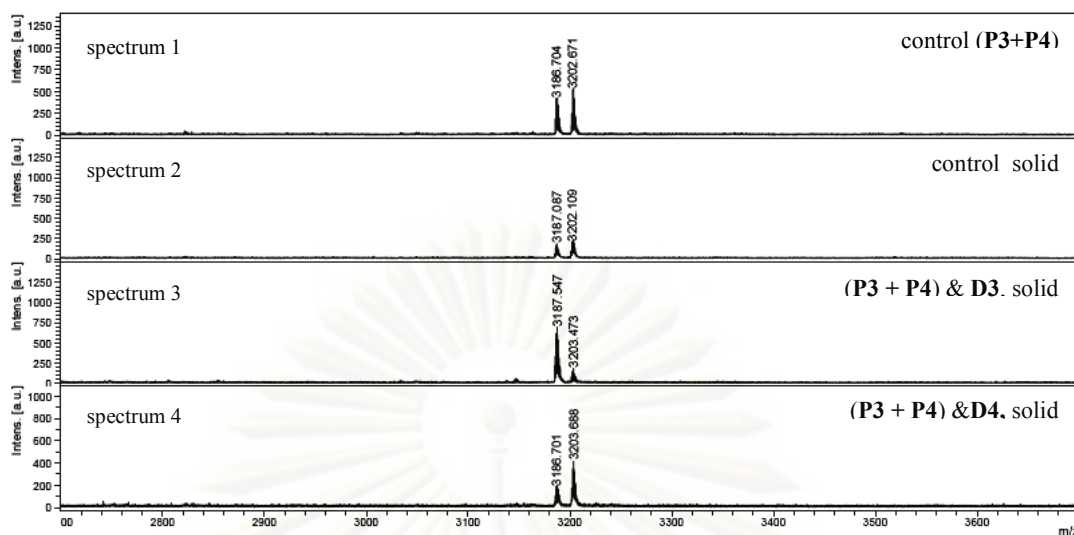
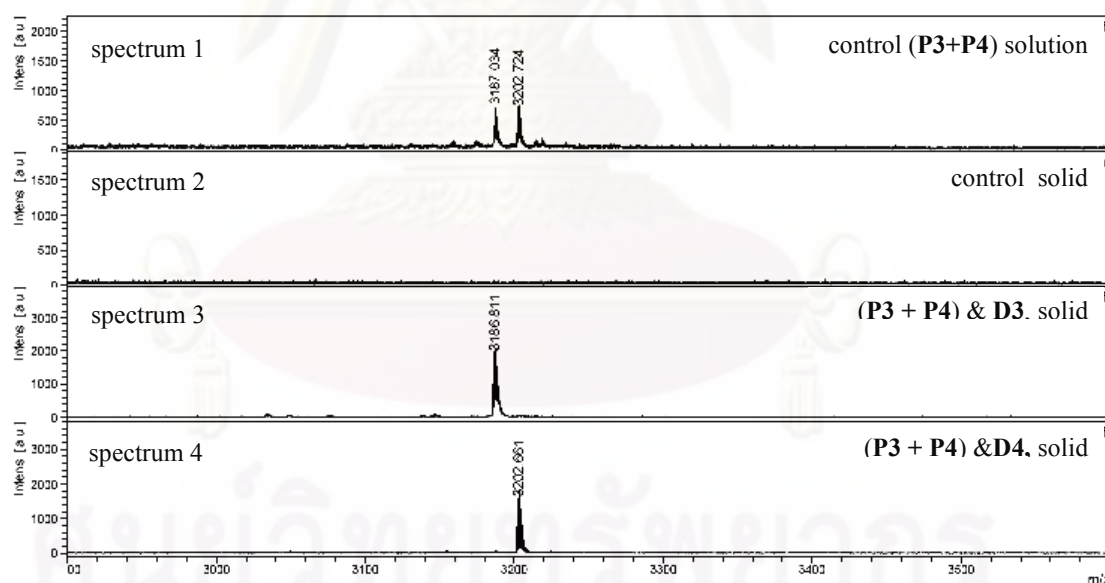


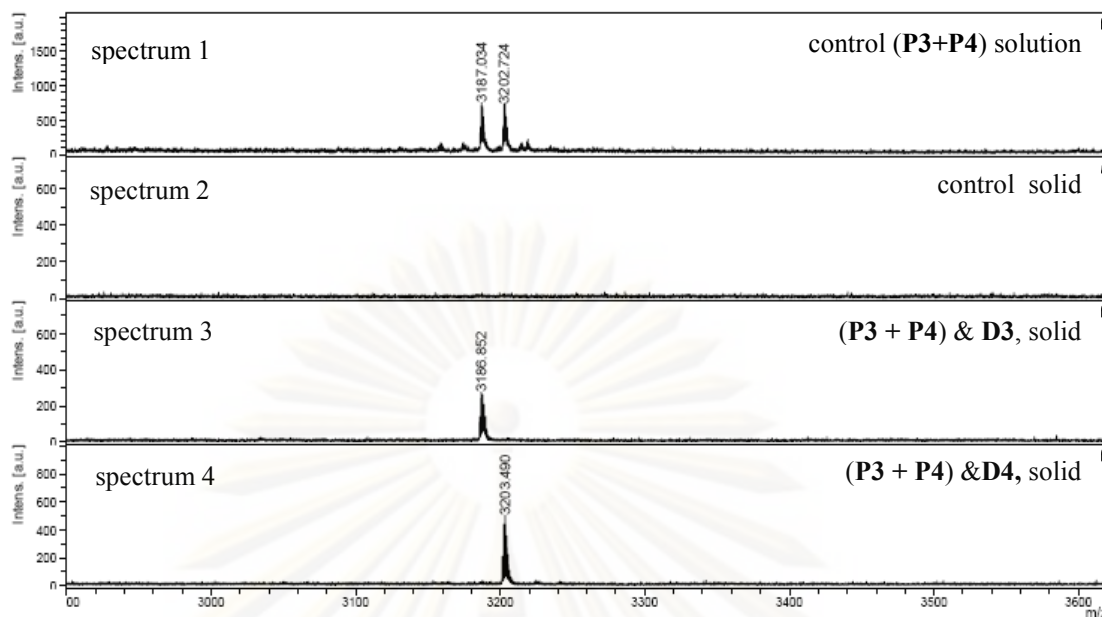
**Figure 3.19** MALDI-TOF analysis of a mixture of two PNA probes, **P3** and **P4**, after hybridization with the DNA targets (**D3** or **D4**) using anion exchanger (SAX) as solid support. Experiments from top to bottom: no DNA (solution), no DNA (solution), +**D3** (solid), +**D4** (solid)

From the above figure, the spectrum 1 was obtained from the solution of the PNA probes without DNA after removing the solid support. This was a solution control experiment and two PNA signals are expected. Spectrum 2 was obtained from the separated solid support in the absence of DNA. This was a solid control experiment and no PNA signals are expected. However, the two PNA signals could be observed in both control experiments indicating that non-specific absorption of the PNA onto the solid support could take place to some extent. However, the intensity of the probe signals in solution was substantially higher than in the solid. Upon addition of **D3** (complementary with PNA **P3**) to the mixed PNA probe solutions, spectrum 3 was obtained from the washed solid support. In this case the signal of PNA **P3** was observed as the major component. On the other hand, spectrum 4 was obtained from the washed support after adding DNA **D4** (complementary with PNA **P4**). The result revealed the signal of PNA **P4** as the major component. The experiments therefore validated the ion exchange capture concept. However, significant background absorption of the non-complementary PNA probes was also observed on the solid support. The background absorption of the non-complementary PNA probe was assumed to involve hydrophobic interaction between PNA probes and the support.

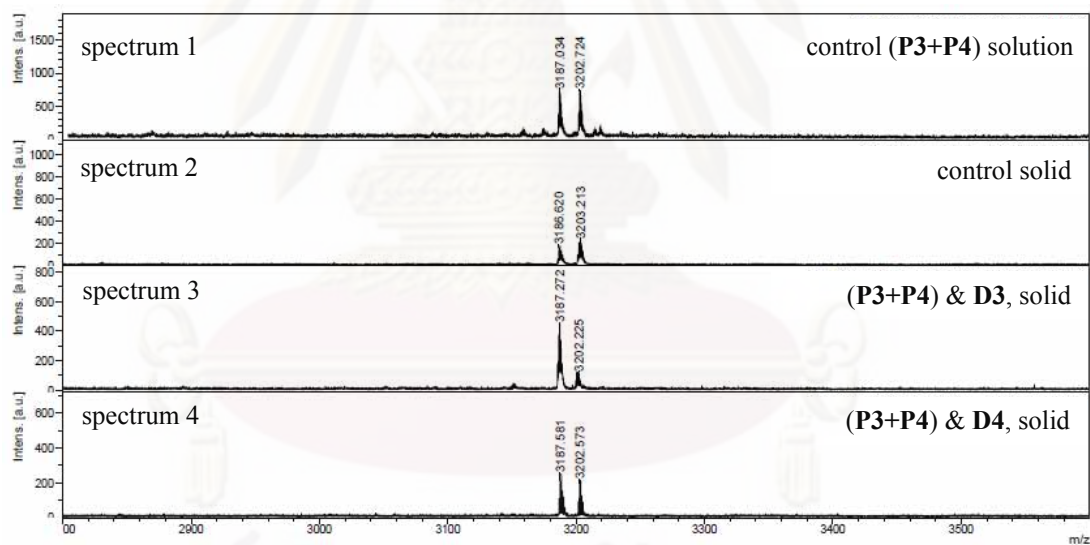
Ross and co-workers have previously reported that the inclusion of 37.5% formamide and 0.1% bovine serum albumin (BSA) in the binding buffer can reduce the hydrophobic interaction between PNA probe and solid support (streptavidin-magnetic bead in that case) and destabilize the non-complementary PNA·DNA hybrids [74]. A study of the effect of formamide and BSA to remove non-specific adsorption was performed according to the literature. Three different binding buffers were employed, the first one was the original binding buffer containing 30% formamide, the second binding buffer contained both 30% formamide and 0.1% BSA and the third buffer contained only 0.1% BSA. In the experiments, the PNA **P3** and **P4**, and DNA **D3** and **D4** were again used as models. The mixture of two PNA probes (100 pmol each) was mixed in 30  $\mu$ L of each of binding buffer and then hybridize with each of the DNA target. After 15 min of hybridization, the ion exchange support ( $\sim$ 2 mg) was added and left for another 15 min. After washing the support bound PNA·DNA hybrids, the support was directly analyzed by MALDI-TOF mass spectrometry. The results are shown in **Figure 3.20**.



(a) Binding buffer: 10 mM sodium phosphate buffer having 30% formamide



(b) Binding buffer: 10 mM sodium phosphate buffer having 30% formamide and 0.1% BSA



(c) Binding buffer: 10 mM sodium phosphate buffer having 0.1% BSA

**Figure 3.20** The effect of three different hybridization medium to non-specificity background. Experiments from top to bottom: no DNA (solution), no DNA (solid), +D3 (solid), +D4 (solid). All spectra were recorded in reflectron mode.

From above figure, it was found that the nonspecific absorption between the PNA probes and the solid support could be eliminated by using binding buffers containing formamide. As shown in spectra 2a to 2c no signals of PNA probes were observed on the solid support in the absence of added DNA. When DNA **D3** or DNA **D4** was added to the mixed PNA probe solutions, a clear differentiation between complementary and non complementary DNA was achieved when the first and second binding buffer were used as shown in the spectra 3a, 3b, 4a and 4b. These spectra revealed only mass signal of expected PNA probe complementary to the DNA was observed i.e. PNA **P3** for DNA **D3** and **P4** for DNA **D4**. For the buffer 3 consisting of only 0.1% BSA, the signal of PNA **P3** was observed as the major component after adding **D3** target (complementary with PNA **P3**) as shown in spectrum 3c. The signal of PNA **P4** was observed as the major component after adding **D4** target (complementary with PNA **P4**) (spectrum 4c). In this latter case, substantial background absorption of the non-complementary PNA probes was also observed on the solid support. From the results shown above, it was concluded that formamide, but not BSA, can reduce the background absorption. Therefore, the buffer containing only formamide was selected to use in the next experiments. As the presence of formamide can decrease the stability of PNA·DNA hybrids, the amounts of formamide were optimized in the next experiments. In these experiments, 10 mM phosphate buffer pH 7.0 containing formamide (10–50%) were employed as binding buffer. The same two PNA probes (**P3** and **P4**, 100 pmol each) were again used as a model. In the experiment, the mixture of two PNA probe in the binding buffer containing varying percentage of formamide was added the SAX and incubated for 15 min at room temperature. The level of non-specific absorptions was determined by MALDI-TOF analysis of the separated solid support after washing with water. The results are shown in **Figure 3.21**.

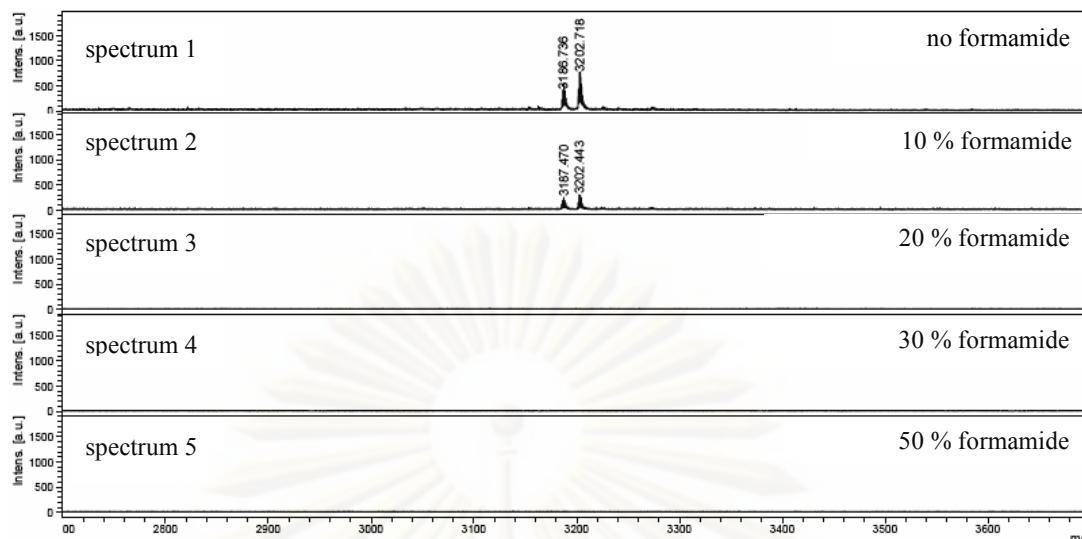


**Figure 3.21** MALDI-TOF analysis of the effect of including formamide in the hybridization medium to non-specificity background. All spectra were acquired in reflectron mode.

From **Figure 3.21** it became clear that the presence of formamide in the hybridization buffer at concentrations of 20–50% could completely eliminate non-specific absorption. As shown in spectra 3, 4 and 5, no signals of PNA probes were observed in the absence of target DNA. The results confirmed that the presence of formamide in the binding buffer could reduce the level of non-specific background absorption of PNA, which is in good agreement with the finding of Ross and co-workers [74]. Therefore, 20% formamide in 10 mM phosphate buffer pH 7.0 was chosen as the binding buffer for hybridization step in the next experiments.

### 3.6.3 The ability of formamide-containing buffer to reduce non-specific absorption of PNA in DNA sequence determination

In order to confirm that the use of 10 mM phosphate buffer pH 7.0 containing 20% formamide could eliminate non-specific background absorption for a variety of PNA sequences, the ability of the present method to distinguish between complementary and non-complementary DNA using this binding buffer was next investigated. The experiment was divided in two parts. In the first part, the experiment was designed to distinguish complementary from completely unrelated DNA targets.

The second experiment was designed to distinguish complementary from single base mismatch DNA targets.

In the first experiment, two PNA probes with unrelated sequences: Ac-TTTTTTTTT-Lys-NH<sub>2</sub> (**P1**,  $m/z = 3179.67$ ) and Ac-GTAGATCACT-Ser-NH<sub>2</sub> (**P2**,  $m/z = 3517.57$ ), were used as models. The DNA (dA<sub>9</sub>, **D1**) that is complementary with PNA **P1** and DNA (dAGTGATCTAC, **D2a**) that is complementary with PNA **P2** were employed as DNA targets. A mixture of the two PNA probes (100 pmol each) was mixed in 30  $\mu$ L of binding buffer and then hybridize with each of the DNA target. After 15 min of hybridization, the solid support ( $\sim 2$  mg) was added and left for another 15 min. After washing the support bound PNA·DNA hybrids with water to remove the unhybridized PNA probe, the solid support was then analyzed by MALDI-TOF mass spectrometry. The results are shown in **Figure 3.22**.

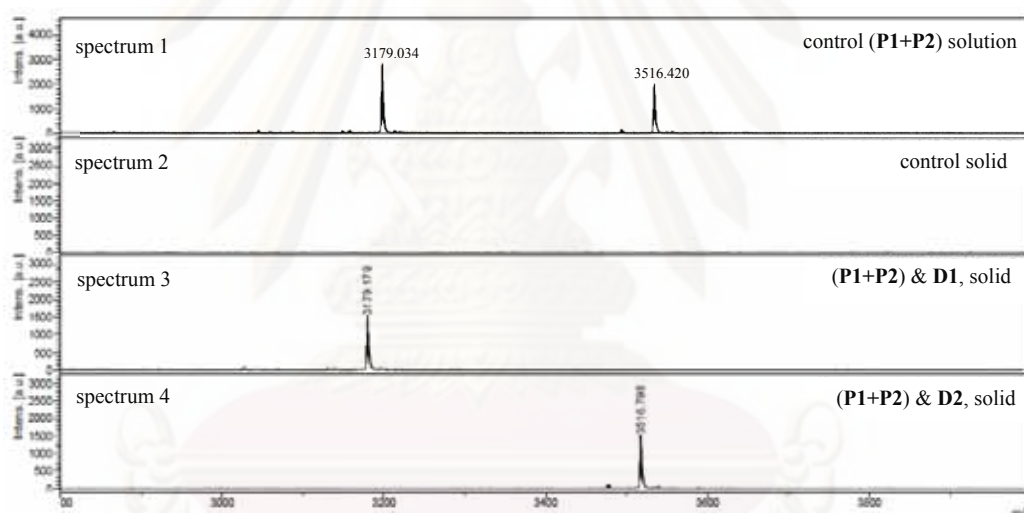


**Figure 3.22** Discrimination between complementary and non-complementary DNA targets (**D1** and **D2a**) by the PNA probes **P1** and **P2**. Experiments from top to bottom: no DNA (solution), no DNA (solid), +**D1** (solid), +**D2a** (solid).

Spectra 1 and 2 (in the **Figure 3.22**) were obtained from the control solution and control solid respectively. The results were encouraging since no mass signals of either of the two PNA probes were observed in spectrum 2, whereas both signal were observed in spectrum 1. This means that the two PNA probes cannot be absorbed onto the anion exchange under the new conditions. When DNA (**D1**) or DNA (**D2a**) was

added to the mixed PNA probe solutions, spectrum 3 and 4 revealed only mass signal of PNA probe complementary to the DNA added was observed i.e. PNA **P1** for DNA **D1** (spectrum 3), and **P2** for DNA **D2a** (spectrum 4). In both cases, a clear differentiation between complementary and non complementary DNA was achieved. As the result, it can be concluded that 20% formamide in 10 mM phosphate buffer was a suitable binding buffer that can eliminate the background absorption of non-complementary PNA probes.

In the second part of the experiment, two PNA probes, Ac-TTTTATTTT-Lys-NH<sub>2</sub> (**P3**,  $m/z = 3186.48$ ) and Ac-TTTTGTTTT-Lys-NH<sub>2</sub> (**P4**,  $m/z = 3202.47$ ) were used as models. The DNA (dAAAATAAAA, **D3**) that is complementary with PNA **P3** and DNA (dAAAACAAAA, **D4**) that is complementary with PNA **P2** were employed as DNA target differing by only one base. The mixture of the two PNA probes (100 pmol each) was mixed in 30  $\mu$ L of binding buffer and then hybridized with each of the DNA target. After 15 min of hybridization, the solid support ( $\sim$ 2 mg) was added and left for another 15 min. After washing the support bound PNA·DNA hybrids with water to remove the unhybridized PNA probe, the support was analyzed by MALDI-TOF mass spectrometry. The results are shown in **Figure 3.23**.

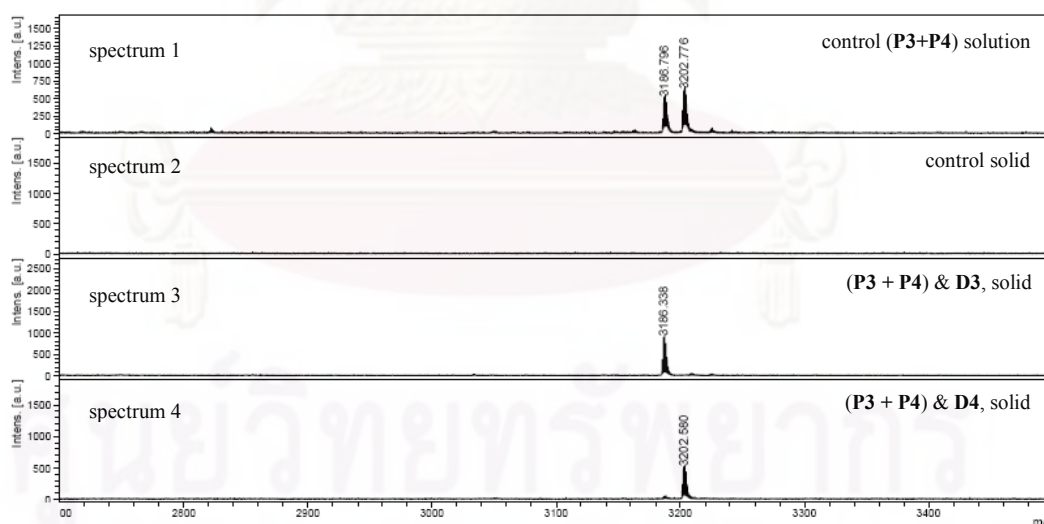


**Figure 3.23** Discrimination between complementary and non-complementary DNA targets (**D3** and **D4**) by the PNA probes **P3** and **P4**. Experiments from top to bottom: no DNA (solution), no DNA (solid), +**D3** (solid), +**D4** (solid). All spectra were acquired in reflectron mode.

From spectrum 2 in this figure, no background absorption of the PNA could be observed on the control solid support in the absence of DNA targets. In the presence of the complementary DNA target, the negatively charged PNA·DNA complex formed was preferentially absorbed onto the solid support. Analysis by MALDI-TOF mass spectrometry revealed only the mass signal corresponding to the expected PNA probe as shown in spectra 3 and 4. In both cases, the background absorption due to the non-complementary probe was minimal. As a result, a clear differentiation between complementary and single base mismatch could be easily achieved.

The experiments carried out so far demonstrated the potential utility of PNA probe and anion exchange support in DNA sequence analysis by MALDI-TOF mass spectrometry. Complete elimination of non-specific PNA probe absorption and thus a clear differentiation between complementary and single base mismatch were achieved by employing a hybridization buffer containing 20% formamide. Nevertheless, the amount of the PNA probe and DNA target required in these experiments were still relative high (100–200 pmol). Therefore, the minimum quantity of PNA and DNA that could be detected by MALDI-TOF mass spectrometry with a reasonable signal-to-noise ratio was next investigated. The same two PNA probes (**P3** and **P4**) and DNA targets (**D3** and **D4**) were selected as models for the next experiments.

In the experiment, the amount of PNA was varied in range between 100, 10 and 1 pmol, whereas the quantity of DNA target was fixed at 100 pmol. The hybridization and ion exchange capture procedure was accomplished in the same way as described above with the hybridization step performed at room temperature. After washing of the solid support to remove the unhybridized PNA probe, the resulting solid support was analyzed by MALDI-TOF mass spectrometry as described previously. The results are shown in **Figure 3.24**.

ศูนย์วิทยทรัพยากร

จุฬาลงกรณ์มหาวิทยาลัย



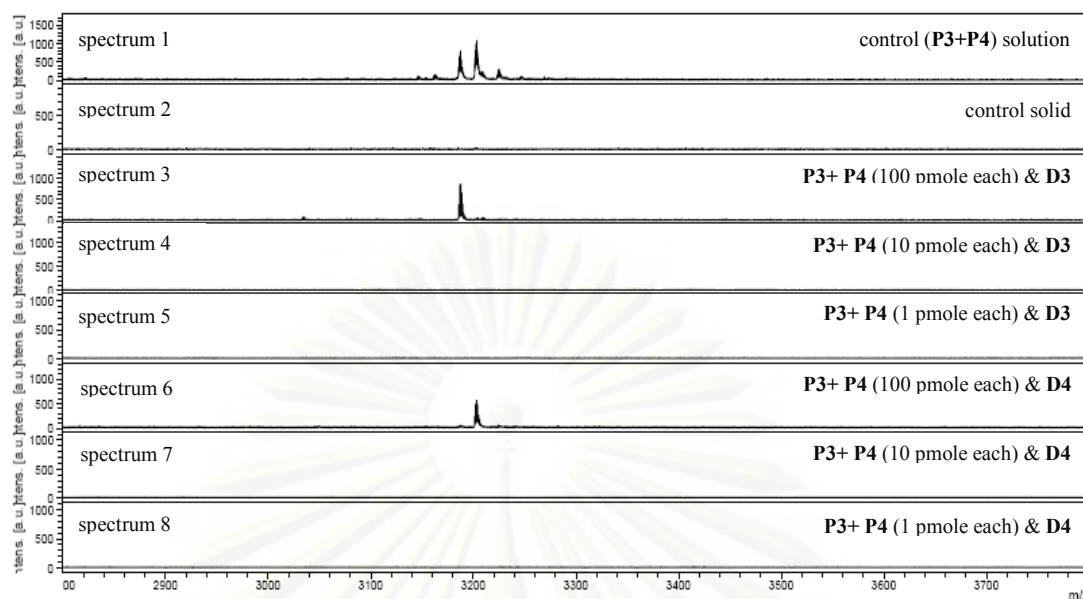


**Figure 3.24** Estimation of the optimum quantity of PNA probes by MALDI-TOF analysis employing **P3** and **P4**. All spectra were obtained in reflectron mode.

From the above spectra, it was apparent that the minimum amount of PNA probe that can show a reasonable single-to-noise ratio was 100 pmol as shown in spectra 3 and 6. When, the amount of PNA probe was lower (10 and 1 pmol) no signal could be observed (spectra 4, 5, 7, 8).

From the above results, it can be summarized that the minimum amounts of PNA probe and DNA target that allow clear differentiation between complementary and single mismatch DNA targets and provided a good signal-to-noise ratio were 100 pmol each. Therefore, these quantities were used in the next experiments.

In the next step, the ability of the present technique to distinguish between complementary and single base mismatch DNA having different types of mismatches at the middle position of the strand was carried out using a single PNA probe. The 10mer mixed base PNA (**P2**) was used as a probe model and the DNA **D2a** as a complementary DNA target. Three other DNAs (**D2b**, **D2c** and **D2d**) were used as single mismatched DNA targets. The sequences of PNA probe and DNA targets are illustrated below.

PNA (**P2**) : Ac-GTAGATCACT-Ser-NH<sub>2</sub>

DNA (**D2a**) : 5'-AGTGATTCTAC-3' (complementary with PNA **P2**)

DNA (**D2b**) : 5'-AGTGAACTAC-3' (single base mismatch,A, with PNA **P2**)

DNA (**D2c**) : 5'-AGTGACCTAC-3' (single base mismatch,G, with PNA **P2**)

DNA (**D2d**) : 5'-AGTGAGGCTAC-3' (single base mismatch,C, with PNA **P2**)

In the experiment, the PNA probe (100 pmol) was hybridized with each of the DNA target (100 pmol) in 30  $\mu$ L of binding buffer (10 mM phosphate buffer pH 7 containing 20 % formamide). After hybridization and washing, the solid support was analyzed by MALDI-TOF mass spectrometry. A clear discrimination between complementary and all three single mismatched targets was successfully achieved. The results are shown in **Figure 3.25**.

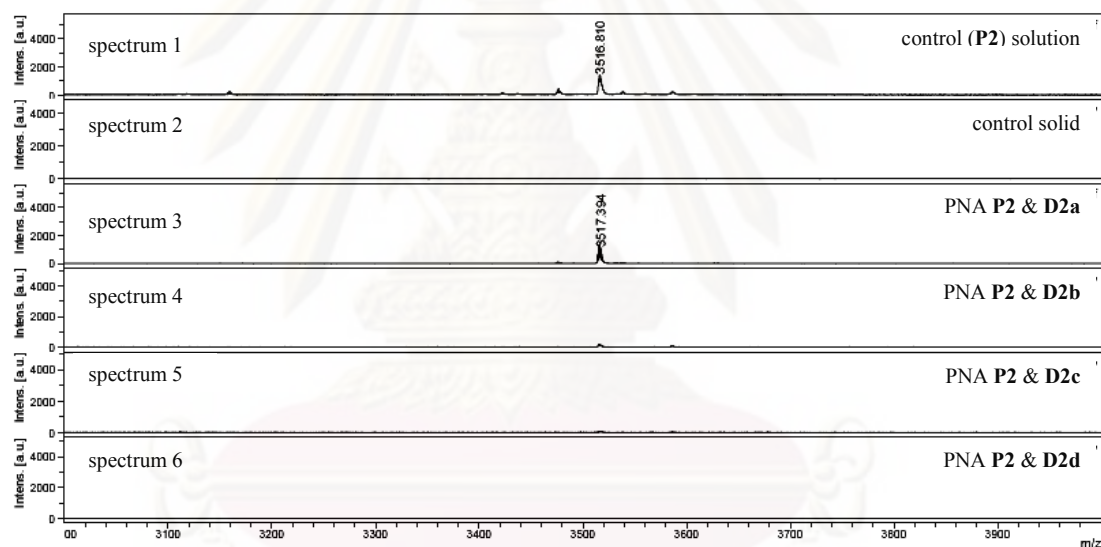


**Figure 3.25** Discrimination between complementary and various types of single mismatch DNA targets by PNA probe **P2**. Experiments from top to bottom: no DNA (solution), no DNA (solid), +**D2a** (solid), +**D2b**(solid), +**D2c** (solid), +**D2d** (solid). All spectra were operated in reflectron mode.

The results in **Figure 3.25**, spectrum 2 (solid control) demonstrated that the PNA probe could not be absorbed in the absence of any DNA. In addition, a clear discrimination between complementary and single base mismatch targets was possible, regardless of the type of the mismatched nucleobases. Mass spectrometric

analysis of the washed supports showed the mass signal of the PNA **P2** probe only when the DNA target was **D2a** (spectrum 3). The mass signal of the probe could not be observed upon addition of the other three single base mismatch targets (**D2b–D2d**) (spectra 4, 5, 6) suggesting that the single mismatch PNA·DNA hybrids could not form. These results demonstrate the high efficiency of the present technique in DNA sequence analysis, which can be attributed to the specificity of the PNA probe. Importantly, DNA targets with similar length and only minor variation in the nucleotide sequence can be readily distinguished on the basis of accurate mass assignment.

Analysis of real DNA samples usually requires a probe longer than 10 bases. For example, a 16 base long sequence is statistically unique in a human genome. In order to investigate the applicability of longer PNA probes, the 15mer PNA **P5** was chosen to investigate the ability to differentiate between complementary and single base mismatch DNA targets. The DNA **D5a** and **D5d** were used as complementary and single mismatched DNA targets, respectively. The sequences of the PNA probe and DNA targets are illustrated below.

PNA (**P5**) : Ac-TGTACGTCACA ACTA-Lys-NH<sub>2</sub> ( $m/z = 5209.38$ )

DNA (**D5a**) : 5'- TAGTTGTGACGTACA-3' (complementary with **P5**)

DNA (**D5d**) : 5'- TAGTTGTAACGTACA-3' (single base mismatch with **P5**)

The experiment was performed in the same way as described for the 10mer mixed base PNA probe. After washing the support, the resulting support-bound PNA-DNA hybrid was analyzed by MALDI-TOF mass spectrometry. The results are shown in **Figure 3.26**.

ศูนย์วิทยทรัพยากร  
จุฬาลงกรณ์มหาวิทยาลัย

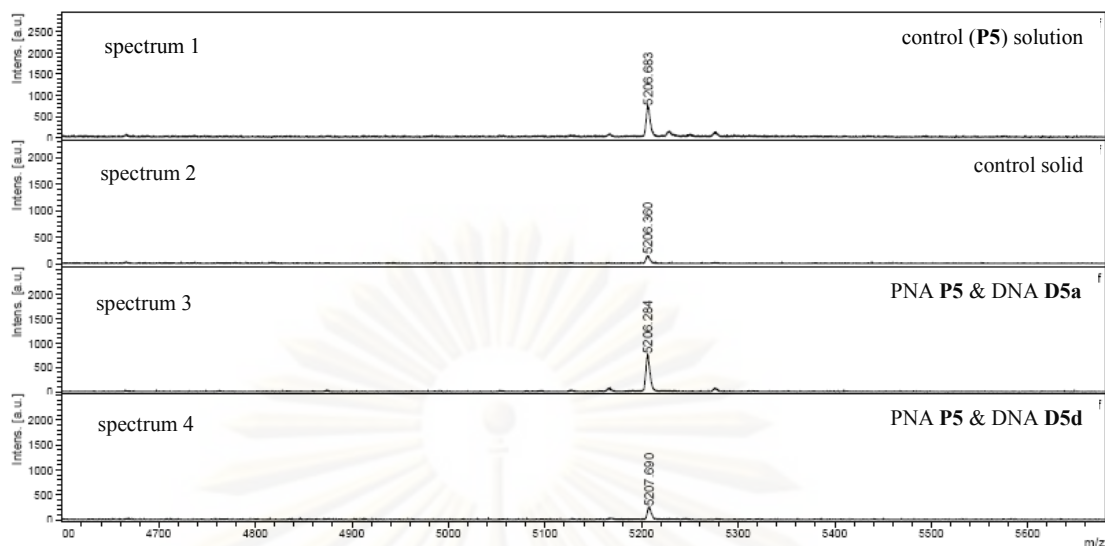


**Figure 3.26** Discrimination between complementary and single mismatched DNA targets using 15mer mixed base PNA **P5** probes. Experiments from top to bottom: no DNA (solution), no DNA (solid), +**D5a** (solid), +**D5d** (solid). All spectra were obtained in linear mode.

From the above spectra, it was found that in the absence of DNA, the 15 mer PNA (**P5**) probe was partially absorbed on the SAX support even when 20% formamide was present in the binding buffer (spectrum 2, solid control). Not surprisingly, substantial background signal of the PNA was observed on the solid support in the presence of non-complementary target as revealed in spectrum 4. It was possible that long PNA sequences might be more hydrophobic than the shorter sequences (9mers and 10mers PNA probes), which resulted in higher background absorption. Therefore, attempts have been made to eliminate this non-specific absorption by varying the percentage of formamide (30, 40 and 50%) in the binding buffer to find the conditions that can minimize the non-specific absorption of **P5** on SAX. The SAX support was added to the 15mer PNA probe (**P5**, 100 pmol) in the binding buffers containing varying amounts of formamide and incubated at room temperature for 15 min. The solid support was washed with water and subsequently analyzed by MALDI-TOF mass spectrometry. The results are shown in **Figure 3.27**.

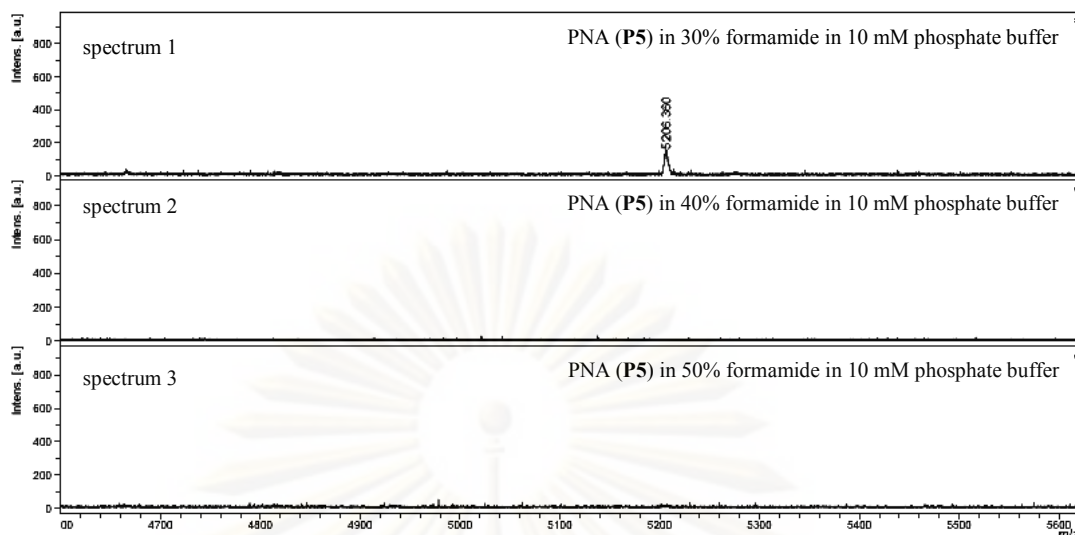


**Figure 3.27** MALDI-TOF analysis revealing the effect of formamide in the hybridization medium to eliminate non-specificity background. All spectra were obtained in linear mode.

The results showed that 40 and 50% formamide in phosphate buffer can completely eliminate the non-specific absorption of the 15mer PNA probe as shown in spectra 2 and 3. This suggested that the non-specific absorption of the longer PNA probes on the support could be reduced by increasing formamide in the binding buffer. The formamide may effectively destroy the hydrophobic interaction between the PNA and the solid support. According to the results shown above, the phosphate buffer consisting of 20% formamide should be employed for the short PNA probes such as 9mer and 10mer, whereas at least 40% formamide is required for longer PNA probes such as 15mer.

Discrimination between complementary and single base mismatch DNA targets using the hybridization buffer containing 40% formamide was next investigated. In the experiment, the mixed base 15mer PNA probe **P5** and DNA targets (**D5a–D5d**, **D6a–D6b**) having different types and different position of nucleobase were employed as model. The sequences of DNA targets are as shown below:

DNA (**D5a**): 5'-TAGTTGTGACGTACA-3' (complementary with PNA **P5**)

DNA (**D5b**): 5'-TAGTTGTAACGTACA-3' (single mismatch, with PNA **P5**, dA·pC)

DNA (**D5c**): 5'-TAGTTGTCACGTACA-3' (single mismatch, with PNA **P5**, dC·pC)

DNA (**D5d**): 5'-TAGTTGTTACGTACA-3' (single mismatch, with PNA **P5**, dT·pC)

DNA (**D6a**): 5'-TAGTTGTGTCGTACA-3' (single mismatch, with PNA **P5**, dT·pC at position 9)

DNA (**D6b**): 5'-TAGTTGTGAAGTACA-3' (single mismatch, with PNA **P5**, dT·pC at position 10)

All experiments were carried out at 100 pmol of PNA probe, 200 pmol of each DNA target in 10 mM phosphate buffer pH7 containing 40% formamide as the binding buffer. The experiment was carried out in the same way as described above. The results are shown in **Figure 3.28**.

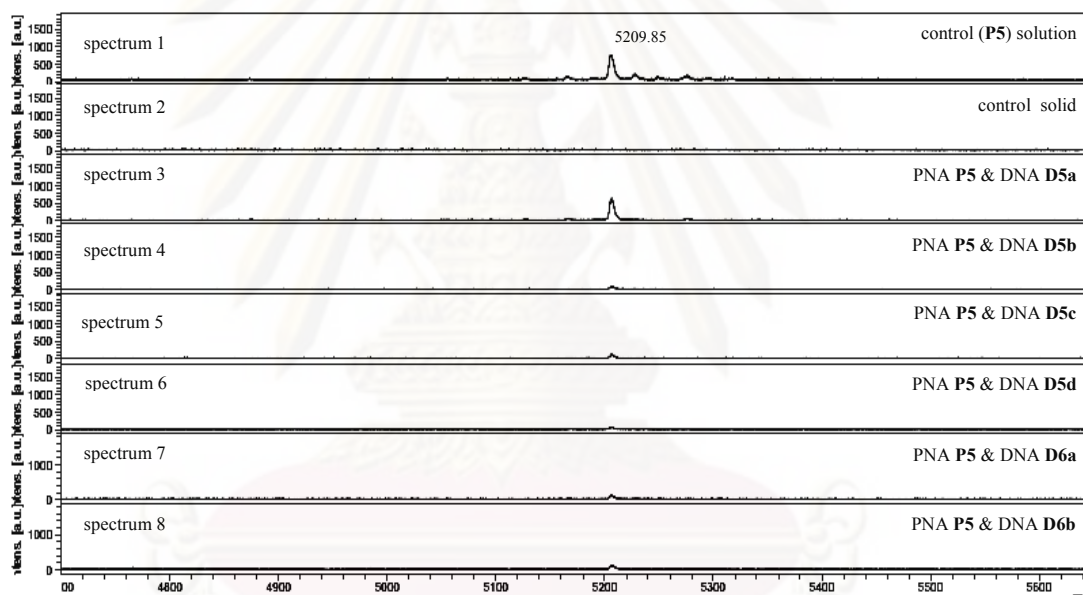


**Figure 3.28** Discrimination between complementary and various types of single mismatch DNA targets by PNA **P5** probe. Experiments from top to bottom: no DNA (solution), no DNA (solid), +**D5a** (solid), +**D5b** (solid), +**D5c** (solid), +**D5d** (solid), +**D6a** (solid), +**D6b** (solid). All spectra were obtained in linear mode.

From the above figure, non-specific background absorption of the PNA (**P5**) probe could not be observed on the solid support in the absence of any DNA target as shown in spectrum 2 (solid control). Furthermore, satisfactory discrimination of single-base mismatch targets was accomplished by using the 15-mer mixed base PNA probe (**P5**), regardless of types and position of the mismatch nucleobase. Mass

spectrometric analysis of the support revealed the mass signal of the PNA probe in case of the complementary DNA target as shown in spectrum 3. The presence of a single base mismatch in the DNA targets at various positions inhibited PNA·DNA hybrids formation. As a result, the mass signal of the PNA probe could not be observed in the spectra 4–8.

According to the above results, it can be concluded that the presence of formamide in the hybridization buffer influences the level of non-specific background absorption. It was observed that the percentage of formamide in the binding buffer had to be increased when the longer PNA probe was employed to avoid non-specific background. It was possible that longer PNA probes might be more hydrophobic and thus absorbed more strongly than short PNA probes. In addition, it can be explained in term of a higher melting temperature between the 15mer mixed base PNA and single base mismatch DNA targets (61.1–63.1 °C) as compared to the 9mer PNA (39.0–48.0 °C) and the 10mer PNA (34.0–37.0 °C) [8]. The strong binding affinity of 15mer mixed base PNA with single base mismatch DNA target can contribute to the background absorption of non-complementary probes on the solid support. This can lower the specificity of the method compared to shorter PNA probes. Fortunately, increasing the percentage of formamide in binding buffer to 40% was found to more or less completely destroy the absorption of non-complementary PNA probes on solid support.

From these preliminary experiments, although SAX was successfully employed as solid anion-exchange support in combination with the pyrrolidiny PNA probes and MALDI-TOF mass spectrometry for DNA sequence analysis, the non-specific background absorption of the PNA probes were still problematic. Although the background absorption could be eliminated by addition of formamide in the binding buffer, different PNA probes required different conditions (ie, concentration of formamide) to eliminate non-specific absorption. For example, only 20% formamide in 10 mM phosphate buffer pH 7.0 was sufficient to eliminate background absorption of 9-10 mer. On the other hand, 40% formamide was required in the binding buffer for 15mer PNA probes. Therefore, it was difficult to set up one general condition to do simultaneous analysis using several PNA probes. Furthermore, it was possible that formamide might also be interfering with the hybridization between PNA and DNA targets. In order to simplify the hybridization while maintaining sequence specificity

without using formamide, other less hydrophobic anion exchange supports were explored next.

### 3.6.4 Investigation of alternative solid supports to eliminate non-specific absorption

As the non-specific absorption was thought to involve mainly hydrophobic interactions, other less hydrophobic anion exchange supports were studied in order to minimize such undesired background absorption. Five ion exchange materials [102] including ethylenediamine-N-propyl silica (PSA), diethylaminoethyl cellulose (DEAE cellulose), diethylaminoethyl sepharose (DEAE sepharose), quaternary ammonium sepharose (Q sepharose) and chitosan were tested. The structures of anion exchangers used in this study are shown in **Figure 3.29**.

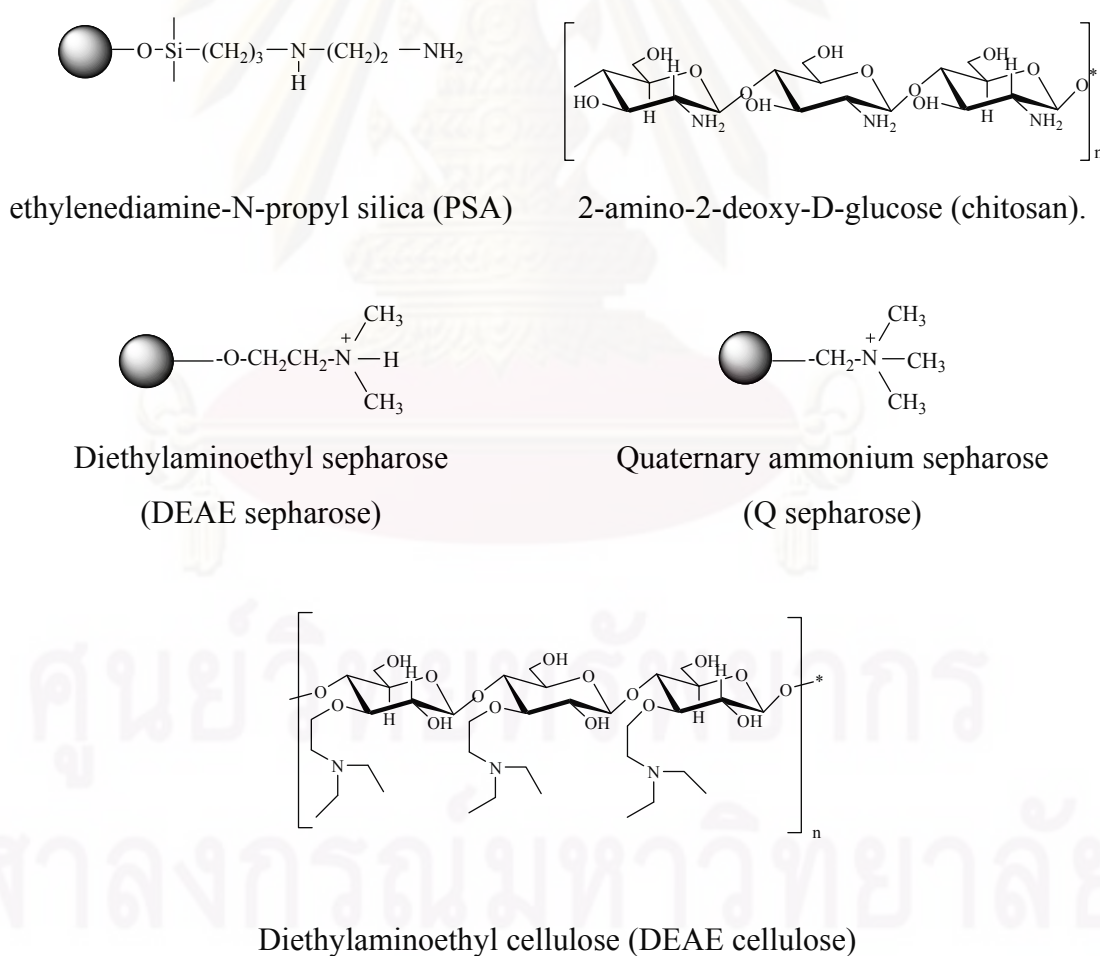


**Figure 3.29** Structures of anion exchange supports used in this study [102].



The degree of absorption of the PNA probe and all solid supports, which give rise to non-specific background, was determined. Two PNA probes, PNA **P1** ( $m/z = 3179.68$ ) and mixed base PNA **P2** ( $m/z = 3517.57$ ), were used as model probes. In the experiment, the two PNA probes (100 pmol each) were mixed in 10 mM phosphate buffer (30  $\mu$ L, then the solid support ( $\sim 2$  mg) was added to the PNA probes mixture followed by incubation at room temperature (30  $^{\circ}$ C). After 15 minutes of incubation, the support was washed with water and subsequently analyzed by MALDI-TOF mass spectrometry. The results are shown in **Figure 3.30**.

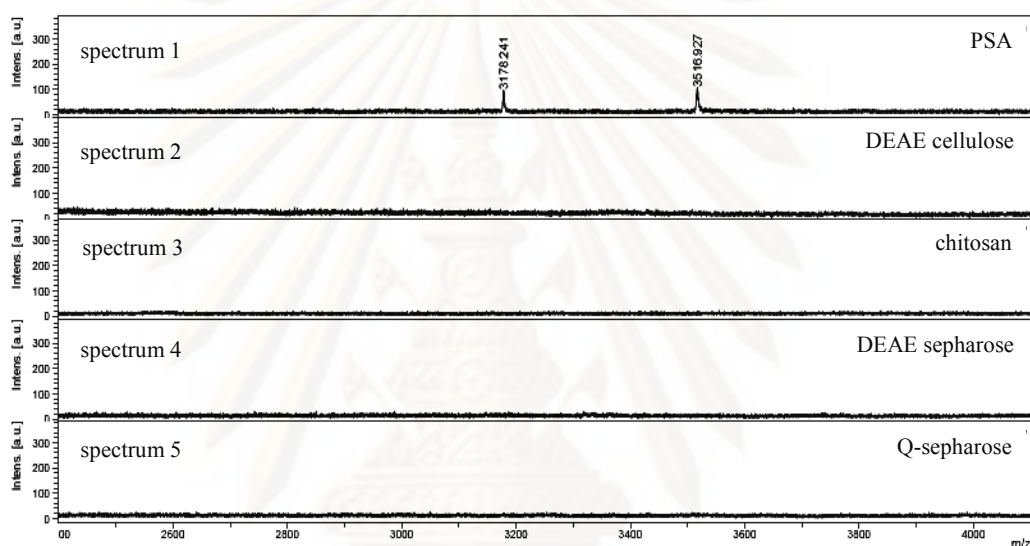


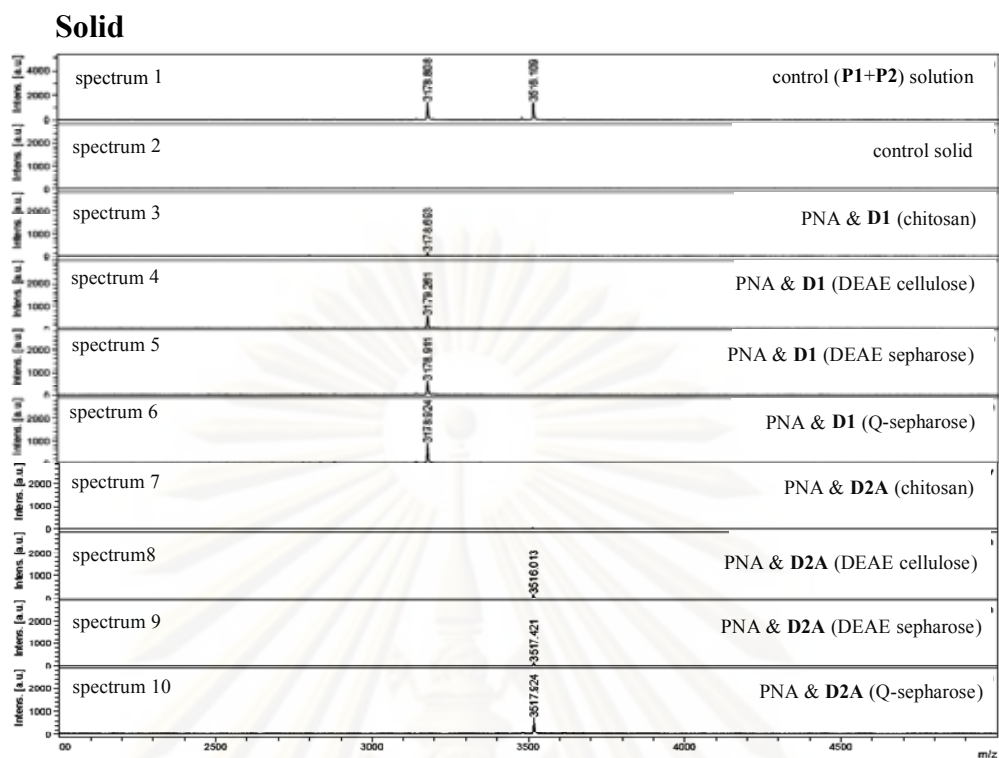
**Figure 3.30** MALDI-TOF analysis of study of hydrophobic interaction between PNA probe and various solid supports in the absence of DNA targets and formamide. For other conditions see text.

The results in **Figure 3.31** revealed that even in the absence of formamide, no significant absorption of the two PNA probes could be observed in most supports except PSA (and SAX as observed in earlier experiments). It can be explained by the fact that the PSA support consists of a silica core similar to SAX. The silica surface of these two supports must be modified by silane chemistry to provide the desired charged functional groups, which may give rise to a hydrophobic surface. It is therefore not surprising to observe non-specific binding of the PNA probes. As a result, this support was not considered further.

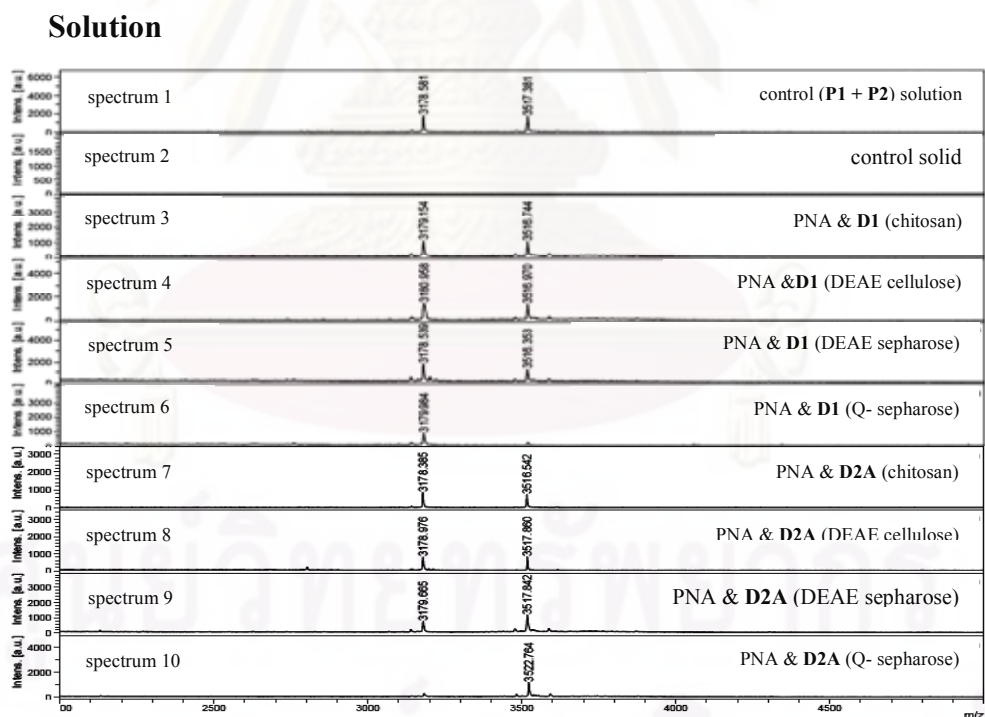
Thereafter, the remaining ion exchange solid supports were next investigated in term of their ability to differentiate between complementary and non-complementary PNA·DNA hybrids. In these experiments, the DNA complementary to each of the PNA probe was added. The mass signal of the PNA·DNA mixture solution before and after adding the solid support was then observed. Ideally, a good solid support should capture all of the negatively charged PNA·DNA hybrid in the presence of the complementary DNA target. Consequently, the remaining solution after removal of the support should contain only the unhybridized non-complementary PNA probe. An efficient ion exchange support should selectively and completely capture the complementary PNA strand and leave the noncomplementary PNA in the solution, and the spectra of both the solid and solution should provide only one mass signal of the complementary and noncomplementary PNA probe, respectively. In the experiment, the same model PNA probes (PNA **P1** and PNA **P2**) were used in conjunction with two DNA targets dA<sub>9</sub> (**D1**, complementary to **P1**) and DNA dAGTGATCTAC (**D2A**, complementary to **P2**). The two PNA probes (100 pmol each) were mixed in the binding buffer (10 mM phosphate buffer pH 7.0, 30  $\mu$ L) and hybridized with each of the DNA target (100 pmol). The hybridization was allowed to proceed at room temperature for 15 min, then each of the solid support was added to the mixture. After 15 min incubation at room temperature, the support bound PNA·DNA hybrid was separated from the solution, and then washed with water to remove any unhybridized PNA. The solution after removal of the solid support and the separated solid support were subsequently analyzed by MALDI-TOF mass spectrometry. The results are shown in **Figure 3.31**.

ศูนย์วิทยทรัพยากร

จุฬาลงกรณ์มหาวิทยาลัย



(a)



(b)

**Figure 3.31** (a) MALDI-TOF analysis of solid support after hybridization with the DNA target **D1** or **D2A**  
 (b) MALDI-TOF analysis of a mixture of two PNA probes, **P1** and **P2**, after hybridization with the DNA target **D1** or **D2A**

The spectra above revealed that Q-sepharose was the best solid support. A clear signal of the complementary PNA probes can be observed on the solid support (spectra 6 and 10 in **Figure 3.31a**). Most importantly, in the remaining solution after removal of the support, only one mass signal due to the non-complementary probe remained (spectra 6 and 10 in **Figure 3.31b**). This means that Q-sepharose can completely absorb the negatively charged complementary PNA·DNA hybrids without leaving any free PNA probe in the solution. On the other hand, other solid supports seemed to have lower capacity to bind the negatively charged PNA·DNA hybrids despite the observed high specificity. This is evidenced by analysis of the PNA·DNA solution after removing the support. In many cases, the mass signal of both PNA probes were observed as shown in **Figure 3.31b** (spectra 3–5, 7–9), while only signal of the complementary probe was observed on the solid support. The results can be explained by the fact that Q-sepharose is a strong anion exchanger due to the presence of quaternary ammonium groups, whereas the other solid supports are weak anion exchangers having primary or secondary amino groups (**Figure 3.29**). In addition, the Q-sepharose showed a good ionic capacity as shown in **Table 3.5** and it was therefore selected for further use as the anion exchanger in conjunction with PNA probes for DNA sequence determination in the next experiments.

**Table 3.5** Type and ionic capacity of each of solid anion exchanger support [102, 103]

Solid support	Type of anion exchanger	Total ionic capacity
PSA	Weak	1.1–1.4 mmol/g
Q sepharose	Strong	0.18–0.25 mmol/mL gel
DEAE sepharose	Weak	0.11–0.16 mmol/mL gel
DEAE cellulose	Weak	~ 1 mmol/g
chitosan	Weak	2.5–2.8 mmol/g

With the new solid support, the quantity of PNA probe and DNA target that can be detected by MALDI-TOF mass spectrometry following the Q-sepharose capture was optimized again. The PNA **P1** ( $m/z= 3179.68$ ) probe and its complementary DNA target DNA **D1** (dA<sub>9</sub>) were selected as models for further optimization. In the protocol, the PNA probe was hybridized with DNA target (10

mM phosphate buffer pH 7.0, 30  $\mu$ L) and incubated at room temperature for 15 min. Subsequently, the pre-equilibrated Q-sepharose was added to this PNA·DNA hybrid solution and left for another 15 min. After extensive washing of the support with water, the resulting support-bound PNA·DNA hybrid was analyzed by MALDI-TOF mass spectrometry.

In the first part of the experiment, the amount of PNA was varied in range between 100, 10, 1 and 0.1 pmol, whereas the quantity of DNA target was fixed at 100 pmol. The results are shown in **Figure 3.32**.

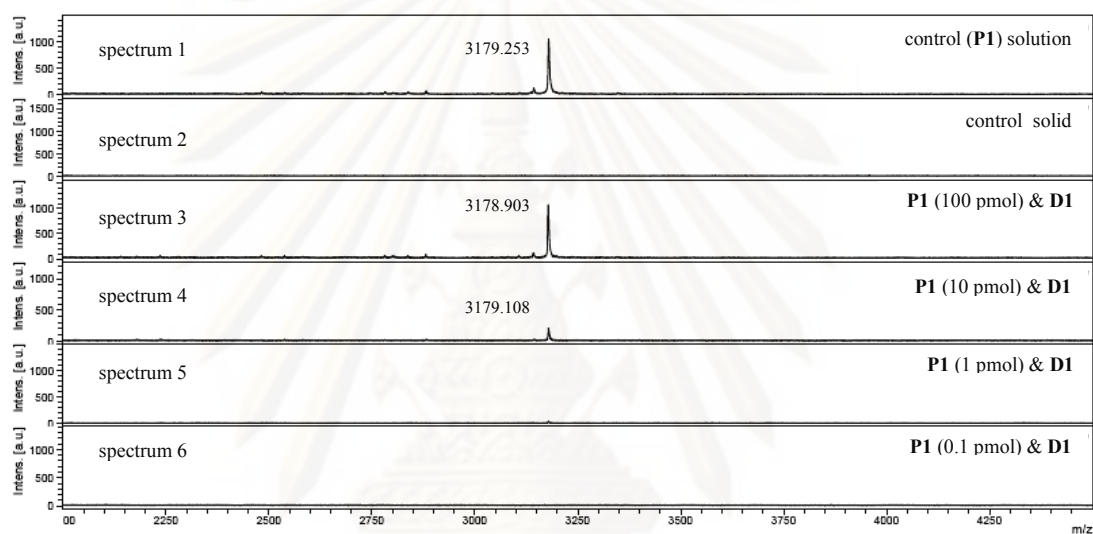


**Figure 3.32** Determination of the limit of detection for PNA probe **P1** with DNA **D1** target (fixing the amount DNA target at 100 pmol/ 30  $\mu$ L hybridization reaction)

From these spectra, it was found that the minimum amount of PNA probe that can be employed conjunction with Q-sepharose for detection of DNA sequence with a reasonable signal-to-noise ratio (27.9) was 10 pmol (spectrum 4). No signal could be detected when the probe quantity was less than 10 pmol as shown in spectrum 5 (S/N=6.6, 1 pmol of probe) and spectrum 6 (0.1 pmol of probe). Therefore the quantity at 10 pmol was selected as the appropriate amount of PNA probe for the next experiments.

In the second part, the amount of DNA was varied between 100, 50, 10 and 1 pmol, whereas the quantity of PNA probe was fixed at 10 pmol. The results are shown in **Figure 3.33**.

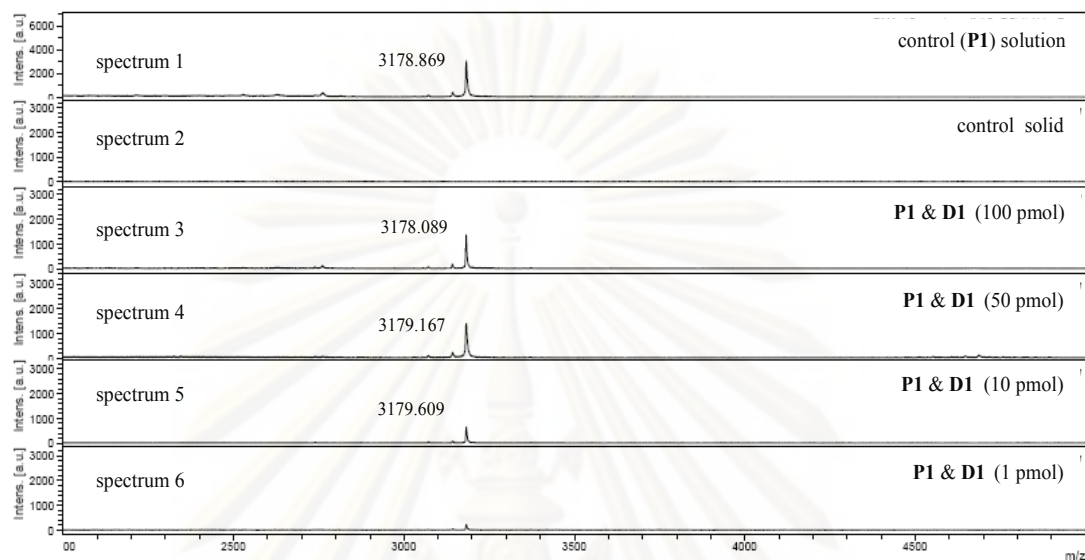


**Figure 3.33** Determination of the limit of detection for DNA target using PNA probe **P1** (fixing the amount PNA probe at 10 pmol/ 30  $\mu$ L hybridization reaction)

The results in the above figure demonstrated that the minimum amount of DNA target that can be used while a reasonable signal-to-noise ratio (75.9) still observed was 10 pmol (spectrum 5). Although a weak signal of the PNA probe could be observed when the DNA quantity was 1 pmol as shown in spectrum 6 (S/N=15.2, 1 pmol of target), the DNA quantity of 10 pmol was used in other experiments.

From the results in **Figure 3.32** and **Figure 3.33**, it is possible to detect the DNA sequence using PNA probe coupled with Q-sepharose and MALDI-TOF mass spectrometry with the sensitivity of 10 pmol/hybridization reaction for both PNA probes and targets. Since the specificity and detection limit obtained by Q-sepharose was better compared to SAX or other ion exchange, these conditions were further employed to detect DNA sequence in the next experiments.

### 3.6.5 The effectiveness of the Q-sepharose based method in detection of PNA·DNA hybridization.

This section will mainly focus on the ability to distinguish between fully complementary and single mismatched DNA targets using PNA probes. Firstly, the effect of type of single base mismatch in the DNA targets was studied. In the experiment, the discrimination between complementary and single base mismatch DNA containing different types of nucleobase at the middle position. A single PNA probe was used in conjunction with Q-sepharose as anion exchange support. The experiment was separated into three parts and all parts were performed under identical conditions. In the procedure, the mixture of PNA probe (10 pmol) in 10 mM phosphate buffer pH 7.0 (30  $\mu$ L) was hybridized with one of the DNA target (10 pmol) and incubated at room temperature for 15 min. Subsequently, the Q-sepharose support (~3  $\mu$ L) was added to the PNA·DNA solution and incubated for another 15 min. After separation and washing the support to remove any unhybridized PNA probe, the resulting support was analyzed by MALDI-TOF mass spectrometry.

In the first part, the PNA Ac-T<sub>9</sub>-Lys-NH<sub>2</sub> (**P1**) was employed as a model. The DNA dA<sub>9</sub> (**D1**) was employed as the complementary DNA target. Several other single base mismatch targets having different types of nucleobase at the middle position of the strand (dAAAATAAAA, dAAAACAAAA, dAAAAGAAAA) were also included in the study. The results obtained from MALDI-TOF analysis of the washed solid support are shown in **Figure 3.34**.

ศูนย์วิทยทรัพยากร

จุฬาลงกรณ์มหาวิทยาลัย

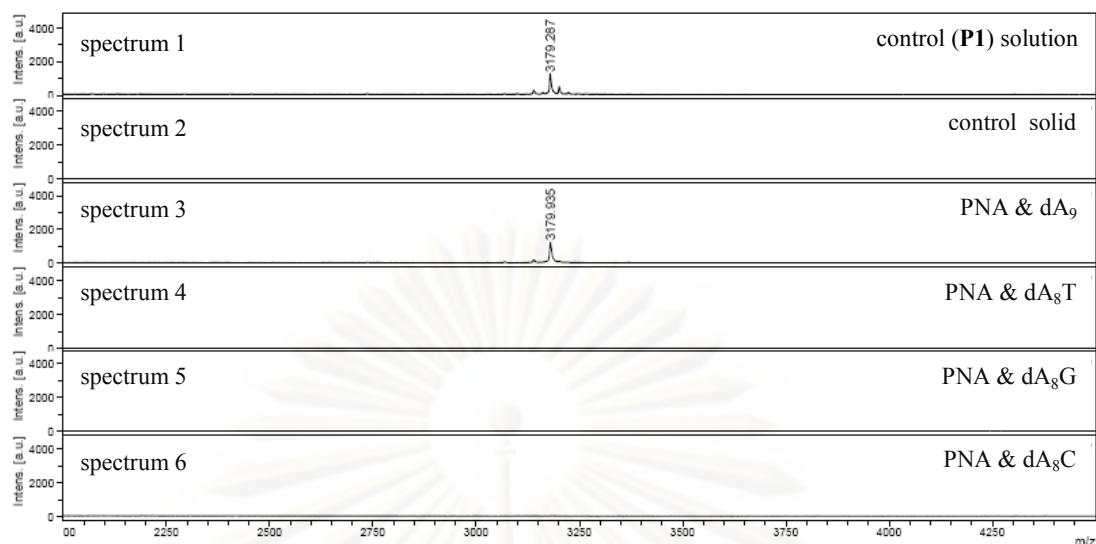


**Figure 3.34** Discrimination between complementary and various types of single mismatch DNA targets by using homothymine nonamer PNA probe **P1**.

The results in **Figure 3.34** indicated the high specificity of the PNA probe **P1** in distinguishing complementary and single mismatch DNA targets. The mass signal of the PNA probe **P1** was observed only in the presence of its complementary DNA target as shown in spectrum 3. On the other hand, in the presence of all single base mismatch DNA targets, the mass signal of probe could not be observed as revealed in spectra 4, 5 and 6. Spectra 1 and 2 were control solution and control solid in the absence of any DNA. As a result, it can be concluded that the present technique showed the potential to discriminate between complementary and single mismatched DNA targets, regardless of the types of the mismatched nucleobase. In all cases, the results were unambiguous and easily interpreted.

In the second part, the hybridization specificity between a mixed base PNA probe and DNA targets was next determined. The 10mer mixed base PNA probe **P2** and various DNA targets (**D2A** as complementary, **D2B**, **D2C**, **D2D**: single base mismatched target containing a different type of nucleobase at the middle position of the strand) were employed as a model. The sequence of the PNA probe and DNA targets were illustrated below. The results obtained from MALDI-TOF analysis of the washed solid support is shown in **Figure 3.35**.



PNA **P2** : Ac-GTAGATCACT-Ser-NH<sub>2</sub>

DNA (**D2A**) : 5'-AGTGATCTAC-3' (complementary with PNA **P2**)

DNA (**D2B**) : 5'-AGTGA<sup>A</sup>ACTAC-3' (single base mismatch,A, with PNA **P2**)

DNA (**D2C**) : 5'-AGTGAC<sup>G</sup>CTAC-3' (single base mismatch,G, with PNA **P2**)

DNA (**D2D**) : 5'-AGTGAG<sup>C</sup>CTAC-3' (single base mismatch,C, with PNA **P2**)

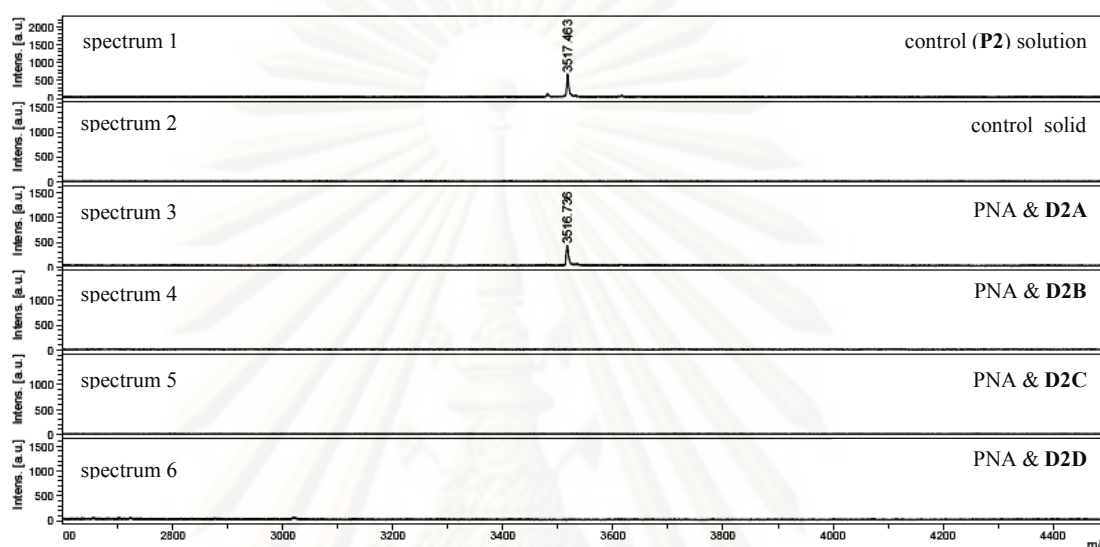


**Figure 3.35** Discrimination between complementary and various types of single mismatch DNA targets by using mixed base 10mer PNA probe **P2**.

The results in **Figure 3.35** illustrated that very high specificity was also observed with the mixed base PNA probe. Spectra 1 and 2 were used as the control described in previous experiments. The mass signal of the PNA probe was observed only in the presence of the complementary DNA target as revealed in spectrum 3, On the other hand no signal of the PNA probe could be observed in the presence of all single base mismatch DNA targets as shown in spectra 4, 5 and 6. The experiment demonstrated the absolute specificity of the 10mer mixed base PNA probe in differentiating between complementary and various types of single base mismatched DNA targets when used in combination with Q-sepharose as solid support.

In the last part of the experiment, testing of the present technique with a longer PNA probe was investigated. A 15mer mixed base PNA **P5** probe ( $m/z = 5208.38$ ) and a variety of DNA target including complementary target and single base mismatch targets having different types of nucleobase at the middle position were used as models. The sequences of the PNA probe **P5** and all DNA targets are shown at below.

- PNA (**P5**) : Ac-TGTACGTCACA ACTA-Lys-NH<sub>2</sub>
- DNA (**D5A**) : 5'-TAGTTGTGACGTACA-3' (complementary with PNA **P5**)
- DNA (**D5B**) : 5'-TAGTTGTAACGTACA-3' (single mismatch,A, with PNA **P5**)
- DNA (**D5C**) : 5'-TAGTTGTCACGTACA-3' (single mismatch,C, with PNA **P5**)
- DNA (**D5D**) : 5'-TAGTTGTTACGTACA-3' (single mismatch,T, with PNA **P5**)

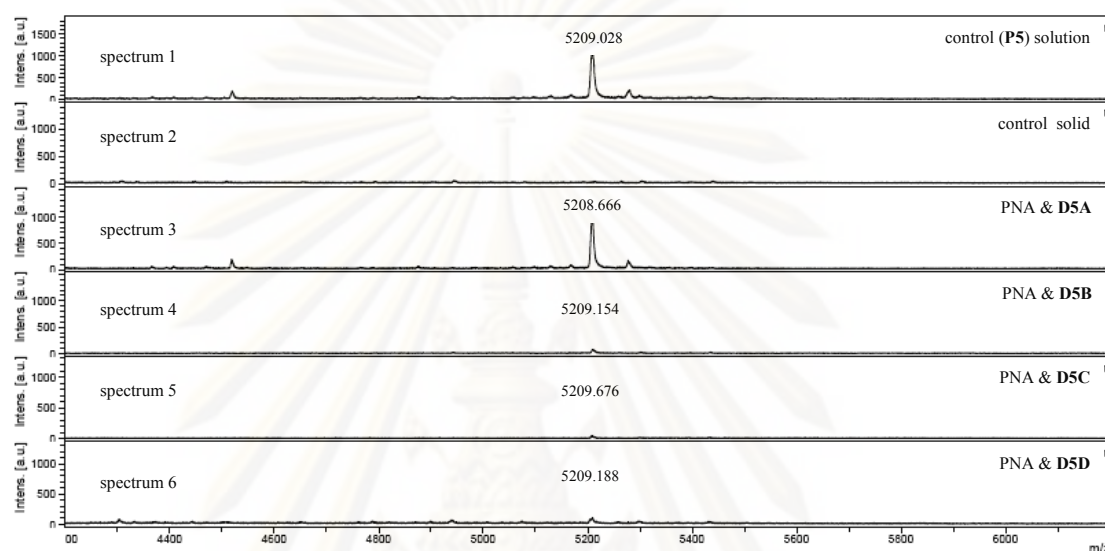


**Figure 3.36** Discrimination between complementary and various types of single mismatch DNA targets by using mixed base 15mer PNA probe **P5**.

In the presence of the complementary DNA target (**D5A**), the mass signal of PNA probe was detected as expected in spectrum 3 of **Figure 3.36**. However, after washing the support with water and MALDI-TOF MS analysis, significant background signal of the PNA was detected in the presence of all single base mismatch DNA targets as shown in the spectra 4, 5 and 6 ( $S/N=18.2, 17.4$  and  $15.4$ , respectively) as compared with the control solution and control solid (spectra 1 and 2). Since no signals were observed in the case of control solid (spectrum 2), the presence of these signals are not due to nonspecific absorption of the PNA on the solid support. In these cases, the mismatched PNA·DNA hybrids appeared to be sufficiently stable to be present in the solution and absorbed on the support. The assumption is supported by the higher melting temperature ( $T_m$ ) of hybrids formed between PNA **P5** and single base mismatched DNA targets ( $61.1\text{--}63.1$  °C) as compare to that of 9mer PNA **P1** ( $39.0\text{--}48.0$  °C) and 10mer mixed base PNA **P2** ( $34.0\text{--}37.0$  °C).

In order to eliminate non-specific absorption signal, a more stringent washing condition was required. Raising the temperature during hybridization/washing is theoretically possible so that the mismatched hybrids are destroyed. This strategy has been used to solve similar problems in other works [74]. Alternatively, single strand specific nucleases may be used to improve the specificity. However, having to control temperature or use an enzyme would complicate the analysis and would not be practical for high throughput applications. In this experiment, it was decided to explore other washing conditions that allow all steps to be carried out at room temperature (30 °C) for the sake of simplicity. Based on literature precedent that the stability of PNA·DNA hybrids are sensitive to organic solvent, it was proposed that an addition of organic solvent in the hybridization or washing buffer should improved the specificity of the technique. To validate the concept, a series of  $T_m$  experiment between the 10mer PNA probe **P2** and its complementary DNA target (**D2A**) in 10 mM phosphate buffer containing varying amount of acetonitrile as co-solvent. The results are summarized in **Figure 3.37** and **Table 3.6**.

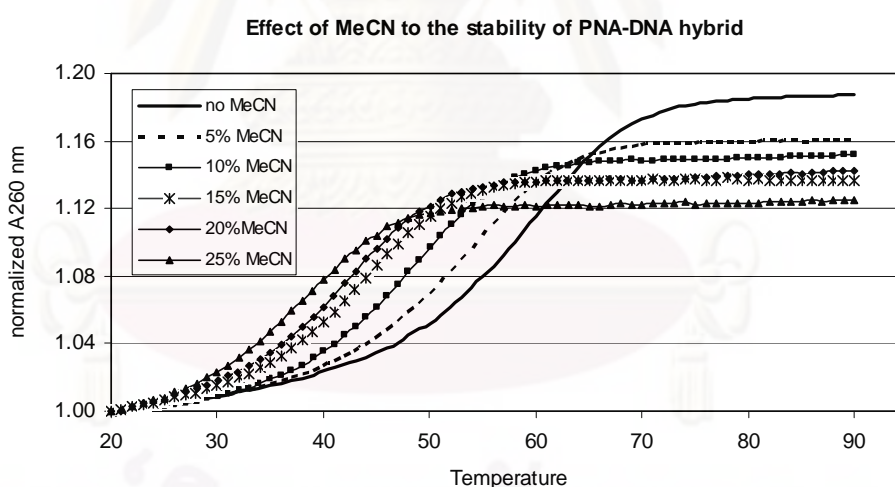


**Figure 3.37**  $T_m$  curves of **P2-D2A** hybrid in the presence of various hybridization buffer: Condition PNA:DNA = 1:1, [PNA] = 1  $\mu$ M, heating rate 1.0 °C/min.

**Table 3.6** Effect of acetonitrile on  $T_m$  of 1:1 **P2·D2A** Condition: ratio of PNA:DNA = 1:1, [PNA] = 1  $\mu$ M, heating rate 1.0  $^{\circ}$ C/min.

Percentage of MeCN in 10 mM phosphate buffer pH 7.0	$T_m$ ( $^{\circ}$ C)
0	58.1
5	52.3
10	46.2
15	42.4
20	40.3
25	35.6

From the above data, it becomes clear that increasing acetonitrile content in the hybridization buffer can destabilize PNA·DNA hybrids. It should therefore be possible to find an appropriate acetonitrile content that decrease the  $T_m$  of mismatched hybrids to below ambient temperature (30  $^{\circ}$ C) while that of the complementary hybrids is still well above that temperature. Provided that the kinetic of the dissociation is fast enough, it should also be possible to include acetonitrile only in the washing step. To study the appropriate conditions for destroying noncomplementary hybrids, the washing step was carried out using various percentage of acetonitrile in water (3–10%). Pleasingly, it was found that a washing solution containing 10% aqueous acetonitrile could more or less completely eliminate the signals from single mismatched hybrids between 15mer PNA and DNA. The results are shown in the **Figure 3.38**.

ศูนย์วิทยทรัพยากร  
จุฬาลงกรณ์มหาวิทยาลัย

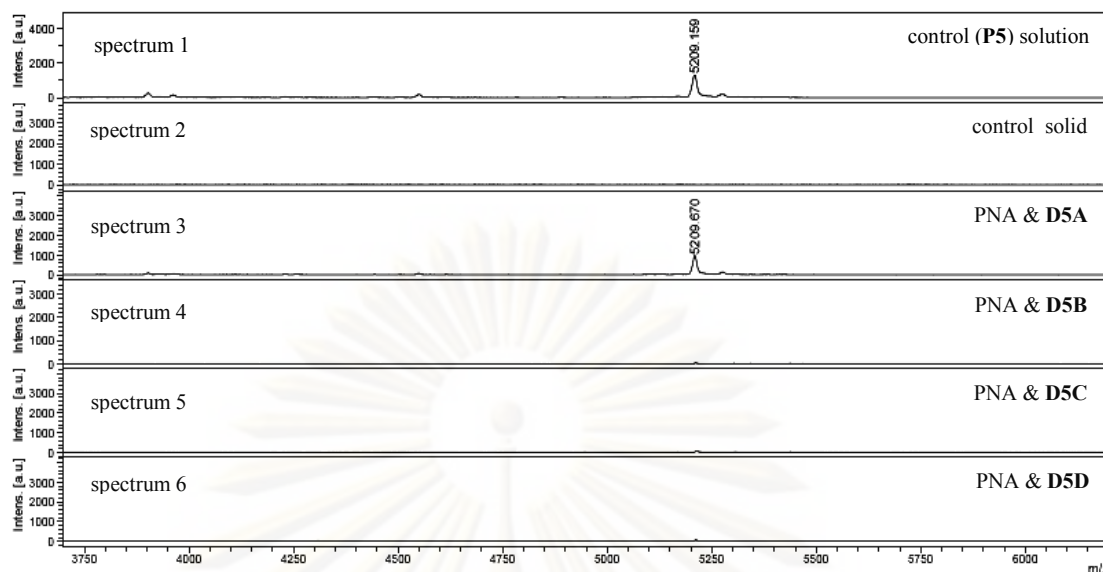


**Figure 3.38** MALDI-TOF analysis of the effect of including acetonitrile in the washing medium to eliminate non-specificity background

MALDI-TOF MS spectra obtained from the solid support after washing with 10% aqueous acetonitrile did not show any background signal in the presence of all single base mismatch targets (**D5B**, **D5C**, **D5D**) as shown in spectra 4, 5 and 6. In contrast, in the presence of complementary DNA target (**D5A**), a signal of PNA **P5** probe was clearly detected in spectrum 3. As a result, it can be concluded that aqueous acetonitrile can eliminate any mismatched PNA·DNA hybrids that might have occurred. Therefore, acetonitrile (3–10%) was always included in the washing step for longer PNA probes (>10mers).

### 3.6.6 Applications in SNP analysis: Validation of present method with synthetic single stranded DNA

The present mass spectrometric analysis of PNA·DNA hybrid on Q-sepharose using single PNA as probe provided a good specificity in differentiating complementary from single base mismatched DNA target. This technique is therefore potentially useful for detection of DNA sequences especially for Single Nucleotide Polymorphism (SNP) analysis. SNPs have important implications in human genetic studies and great potential increasingly useful as genetic markers for genome mapping studies, medical diagnostics, and human identity testing. The presence of the specific SNP allele can be implicated as a causative factor in human genetic disorders [61]. It

has been suggested that an appropriate set of SNP markers could be used to identify genetic factors associated with complex disease traits. SNPs that vary across differing population will also be useful for the purpose of human identification [104].

For SNP genotyping, a combination of two PNA probes is commonly used for one experiment; each probe should be complementary to each type of SNP so as to provide a mechanism for self-validation. For this reason, detection of DNA sequence using two PNA probes should be next investigated. An experimental model was established to verify the efficiency of the present technique for DNA sequence analysis, using synthetic DNA targets which are different at one base position.

To validate the technique using single stranded synthetic DNA, the experiments were separated into three parts. All experiments were performed under the same conditions, using different PNA probes. In the protocol, an equimolar quantity of two PNA probes (10 pmol each) was mixed with one of synthetic single-stranded DNA target (10 pmol) in 10 mM phosphate buffer pH 7.0 as binding buffer (30  $\mu$ L) and incubated at room temperature for 15 min. After the usual hybridization-absorption-washing (by water or acetonitrile) cycles, the support was then analyzed by MALDI-TOF mass spectrometry. The sequences of the PNA probes and DNA targets employed in each experiment are shown in **Table 3.7**.

**Table 3.7** PNA probes and DNA targets were employed in these experiments.

Experiment section	PNA probes (N to C)	DNA targets (5' to 3')
1	<b>P1</b> Ac-TTTTTTTTT-Lys-NH <sub>2</sub> <b>P2</b> Ac-GTAGATCACT-Ser-NH <sub>2</sub>	<b>D1</b> dAAAAAAAAA <b>D2A</b> dAGTGATCTAC
2	<b>P3</b> Ac-TTTTATTTT-Lys-NH <sub>2</sub> <b>P4</b> Ac-TTTTGTTTT-Lys-NH <sub>2</sub>	<b>D3</b> dAAAATAAAA <b>D4</b> dAAAACAAAA
3	<b>P5</b> Ac-TGTACGTCACAACTA-Lys-NH <sub>2</sub> <b>P6</b> Ac-TGTACGTAACAACCTA-Lys-NH <sub>2</sub>	<b>D5A</b> dTAGTTGTGACGTACA <b>D6A</b> dTAGTTGTTACGTACA

In the first part, the ability of a mixture of two different PNA probes to differentiate between complementary and non-complementary DNA target was tested. Using two PNA probes containing completely different sequences, namely Ac-T<sub>9</sub>-Lys-NH<sub>2</sub> (**P1**  $m/z$  = 3179.68) and Ac-GTAGATCACT-Ser-NH<sub>2</sub> (**P2**  $m/z$  = 3517.57)

as models. Two synthetic DNA dA<sub>9</sub> (**D1**) and dAGTGATCTAC (**D2A**), which are complementary with **P1** and **P2**, respectively, were employed as DNA targets. MALDI-TOF analysis results are shown in **Figure 3.39**.

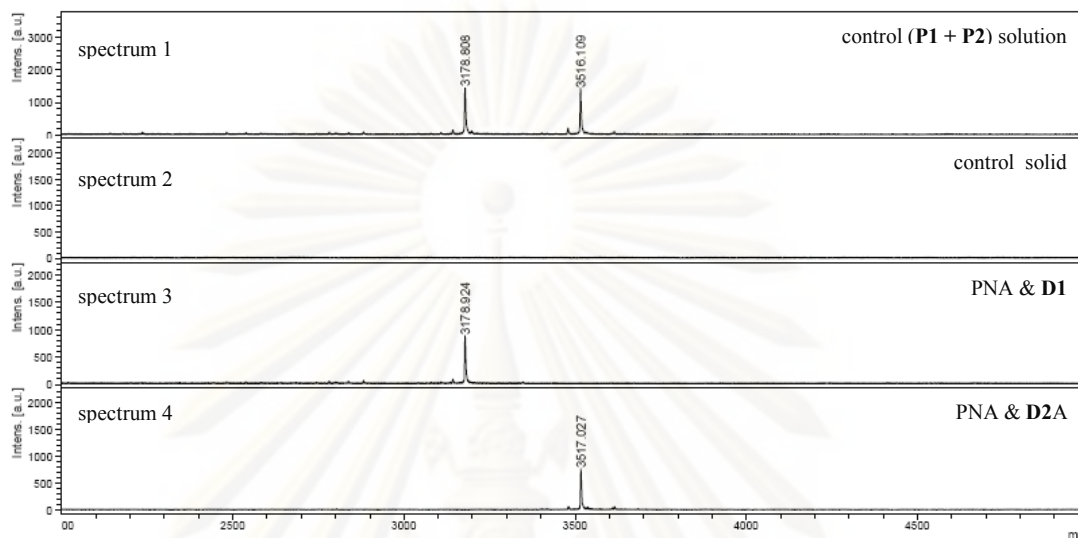


**Figure 3.39** Discrimination between complementary and fully mismatched DNA targets using a combination of two PNA probes **P1** and **P2**. Hybridization conditions: PNA 10 pmol each and DNA 10 pmol in 30  $\mu$ L binding buffer at 30  $^{\circ}$ C. Experiments from top to bottom: no DNA target (solution, positive control), no DNA target (solid, negative control), +**D1** (complementary to **P1**, single mismatch to **P2**), +**D2A** (complementary to **P2**, single mismatch to **P1**).

The results in the **Figure 3.39** revealed that in the control solution (spectrum 1) the mass signals of both PNA probes were observed. As expected, the solid control did not show any signals. Upon addition of either DNA **D1** or DNA **D2A** to the mixed PNA probe solution, only one of the mass signals of PNA probes corresponding to their complementary DNA targets was observed in the washed solid support (spectra 3 and 4). In both case, no absorption of the non-complementary PNA probe was observed.

In the second part of the experiment, differentiation between complementary and single base mismatch using a mixture of two PNA probes differing at only one base was investigated. Two PNA probes containing single base mismatch to each other at the middle position: Ac-TTTTATTTT-Lys-NH<sub>2</sub> (**P3**,  $m/z = 3186.48$ ) and Ac-TTTTGTTTT-Lys-NH<sub>2</sub> (**P4**,  $m/z = 3202.47$ ) were used as models. Two synthetic DNA dAAAATAAAA (**D3**) and dAAAACAAAA (**D4**), which are complementary

with **P3** and **P4** respectively, were employed as targets. MALDI-TOF analysis results are shown in **Figure 3.40**.

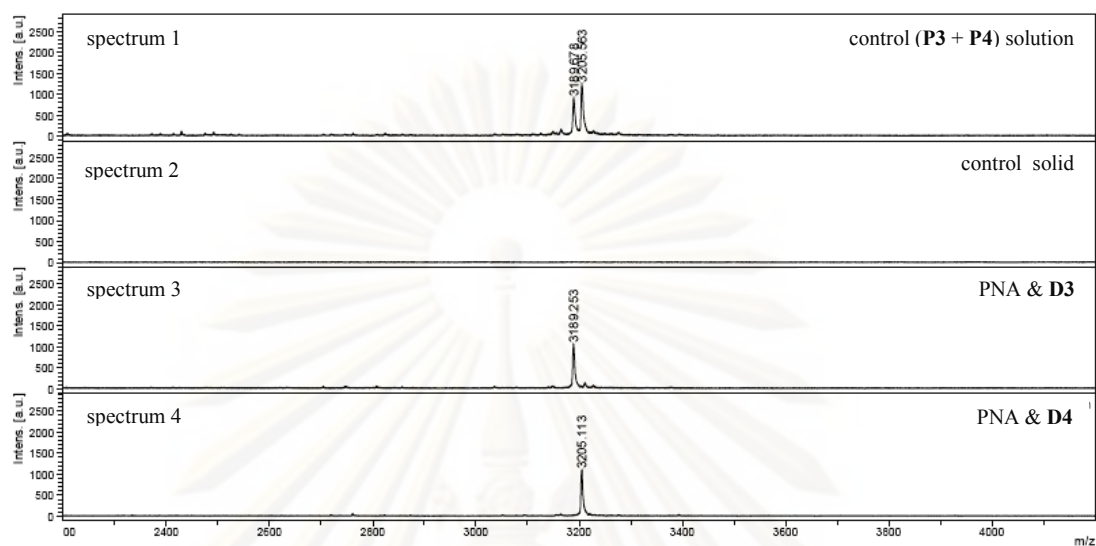


**Figure 3.40** Discrimination between complementary and fully mismatched DNA targets using a combination of two PNA probes **P3** and **P4**. Hybridization conditions: PNA 10 pmol each and DNA 10 pmol in 30  $\mu$ L binding buffer at 30  $^{\circ}$ C. Experiments from top to bottom: no DNA target (solution, positive control), no DNA target (solid, negative control), +**D3** (complementary to **P3**, single mismatch to **P4**), +**D4** (complementary to **P4**, single mismatch to **P3**).

The result shown in **Figure 3.40** indicated only mass signal of the complementary PNA probe to the DNA target when the complementary DNA target was present (spectra 3 and 4). Background absorption of non-complementary probe did not occur on the solid support therefore unambiguous differentiation between complementary and single base mismatch were easily achieved.

In the third part, two 15mers mixed base PNA probes, **P5** and **P6**, having a single base mismatch to each other were used as models. The **D5A** that is complementary with **P5** and **D6A** that is complementary with **P6** were used as targets.

The sequences of PNA probes and DNA targets are as follow.



- PNA (**P5**) : Ac-TGTACGTCACA ACTA-Lys-NH<sub>2</sub> ( $m/z = 5209.38$ )  
 PNA (**P6**) : Ac-TGTACGTAACA ACTA-Lys-NH<sub>2</sub> ( $m/z = 5232.37$ )  
 DNA (**D5A**) : 5'-TAGTTGTGACGTACA-3'  
 (complementary with **P5**, single mismatch with PNA **P6**)  
 DNA (**D6A**) : 5'-TAGTTGTTACGTACA-3'  
 (complementary with **P6**, single mismatch with PNA **P5**)

For these longer PNA probes, 10% aqueous acetonitrile was employed for washing of the solid support after the hybridization and ion-exchange capture in order to eliminate the background due to the non-complementary probe. The results from MALDI-TOF mass spectrometric analysis of the washed support are illustrated in **Figure 3.41**.

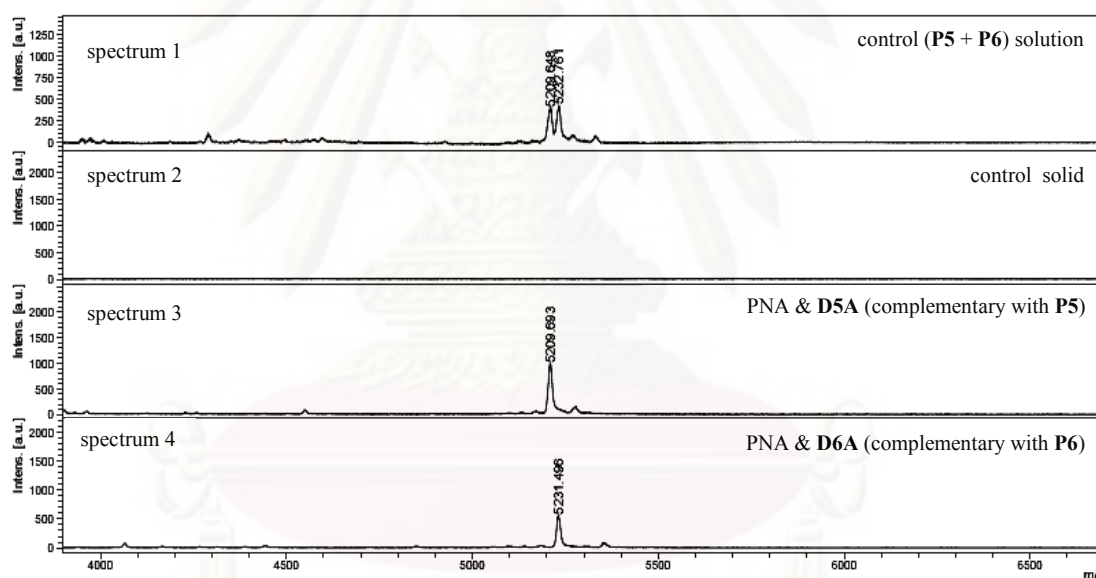


**Figure 3.41** Discrimination between complementary and fully mismatched DNA targets using a combination of two PNA probes **P5** and **P6**. Hybridization conditions: PNA 10 pmol each and DNA 10 pmol in 30  $\mu$ L binding buffer at 30  $^{\circ}$ C. Experiments from top to bottom: no DNA target (solution, positive control), no DNA target (solid, negative control), +**D5A** (complementary to **P5**, single mismatch to **P6**), +**D6A** (complementary to **P6**, single mismatch to **P5**).

From the above spectra, it was observed that after hybridization and washing with 10% aqueous acetonitrile, a satisfactory discrimination between complementary and single base mismatched 15mer DNA targets was achieved since only the mass signal of the expected PNA probe could be observed (spectra 3 and 4). The results

confirmed that aqueous acetonitrile could effectively destroy any mismatched PNA·DNA hybrids that might have formed when longer PNA probes were employed.

The results above clearly demonstrated the potential of the present technique in discrimination between complementary and single base mismatch with high specificity. The background absorption was not detected even when the hybridization and washing were carried out at room temperature.

### 3.6.7 Applications in SNP analysis: Validation of present method with synthetic double stranded DNA

All previous experiments were performed with synthetic single-stranded DNA target. In reality, DNA samples obtained from extraction and/or PCR technique are double-stranded. In this section, synthetic double-stranded DNA was employed as targets to validate the technique before applying to the real samples. In the experiment, a synthetic 15mer double-stranded DNA and 15mer mixed base PNA **P5** probe were used as models. The experiment was divided into three parts to address factors that influence the PNA·DNA hybridization including salt concentration, temperature and the length of DNA target.

The first part of the experiment was designed to study the effect of salt concentration on the formation of the hybrid between PNA and one of the DNA strand in a double-stranded DNA target. A synthetic double-stranded DNA (**D5A/D5A'**) having one of the strands (**D5A**) complementary with the PNA **P5** probe was used as a target model. The sequences of the DNA are shown below.

DNA (**D5A**) = 5'- TAGTTGTGACGTACA-3' (complementary with PNA **P5**)

DNA (**D5A'**) = 5'- TGTACGTCACA ACTA -3' (complementary with DNA **D5A**)

Two binding buffers containing different salt concentration were evaluated. Buffer 1 consisted of 10 mM phosphate buffer pH 7 containing 100 mM NaCl and buffer 2 consisted of 10 mM phosphate buffer pH 7 without added NaCl.

In the procedure, the DNA **D5A** and **D5A'** (10 pmol each) were mixed in 30  $\mu$ L of binding buffer. The hybridization was incubated at room temperature for 15 min and then denatured to their single stranded DNA components in a boiling water bath for 5 min. The mixture was rapidly cooled down at 0 °C and then the PNA probe

**P5** (10 pmol) was immediately added. The hybridization reaction was performed at room temperature for 15 min to allow complete hybridization. The pre-equilibrated solid support was then added to the PNA·DNA hybrid mixture and left for another 15 min. After that, the solid support was washed with the 10% aqueous acetonitrile. The results from MALDI-TOF mass spectrometric analysis of the washed solid support are shown in **Figure 3.42**.

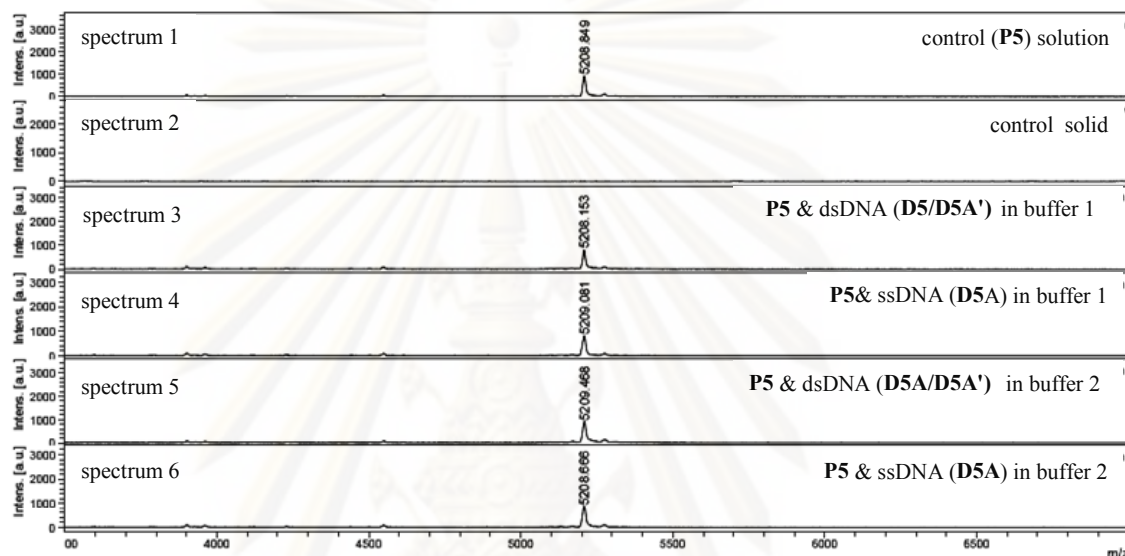


**Figure 3.42** Determination of the effect of salt concentration to the hybridization between PNA and synthetic double strand DNA

From above figure, it was apparent that the efficiency of the hybridization between PNA and synthetic double-stranded DNA in the presence of 10 mM phosphate buffer in the absence of NaCl (buffer 2) was comparable to that in the presence of NaCl (buffer 1) (spectra 3 and 5). This is in agreement with the relatively low sensitivity of PNA·DNA hybrids to ionic strength. In addition, it was also observed that the hybridization of PNA to dsDNA was at least as efficient as to ssDNA as shown by the comparable signal intensities and signal-to-noise ratio in all case. As a result, it can be concluded that dsDNA can be used as targets and that salt concentration did not effect the hybridization between PNA and dsDNA.

From the above results, 10 mM phosphate buffer pH 7 without NaCl was selected as the binding buffer for further experiments with both single-stranded and double-stranded DNA targets. The low salt hybridization buffer is beneficial in destabilizing dsDNA and minimizing secondary and tertiary structure formation. It

also simplified the reaction set-up and analysis since it is well known that high concentration of salt may interfere with MALDI-TOF analysis.

In the next part of the experiment, the differentiation between complementary and single mismatched double stranded DNA compared to the single stranded DNA was investigated. The 15mer PNA probes **P5** was employed as models. The synthetic double-stranded 15mer DNAs carrying complementary (dsDNA **D5A/D5A'**) and single base mismatched sequences (dsDNA **D5C/D5C'**) were employed as targets. The sequences of the PNA probes and DNA targets are illustrated below.

- PNA (**P5**) : Ac-TGTACGTCACA ACTA-Lys-NH<sub>2</sub> ( $m/z = 5209.38$ )  
 DNA (**D5A**) : 5'-TAGTTGTGACGTACA-3' (complementary with PNA **P5**)  
 DNA (**D5A'**) : 5'-TGTACGTCACA ACTA-3' (complementary with **D5A**)  
 DNA (**D5C**) : 5'-TAGTTGTTACGTACA-3' (single mismatch with PNA **P5**)  
 DNA (**D5C'**) : 5'-TGTACGTAACA ACTA-3' (complementary with **D5C**)

In the procedure, one of the dsDNA target (10 pmol each) were mixed in 30  $\mu$ L of binding buffer (10 mM phosphate buffer pH 7.0) and incubated at room temperature for 15 min. The mixture was then heated in boiling water bath for 5 min and rapidly cooled down at 0°C and solid support was added to mixture immediately. The PNA probe **P5** (10 pmol) was added to mixture immediately. The mixture was incubated at room temperature for 15 min to allow complete hybridization. After the usual hybridization-absorption-washing cycle (with 10% aqueous acetonitrile to remove non-specifically bound probes), the support bound PNA·DNA hybrid was analyzed by MALDI-TOF mass spectrometry. The results are shown in **Figure 3.43**.

ศูนย์วิทยทรัพยากร  
จุฬาลงกรณ์มหาวิทยาลัย

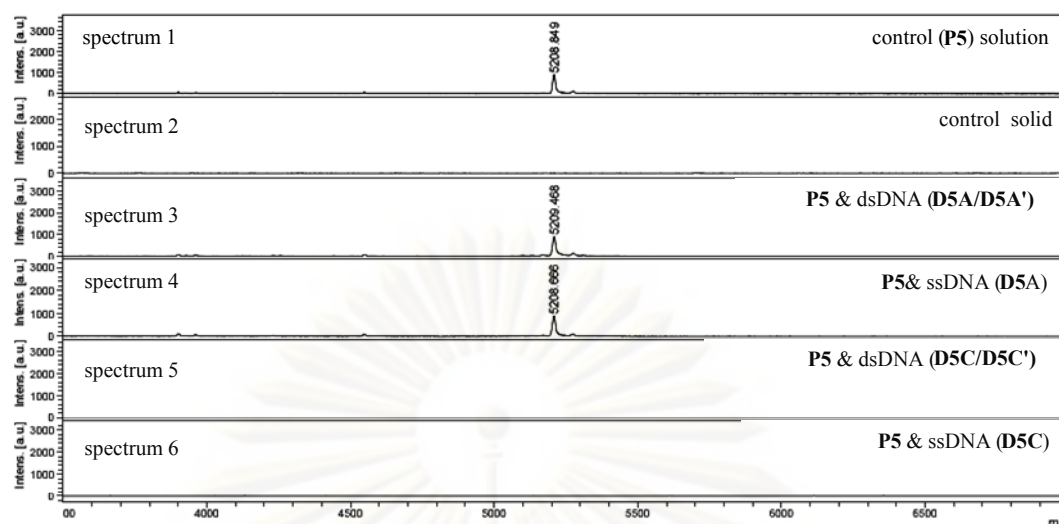


**Figure 3.43** Discrimination between complementary and single mismatch in double stranded DNA targets by the 15mer PNA probe **P5**. Hybridization conditions: PNA 10 pmol, DNA 5 pmol, 10 mM sodium phosphate buffer pH 7.0 (30  $\mu$ L) at 30  $^{\circ}$ C. Experiments from top to bottom: no DNA target (solution, positive control), no DNA target (solid, negative control), +ds**D5A/D5A'** (complementary, double-stranded), +**D5A** (complementary, single-stranded), +ds**D5C/D5C'** (C·T single mismatch, double-stranded), +**D5C** (C·T single mismatch, single-stranded),

From the **Figure 3.43**, it was illustrated that the present method can clearly differentiate between the complementary duplex (dsDNA **D5A/D5A'**) and single base mismatched duplex (dsDNA **D5C/D5C'**) as shown in spectra 3 and 5 with comparable results (signal intensity, S/N ratio) to the corresponding single stranded DNA (**D5A** and **D5C**) as revealed in spectra 4 and 6 under the same conditions.

Hybrid formation with longer double stranded DNA is potentially difficult due to the expected high stability of the dsDNA. Prior dissociation of the duplex to single stranded DNA under a suitable condition, such as heating, before the hybridization should facilitate the hybridization process. Therefore, in the last part of the experiment, applicability of this technique with long synthetic double stranded DNA sequences was verified. In the experiment, hybridization between PNA probe hybrid and dsDNA target under the standard protocol (without heating) and the new protocol with an additional heating step to denature double stranded to single strand DNA just before hybridization with the PNA probe were made. The experiment employed the 15 mer PNA probes **P5** as model and two 30mer synthetic double-stranded DNA having complementary sequence at the terminal (**D15A/15B**) and middle (**D16A/16B**) position of the sequence as targets. Their sequences are shown as follows.

PNA (**P5**) : Ac-TGTACGTCACA ACTA-Lys-NH<sub>2</sub> ( $m/z = 5209.38$ )

dsDNA (**D15A·D15B**)

DNA (D15A) : 5'-TAGTTGTGACGTACACGTAAGTGACCGTCA-3'

DNA (D15B) : 3'-ATCAACACTGCATGTGCATTCACTGGCAGT-5'

dsDNA (**D16A·D16B**)

DNA (D16A) : 5'-ATCTAGCTAGTTGTGACGTACATACGCATC-3'

DNA (D16B) : 3'-TAGATCGATCAACACTGCATGTATGCGTAG-5'

In all cases, the hybridization steps were carried out in 10 mM phosphate buffer pH 7.0. The solid supports were washed with the 10% aqueous acetonitrile. The results from MALDI-TOF analysis of the washed support are shown in **Figure 3.44**.

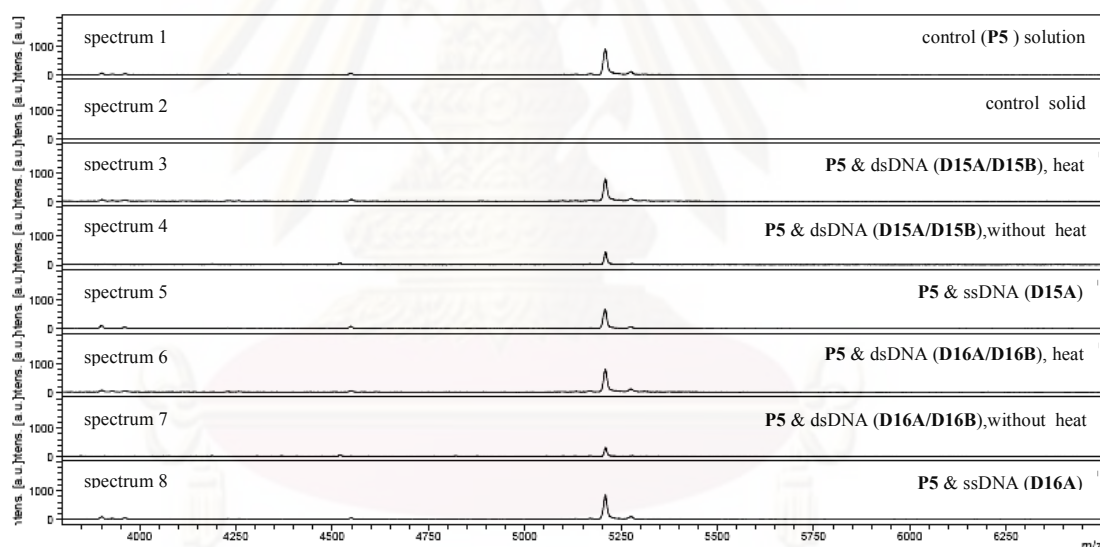


**Figure 3.44** Comparison the efficacy of PNA·DNA hybridization under usual condition and new condition with additional heating step

From the above results, it was apparent that the efficiency of the hybridization between PNA probe and two 30mers synthetic double-stranded DNA sequence was better using the new hybridization procedure with the additional heating step. As shown in spectra 3 (**D15A·D15B**) and 6 (**D16A·D16B**) (with heating) compared to the usual conditions (without heating) in spectra 4 (**D15A·D15B**) and 7 (**D16A·D16B**), the signals intensity and S/N ratio obtained from the new protocol were better. The

efficiency of the hybridization between PNA and synthetic 30mers double-stranded DNA with additional heating step was comparable to that of the corresponding single-stranded DNA targets as indicated in spectra 5 (**D15A**) and 8 (**D16A**). The position of the sequence to be detected in the DNA targets had no effect on the hybridization efficiency. In addition, the order of hybridization and absorption steps could be reversed without any observable difference. Under the usual hybridization conditions (without heating), the longer double-stranded DNA might be more stable than the short double-stranded DNA making it difficult for the PNA to dissociate and hybridize with one strand of the DNA target. The heating step used was necessary to first dissociate the DNA duplex. Upon rapid cooling, the DNA remained in its single stranded form. Therefore, in case of real DNA samples detection, it was preferable to include of the heating step to denature the dsDNA before hybridization with the PNA.

Although all above results suggested that the *acpc*PNA in combination with Q-sepharose capture and MALDI-TOF MS can be potentially useful for DNA sequence analysis, the sensitivity of the analysis was still less than satisfactory since at least 10 pmol of PNA probes and DNA samples are usually required to obtain acceptable S/N ratio. Although these quantities of DNA are available by standard PCR, it is quite wasteful of the expensive PNA probes. Therefore, the improvement of the sensitivity of PNA probe for detecting DNA sequence was next studied.

### **3.6.8 Investigation of the effect of positively charged labeling groups on PNA to enhance the sensitivity of the detecting DNA sequence**

Since the PNA probe is analyzed in positive ion time-of-flight mode by MALDI-TOF mass spectrometry, attaching a charged labeling group on the PNA probe might enhance the sensitivity of the detection further [73]. Therefore, the effect of modification of the PNA with positively charged labeling groups to the detection limit was next studied. To assess the effectiveness of positively charged labeling groups, a simple PNA probes (Ac-TTTT-ser-NH<sub>2</sub>) was modified by at the N-termini capping with arginine or carboxybutyltriphenylphosphonium group and directly compared with the unmodified sequence. The structures of arginine and carboxybutyltriphenylphosphonium group are shown in **Figure 3.45**.

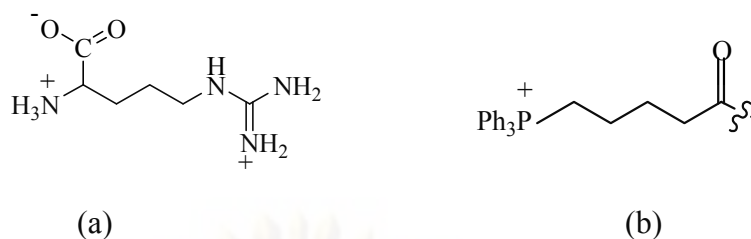
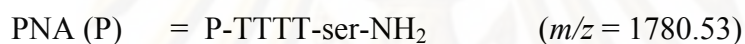
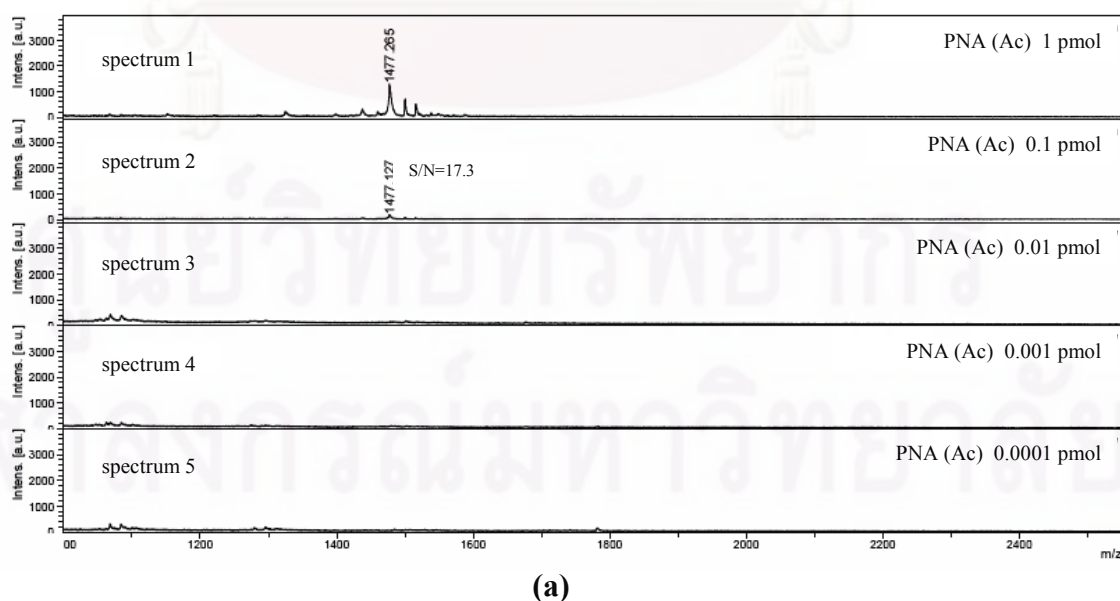


**Figure 3.45** Structure of (a) arginine and (b) carboxybutyl triphenyl phosphonium group

The sequences of the modified PNA probes used in this study are shown below.

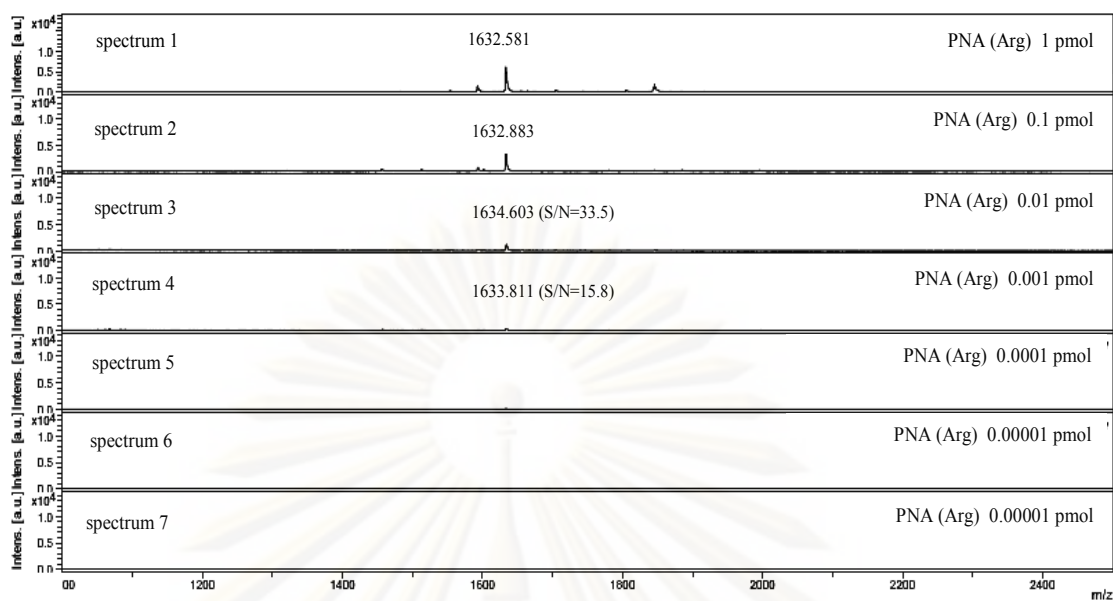


In the experiment, the amount of each PNA probe deposited on the MALDI-TOF target was varied in range between 10 pmol to 0.00001 pmol. One microliter of the stock PNA solution was mixed with the matrix solution (10  $\mu$ L). The resulting sample mixture (1  $\mu$ L) was deposited onto the target and analyzed by MALDI-TOF mass spectrometry. The results are illustrated in **Figure 3.46**.

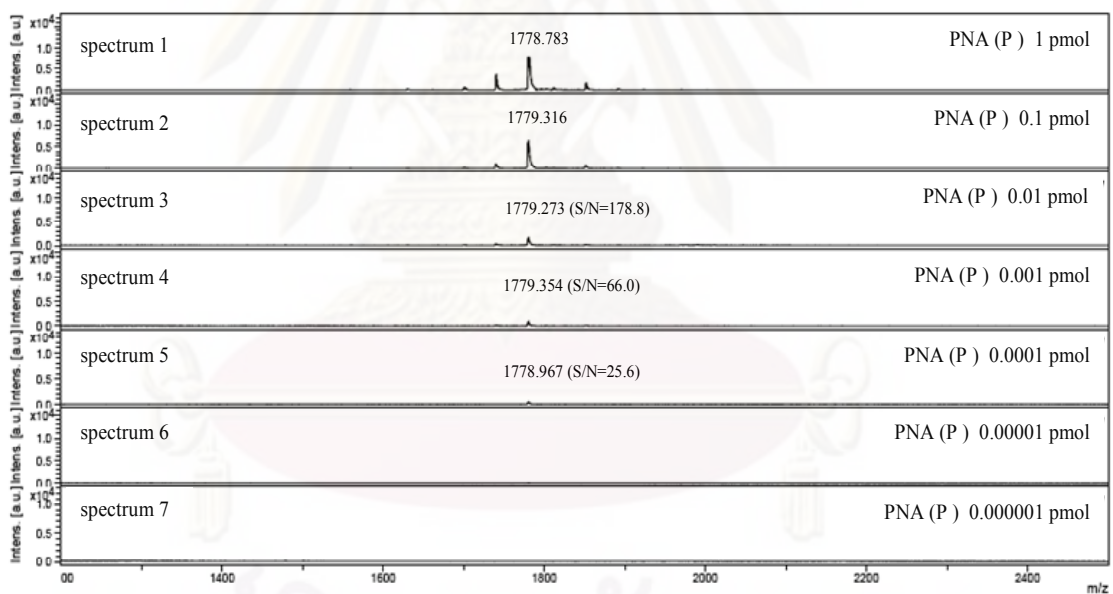


(a)





(b)



(c)

**Figure 3.46** Determination of the limit of detection of

(a) unmodified PNA (PNA (Ac))

(b) PNA with N-terminal arginine group (PNA (Arg))

(c) PNA with N-terminal carboxybutyltriphenylphosphonium group (PNA (P))

From the spectra, the minimum amount of PNA (Ac), PNA (Arg) and PNA (P) that could be detected were 0.1, 0.001 and 0.0001 pmol (at S/N ratio= 17.3, 15.8 and 25.6) as shown in **Figures 3.46** respectively. It can be concluded that attaching a positively charged labelling group can improve the sensitivity of PNA detection using mass spectrometry. Therefore, PNA probes used in later experiments were modified with *N*-arginine or carboxybutylphosphonium to improve sensitivity of the detection.

At this stage, it was considered that the technique was sufficiently robust to allow determination of real DNA sequences. Applications of the technique in analysis of meat products and human DNA will be discussed in the next section.

### **3.7 Investigation of the applicability of this method in real DNA samples derived from PCR amplification.**

#### **3.7.1 Identification of meat products in feedstuff.**

To demonstrate its applications, the present technique was applied for the identification of meat species in feedstuffs using a fragment of mitochondrial cytochrome *b* gene from bovine (*Bos taurus*) and porcine (*Sus scrofa*). The DNA sequence information was obtained using Clustal W2 and BLASTN analysis of the National Center for Biotechnology Information (NCBI database). For identification, 53bp DNA fragments (nucleotides 628–680) containing a single diagnostic T/C difference at nucleotide position 654 were prepared from the meat samples by PCR amplifying the cytochrome *b* gene covering the desired this SNP site using 5'-GGAATCTCTCAGAC-3' and 5'-TTAATAGTGTAGTA-3' primers and hybridized with two 11mer arginine-labeled PNA probes **P7** and **P8**, which were specific for bovine and porcine species respectively. The results were compared with a standard process, PCR-RELF [105–106]. The sequences of the PNA **P7**, **P8** and the bovine and porcine target having the SNP site of the cytochrome *b* gene are shown below.

PNA **P7** = Ac-Arg-AAAATCCCATT-ser-NH<sub>2</sub> ( $m/z = 3961.46$ )

PNA **P8** = Ac-Arg-AAAATTCCATT-ser-NH<sub>2</sub> ( $m/z = 3976.21$ )

(a)

	▼ 628	▼ 654	Accession No. ▼ 680
<i>Sus scrofa</i>	GGAATCTCATCAGACATAGACAAAATtCCATTTCACCCATACTACACTATTAA		AM492627
<i>Sus scrofa</i>	GGAATCTCATCAGACATAGACAAAATtCCATTTCACCCATACTACACTATTAA		DQ334861
<i>Bos javanicus</i>	GGAATCTCCTCAGACATAGACAAAATtCCATTTCACCCCTACTACACTATTAA		EF685914
<i>Bos indicus</i>	GGAATCTCCTCAGACATAGACAAAATtCCATTTCACCCCTACTACACTATTAA		EF061240
<i>Bos taurus</i>	GGAATCTCCTCAGACATAGACAAAATtCCATTTCACCCCTACTACACTATTAA		DQ186269

(b)

**Figure 3.47 (a)** Sequence of PNA **P7** and PNA **P8**

**(b)** Target cytochrome b sequence used for identification of meat samples

Prior to applying the method to a real system, the fidelity of the hybridization was first established by using two 11bp synthetic oligonucleotides (DNA **D7** and **D8**) as targets. The sequences of the two synthetic DNA are shown as follow.

DNA **D7** = 5'- AATGGGATTTT -3' (complementary with PNA **P7**)

DNA **D8** = 5'- AATGGAATTTT -3' (complementary with PNA **P8**)

In the experiment, an equimolar mixture of the two PNA probes (10 pmol each) was mixed with 10 pmol of either **D7** or **D8** in 10 mM sodium phosphate buffer (30  $\mu$ L) and incubated at room temperature. After 15 min of hybridization, Q-sepharose ( $\sim$ 3  $\mu$ L) was added to the mixture and left for another 15 min. The solid supports were then washed with water. The results from MALDI-TOF mass spectrometric analysis of the washed anion exchange support are shown in **Figure 3.48**.

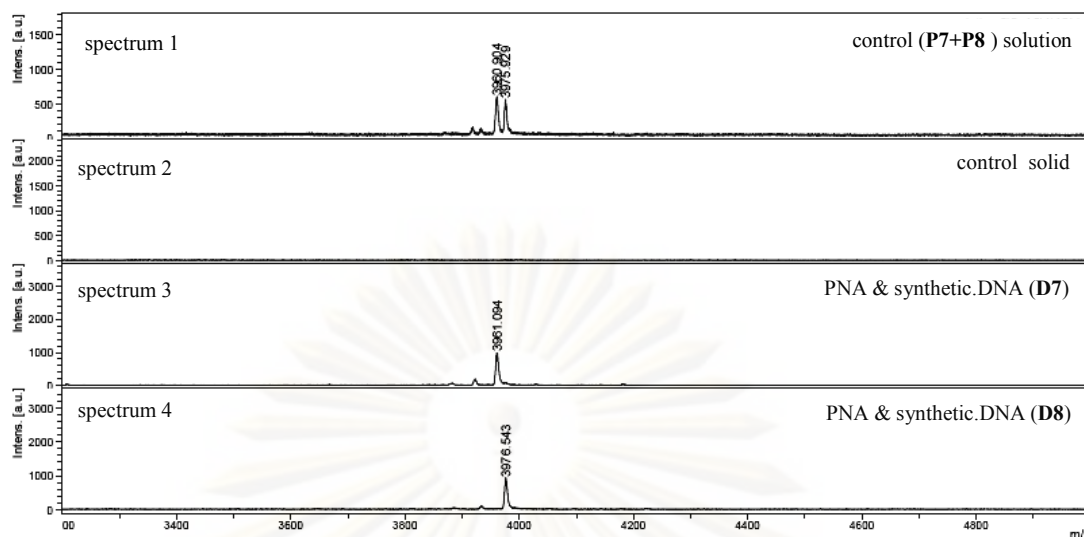


**Figure 3.48** Identification of bovine and porcine DNA in meat products by the 11mer PNA probes **P7** and **P8**. Hybridization conditions: PNA 10 pmol each, DNA 10 pmol, 10 mM sodium phosphate buffer pH 7.0 (30  $\mu$ L) at 30  $^{\circ}$ C. Experiments from top to bottom: no DNA target (solution, positive control), no DNA target (solid, negative control), +**D7** (complementary to **P7**), +**D8** (complementary to **P8**)

The results clearly revealed the high sequence specificity between the probes and their complementary targets. Complementary and single base mismatched targets could be readily distinguished. In the presence of the DNA **D7** (complementary with the PNA **P7**) the result showed a mass signal at  $m/z = 3961.1$  corresponding to the PNA **P7** (spectrum 3). On the other hand, spectrum 4 showed only the mass signal of PNA **P8** at  $m/z = 3976.5$  in the presence of the DNA **D8** (complementary with PNA **P8**). For such short PNA probes (11 mer), a clear differentiation between complementary and single base mismatch was achieved when using water alone in the washing step. The high specificity can be described in term of the difference in melting temperature ( $T_m$ ) between the complementary and single mismatched PNA·DNA hybrids. The  $T_m$  value of single mismatched **P7·D8** duplex and **P8·D7** duplex (Table 3.6) were 37.8  $^{\circ}$ C and 38.7  $^{\circ}$ C, respectively. These figures are considerably lower than that of the perfectly matched **P7·D7** (63.1  $^{\circ}$ C) and **P8·D8** (65.9  $^{\circ}$ C) hybrids ( $\Delta T_m = -28.1$   $^{\circ}$ C and  $-24.4$   $^{\circ}$ C, respectively). The difference  $T_m$  between the complementary and single mismatch duplex of both sequence was very high which explained the high discrimination power of the present PNA probes. The  $T_m$  of both mismatched hybrids was also low, thereby using only water in washing step was sufficient eliminate the non-specific signal from the support-bound mismatched PNA·DNA hybrid. However,

since the  $T_m$  is concentration dependent, one should be careful in relying on the  $T_m$  data obtained under different concentrations (1  $\mu\text{M}$ ) from the actual hybridization conditions. In these cases, the explanation based on  $T_m$  should still be valid since all probes are compared under more or less the same concentration (in the range of 1–10 pmol/30  $\mu\text{L}$ , equivalent to 0.03–0.3  $\mu\text{M}$ ).

From the satisfactory results obtained with synthetic DNA targets, this method was further applied in real DNA sample derived from PCR amplification for detection of bovine and porcine species in meat products. A total of 14 DNA samples from meats and feedstuffs were analyzed. In the protocol, each of double-stranded DNA sample ( $\sim 5$   $\mu\text{L}$ ) was mixed with 30  $\mu\text{L}$  of 10 mM sodium phosphate buffer pH 7.0 and denatured in a boiling water bath for 5 minutes. The mixture was rapidly cooled down to 0°C and then a pre-equilibrated Q-sepharose support (3  $\mu\text{L}$ ,  $\sim 3$  mg) was immediately added to immobilize single-stranded DNA on the solid support. After 15–20 min at room temperature (30 °C), the solid support was extensively washed with 10 mM sodium phosphate buffer pH 4.0 and re-suspended in 30  $\mu\text{L}$  of the hybridization buffer. This procedure allowed extensive washing of the support-bound DNA to remove impurities like salts, proteins and nucleotides in the PCR samples before subsequent hybridization with the PNA probe. For hybridization, a mixture containing an equimolar quantity of each PNA probe (10 pmol) was added to this support-bound DNA suspension. The hybridization mixture was then incubated at room temperature for another 15–20 min. After the usual hybridization-absorption-washing cycle (with water), the solid support was analyzed by MALDI-TOF mass spectrometry. The results are shown in **Figure 3.49** and **Table 3.8**.

ศูนย์วิทยทรัพยากร

จุฬาลงกรณ์มหาวิทยาลัย

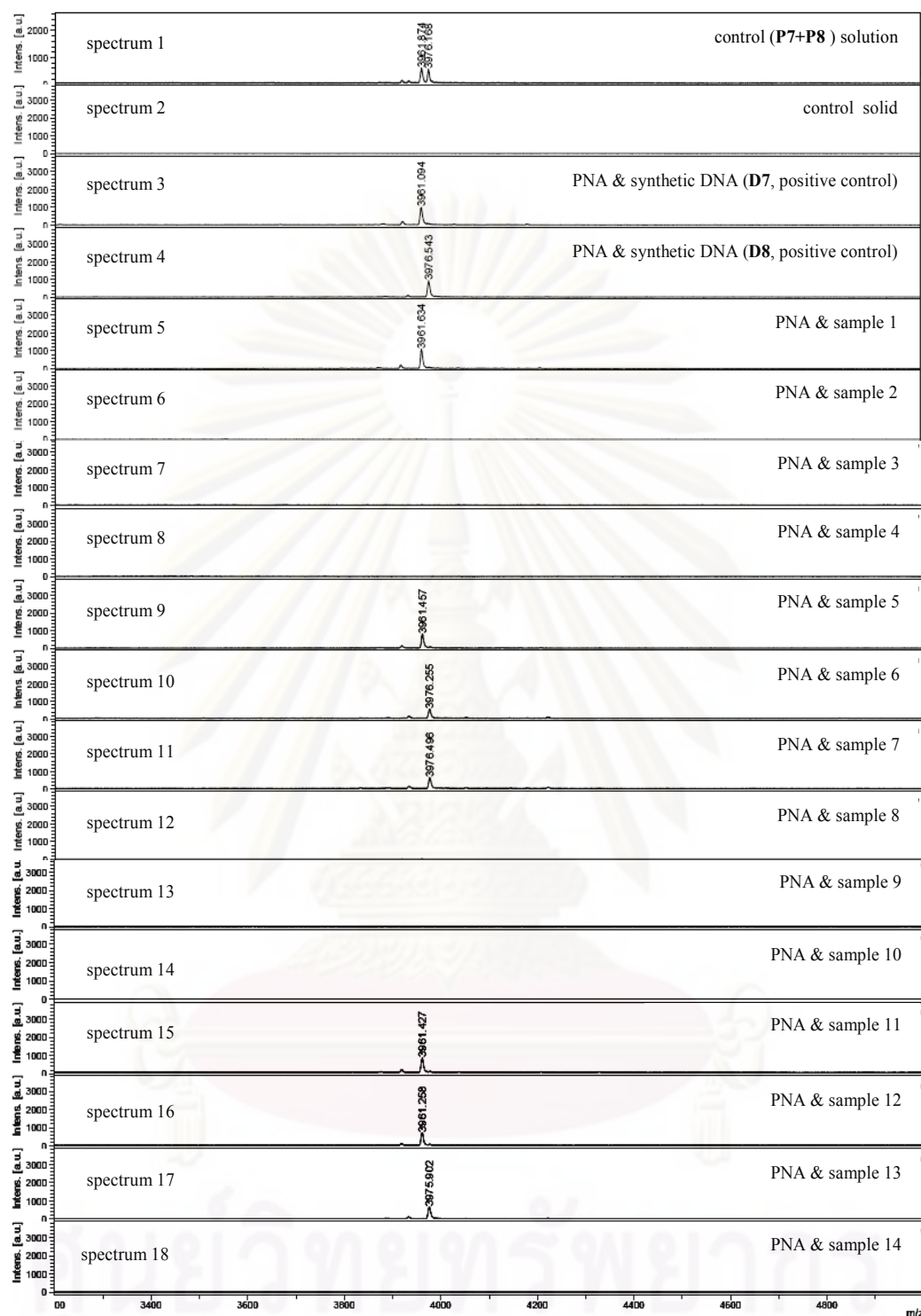


**Figure 3.49** Identification of bovine and porcine DNA in meat products by using the PNA probes **P7** and **P8**.

The result in above spectra revealed the potential of this technique in detection of the bovine and porcine species in the DNA samples by using PNA **P7** and **P8** as probes. The results are in complete agreement with the origin of the samples and with two independent analysis techniques (PCR-RFLP and electrochemical biosensor) [105–106]. Amongst the samples tested, it was found that the mass signal of PNA **P7**, but not **P8**, was observed in sample 1, 5, 11 and 12. It can therefore be concluded that these samples contain only bovine meats. On the other hand, analysis of samples 6, 7 and 13 revealed only mass signal corresponding to PNA **P8**. Consequently, such samples contained only porcine meat. The remaining samples exhibited neither signals of **P7** nor **P8** hence they did not contain bovine and porcine meat. The mass present in these samples were obtained using an external calibration at the beginning of the experiment. A mass error range lower than 150 ppm was obtained which were more than adequate to unambiguously discriminate between the two PNA probes ( $\Delta m/z = 15.1$ ) in the whole set of experiments. The results from the above spectra are also summarized in **Table 3.8**.

**Table 3.8** Analysis results of DNA samples obtained from meat products

sample no.	description	observed $m/z$ (error, ppm)	results	independent analysis <sup>a,b</sup>
DNA D7	bovine positive control (synthetic)	3961.1 (-25.2)	bovine	N/A
DNA D8	porcine positive control (synthetic)	3976.5 (+75.4)	porcine	N/A
Sample-1	Cloned target DNA (bovine positive)	3961.4 (+50.4)	bovine	bovine
sample-2	Soybean genomic DNA	None	negative	negative
sample-3	Non template control	None	negative	negative
sample-4	Poultry meat (Thai)	None	negative	negative
sample-5	Ruminant meat (Thai)	3961.5 (+75.7)	bovine	bovine
sample-6	Pig meat (Thai)	3976.3 (+50.3)	porcine	porcine
sample-7	Pig bone meat (Netherlands)	3976.5 (+75.4)	porcine	porcine
sample-8	Hydrolyzed feather (Australia)	None	negative	negative
sample-9	Chicken blood meal (Australia)	None	negative	negative
sample-10	Poultry meal (France)	None	negative	negative
sample-11	Pet food paste 7% protein (cattle & poultry , Thai)	3961.4 (+50.4)	bovine	bovine
sample-12	Pet food paste 8% protein (cattle & poultry, France)	3961.3 (+25.2)	bovine	bovine
sample-13	Actipro 95PHS (pig & poultry , Netherlands)	3975.9 (-75.4)	porcine	porcine
sample-14	Pet food bar (poultry , Thai)	None	negative	negative

<sup>a</sup> standard PCR-RFLP analysis<sup>b</sup> electrochemical biosensor



### 3.7.2 Genotyping of single nucleotide polymorphism (SNP) in human gene

Apart from identification of meat species in feedstuffs, the present technique was also applied to the detection of SNP in human DNA. The target chosen was human interleukin-10 (*IL-10*) promoter gene, which was believed to be associated with autoimmune disease like systemic lupus erythematosus (SLE) and psoriasis [107–108]. Three regions in the *IL-10* promoter gene: rs1800896 (–1082 G/A), rs1800871 (–819 C/T) and rs1800872 (–592 A/C) were selected as representative cases. The DNA sequences of the three respective regions are shown in **Figure 3.50**.

#### Substrate DNA PCR product:

rs1800896 (–1082 G/A)

5'-CCCTTACTTTTCCTTACCTATCCCTACTTCCCC(c/t)TCCCAAAGAAGCCTTAGTAGTGTTGTCTTGGATT-3'  
3'-GGGAATGAAAGGAGAATGGATAGGGATGAAGGGG(g/a)AGGGTTTCTTCGGAATCATCACAACAGAACCTAA-5'

rs1800871 (–819 C/T)

5'-TATTTTATAGTGAGCAAAGTCTGAGGCACAGAGAT(a/g)TTACATCACCTGTACAAGGGTACACCAGTGC-3'  
3'-ATAAAATATCACTCGTTTGACTCCGTGCTCTA(t/c)AATGTAGTGGACATGTTCCCATGTGGTCACG-5'

rs1800872 (–592 A/C)

5'-CCATTTACTTTCCAGAGACTGGCTTCTACAG(g/t)ACAGGCGGGGTCACAGGATGTGTTCCAGGC-3'  
3'-GGTAAAATGAAAGGTCTCTGACCGAAGGATGTC(c/a)TGTCGCCCCAGTGTCTACACAAGGTCCG-5'

**Figure 3.50** *IL-10* promoter gene sequence

The first experiments focused on two SNP sites, rs1800896 (–1082 G/A) and rs1800871 (–819 C/T). Four PNA probes (**P9–P12**) corresponding to the two SNP sites were designed. The probes **P9** and **P10** corresponded to SNPs –1082G and –1082A, whereas **P11** and **P12** corresponded to SNPs –819C and –819T respectively. All PNA probes were 13 bases long. Probes shorter than 10 and longer than 15 bases tend to be less specific due to non-uniqueness of the sequences in the genome and the high stability of single mismatched duplex, respectively. The carboxybutyltriphenyl phosphonium label was attached to the *N*-termini of the PNA probes to enhance the sensitivity of the detection by MALDI-TOF MS. Using these phosphonium-labeled probes, the quantity of the PNA probe desired for one experiment could be reduced to 10 fmol while clear signals was still obtained. In the actual experiments, it was

purposely decided to employ significantly larger amounts of probes (1 pmol) than this detection limit to ensure reproducibility and to obtain high quality spectra with reasonable signal-to-noise ratio. The sequences and polymorphisms of the SLE alleles (**Figure 3.50**) as well as the PNA probes used to recognize this polymorphism were indicated in the **Table 3.9**.

**Table 3.9** Sequence polymorphism of PCR product and corresponding PNA probe

<u>rs1800896</u>	
-1082G	5'.....GGCTTCT <u>TTGGGAGGGGGAA</u> GTAGGGA.....-3' PNA ( <b>P9</b> ) P- TTCCCC <u>C</u> TCCCAA-ser-NH <sub>2</sub> ( <i>m/z</i> = 4668.01 )
-1082A	5'.....GGCTTCT <u>TTGGGAAGGGGAA</u> GTAGGGA.....-3' PNA ( <b>P10</b> ) P-TTCCCC <u>T</u> TCCCAA-ser-NH <sub>2</sub> ( <i>m/z</i> = 4683.36 )
<u>rs1800871</u>	
-819C	5'.....GAGGCACAGAGATGTTACATCACCTGTACA.....-3' PNA ( <b>P11</b> ) P-ATGTAAC <u>A</u> TCTCT -ser-NH <sub>2</sub> ( <i>m/z</i> = 4785.75 )
-819T	5'.....GAGGCACAGAGATATTACATCACCTGTACA.....-3' PNA ( <b>P12</b> ) P-ATGTAAT <u>A</u> TCTCT -ser-NH <sub>2</sub> ( <i>m/z</i> = 4801.46 )

P = carboxybutyltriphenyl phosphonium

Before attempting to genotype real DNA samples, a model analysis on synthetic DNA was first investigated to study the ability of each probe to specifically recognize their complementary DNA. In addition, two homozygous DNA samples namely S64 (-1082G, -819C) and N2 (-1082A, -819T) from individuals known to possess the target polymorphism were generated by amplifying the region of human *IL-10* promoter carrying the desired SNP sites and also included in the samples.

As a model for rs1800896 typing, **P9** and **P10** were used as probes (1 pmol each). Two synthetic DNA (5 pmol each) namely 5'-TTGGGGGAGGGAA-3' (**D9**, complementary with **P9**) and 5'-TTGGGGAAGGGAA-3' (**D10**, complementary with **P10**) were used as positive controls. Following the standard protocol, the results from MALDI-TOF mass spectrometric analysis of the washed solid support are shown in **Figure 3.52**.

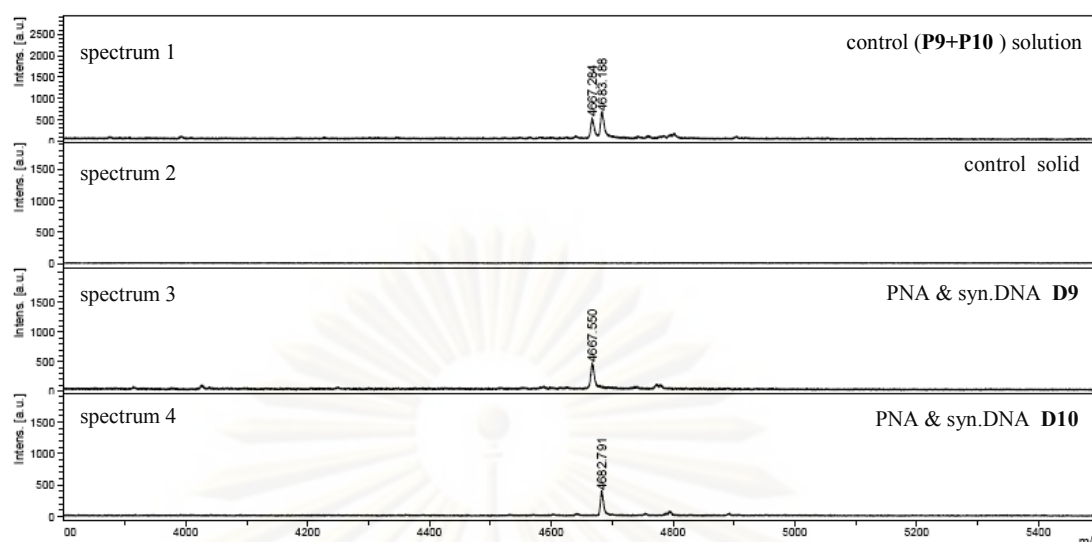


**Figure 3.51** Discrimination between complementary and single mismatched DNA targets using a combination of two PNA probes **P9** and **P10**. Hybridization conditions: PNA 1 pmol each and DNA 5 pmol in 30  $\mu$ L binding buffer at 30  $^{\circ}$ C. Experiments from top to bottom: no DNA target (solution, positive control), no DNA target (solid, negative control), +**D9** (complementary to **P9**, single mismatch to **P10**), +**D10** (complementary to **P10**, single mismatch to **P9**).

The spectra 3 and 4 in **Figure 3.52** clearly showed that the two DNA corresponding to each different SNP at the position  $-1082$  (rs1800896) could be readily distinguished. The mass signal at 4667.7 in the spectrum 3 corresponded to **P9** which is complementary with **D9**. Spectrum 4 showed a mass signal at 4682.8 of **P10** whose sequences correspond to **D10**. No signals were detected in the absence of any DNA (spectrum 2), indicating no non-specific absorption of the PNA probes.

As models for SNP typing at the position  $-819$  (rs1800871), **P11** and **P12** were employed as probes (1 pmol each). Two synthetic DNA (5 pmol each) namely 5'-AGAGATGTTACAT-3' (**D11**, complementary with **P11**) and 5'-AGAGATATTACAT-3' (**D12**, complementary with **P12**) were used as positive controls. The results from MALDI-TOF mass spectrometric analysis of the washed solid support are shown in **Figure 3.52**.

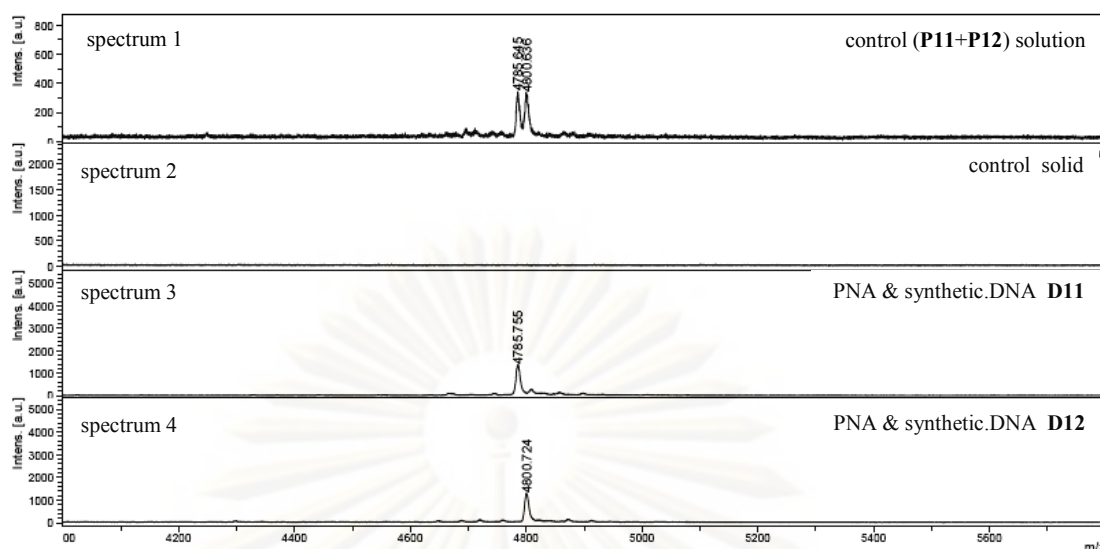


**Figure 3.52** Discrimination between complementary and single mismatched DNA targets using a combination of two PNA probes **P11** and **P12**. Hybridization conditions: PNA 1 pmol each and DNA 5 pmol in 30  $\mu$ L binding buffer at 30  $^{\circ}$ C. Experiments from top to bottom: no DNA target (solution, positive control), no DNA target (solid, negative control), +**D11** (complementary to **P11**, single mismatch to **P10**), +**D12** (complementary to **P12**, single mismatch to **P11**).

Again, spectra 3 and 4 in **Figure 3.52** clearly showed that the two DNA corresponding to each SNP at the position  $-819$  (rs1800871) could be readily distinguished. The mass signal at  $m/z = 4785.8$  in the spectrum 3 corresponded to **P11** which is complementary with **D11**. Spectrum 4 showed a mass signal at 4800.7 of **P12** whose sequences correspond to the **D12**. No signals were detected in the absence of any DNA (spectrum 2).

Although the two model SNP typing experiments were successful, different washing conditions were required for the two typing experiments. After washing the support with water, a clear differentiation between complementary and single base mismatch was achieved in case of using **P9** and **P10** as probe (**Figure 3.51**). On the other hand, when **P11** and **P12** were employed as probes, the support had to be washed with aqueous acetonitrile (3% MeCN in  $H_2O$ ) to give a clear discrimination between complementary and single base mismatch. This can be explained in term of the difference in melting temperature ( $T_m$ ) between the perfectly matched duplex and mismatched duplexes. In case of using **P9** and **P10** as probes, the  $T_m$  of mismatched **P9**·**D10** duplex (32.8  $^{\circ}$ C) was comparable to that of **P10**·**D9** duplex (32.4  $^{\circ}$ C) and these numbers were very different from the  $T_m$  of the perfectly matched **P9**·**D9** duplex

(63.8 °C,  $\Delta T_m = 35.1$  °C) and **P10·D10** duplex (67.9 °C,  $\Delta T_m = 31.4$  °C). The low stability of mismatched duplex means that washing with water was sufficient to destroy the support-bound PNA–DNA hybrid and a clear discrimination was achieved (**Figure 3.52**).

On the contrary, when **P11** and **P12** were used as probes, it was found that the  $T_m$  of the mismatched duplexes **P11·D12** (43.9 °C) and **P12·D11** (52.8 °C) were much higher than that of mismatched duplexes **P9·D10** and **P10·D9**. The  $T_m$  of the mismatched **P12·D11** duplex was less different from the fully complementary **P12·D12** duplex (75.8 °C,  $\Delta T_m = 19.8$  °C). Furthermore, the mismatched duplexes in these cases had  $T_m$  values above room temperature. This may allow partial absorption of the mismatched duplexes on the support. Fortunately, washing of support-bound PNA·DNA hybrid with 3% aqueous acetonitrile after hybridization could completely remove the mismatched hybrid signal and clearly distinguish between complementary and single base mismatch.

Encouraged by the above results, the singleplex SNP genotyping in the real human DNA sample derived from PCR amplification (S64 and N2) using the above mentioned PNA sequences as probe was further investigated.

In the experiments, each of double-stranded DNA sample (~5  $\mu$ L) was mixed with 30  $\mu$ L of 10 mM sodium phosphate buffer pH 7.0 and denatured in boiling water bath for 5 min. The mixture was then rapidly cooled down at 0 °C followed by addition of the pre-equilibrated solid support (3  $\mu$ L, ~3 mg) to immobilize single-stranded DNA. After incubation for 15–20 min at room temperature (30 °C), the solid support was extensively washed with 10 mM sodium phosphate buffer pH 4.0 and resuspended in 30  $\mu$ L of the hybridization buffer. For hybridization, a mixture containing equimolar quantity of each PNA probe (1 pmol), **P9** and **P10** for –1082 g/a, **P11** and **P12** for –819 c/t, was added to support-bound DNA sample suspended in binding buffer and incubated at room temperature for 15–20 min. After the usual hybridization-absorption-washing cycle (with water or aqueous acetonitrile), the anion exchange support was analyzed by MALDI-TOF mass spectrometry. The results are shown in **Figures 3.53** and **3.54**.

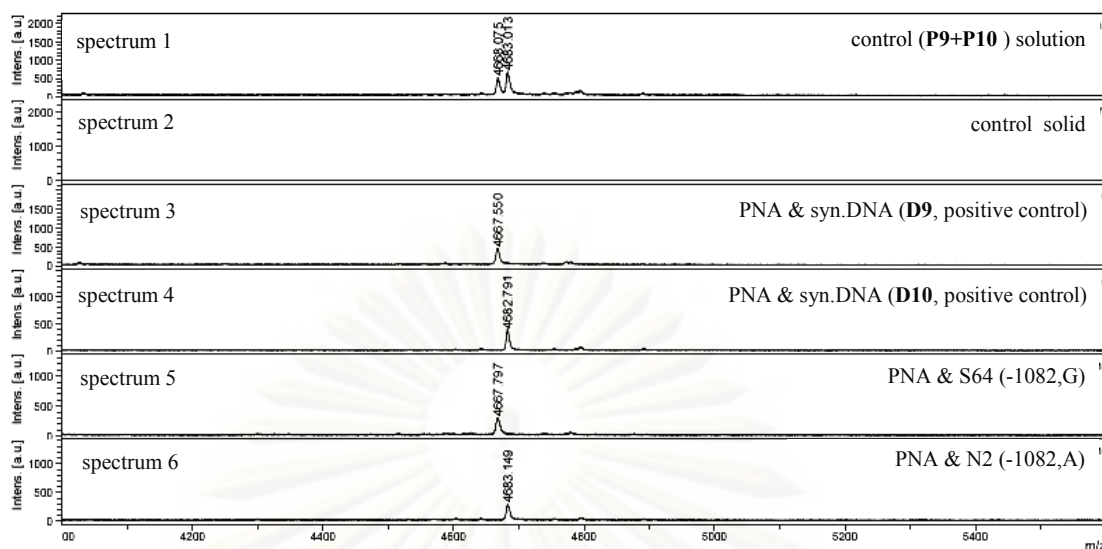


**Figure 3.53** Singleplex SNP typing of the  $-1082$  position of the human *IL-10* gene using a two PNA probes **P9** ( $-1082G$  probe) and **P10** ( $-1082A$  probe).

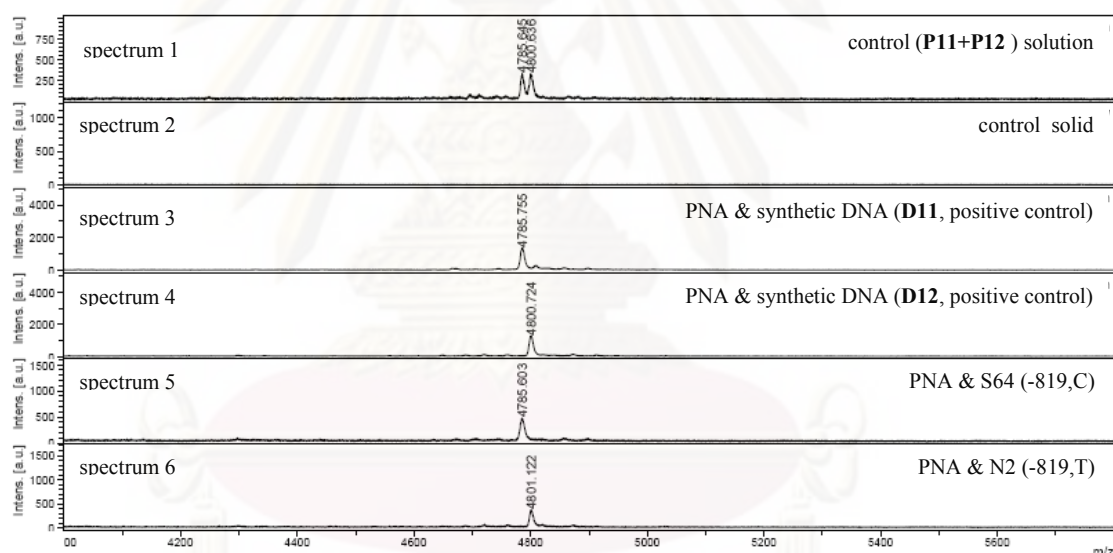


**Figure 3.54** Singleplex SNP typing of the  $-819$  position of the human *IL-10* gene using two PNA probes **P11** ( $-819C$  probe) and **P12** ( $-819T$  probe).

From **Figure 3.53**, the presence of a mass signal of **P9** at  $m/z = 4667.8$  in spectrum 5 indicated that the SNP genotype at the position  $-1082$  of the S64 sample was G. Spectrum 6 showed a mass signal of **P10** at  $m/z = 4683.1$  indicating that the SNP genotype at the position  $-1082$  of the N2 sample was A. In the **Figure 3.54** the mass signal of **P11** at  $m/z = 4785.6$  was observed in spectrum 5 indicating that the SNP genotype at the position  $-819$  in the S64 sample was C. Spectrum 6 showed a mass signal of **P12** at  $m/z = 4801.1$  indicating that the SNP at the position  $-819$  of the

N2 sample was T. The presence of only one signal in each SNP region is consistent with the fact that both human DNA samples came from homozygous individuals. Synthetic DNA controls (**D9–D12**) gave the expected results (spectra 3 and 4, **Figure 3.53** and **3.54**), while in the absence of DNA no PNA signals were observed (spectra 1 and 2, **Figure 3.53** and **3.54**).

From positive results obtained in these earlier experiments, an opportunity to carry out a more challenging simultaneous multiplex genotyping employing the present method was next investigated. Two homozygous 420bp double-stranded DNA samples from the same individuals used in previous experiments (S64 and N2) were obtained by standard PCR technique in such a way that each of PCR product consists of both SNP sites (–819 and –1082). The same set of PNA (**P9/P11** and **P10/P12**) were used as probes for simultaneous detection of two SNP sites

Since the washing condition for detection of the two SNP sites are not identical, it was decided to perform a model experiment using synthetic DNA targets carrying both SNP sites first to establish a general washing condition. The sequences of the synthetic DNA targets are shown below.

DNA **D17A** = 5'-GTGCAGAGATGTTACATGCATCATTGGGAGGGGGAATCTA-3'

DNA **D17B** = 5'-GTGCAGAGATATTACATGCATCATTGGGAAGGGGAATCTA-3'

The experiment was carried out at 1 pmol each probe and 5 pmol each synthetic DNA target. After the hybridization, the Q-sepharose was washed with water and then 3% aqueous acetonitrile to eliminate the non-specific probe. The results from MALDI-TOF mass spectrometric analysis of the washed solid support are shown in **Figure 3.55**.

ศูนย์วิทยุทรัพยากร

จุฬาลงกรณ์มหาวิทยาลัย

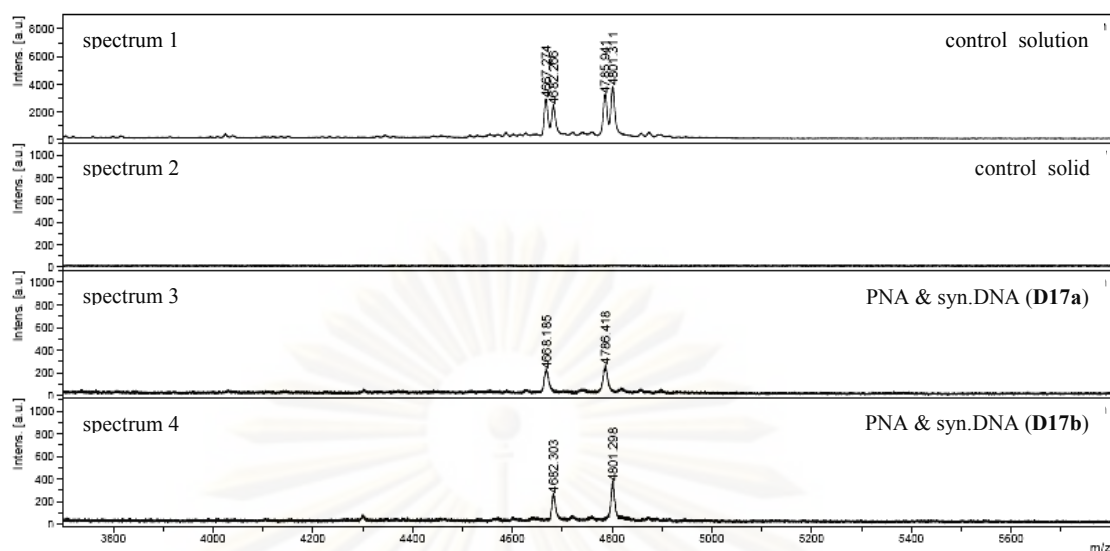


**Figure 3.55** Duplex SNP typing in the synthetic DNA using four PNA probes (**P9**, **P10**, **P11** and **P12**). Hybridization conditions: PNA 1 pmol each and DNA 5 pmol in 30  $\mu$ L binding buffer at 30  $^{\circ}$ C. Experiments from top to bottom: no DNA target (solution, positive control), no DNA target (solid, negative control), +**D17a** (complementary to **P9** and **P11**, single mismatch to **P10** and **P12**), +**D17b** (complementary to **P10** and **P12**, single mismatch to **P9** and **P11**).

The results in above figure indicated that the two SNP positions, which were incorporated into the 40bp synthetic DNA targets, can also be simultaneously genotyped using four PNA probes in just one common washing condition (water followed by 3% MeCN). Unambiguous signals corresponding only to the expected PNA probe were observed as shown in spectra 3 and 4 hence allowing a clear discrimination between different SNP genotype.

The experiment above suggested that the two SNP sites could be genotyped in a single experiment by using present technique. Next, genotyping of the two SNP sites in real PCR product (**Table 3.9**) was attempted. The experiments were performed in the same way as described in the singleplex SNP genotyping. After the denaturation-absorption-hybridization-washing cycle, the Q-sepharose was analyzed by MALDI-TOF mass spectrometry. The results are shown in **Figure 3.56**.



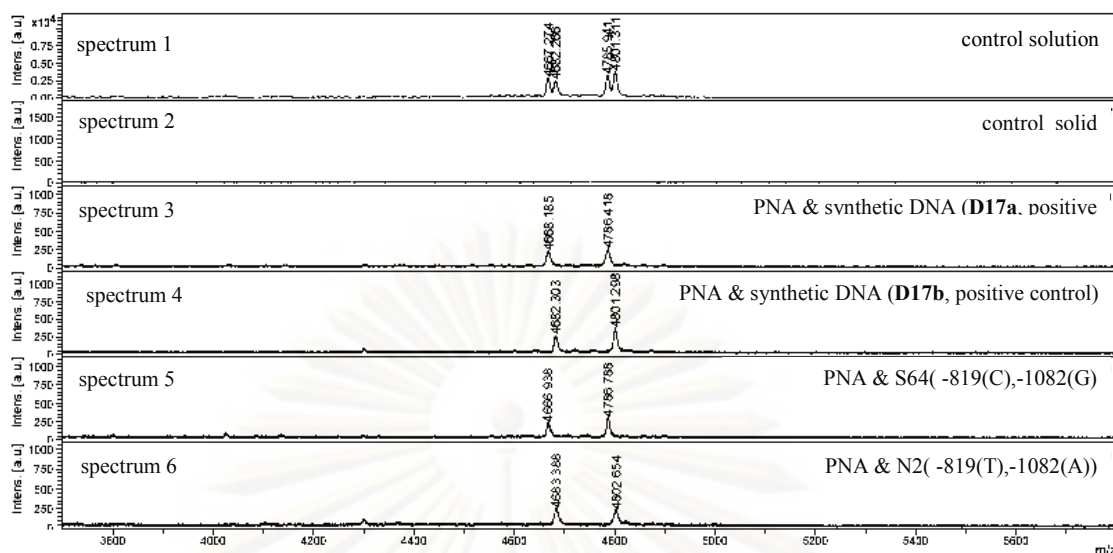


**Figure 3.56** Duplex SNP genotyping of the –819 position and -1082 position of the human *IL-10* gene using four PNA probes **P9** (–1082G probe), **P10** (–1082A probe), **P11** (–819T probe) and **P12** (–819C probe). Hybridization conditions: PNA 1 pmol each, DNA sample (from PCR) 5 pmol, 10 mM sodium phosphate buffer pH 7.0 (30  $\mu$ L) at 30  $^{\circ}$ C. Experiments from top to bottom: no DNA target (solution, positive control), no DNA target (solid, negative control), +**D17a** (positive control), +**D17b** (positive control), +DNA sample **S64** (–819C/C and –1082G/G homozygous), +DNA sample **N2** (–819T/T and –1082A/A homozygous).

The two 40bp synthetic DNA targets (**D17A** and **D17A**) were used as positive controls (spectra 3 and 4). Results in **Figure 3.56** revealed that the simultaneous genotyping in PCR products using four different PNA probes sample was successful. The two peaks in the mass spectrum are well separated and could be identified without ambiguity. With the S64 DNA sample, two mass signals were observed at  $m/z = 4666.9$  (**P9**) and  $4786.7$  (**P11**) (spectrum 5) indicated that the SNP genotype of this individual was –819C and –1082G. On the other hand, in the presence of the N2 DNA sample, two mass signals were observed at  $m/z = 4683.3$  (**P10**) and  $4802.6$  (**P12**) (spectrum 6) indicated the SNP genotype of this individual was –819T and –1082A. In addition, synthetic DNA controls (**D17a** and **D17b**) gave the expected results as shown in spectra 3 and 4, while in the absence of DNA no PNA signals were observed as shown in spectrum 2.

From the perspective of high throughput analysis, it is desirable to develop a multiplex SNP typing whereby different SNP sites can be genotyped in the same experiment. Therefore, the possibility of using this new technique for simultaneous

genotyping of three SNP sites in the same DNA target was further evaluated. In the next experiments, two new probes (**P13** and **P14**) designed to detect an additional SNP site at the position  $-592$  of the *IL-10* promoter (rs1800872) whose sequences shown below were included in addition of the four 13bp PNA probes (**P9–P12**) previously employed. Two homozygous 550bp double-stranded DNA (S64 and N2 samples) containing all three SNP sites ( $-1082$ ,  $-819$ ,  $-592$ ) were prepared by PCR amplification.

PNA **P13** = P-GCCTGTCCTGTAG -ser-NH<sub>2</sub> ( $m/z = 4818.62$ )

PNA **P14** = P-GCCTGTACTGTAG -ser-NH<sub>2</sub> ( $m/z = 4843.02$ )

The triplex SNP genotyping using six different PNAs as probe was performed with the two DNA samples in the same way as described in the singleplex and duplex SNP genotyping. The results from MALDI-TOF mass spectrometric analysis of the washed solid support are shown in **Figure 3.57**.

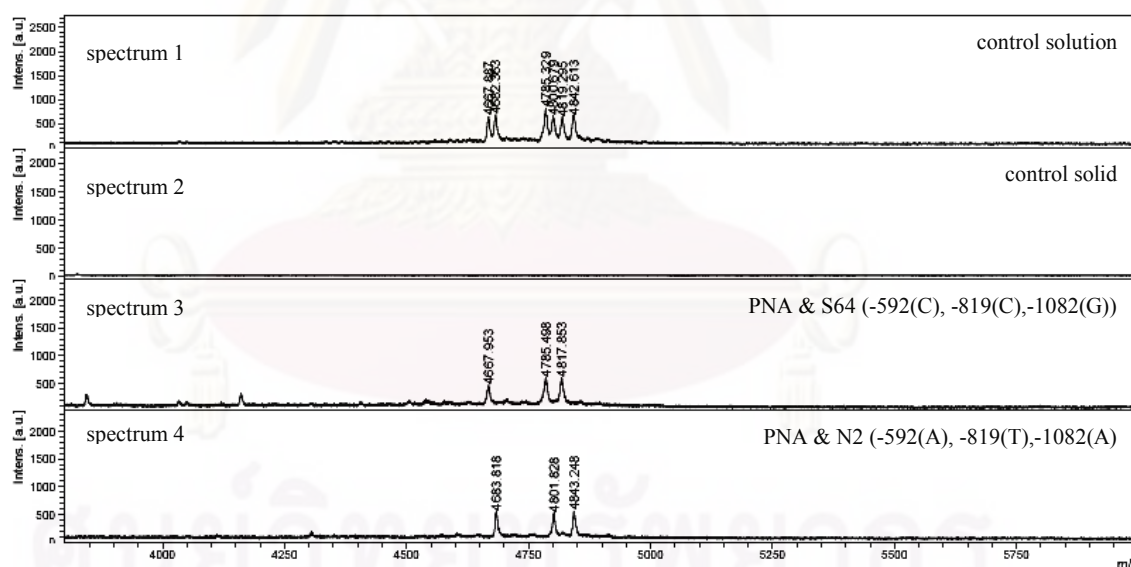


**Figure 3.57** Simultaneous multiplex typing of the human *IL-10* gene promoter at SNP positions  $-1082$ ,  $-819$  and  $-592$  using a combination of six PNA probes **P9** ( $-1082G$  probe), **P10** ( $-1082A$  probe), **P11** ( $-819T$  probe), **P12** ( $-819C$  probe), **P13** ( $-592C$  probe) and **P14** ( $-592A$  probe).

The spectra depicted in **Figure 3.57** revealed that this technique can be used to simultaneously detect three SNP sites in a single experiment. With the S64 sample, only three out of six PNA mass signals were observed. The  $m/z$  of 4667.9 (**P9**), 4785.5 (**P11**) and 4817.9 (**P13**) observed in the spectrum 3 indicated that the SNP genotype of this individual was -592C, -819C and -1082G. On the contrary, the  $m/z$  of 4683.8 (**P10**), 4801.8 (**P12**) and 4843.2 (**P14**) observed in the N2 sample (spectrum 4) indicated the SNP genotype of this individual was -592A, -819T and -1082A. Since the smallest mass difference between any two of the six probes is 15 Da (between C and T), the three peaks in the mass spectrum are well separated and all three nucleotide variations (three homozygous genotypes C/A, C/T and G/A) could be identified without ambiguity. The clear differentiation can be explained in term of the difference in melting temperature ( $T_m$ ) between the fully matching duplex and single mismatching duplex. The fully complementary duplexes have  $T_m$  in the range between 64 °C to 76 °C, whereas the  $T_m$  value of single base mismatch hybrids were between 32 °C to 53 °C as shown in **Table 3.4**. The differences in  $T_m$  ( $\Delta T_m$ ) between complementary with lowest stability and single mismatch with highest stability was 11 °C, which was sufficient to allow simultaneous multiplex genotyping under one general condition. The non-complementary probe and non-specific background were easily removed during washing step using 3% aqueous acetonitrile.

To assess the ability of present method to simultaneous multiplex genotyping, a blind-folded study was performed on 10 homo- and heterozygous human DNA samples. The 550bp target DNA samples obtained from PCR amplification as described earlier. The experiments were carried out according to the general protocol for multiplex SNP genotyping described in the previous experiment. After the usual denaturation-absorption-hybridization-washing cycle (with water and then 3% aqueous acetonitrile), the Q-sepharose was analyzed by MALDI-TOF mass spectrometry. The results are shown in **Figure 3.58**.

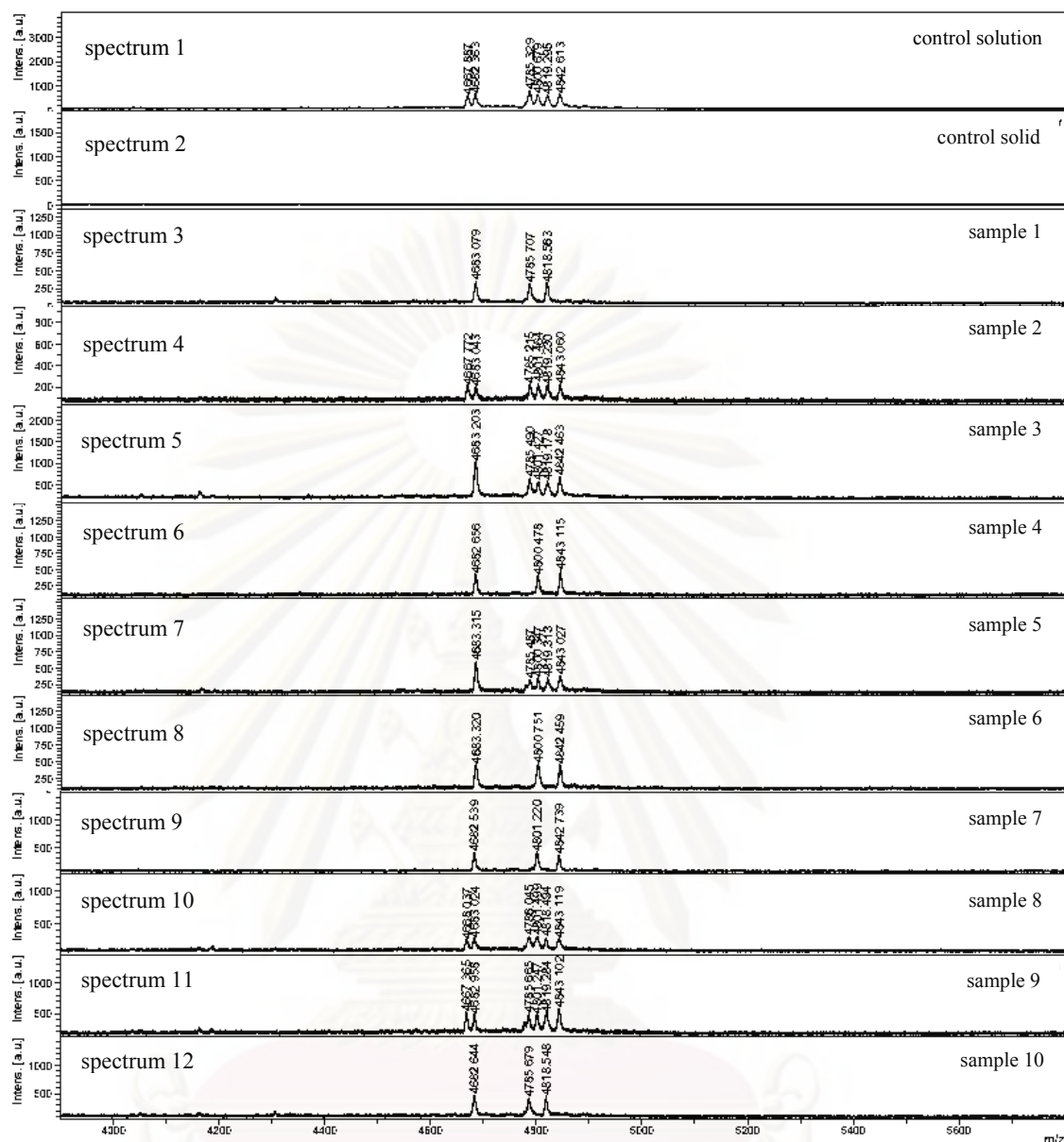


**Figure 3.58** Simultaneous multiplex typing of the human *IL-10* gene promoter of unknown samples using a combination of six PNA probes (P9–P14).

Generally, for the homozygous samples, only one signal due to one specific PNA probe should be detected in each SNP region, while in the presence of the heterozygous samples, signals of both probes should be detected with roughly equal intensities. In addition, the intensity of the signals from homozygous sample are approximately twice of heterozygous. From the above **Figure 3.58**, it was found that three out of ten samples (2, 8, 9) were completely heterozygous at all SNP sites as indicated by the presence of both probe signals at each SNP region (spectra 4, 10 and 11). Samples 1, 4, 6, 7 and 10 were completely homozygous as indicated by

occurrence of only one signal in each SNP region (spectra 3, 6, 8, 9 and 12). The remaining samples (3 and 5) contain both homo- and heterozygous for gene at different SNP sites because of both probe signals were observed in one or more SNP region and their intensities was approximately half of homozygous signal (spectra 5 and 7). In all cases, the signals of the PNA probes showed a reasonable signal-to-noise ratio with mass error range less than 150 ppm. Furthermore, the results are in complete agreement to those obtained from automated sequencing data as shown in **Table 3.10**.

**Table 3.10** Analysis results of *IL-10* SNP from 10 human DNA samples obtained from different origins.

sample code	observed $m/z$ (error, ppm)	results	sequencing
sample-1	4683.1 (+64.0) 4785.7 (-41.7) 4818.6 (-62.2)	-1082 a/a -819 c/c -592 c/c	-1082 a/a -819 c/c -592 c/c
sample-2	4667.7 (-21.4), 4683.0 (+42.7) 4785.2 (-125.4), 4801.5(+124.1) 4819.2(+62.9), 4843.0 (+41.2)	-1082 g/a -819 c/t -592 a/c	-1082 g/a -819 c/t -592 a/c
sample-3	4683.2 (+85.4) 4785.5 (-83.5), 4801.4 (+104.1) 4819.2 (+62.2), 4842.5 (-82.5)	-1082 a/a -819 c/t -592 a/c	-1082 a/a -819 c/t -592 a/c
sample-4	4682.7 (-42.7) 4800.5 (-83.3) 4843.1(+41.2)	-1082 a/a -819 t/t -592 a/a	-1082 a/a -819 t/t -592 a/a
sample-5	4683.3 (+106.7) 4785.5(-83.5),4800.3 (-104.1) 4819.3 (+83.0), 4843.0 (+41.7)	-1082 a/a -819 c/t -592 a/c	-1082 a/a -819 c/t -592 a/c
sample-6	4683.3 (+106.7) 4800.7 (-41.6) 4842.5 (-82.5)	-1082 a/a -819 t/t -592 a/a	-1082 a/a -819 t/t -592 a/a
sample-7	4682.5 (-64.0) 4801.2 (+62.4) 4842.7(-41.2)	-1082 a/a -819 t/t -592 a/a	-1082 a/a -819 t/t -592 a/a
sample-8	4668.0 (+42.8), 4683.0 (+42.7) 4786.0 (+20.8), 4801.5 (+104.1) 4818.5 (-83.0), 4843.1 (+41.2)	-1082 a/g -819 c/t -592 a/c	-1082 a/g -819 c/t -592 a/c
sample-9	4667.4 (-85.6), 4683.0 (+42.7) 4785.7 (-41.7), 4801.2 (+62.4) 4819.3 (+83.0), 4843.1 (+41.2)	-1082 a/g -819 c/t -592 a/c	-1082 a/g -819 c/t -592 a/c
sample-10	4682.6 (+42.7) 4785.7 (-41.7) 4818.5 (-83.0)	-1082 a/a -819 c/c -592 c/c	-1082 a/a -819 c/c -592 c/c

The ability of the new pyrrolidinyl *acpcPNA* to do multiplex SNP typing under ambient conditions is unprecedented. Similar works using Nielsen *aegPNA* in combination with streptavidin capture of biotinylated DNA samples [74–75, 77] failed to achieve the desired level of specificity in a one-experiment assay format. Furthermore, a high temperature and/or denaturing conditions are generally required to achieve the desired level of specificity. Since the capture techniques are different, it is difficult to compare the effectiveness of Nielsen and *acpcPNA* in terms of specificity. To compare the performance of the *acpcPNA* and Nielsen's *aegPNA* as probes for SNP genotyping using the present technique, the ability to discriminate between complementary and single base mismatch DNA targets was studied using the two types of PNA probes under identical conditions. Two *acpcPNA* probes labeled with biotin group at *N*-terminus with sequence corresponding to the SNP were used as model. A biotin-labeled Nielsen's *aegPNA* with identical sequence was used as comparator. The sequences of all PNA used in this study are shown below. The biotin group is not required for the capture experiment, but since the *aegPNA* was obtained with biotin label, the *acpcPNA* were also labeled with biotin for a fair comparison.

Neilsen's PNA (T)	Biotin-TTCCCCCTCCCAA-NH <sub>2</sub>	( <i>m/z</i> = 3890.58)
Pyrrolidinyl PNA(C)	Biotin-TTCCCCCTCCCAA-ser-NH <sub>2</sub>	( <i>m/z</i> = 4691.17)
Pyrrolidinyl PNA(T)	Biotin-TTCCCCCTCCCAA-ser-NH <sub>2</sub>	( <i>m/z</i> = 4706.16)

Two synthetic DNA sequences namely 5'-TTGGGGGAGGGAA-3' (**D9**, complementary with pyrrolidinyl PNA(C)) and 5'-TTGGGGAAGGGAA-3' (**D10**, complementary with original PNA and pyrrolidinyl PNA(T)) were used as targets. In the experiment, an equimolar quantity of the three PNA probes (50 pmol each) was mixed with an excess of the synthetic single-stranded DNA target (1000 pmol) in 10 mM phosphate buffer pH 7.0 (30  $\mu$ L) and incubated at room temperature (30 °C) for 15 min. After the usual hybridization-absorption-washing cycles (with water), the Q-sepharose was analyzed by MALDI-TOF mass spectrometry. The results are shown in **Figure 3.59**.

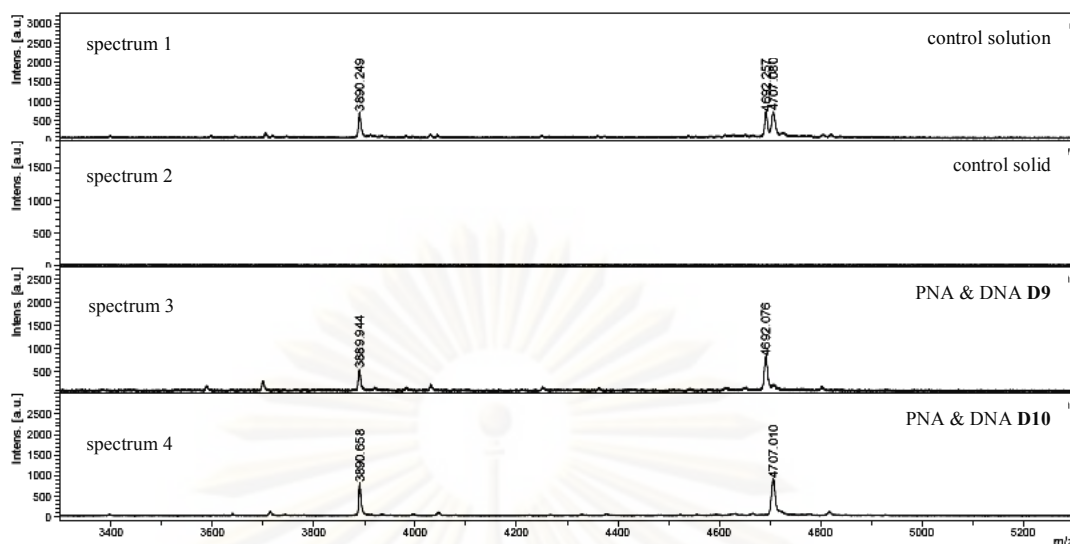


**Figure 3.59** Comparison of specificity between Nielsen's PNA and Vilaivan's pyrrolidinyl PNA

From the above figure, spectrum 1 (solution control) exhibited mass signal of all probes, while spectrum 2 (solid control) did not exhibit any signal. This indicated that both Nielsen's and Vilaivan's PNA could not be absorbed by the anion exchange support (Q-sepharose) in the absence of DNA targets. In the presence of the **D10** DNA target that is complementary to the Nielsen's PNA (**T**) and pyrrolidinyl PNA(**T**), the mass signals at  $m/z$  of 3889.94 and 4702.07 corresponding to the Nielsen PNA and pyrrolidinyl PNA(**T**), were clearly observed as shown in spectrum 4. On the other hand, the mass signal of Nielsen PNA (**T**) (3890.05) and pyrrolidinyl PNA(**C**) (4692.07), but not the pyrrolidinyl PNA(**T**) (4702.07), were observed in the presence the **D9** DNA target (complementary with pyrrolidinyl PNA(**C**) and single base mismatch with Nielsen PNA (**T**) and pyrrolidinyl PNA(**T**)). This indicated the higher specificity of Vilaivan's *acpc*PNA. The results can be explained in term of the melting temperature of three PNA probes and DNA targets as shown in **Table 3.11**.

**Table 3.11** Comparison of  $T_m$  between Nielsen's *aeg*PNA and Vilaivan's *acpc*PNA

PNA <sup>a</sup>	$T_m$ with <b>D9</b> (°C) <sup>b</sup>	$T_m$ with <b>D10</b> (°C) <sup>b</sup>
Neilsen's PNA	49.2 (single base mismatch)	60.5 (complementary)
Pyrrolidinyl PNA( <b>C</b> )	56.7 (complementary)	40.4 (single base mismatch)
Pyrrolidinyl PNA( <b>T</b> )	35.7 (single base mismatch)	60.0 (complementary)

<sup>a</sup>Neilsen's PNA was a high gift from Dr. Su Xiaodi, Institute of Materials Research & Engineering (IMRE), Singapore.

<sup>b</sup> $T_m$  values were provided by Miss Cheeraporn Ananthanawat ( $T_m$  were measured at [DNA] = [PNA] = 1  $\mu$ M, 10 mM sodium phosphate buffer, pH 7.0, heating rate 1.0 °C/min. Corrected values, as described in section 2.6)

From above Table, the  $T_m$  of the hybrid between Nielsen PNA and single base mismatch DNA target is higher than that of the corresponding mismatched DNA hybrids of pyrrolidinyl PNA(**C**) and pyrrolidinyl PNA(**T**). In addition, the melting temperature of the mismatched Nielsen PNA ·DNA hybrid was only slightly different from that of the complementary hybrid ( $\Delta T_m = 11.3$  °C). Much larger differences were observed for the corresponding pyrrolidinyl PNA(**C**) ( $\Delta T_m = 16.3$  °C) and pyrrolidinyl PNA(**T**) ( $\Delta T_m = 24.3$  °C). The high stability of the mismatched hybrid between Nielsen PNA and the mismatched DNA target (**D9**) might be responsible for the non-specific signal observed on the support. These results implied that the pyrrolidinyl *acpc*PNA offers higher sequence specificity than that of the original *aeg*PNA, at least for this particular sequence.

ศูนย์วิทยทรัพยากร

จุฬาลงกรณ์มหาวิทยาลัย



## CHAPTER IV

### CONCLUSIONS

In this research, a novel mass spectrometric technique for DNA sequence analysis employing PNA probe has been successfully developed. A new pyrrolidinyI PNA, so called *acpcPNA* was used as probe for detection of DNA sequence in combination with ion exchange method. This method relies on the electrostatic interaction between negative charge of a PNA-DNA hybrid and positive charge of an insoluble anion exchanger. Analysis of the ion exchanger with MALDI-TOF MS revealed the signal corresponding to the molecular weight of the PNA probe only when its complementary DNA was present. A variety of anion exchangers were studied. Q-sepharose was found to give the best results, providing high ion exchange capacity and a low background adsorption. This technique allows differentiation between complementary and single base mismatched 9–15mer DNA targets at room temperature (30 °C) after simple washing. With unmodified PNA probe, the minimum detectable quantity of the PNA probe and DNA target were 10 pmol. In the presence of arginine or phosphonium charge tag on the PNA, the detection limit was reduced from picomole to femtomole level and still showed a reasonable signal-to-noise ratio which allows the use of only small amounts of DNA sample and PNA probe. The technique was validated using synthetic single and double stranded DNA. It was also applied for the identification of bovine and porcine species in feedstuffs and to the detection of SNP in human DNA. The technique was shown to be highly reliable as it provided clear-cut results that were in complete agreement with the source of the sample and data from independent analyses such as automated sequencing technique. The technique allows a straightforward, rapid, inexpensive and highly specific detection of SNPs in PCR amplified DNA. In addition, the calculation of the cost for analyzed the sample by using this method and comparison to that by employed another technique such as standard PCR technique ( ~350-500 bath per sample) and automated sequencing technique ( ~2500 bath per sample), it was found that the present technique is cheaper than that of the standard methods because all experiments in this method could be performed in a one-pot reaction at room

temperature in without the need for labeled DNA samples therefore the unpurified standard PCR product can be directly employed. Most importantly, the technique is applicable for a very challenging simultaneous multiplex SNP analysis, which could not be carried out using conventional PNA probes. Furthermore, this technique also provided clear-cut discrimination between homo- and heterozygous sample, which could not be carried out using other methods.



ศูนย์วิทยทรัพยากร  
จุฬาลงกรณ์มหาวิทยาลัย

## REFERENCES

- [1] Kool, E.T.; Morales, J. C.; and Guckian, K.M. Mimicking the Structure and Function of DNA: Insights into DNA Stability and Replication. **Angew. Chem. Int. Ed.** 39 (2000): 990-1009.
- [2] Watson, J. D.; Crick, F. H. C., A Structure for Deoxyribose Nucleic Acid. **Nature**, 171(1953): 737-738.
- [3] Uhlmann, E.; Peyman, A.; Breipohl, G.; Will, D.W. PNA: Synthesis Polyamide Nucleic Acids with Unusual Binding Properties\*\*. **Angew. Chem. Int. Ed.** 37 (1998): 2796-2823.
- [4] Hyrup, B.; and Nielsen, P.E. Peptide Nucleic Acids (PNA): Synthesis, Properties and Potential Applications. **Bioorgan. Med. Chem.** 4 (1996): 5-23.
- [5] Nielsen, P. E.; Egholm, M.; and Berg, R. H.; Buchardt, O. Sequence-Selective Recognition of DNA by Strand Displacement with a Thymine-Substituted Polyamide. **Science** 254 (1991): 1497-1500.
- [6] Ray, A.; and Norde, B. Peptide Nucleic Acid (PNA): Its Medical and Biotechnical Applications and Promise for the Future. **J. FASEB** 14 (2000): 1041-1060.
- [7] Kumar, V.A.; and Ganesh, K.N. Conformationally Constrained PNA Analogues: Structural Evolution toward DNA/RNA binding Selectivity. **Acc. Chem. Res.** 38 (2005): 404-412.
- [8] Nielsen, P. E.; Egholm, M.; and Buchardt, O. Evidence for (PNA)<sub>2</sub>/DNA Triplex Structure Upon Binding of PNA to dsDNA by Strand Displacement. **J. Mol. Recog.** 7 (1994): 165-170.
- [9] Zhang, X.; Ishihara, T.; and Corey, D.R. Strand Invasion by Mixed Base PNAs and a PNA-Peptide Chimera. **Nucleic Acids Res.** 28 (2000): 3332-3338.
- [10] Betts, L.; Josey, J. A.; Veal, J. M.; and Jordan, S. R. A Nucleic Acid Triple Helix Formed by a Peptide Nucleic Acid–DNA Complex. **Science** 270 (1995): 1838-1841.

- [11] Hyrup, B.; Egholm, M.; Nielsen, P. E.; Wittung, P.; Norden, P. B.; and Buchardt, O. Structure-Activity Studies of the Binding of Modified Peptide Nucleic Acids (PNAs) to DNA. **J. Am. Chem. Soc.** 116 (1994): 7964-7970.
- [12] Hyrup, B.; Egholm, M.; Buchardt, O.; and Nielsen, P. E. A Flexible and Positively Charged PNA Analogue with an Ethylene-linker to the Nucleobase: Synthesis and Hybridization Properties. **Bioorg. Med. Chem. Lett.** 6 (1996): 1083-1088.
- [13] Nielsen, P. E.; and Haaima, G. Peptide Nucleic Acid (PNA). A DNA Mimic with a Pseudopeptide Backbone. **Chem. Soc. Rev.** 8 (1997): 73-78.
- [14] Sforza, S.; Tedeschi, T.; Corradini, R.; and Marchelli, R. A New Concept in Double Duplex DNA Invasion by Chiral PNAs which Simultaneously Depress PNA-PNA and Improve PNA-DNA Duplex Stability. **Nucleic Acids Symposium Series 5** (2007): 19-20
- [15] Kumar, V. A. Structural Preorganization of Peptide Nucleic Acids: Chiral Cationic Analogues with Five- or Six-Membered Ring Structures. **Eur. J. Org. Chem.** (2002): 2021-2032.
- [16] Govindaraju, T.; Kumar, V. A.; and Ganesh, K. N. Synthesis and Evaluation of (1*S*,2*R*/1*R*,2*S*)-Aminocyclohexylglycyl PNAs as Conformationally Preorganized PNA Analogues for DNA/RNA Recognition. **J. Org. Chem.** 69 (2004): 1858-1865.
- [17] Lowe, G.; and Vilaivan, T. Amino Acids Bearing Nucleobases for the Synthesis of Novel Peptide Nucleic Acids. **J. Chem. Soc., Perkin Trans. 1** (1997): 539-546.
- [18] Lowe, G.; and Vilaivan, T. Dipeptides Bearing Nucleobases for the Synthesis of Novel Peptide Nucleic Acids. **J. Chem. Soc.; Perkin Trans. 1** (1997): 547-554.
- [19] Lowe, G.; and Vilaivan, T. Solid Phase Synthesis of Novel Peptide Nucleic Acids. **J. Chem. Soc.; Perkin Trans. I.** (1997): 555-560.
- [20] D'Costa, M.; Kuman, V. A.; and Ganesh, K. N. Aminoethylpropyl (aep) PNA: Mixed Purine / Pyrimidine Oligomers and Binding Orientation Preferences for PNA: DNA Duplex Formation. **Org. Lett.** 3 (2001): 1281-1284.

- [21] D'Costa, M.; Kumar V. A.; Ganesh, K. N. Aminoethylpropyl PNA (aepPNA): Chiral PNA Analogues that from Highly Stable DNA: aepPNA<sub>2</sub> Triplex. **Org. Lett.** 1 (1999): 1513-1516.
- [22] Vilaivan, T.; Khongdeesameor, C.; Harnyuttanakorn, P.; Westwell, M. S.; and Lowe, G. Synthesis and Properties of Chiral Peptide Nucleic Acids with a *N*-Aminoethyl-D-proline Backbone. **Bioorg. Med. Chem. Lett.** 10 (2000): 2541-2545.
- [23] Samuel Tan T. H.; Worthington R. J.; Pritchard R. G.; Morral J.; and Micklefield J. Homopolymeric Pyrrolidine-amide Oligonucleotide Mimics: Fmoc-Synthesis and DNA/RNA Binding Properties. **Org. Biomol. Chem.** 5 (2007): 239-248.
- [24] Samuel Tan T. H.; Worthington R. J.; Pritchard R. G.; Morral J.; and Micklefield J. Mixed-sequence Pyrrolidine-amide Oligonucleotide Mimics: Boc(Z) Synthesis and DNA/RNA Binding Properties. **Org. Biomol. Chem.** 5 (2007): 249-259.
- [25] Gellman, S.H. Foldamers: A Manifesto. **Acc. Chem. Res.** 31 (1998): 173-180.
- [26] Vilaivan, T.; Suparpprom, C.; Duanglaor, P.; Harnyuttanakorn, P.; and Lowe, G. Synthesis and Nucleic Acid Binding Studies of Novel Pyrrolidinyl PNA Carrying an *N*-amino-*N*-methylglycine Spacer. **Tett. Lett.** 44 (2003): 1663-1666.
- [27] Vilaivan, T.; Suparpprom, C.; Harnyuttanakorn, P.; and Lowe, G. Synthesis and Properties of Novel Pyrrolidinyl PNA Carrying  $\beta$ -Amino Acid Spacers. **Tett. Lett.** 42 (2001): 5533-5536.
- [28] Vilaivan, T.; and Lowe, G. A Novel Pyrrolidinyl PNA Showing High Sequence Specificity and Preferential Binding to DNA over RNA. **J. Am. Chem. Soc.** 124 (2002): 9326-9327.
- [29] Suprapprom, C.; Srisuwannaket, C.; Sangvanich, P.; and Vilaivan, T. Synthesis and Oligodeoxynucleotide Binding Properties of Pyrrolidinyl Peptide Nucleic Acids Bearing Prolyl-2-aminocyclopentanecarboxylic Acid (ACPC) Backbones. **Tett. Lett.** 46 (2005): 2833-2837.
- [30] Vilaivan, T.; and Srisuwannaket, C. Hybridization of Pyrrolidinyl Peptide Nucleic Acids and DNA: Selectivity, Base-Pairing Specificity and Direction of Binding. **Org. Lett.** 8 (2006): 1879-1900.

- [31] <http://www.paragene.com>
- [32] Dias, N.; and Stein, C.A. Antisense Oligonucleotides; Basic Concepts and Mechanisms. **Mol. Cancer Ther.** 1 (2002): 347-355.
- [33] Mologni, L.; IeCoutre, P., Nielsen, P. E.; and Gambacorti-Passerini, C., Additive Antisense Effects of Different PNAs on the *in vitro* Translation of the PML/RAR $\alpha$  Gene. **Nucleic Acids Res.** 26 (1998): 1934-1938.
- [34] Lewis, M.R.; Jia, F.; Gallazzi, F.; Wang, Y.; Zhang, J.; Shenoy, N.; Lever, S. Z.; and Hannink, M. Radiometal-Labeled Peptide-PNA Conjugates for Targeting *bcl-2* Expression: Preparation, Characterization, and *in vitro* mRNA Binding. **Bioconjugate Chem.** 13 (2002): 1176-1180.
- [35] Paulasova, P.; and Pellestor, F. The Peptide Nucleic Acids (PNAs): A New Generation of Probe for Genetic and Cytogenetic Analyses. **Ann. Genet-Paris.** 47 (2004): 349-358.
- [36] Zhilina, Z.V.; Ziemba, A. J.; Nielsen, P.E.; and Ebbinghaus, S.W. PNA-Nitrogen Mustard Conjugates Are Effective Suppressors of HER-2/neu and Biological Tools for Recognition of PNA/DNA Interaction. **Bioconjugate Chem.** 17 (2006): 214-222.
- [37] Zhou, P.; Dragulescu-Andrasi, A.; Bhattacharya, B.; O’Keefe, H.; Vatta, P.; Hyldig-Nielsen, J. J.; and Ly, D. H. Synthesis of Cell-Permeable Peptide Nucleic Acids and Characterization of their Hybridization and Uptake Properties. **Bioorg. Med. Chem. Lett.** 16 (2006): 4931–4935.
- [38] Nielsen, P.E. Peptide Nucleic Acid: A Versatile Tool in Genetic Diagnostics and Molecular Biology. **Curr. Opin. Biotech.** 12 (2001): 16-20.
- [39] Thiede C.; Bayerdörffer E.; Blasczyk R.; Wittig B.; and Neubauer A. Simple and Sensitive Detection of Mutations in the Ras Proto-oncogenes Using PNA-mediated PCR Clamping. **Nucleic Acids Res.** 24 (1996): 983–984.
- [40] Behn, M.; and Schuermann, M. Sensitive Detection of p53 Gene Mutations by a “Mutant Enriched” PCR-SSCP Technique. **Nucleic Acids Res.** 26 (1998): 1356-1358.

- [41] Murdock, D. G.; Christacos, N. C.; and Wallace, D. C. The Age-related Accumulation of a Mitochondria DNA Control Region Mutation in Muscle, but not Brain, Detected by a Sensitive PNA-Directed PCR Clamping Based Method. **Nucleic Acids Res.** 28 (2000): 4350-4355.
- [42] Pellestor, F.; Paulasova, P.; Macek, M.; and Hamamah, S. The Use of Peptide Nucleic Acids for In Situ Identification of Human Chromosomes. **J. Histochem. Cytochem.** 53 (2005): 395-400.
- [43] Sassolas, A.; Leca-Bouvier, B.D.; and Blum, L.J. DNA Biosensors and Microarrays. **Chem. Rev.** 108 (2008): 109-139.
- [44] Kuzuya, A.; Zhou, J-M.; and Komiyama, M. DNA, PNA, and Their Derivatives for Precise Genotyping of SNPs. **Mini-Rev. Org. Chem.** 1 (2004): 125-131.
- [45] Willhelmsson, L.M.; Nordén, B.; Mukherjee, K.; Dulay, M.T.; and Zare, R.N. Genetic Screening Using the Colour Change of a PNA-DNA Hybrid-Binding Cyanine Dye. **Nucleic Acids Res.** 30 (2002): e3.
- [46] Komiyama, M.; Ye, S.; Liang, X.; Yamamoto, Y.; Tomita, T.; Zhou, J-M.; and Aburatani, H. PNA-for One-Base Differentiating Protecting of DNA from Nuclease and Its Use for SNPs Detection. **J. Am. Chem. Soc.** 125 (2003): 3758-3762.
- [47] Zhang, N.; and Appella, D. H. Colorimetric Detection of Anthrax DNA with a Peptide Nucleic Acid Sandwich-Hybridization Assay. **J. Am. Chem. Soc.** 129 (2007): 8424-8425.
- [48] Svanvik, N.; Westman, G.; Wang, D.; and Kubista, M. Light-Up Probes: Thiazole-Orange-Conjugated Peptide Nucleic Acid for Detection of Target Nucleic Acid in Homogeneous Solution. **Anal. Biochem.** 281 (2000): 26-35.
- [49] Socher, E.; Jarikote, D.V.; Knoll, A.; Rüglin, L.; Burmeister, J.; and Seitz, O. FIT Probes: Peptide Nucleic Acid Probes with a Fluorescent Base Surrogate Enable Real-Time DNA Quantification and Single Nucleotide Polymorphism Discovery. **Anal. Biochem.** 375 (2008): 318-330.
- [50] Gaylord, B.S.; Heeger, A.J.; and Bazan, G.C. DNA Detection Using Water-Soluble Conjugated Polymers and Peptide Nucleic Acid Probes. **Proc. Natl. Acad. Sci. USA.** 99 (2002): 10954-10957.

- [51] Liu, B.; and Bazan, G.C. Methods for Strand-Specific DNA Detection with Cationic Conjugated Polymers Suitable for Incorporation into DNA Chips and Microarrays. **Proc. Natl. Acad. Sci. USA.** 102 (2005): 589-593.
- [52] Baker, E.S.; Hong, J.W.; Gaylord, B.S.; Bazan, G.C.; and Bowers, M.T. PNA/dsDNA Complexes: Site Specific Binding and dsDNA Biosensor Applications. **J. Am. Chem. Soc.** 128 (2006): 8484-8492.
- [53] Hwang, G.T.; Seo, Y.J.; and Kim, B.H. A Highly Discriminating Quencher-Free Molecular Beacon for Probing DNA. **J. Am. Chem. Soc.** 126 (2004): 6528-6529.
- [54] Kuhn, H.; Demidov, V.V.; Coull, J.M.; Fiandaca, M.J.; Gildea, B.D.; and Frank-Kamenetskii, M.D. Hybridization of DNA and PNA Molecular Beacons to Single-Stranded and Double-stranded DNA targets. **J. Am. Chem. Soc.** 124 (2002): 1097-1103.
- [55] Ye, S.; Miyajima, Y.; Ohnishi, T.; Yamamoto, Y.; and Komiyama, M. Combination of Peptide Nucleic Acid Beacon and Nuclease S1 for Clear-cut Genotyping of Single Nucleotide Polymorphisms. **Anal. Biochem.** 363 (2007): 300-302.
- [56] Englund, E.A.; and Appella, D.H. Synthesis of  $\gamma$ -Substituted Peptide Nucleic acids: A New Place to attach Fluorophores without Affecting DNA Binding. **Org. Lett.** 7 (2005): 3465-3467.
- [57] Totsingan, F.; Rossi, S.; Corradini, R.; Tedeschi, T.; Sforza, S.; Juris, A.; Scaravelli, E.; and Marchelli, R. Label-free Selective DNA Detection with High Mismatch Recognition by PNA Beacons and Ion Exchange HPLC. **Org. Biomol. Chem.** 6 (2008): 1232-1237.
- [58] Hahn, J.-I.; and Lieber, C.M. Direct Ultrasensitive Electrical Detection of DNA and DNA Sequence Variations Using Nanowire Nanosensors. **Nano. Lett.** 4 (2004): 51-54.
- [59] Gao, Z.; Agarwal, A.; Trigg, A.D.; Singh, N.; Fang, C.; Tung, C.-H.; Fan, Y.; Buddharaju, K.D.; and Kong, J. Silicon Nanowire Arrays for Label-Free Detection of DNA. **Anal. Chem.** 79 (2007): 3291-3297.



- [60] Zhang, G.-J.; Chua, J.H.; Chee, R.-E.; Agarwal, A.; Wong, S.M.; Buddharaju, K. D.; and Balasubramanian, N. Highly Sensitive Measurements of PNA-DNA Hybridization Using Oxide-etched Silicon Nanowire Biosensors. **Biosensor Bioelectron.** 23 (2008): 1701-1707.
- [61] Rockenbauer, E.; Peterson, K.; Vogel, U.; Bolund, L.; Kølvråa, S.; Nielsen, K.V.; and Nexø, B.A. SNP Genotyping Using Microsphere-Linked PNA and Flow Cytometric Detection. **Cytom. Part A** 64A (2005): 80-86.
- [62] Kerman, K.; Matsubara, Y.; Morita, Y.; Takamura, Y.; and Tamiya, E. Peptide Nucleic Acid Modified Magnetic Beads for Intercalator Based Electrochemical Detection of DNA Hybridization. **Sci. and Technol. Adv. Mater.** 5 (2004): 351-357.
- [63] Edwards, J.R.; Ruparel, H.; and Ju, J. Mass-spectrometry DNA sequencing. **Mutat. Res.** 573 (2005): 3-12.
- [64] Tang, K.; Opalsky, D.; Abel, K.; Boom, D.; Yip, P.; Mistro, G.D.; Braun, A.; and Cantor, C.R. Single Nucleotide Polymorphism Analyses by MALDI-TOF MS. **Int. J. Mass Spectrom.** 226 (2003): 37-54.
- [65] Pröll, F.; Möhrle, B.; Kumpf, M.; and Gauglitz, G. Label-free Characterization of Oligonucleotide Hybridization Using Reflectometric Interference Spectroscopy. **Anal. Bioanal. Chem.** 382 (2005): 1889-1894.
- [66] Boll, I.; Krämer, R.; Brunner, J.; and Mokhir, A. Templated Metal Catalysis for Single Nucleotide Specific DNA Sequence Detection. **J. Am. Chem. Soc.** 127 (2005): 7849-7856.
- [67] Al Attar, H.A.; Norden, J.; O'Brien, S.; and Monkman, A.P. Improved Single Nucleotide Polymorphisms Detection Using Conjugated Polymer/Surfactant System and Peptide Nucleic Acid. **Biosensor Bioelectron.** 23 (2008): 1466-1472.
- [68] Tost, J.; and Gut, I.G. Genotyping Single Nucleotide Polymorphism by MALDI Mass Spectrometry in Clinical Application. **Clin. Biochem.** 38 (2005): 335-350.
- [69] Tost, J.; and Gut, I.G. Genotyping Single Nucleotide Polymorphism by Mass Spectrometry. **Mass Spectrom. Rev.** 21 (2002): 388-418.
- [70] Meng, Z.; Simmons-Willis, T.A.; and Limbach, P. A. The Use of Mass Spectrometry in Genomics. **Biomol. Eng.** 21 (2004): 1-13.

- [71] Griffin, T.J.; and Smith, L.M. Single-Nucleotide Polymorphism Analysis by MALDI-TOF Mass Spectrometry. **Trends Biotechnol.** 18 (2000): 77–84.
- [72] Marvin, L.F.; Roberts, M.A.; and Fay, L.B. Matrix-Assisted Laser Desorption/Ionization Time-of-Flight Mass Spectrometry in Clinical Chemistry. **Clin. Chim. Acta** 337 (2003): 11-21.
- [73] Bauer, O.; Guerasimova, A.; Sauer, S.; Thamm, S.; Steinfath, M.; Herwig, R.; Janitz, M.; Lehrach, H.; and Radelof, U. Multiplexed Hybridizations of Positively Charge-Tagged Peptide Nucleic Acids Detected by Matrix-Assisted Laser Desorption/Ionization Time-of-Flight Mass Spectrometry. **Rapid Commun. Mass Spectrom.** 18 (2004): 1821–1829.
- [74] Ross, P.L.; Lee, K.; and Belgrader, P. Discrimination of Single-Nucleotide Polymorphisms in Human DNA Using Peptide Nucleic Acid Probed Detected by MALDI-TOF Mass Spectrometry. **Anal. Chem.** 69 (1997): 4197-4202.
- [75] Jiang-Baucom, P.; Girard, J.E.; Butler, J.; and Belgrader, P. DNA typing of Human Leukocyte Antigen Sequence polymorphisms by Peptide Nucleic Acid Probes and MALDI-TOF Mass Spectrometry. **Anal. Chem.** 69 (1997): 4894-4898.
- [76] Ren, B.; Zhou, J.-M.; and Komiyama, M. Straightforward Detection of SNPs in Double-Stranded DNA by Using Exonuclease III/Nuclease S1/PNA System. **Nucleic Acids Res.** 32 (2004): e42.
- [77] Timothy, J.; Tang, W.; and Smith, L. M. Genetic Analysis by Peptide Nucleic Acid Affinity MALDI-TOF Mass Spectrometry. **Nat. Biotech.** 15 (1997): 1368-1372
- [78] Schatz, P.; Distler, J.; Berlin, K.; and Schuster, M. Novel Method for High Throughput DNA Methylation Marker Evaluation Using PNA-Probe Library Hybridization and MALDI-TOF Detection. **Nucleic Acids Res.** 34 (2006): e59.
- [79] Mattes, A.; and Seitz, O. Mass-Spectrometric Monitoring of a PNA-Based Ligation Reaction for the Multiplex Detection of DNA Single-Nucleotide Polymorphism. **Angew. Chem. Int. Ed.** 40 (2001): 3178-3181.

- [80] Bauer, O.; Guerasimova, A.; Sauer, S.; Thamm, S.; Steinfath, M.; Herwig, R.; Janitz, M.; Lehrach, H.; and Radelof, U. Multiplexed Hybridizations of Positively Charge-tagged Peptide Nucleic Acids Detected by Matrix-assisted Laser Desorption/Ionization Time-of-flight Mass Spectrometry. **Rapid Commun. Mass Spectrom.** 18 (2004): 1821–1829.
- [81] Stoerker, J.; Mayo, J. D.; Tetzlaff, C. N.; Sarracino, D. A.; Schwöpe, I.; and Richert, C. Rapid Genotyping by MALDI-monitored Nuclease Selection From Probe Libraries. **Nat. Biotech.** 18 (2000): 1213-1216.
- [82] Mengel-Jørgensen, J.; Sanchez, J. J.; Børsting, C.; Kirpekar, F.; and Morling, N. MALDI-TOF Mass Spectrometric Detection of Multiplex Single Base Extended Primers. A Study of 17 Y-Chromosome Single-Nucleotide Polymorphisms. **Anal. Chem.** 76 (2004): 6039-6045.
- [83] Vilaivan, T. Synthesis and Properties of Novel Nucleopeptides. Doctoral Dissertation, University of Oxford, 1996.
- [84] Ngamviriyavong, P.; Synthesis of Peptide Nucleic Acid Containing Aminoethyl Linkers. Master's Thesis, Department of chemistry, Chulalongkorn University, 2003.
- [85] Srisuwannaket, C.; Synthesis and DNA-Binding Properties of Pyrrolidinyl Peptide Nucleic Acids Bearing (1*S*,2*S*)-2-Aminocyclopentane Carboxylic Acids Spacer. Doctoral Dissertation. Department of chemistry, Chulalongkorn University, 2005.
- [86] Suprapprom, C. Synthesis and Nucleic Acid Properties of Novel Peptide Nucleic Acids Carrying beta Amino Acid Spacer. Doctoral Dissertation, Department of chemistry, Chulalongkorn University, 2006.
- [87] LePlae, P.R.; Umezawa, N.; Lee, H-S.; and Gellman, S.H. An Efficient Route to Either Enantiomer of trans-2-Aminocyclopentanecarboxylic Acid. **J. Org. Chem.** 66 (2001): 5629-5632.
- [88] Kuwahara, M.; Arimitsu, M.; and Sisido, M. Synthesis of  $\delta$ -Amino Acids with an Ether Linkage in the Main Chain and Nucleobase on the Side Chain as Monomer Units for Oxy-Peptide Nucleic Acids. **Tetrahedron.** 55 (1999): 10067-10078.

- [89] Chan, W.C.; and White, P.D. **Fmoc Solid Phase Peptide Synthesis**, pp. 9-13. New York: Oxford University Press Inc, 2004.
- [90] Nielsen, P.E. **Peptide Nucleic acids Protocols and Application**, Great Britain: Cromwell Press. 2004.
- [91] Dueholm, K.L; Egholm, M.; Behrens, C.; Christensen, L.; Hansen, H.F.; Vulpius, T.; Petersen, K.H.; Berg, R.H.; Nielsen, P.E.; and Buchardt, O. Synthesis of Peptide Nucleic Acid Monomers Containing the Four Natural Nucleobase: Thymine, Cytosine, Adenine, and Guanine and Their Oligomerization. **J. Org. Chem.** 59 (1994): 5767-5773.
- [92] Breipohl, G.; Knolle, J.; Langner, D.; O'Malley, G.; and Uhlmann, E. Synthesis of Polyamide Nucleic Acids (PNAs) using a Novel Fmoc/Mmt Protecting-Group combination. **Bioorg. Med. Chem. Lett.** 6 (1996): 665-670.
- [93] Bodanszky, M. **Peptide Chemistry. A Practical Text Book**, pp. 60-68. New York: Springer-Verlag Berlin Heidelberg, 1993.
- [94] Carpino, L. A. 1-Hydroxy-7-azabenzotriazole. An Efficient Peptide Coupling Additive. **J. Am. Chem. Soc.** 115 (1993): 4397-4398.
- [95] Van den Boom, D.; and Berkenkamp, S. **MALDI MS: A Practical Guide to Instrumentation, Methods and Applications**, pp. 131-135. Wiley-VCH, 2007.
- [96] L.G.Wade, Jr. **Organic chemistry**, pp. 150-155. Pearson Education, Inc. 2006.
- [97] Sforza, S.; Corradini, R.; Galaverna, G.; Dossena, A.; and Marchelli, R. The chemistry of peptide nucleic acids. **Mine. Biotech.** 11 (1999): 163-174.
- [98] TentGel is a trademark of Rapp Polymer GmbH, Tübingen, Germany.
- [99] Rink, H. Solid-Phase Synthesis of Protected Peptide Fragments Using a Trialkoxy- Diphenyl-methylester Resin. **Tett. Lett.** 28 (1987): 3787-3790.
- [100] Bodanszky, M, **Peptide Chemistry. A Practical Text Book**, pp. 60-63. New York: Springer-Verlag Berlin Heidelberg. 1993.
- [101] Blackburn, G.M.; and Gait, M.J. **Nucleic acid in chemistry and biology**, pp. 20-25. New York: Oxford University Press Inc. 1996.

- [102] “Ion Exchange Chromatography: Principle and Methods”, Technical Booklet Series Pharmacia. Biotech, Uppsala, Sweden. 1999.
- [103] Korkaew, P.; Synthesis of Fluorescent-labelled PNA and Application Determination of DNA Sequence. Master’s Thesis, Department of chemistry, Chulalongkorn University, 2007.
- [104] Peter M.; Vallone and John M.B. **Encyclopedia of Mass Spectrometry**. 3 (2005): 1-6.
- [105] Wolf, C.; Rentsch, J.; and Hübner, P. PCR–RFLP Analysis of Mitochondrial DNA: A Reliable Method for Species Identification. **J. Agric. Food Chem.** 47 (1999): 1350–1355.
- [106] Chaumpluk, P.; Chikae, M.; Takamura, Y.; and Tamiya, E. Novel Electrochemical Identification and Semi Quantification of Bovine Constituents in Feedstuffs. **Sci. and Technol. Adv. Mater.** 7 (2006): 263-269.
- [107] Hirankarn, N.; Wongpiyabovorn, J.; Hanvivatvong, O.; Netsawang, J.; Akkasilpa, S.; Wongchinsri, J.; Hanvivadhanakul, P.; Korkit, W.; and Avihingsanon, Y. The Synergistic Effect of FC Gamma Receptor IIa and Interleukin-10 Genes on the Risk to Develop Systemic Lupus Erythematosus in Thai Population. **Tissue Antigens.** 68 (2006): 399–406.
- [108] Wongpiyabovorn, J.; Hirankarn, N.; Ruchusatsawat, K.; Yooyongsatit, S.; Asawanonda, P.; and Poovorawan, Y. Association of The Interleukin-10 Distal Promoter (-2763A/C) Polymorphism with Late-Onset Psoriasis. *Experimental Dermatology*. **Clin. Exper. Dermatol.** 33 (2007): 186–189.



## **APPENDICES**

ศูนย์วิทยทรัพยากร  
จุฬาลงกรณ์มหาวิทยาลัย

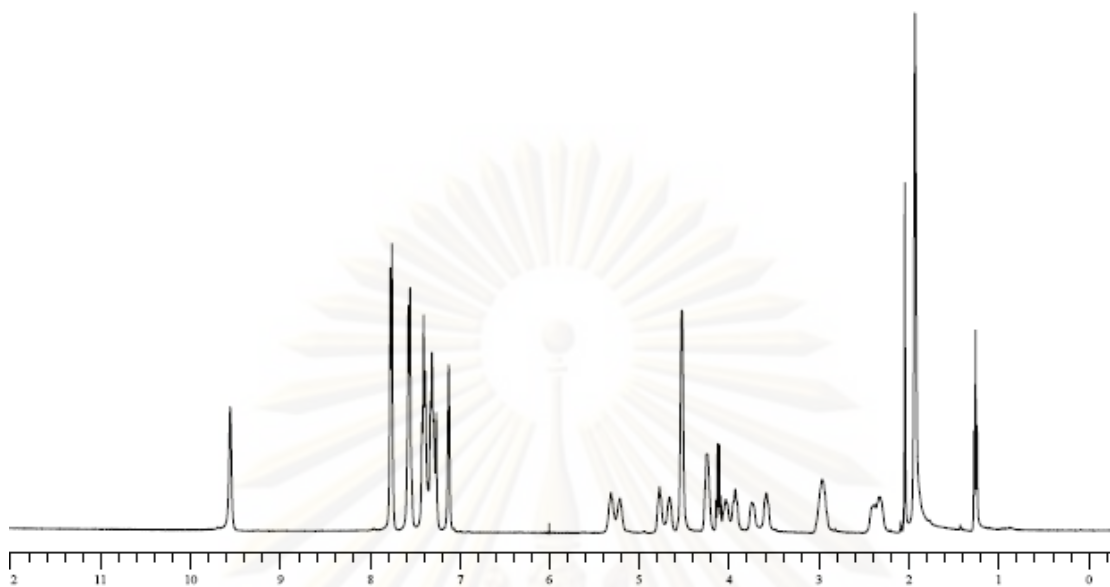


**Figure A.1**  $^1\text{H}$  NMR spectrum of (*N*-Fluoren-9-ylmethoxycarbonyl)-*cis*-4-(thymine-1-yl)-D-proline pentafluorophenyl ester (**11**)

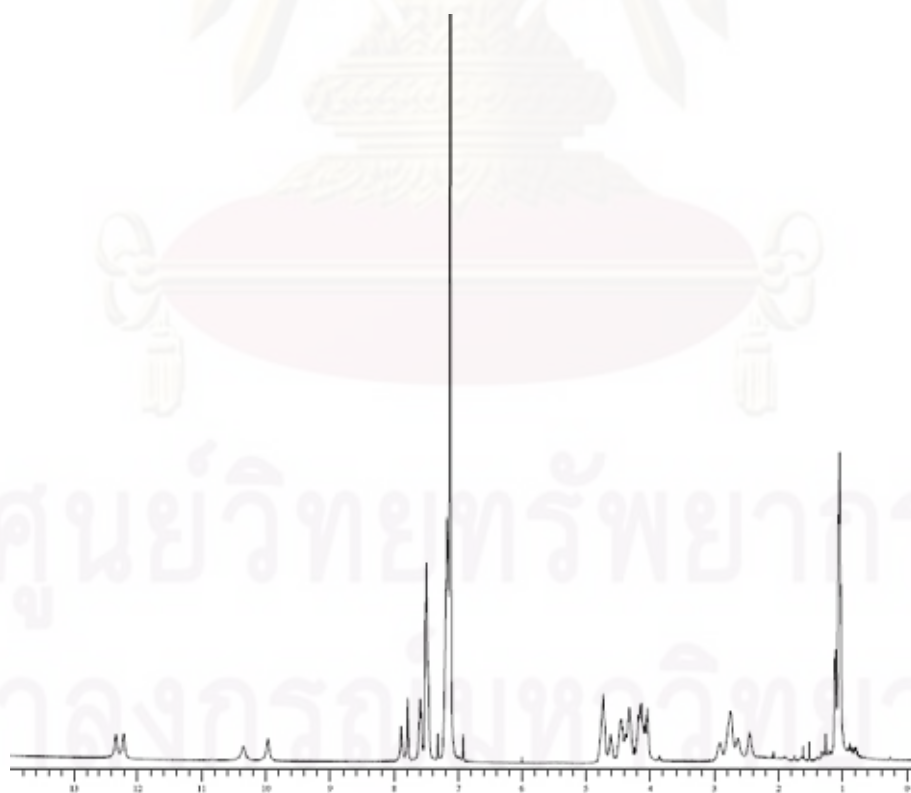


**Figure A.2**  $^1\text{H}$  NMR spectrum of (*N*-Fluoren-9-ylmethoxycarbonylamino)-*cis*-4-(*N*<sup>2</sup>-isobutyrylguanin-9-yl)-D-proline pentafluorophenyl ester (**12**)

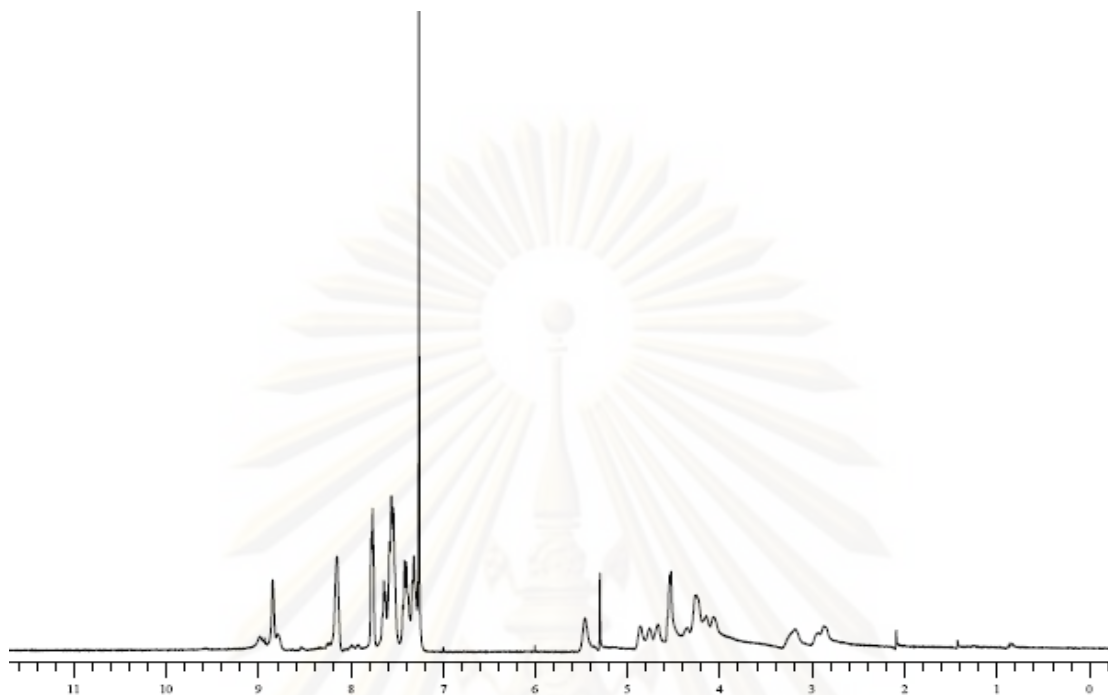


**Figure A.3**  $^1\text{H}$  NMR spectrum of (*N*-Fluoren-9-ylmethoxycarbonyl)-*cis*-4-(*N*<sup>6</sup>-benzoyladenin-9-yl)-D-proline pentafluorophenyl ester (**16**)

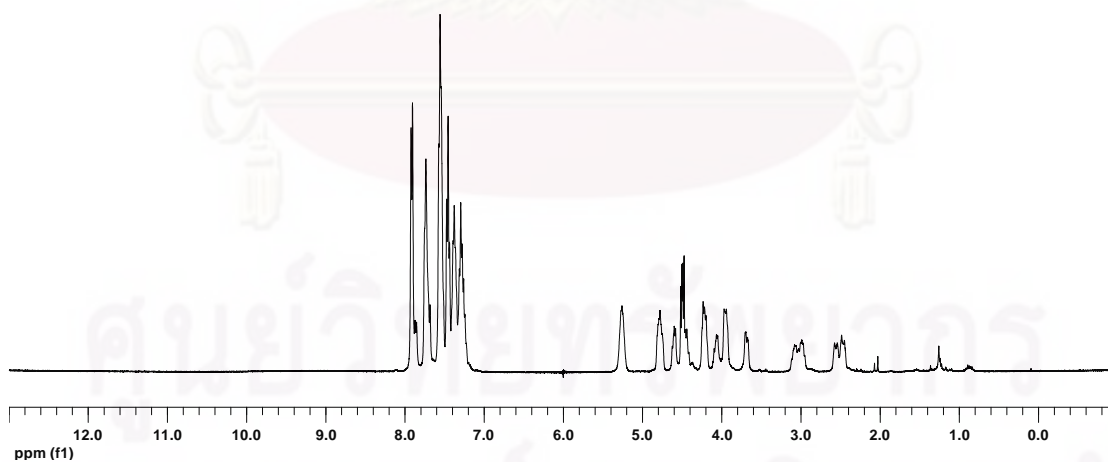


**Figure A.4**  $^1\text{H}$  NMR spectrum of (*N*-Fluoren-9-ylmethoxycarbonyl)-*cis*-4-(*N*<sup>4</sup>-benzoylcytosin-1-yl)-D-proline pentafluorophenyl ester (**17**)



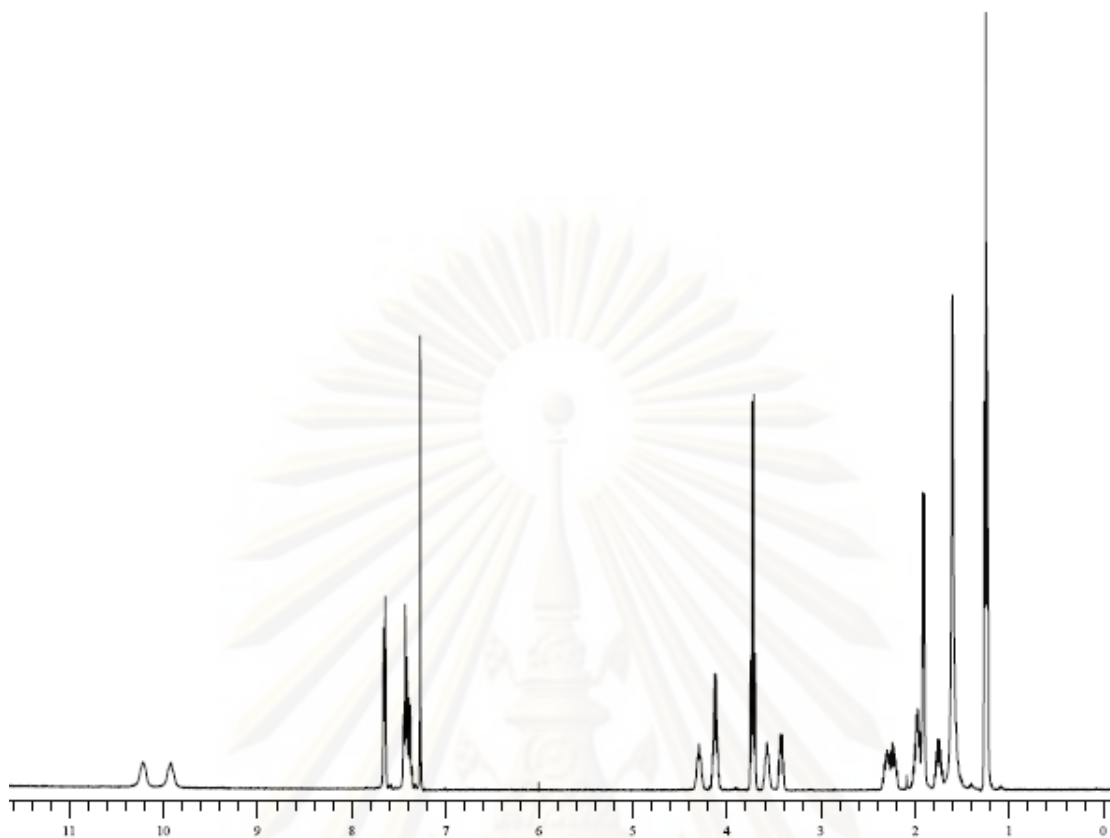


**Figure A.5**  $^1\text{H}$  NMR spectrum of ethyl (1*S*,2*S*)-2-[(1*S*)-phenylethyl]-aminocyclopentane carboxylate (**23**)

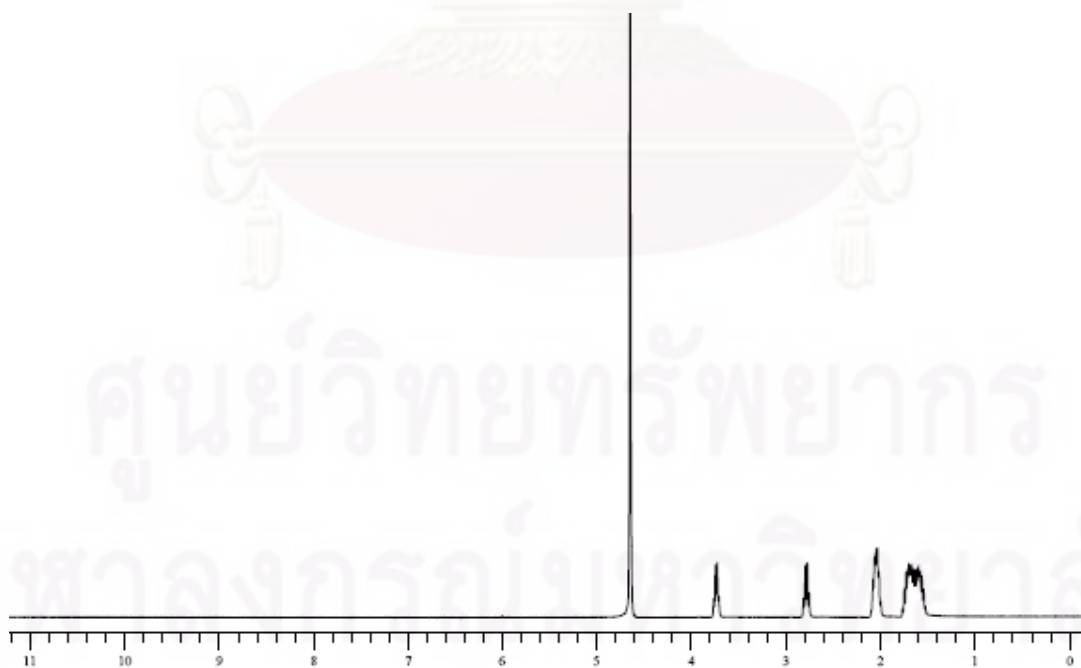


**Figure A.6**  $^1\text{H}$  NMR spectrum of (1*S*,2*S*)-2-Aminocyclopentane carboxylic acid hydrochloride (**24**)

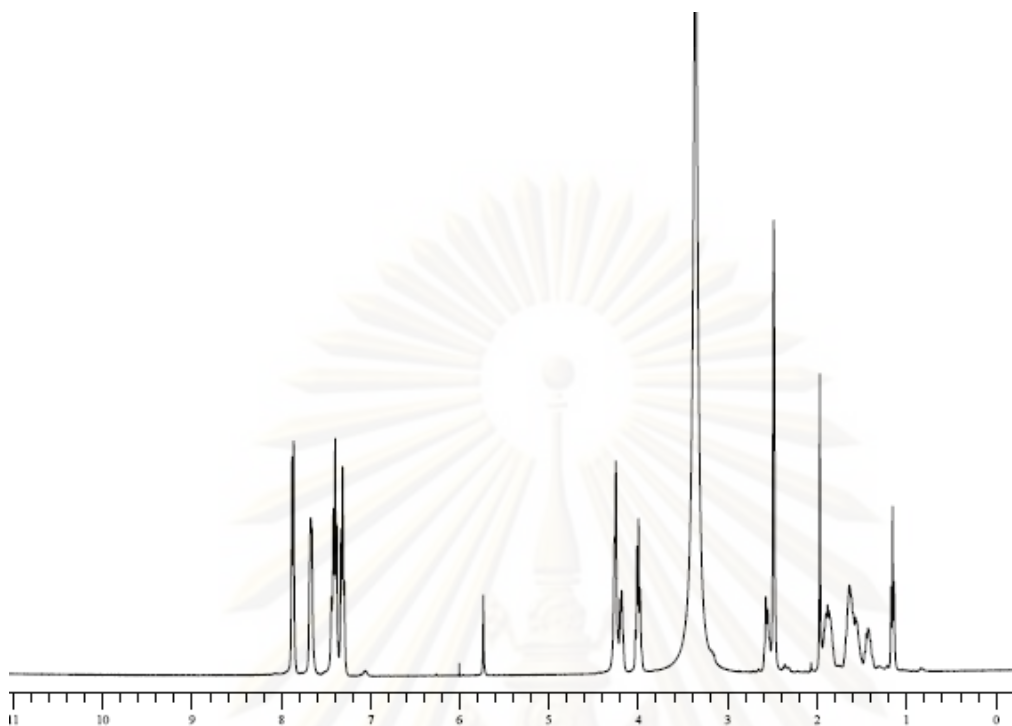


**Figure A.7**  $^1\text{H}$  NMR spectrum of (1*S*,2*S*)-2-(*N*-Fluoren-9-ylmethoxycarbonyl)-aminocyclopentanecarboxylic acid (**26**)

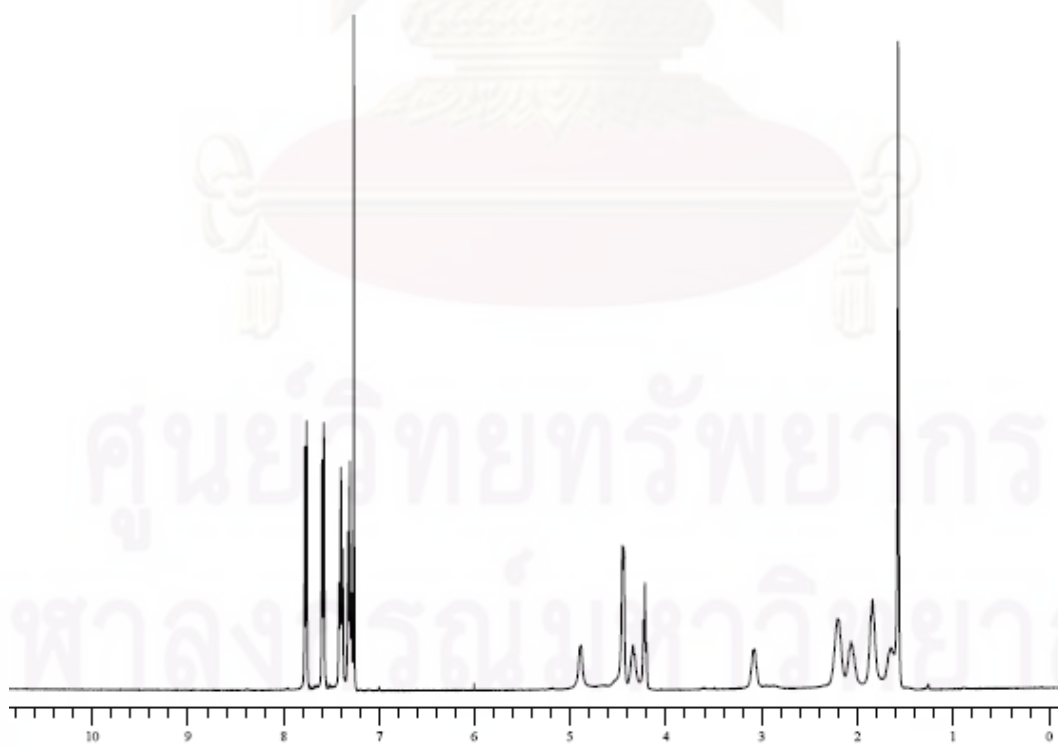


**Figure A.8**  $^1\text{H}$  NMR spectrum of (1*S*,2*S*)-2-(*N*-fluoren-9-ylmethoxycarbonyl)-aminocyclopentane pentafluorophenyl ester (**27**)

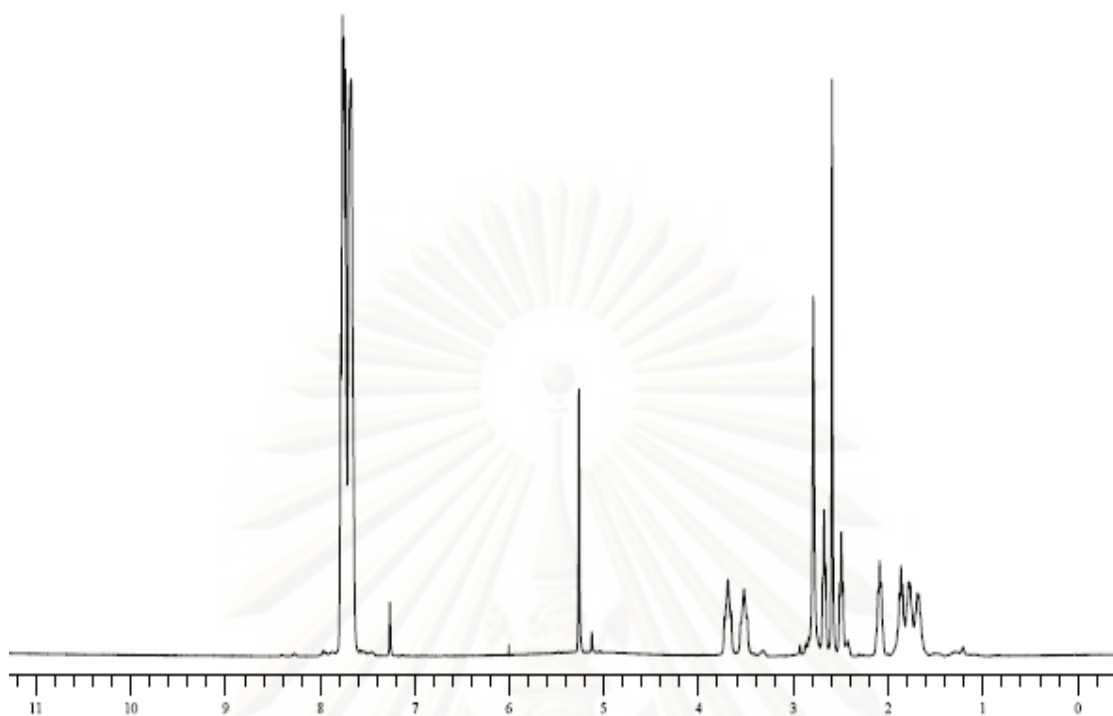


**Figure A.9**  $^1\text{H}$  NMR spectrum of carboxybutyltriphenylphosphonium bromide *N*-hydroxysuccinimidyl ester (**2**)

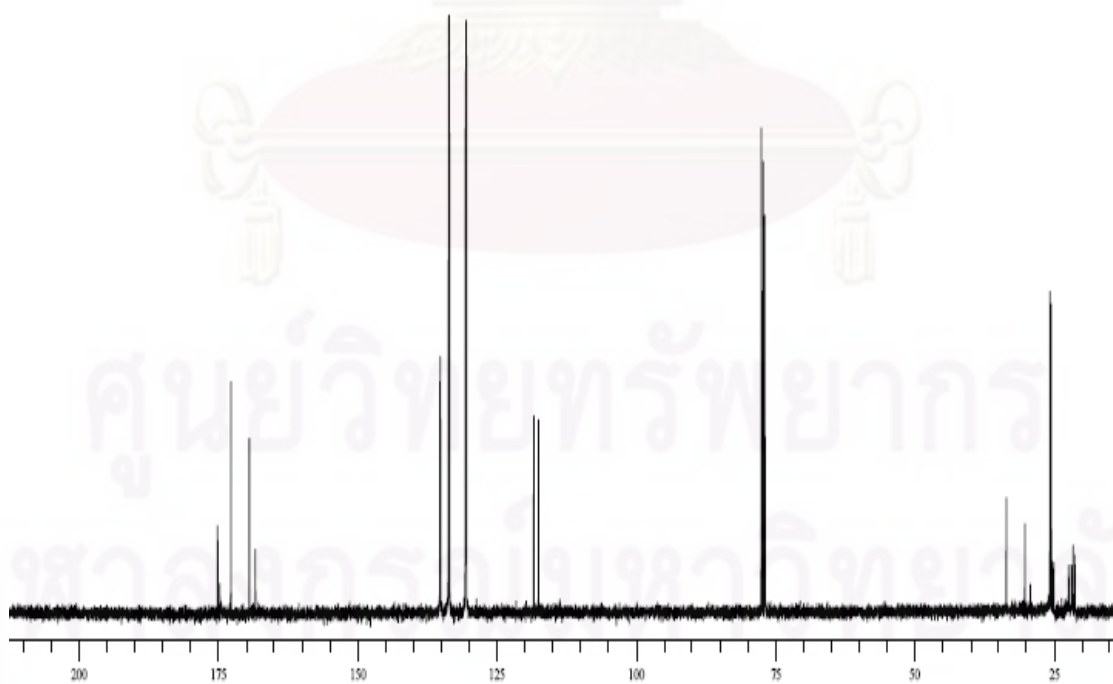


**Figure A.10**  $^{13}\text{C}$  NMR spectrum of carboxybutyltriphenylphosphonium bromide *N*-hydroxysuccinimidyl ester (**2**)

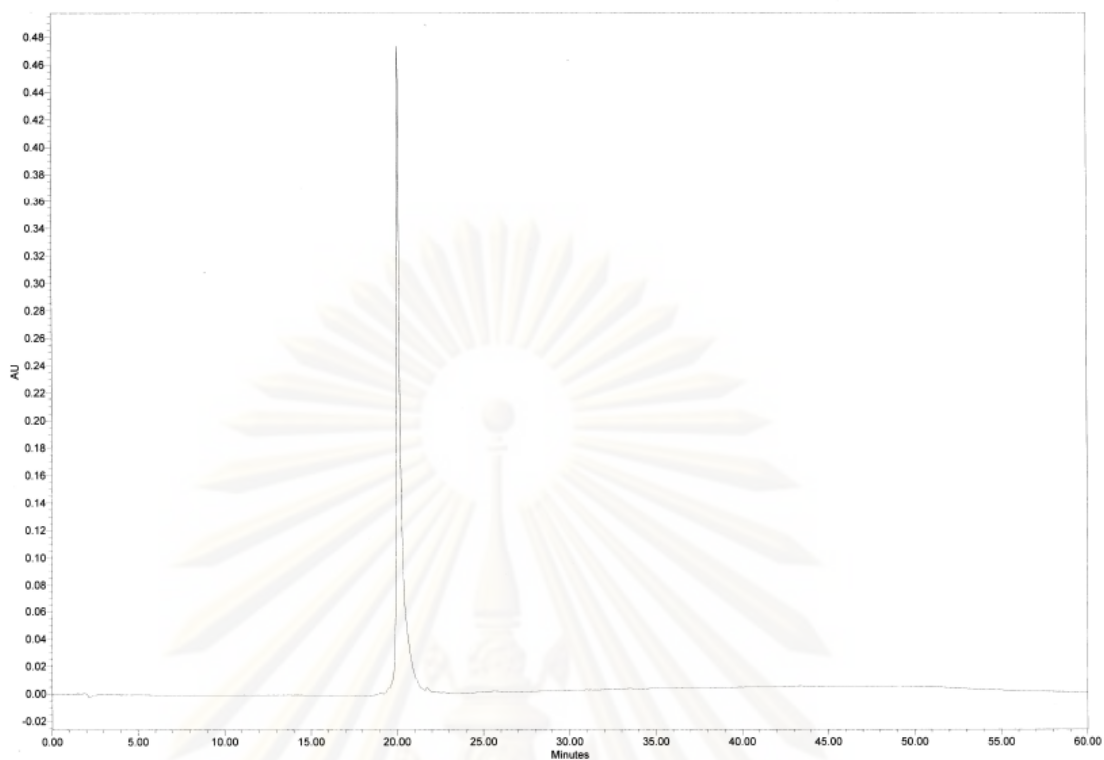


**Figure A.11** HPLC chromatogram of Ac-T<sub>9</sub>-LysNH<sub>2</sub> (P1)

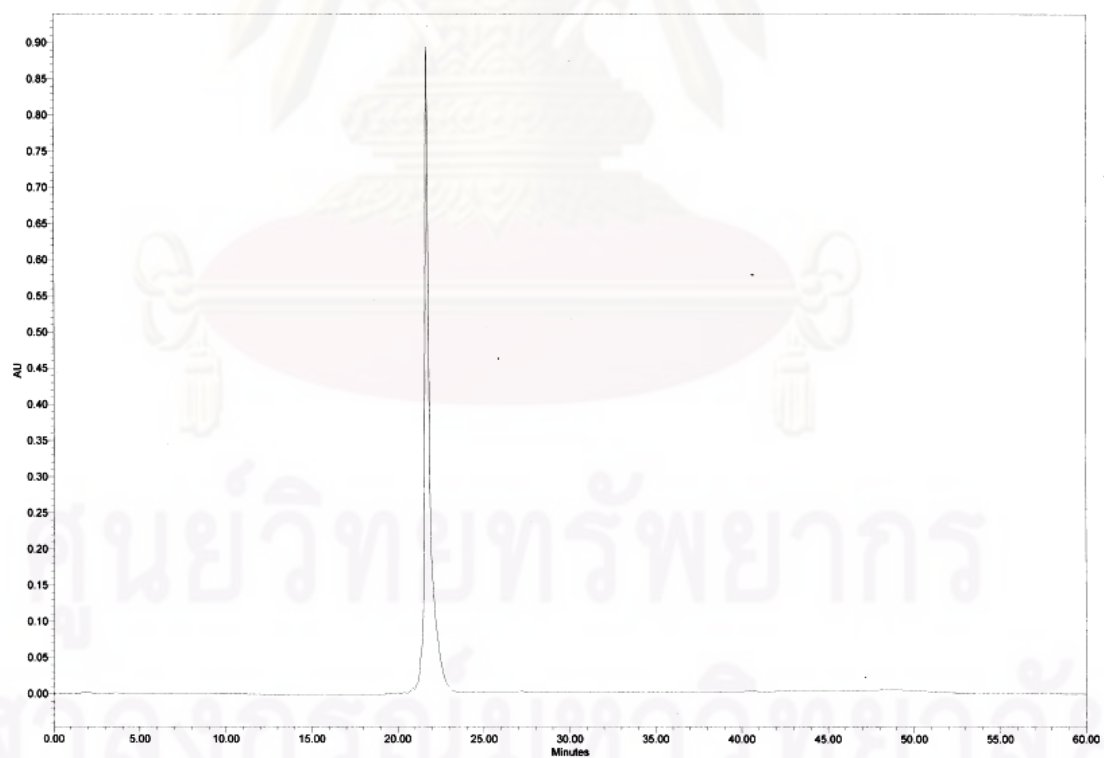


**Figure A.12** HPLC chromatogram of Ac-GTAGATCACT-Ser-NH<sub>2</sub> (P2)

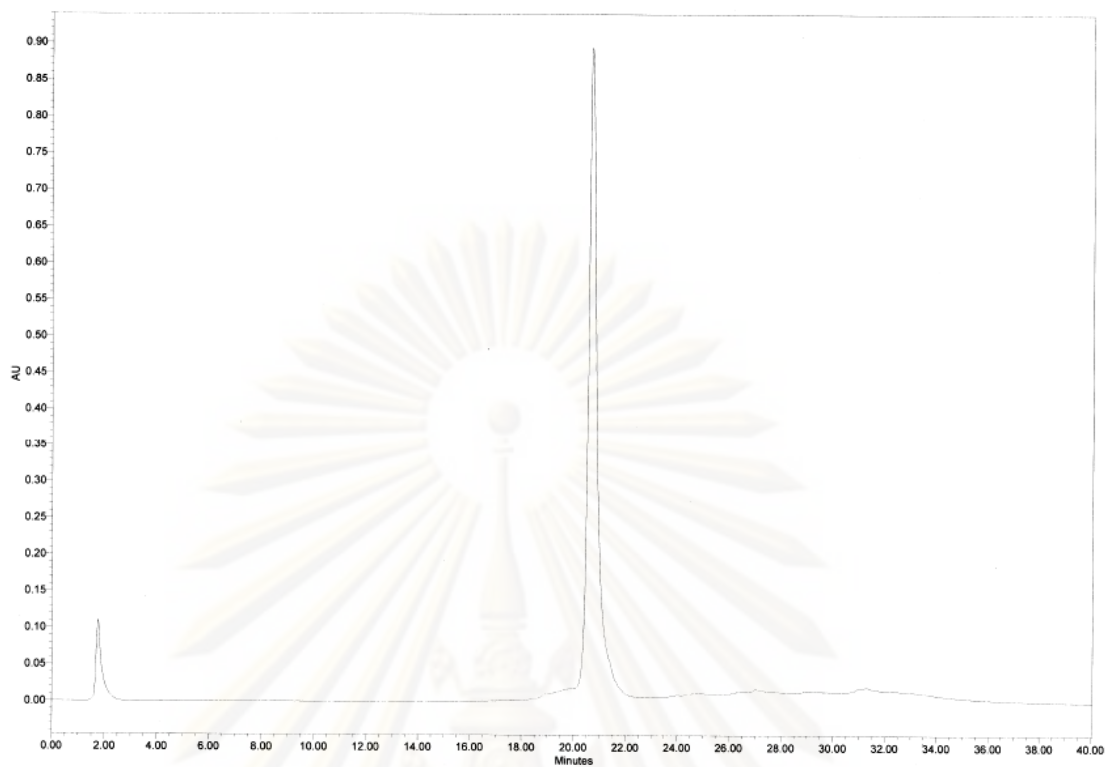


**Figure A.13** HPLC chromatogram of Ac-TGTACGTCACA ACTA-Lys-NH<sub>2</sub> (P5)

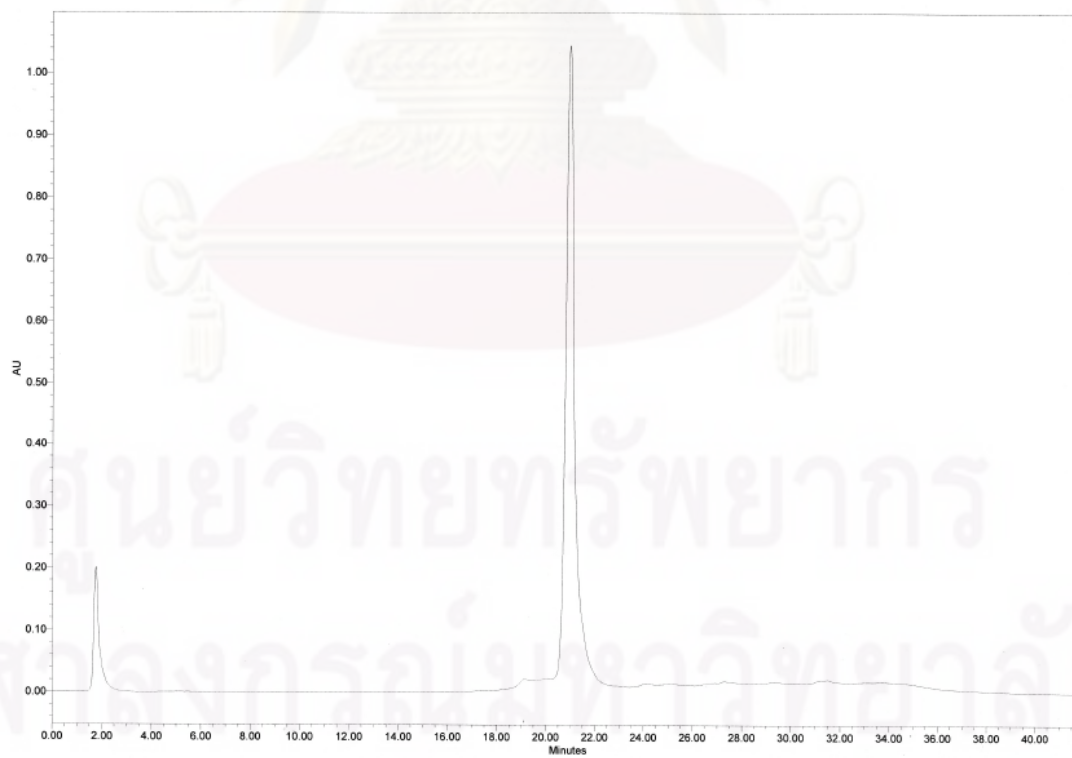


**Figure A.14** HPLC chromatogram of Ac-TGTACGTAACA ACTA-Lys-NH<sub>2</sub> (P6)

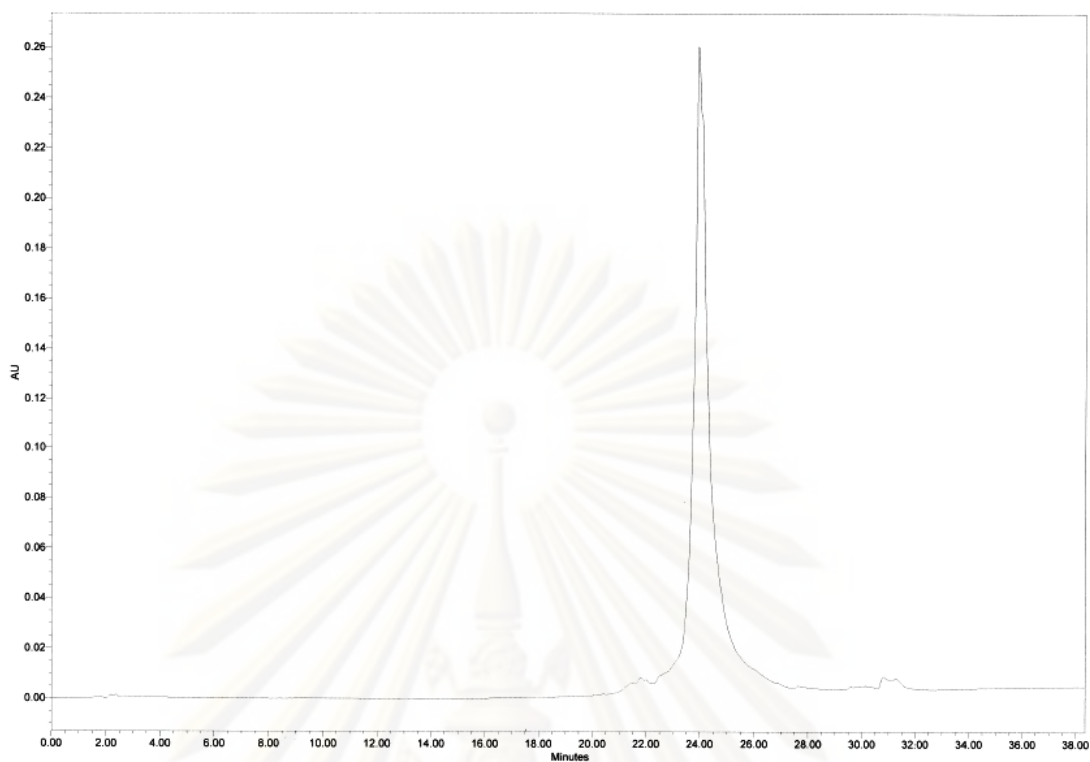


**Figure A.15** HPLC chromatogram of Ac-Arg-AAAATCCATT-Ser-NH<sub>2</sub> (P7)

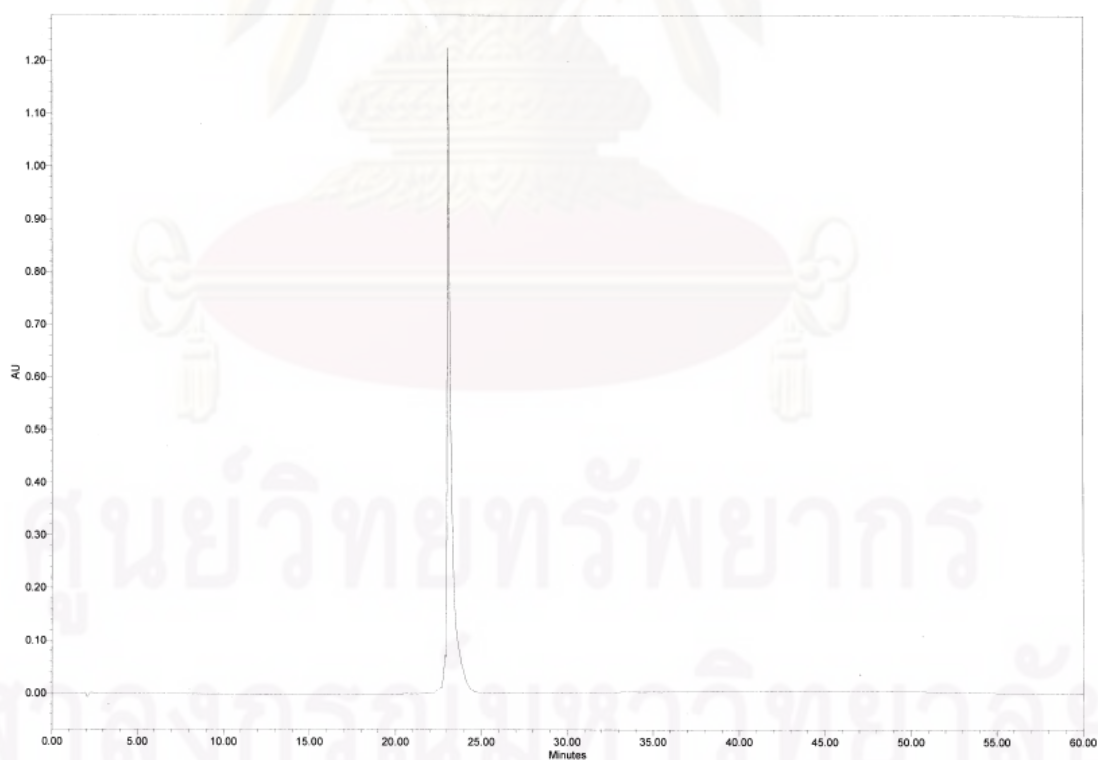


**Figure A.16** HPLC chromatogram of Ac-Arg-AAA ATTCCATT-Ser-NH<sub>2</sub> (P8)

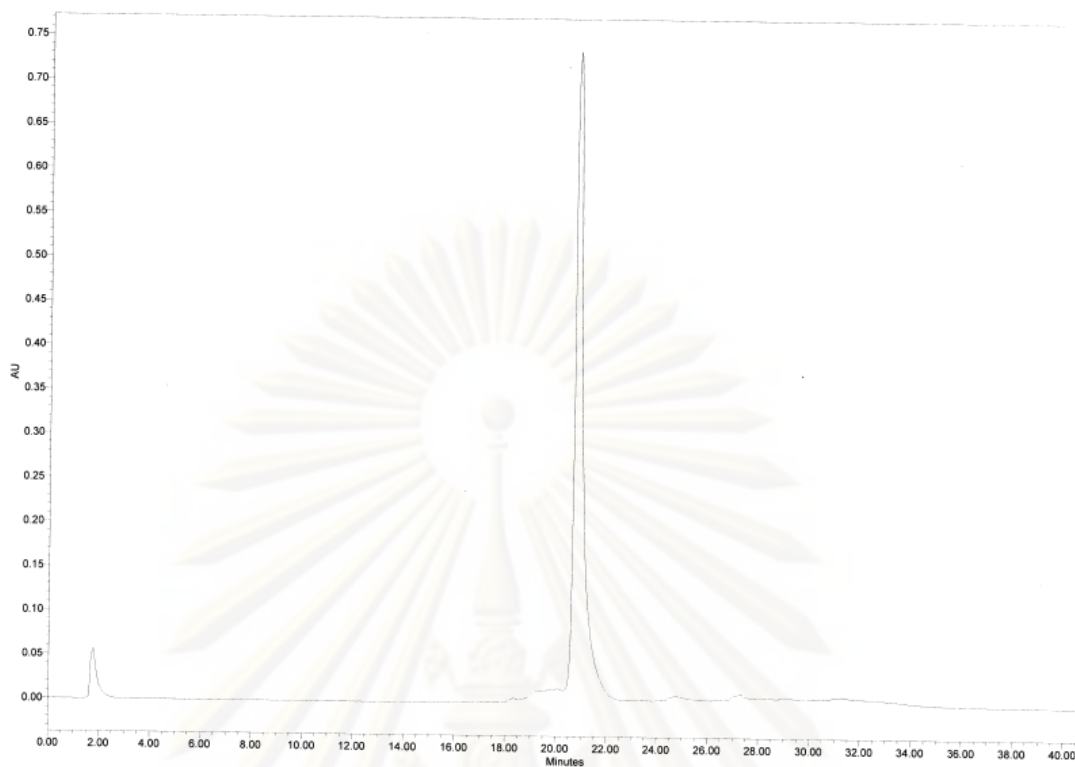


**Figure A.17** HPLC chromatogram of P-TTCCCCCTCCCAA-Ser-NH<sub>2</sub> (**P9**)

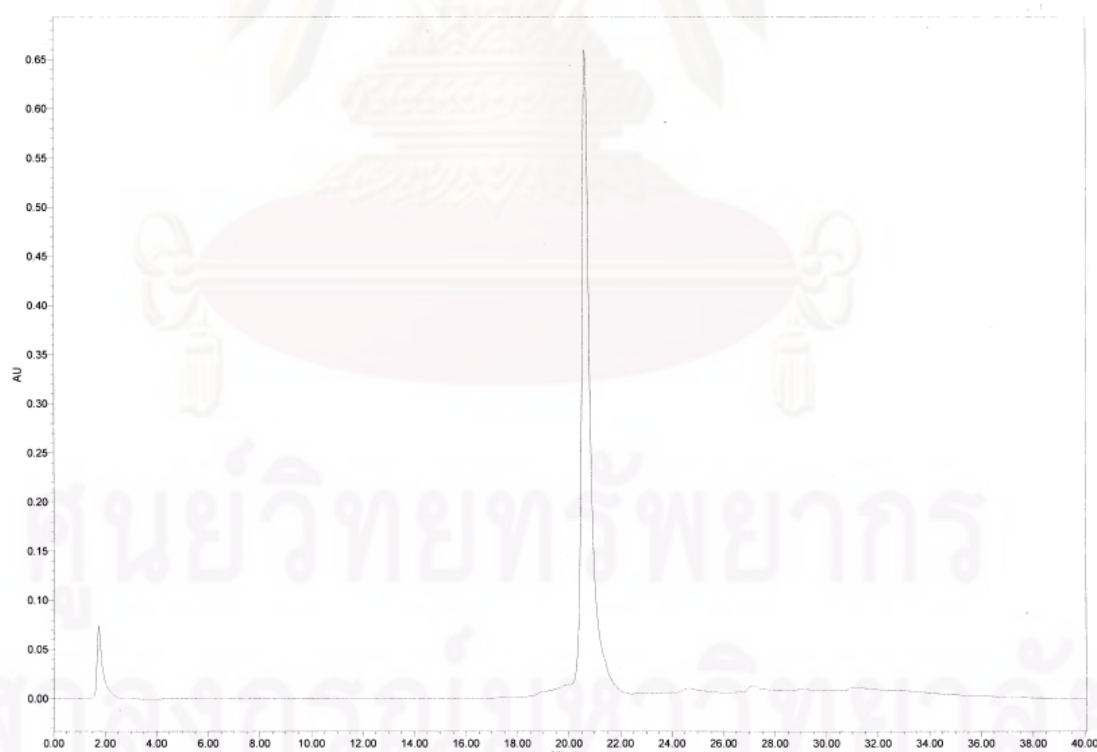


**Figure A.18** HPLC chromatogram of P-TTCCCCCTCCCAA-Ser-NH<sub>2</sub> (**P10**)

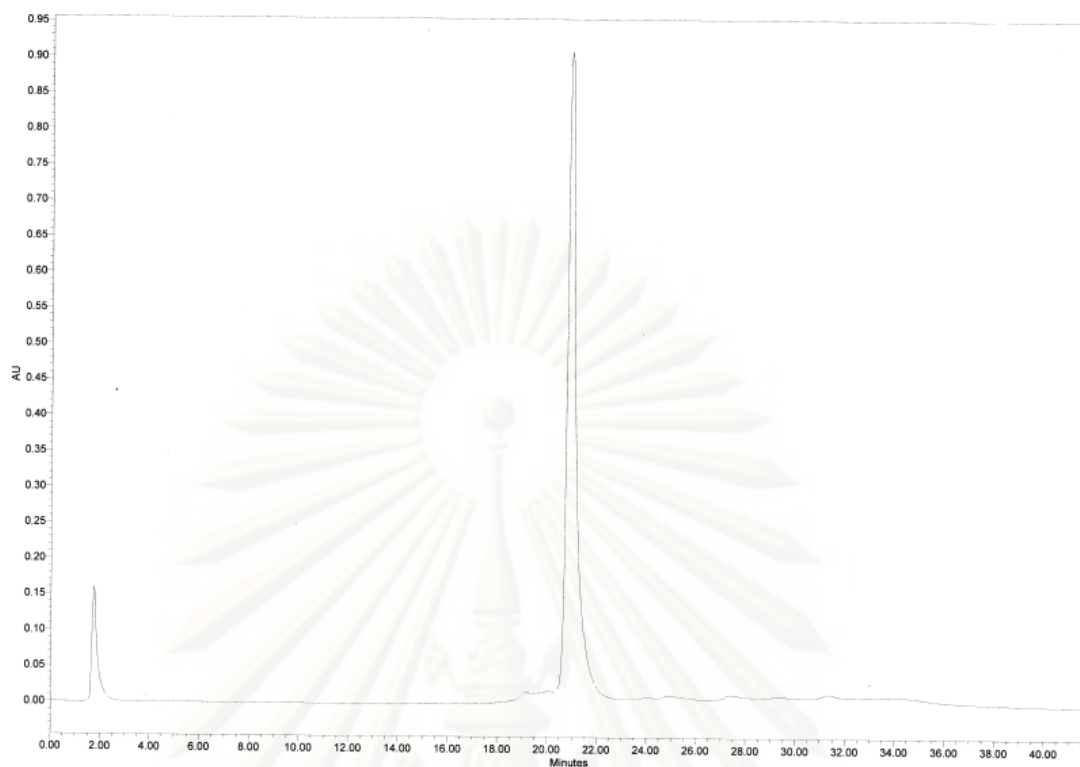


**Figure A.19** HPLC chromatogram of P-ATGTAACATCTCT-Ser-NH<sub>2</sub> (P11)

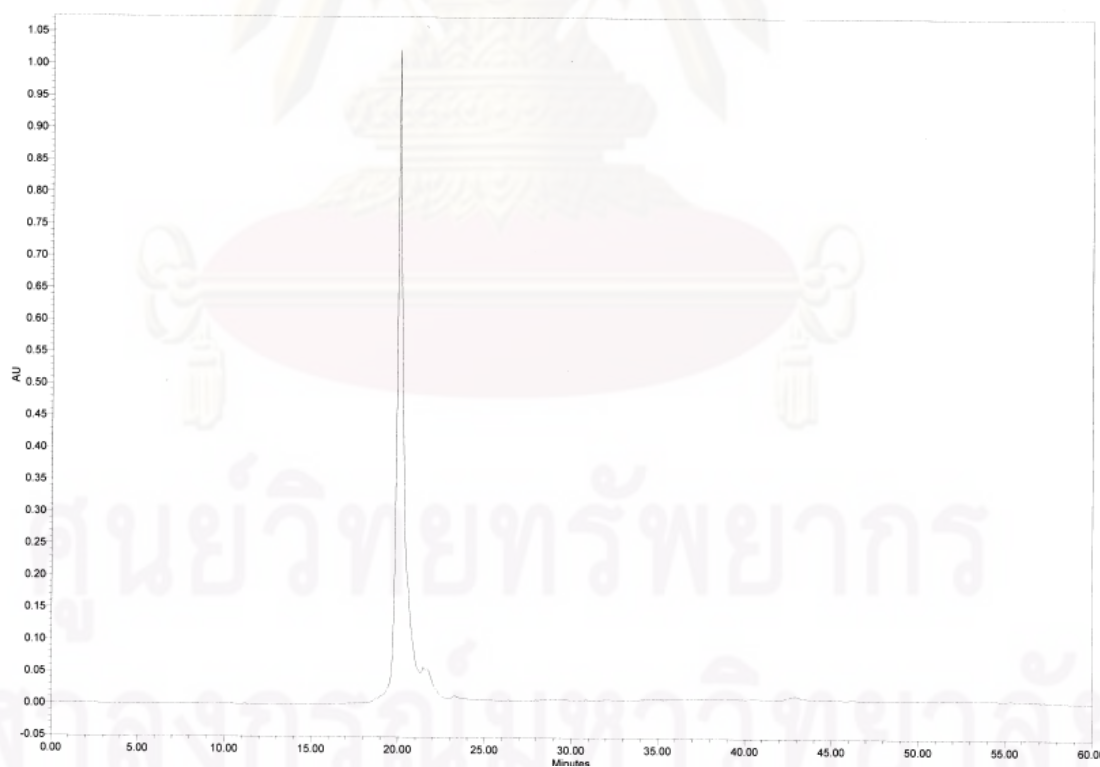


**Figure A.20** HPLC chromatogram of P-ATGTAATATCTCT-Ser-NH<sub>2</sub> (P12)



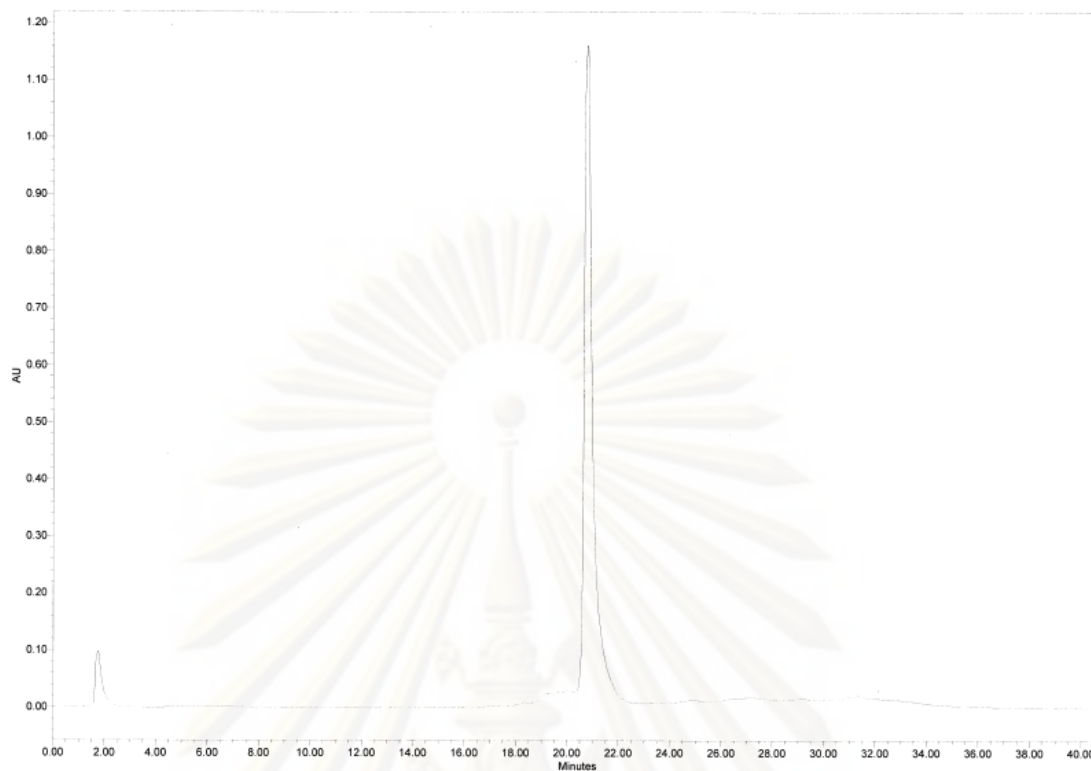


**Figure A.21** HPLC chromatogram of P-GCCTGTACTGTAG-Ser-NH<sub>2</sub> (P13)

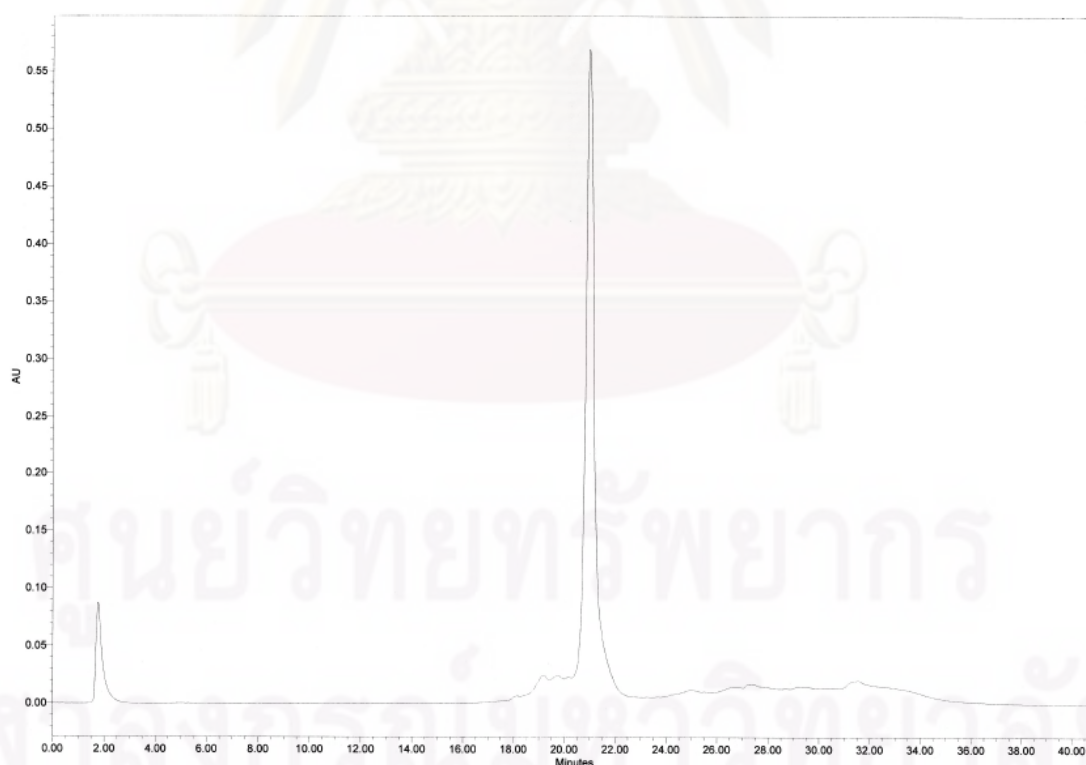


**Figure A.22** HPLC chromatogram of P-GCCTGTCCTGTAG-Ser-NH<sub>2</sub> (P14)

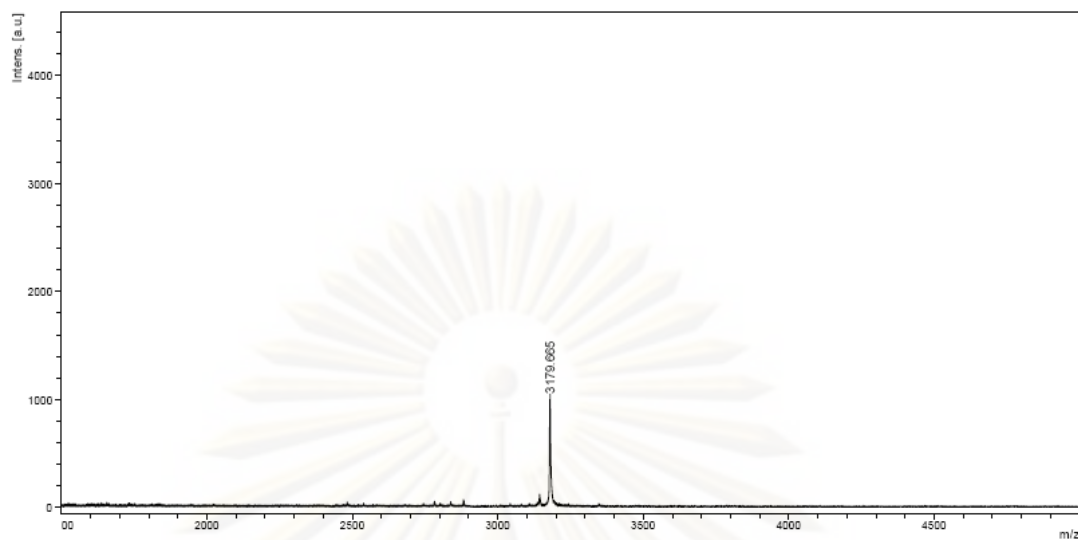


**Figure A.23** MALDI-TOF mass spectrum of Ac-TTTTTTTT-LysNH<sub>2</sub> (**P1**)

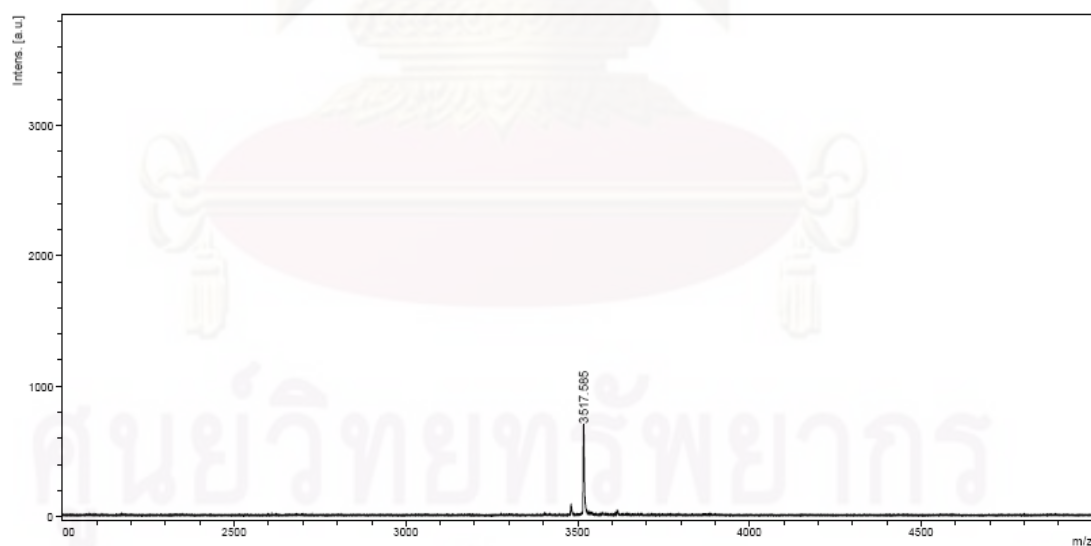


**Figure A.24** MALDI-TOF mass spectrum of Ac-GTAGATCACT-Ser-NH<sub>2</sub> (**P2**)

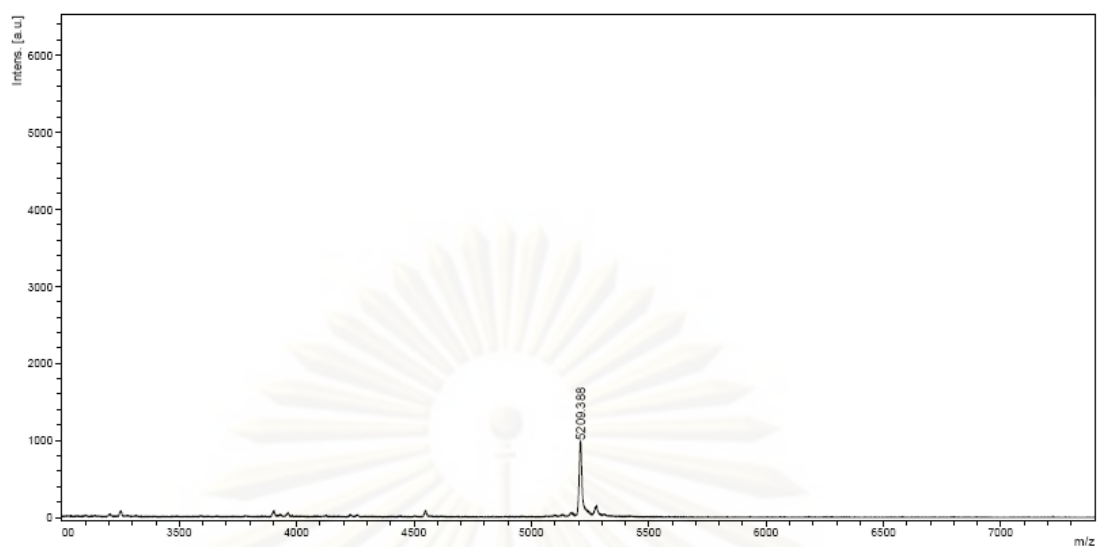


**Figure A.25** MALDI-TOF mass spectrum of Ac-TGTACGTAAACAATA-Lys-NH<sub>2</sub> (**P5**)

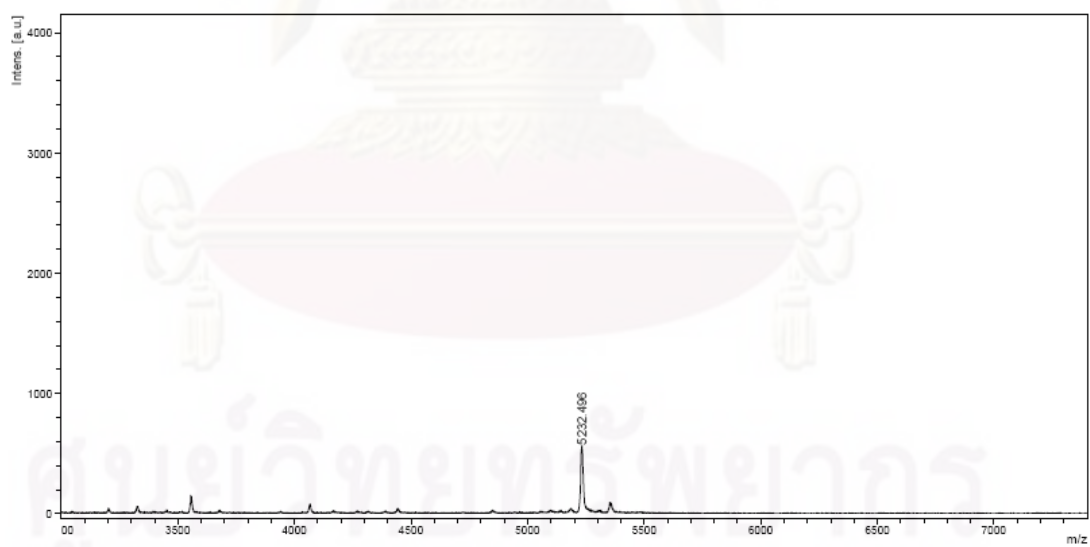


**Figure A.26** MALDI-TOF mass spectrum of Ac-TGTACGTCAACAATA-Lys-NH<sub>2</sub> (**P6**)

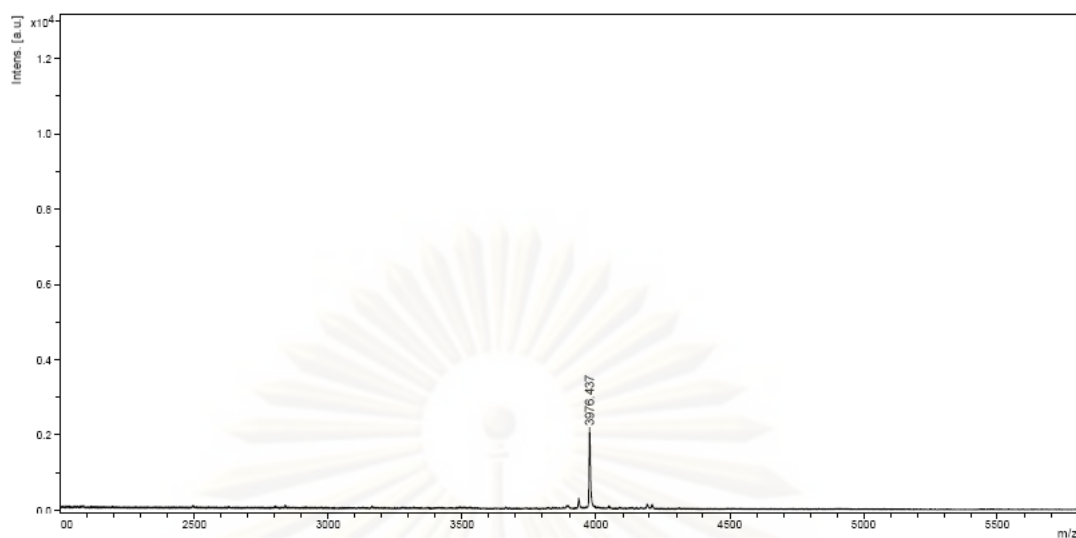


**Figure A.27** MALDI-TOF mass spectrum of Ac-Arg-AAAATCCATT-Ser-NH<sub>2</sub> (**P7**)

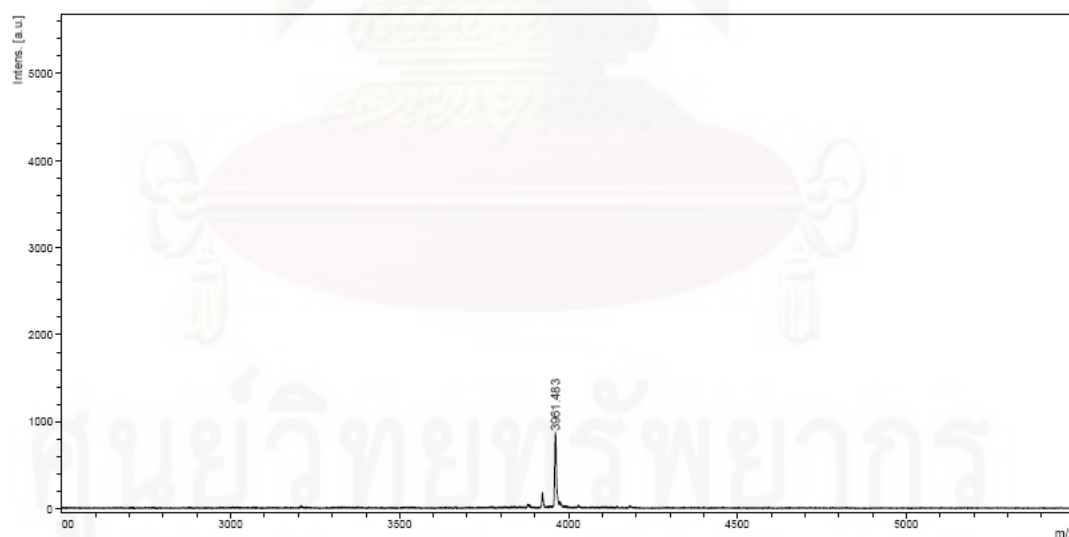


**Figure A.28** MALDI-TOF mass spectrum of Ac-Arg-AAA ATTCCATT-Ser-NH<sub>2</sub> (**P8**)

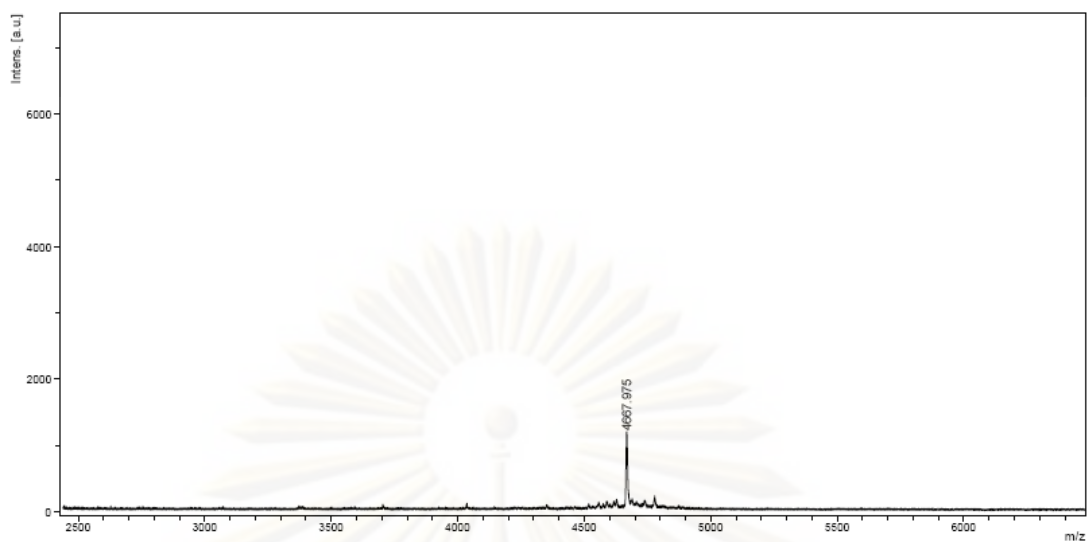


**Figure A.29** MALDI-TOF mass spectrum of P-TTCCCCCTCCCAA-Ser-NH<sub>2</sub> (**P9**)

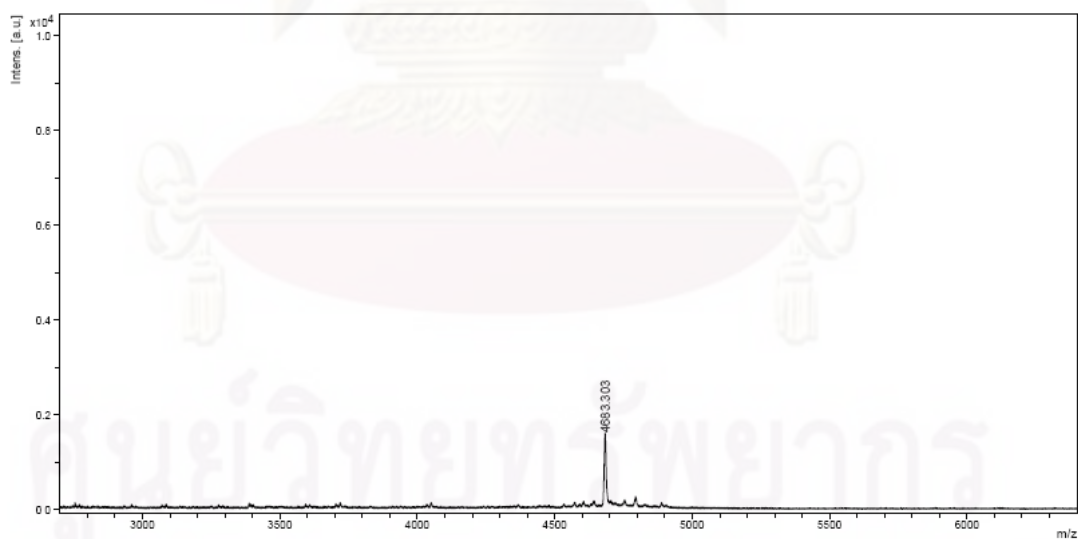


**Figure A.30** MALDI-TOF mass spectrum of P-TTCCCCCTCCCAA-Ser-NH<sub>2</sub> (**P10**)

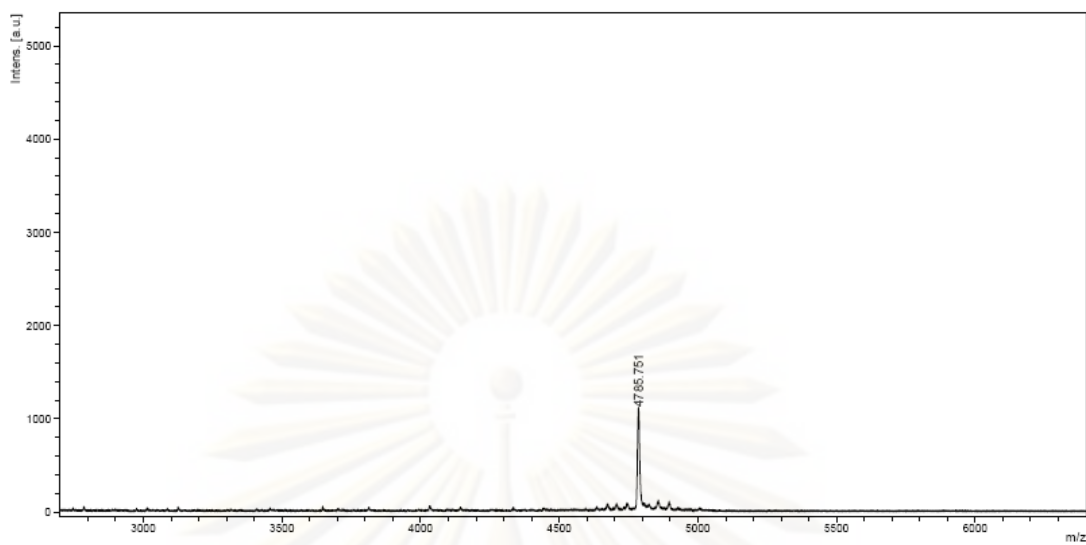


**Figure A.31** MALDI-TOF mass spectrum of P-ATGTAACATCTCT-Ser-NH<sub>2</sub> (**P11**)

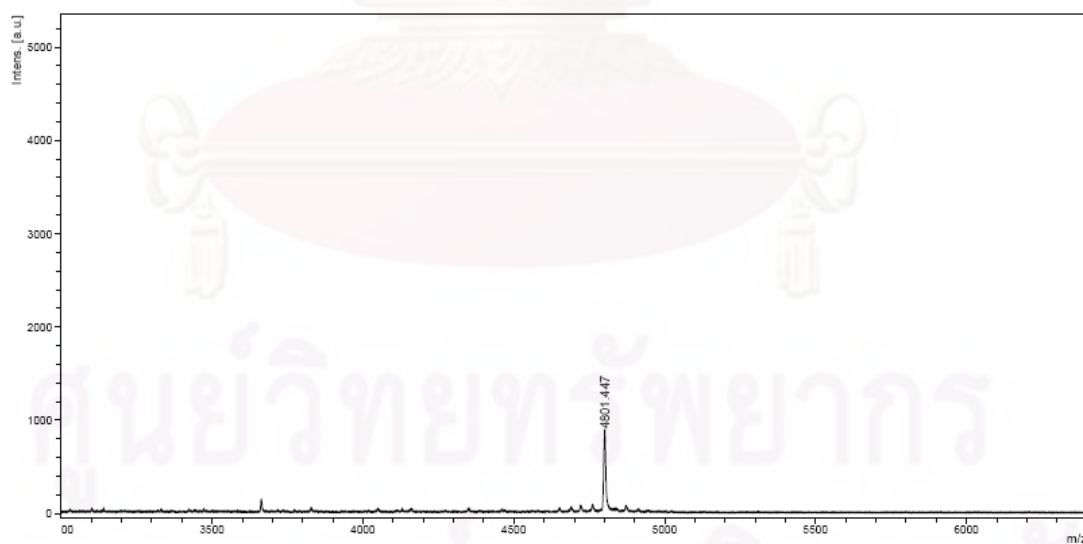


**Figure A.32** MALDI-TOF mass spectrum of P-ATGTAATATCTCT-Ser-NH<sub>2</sub> (**P12**)

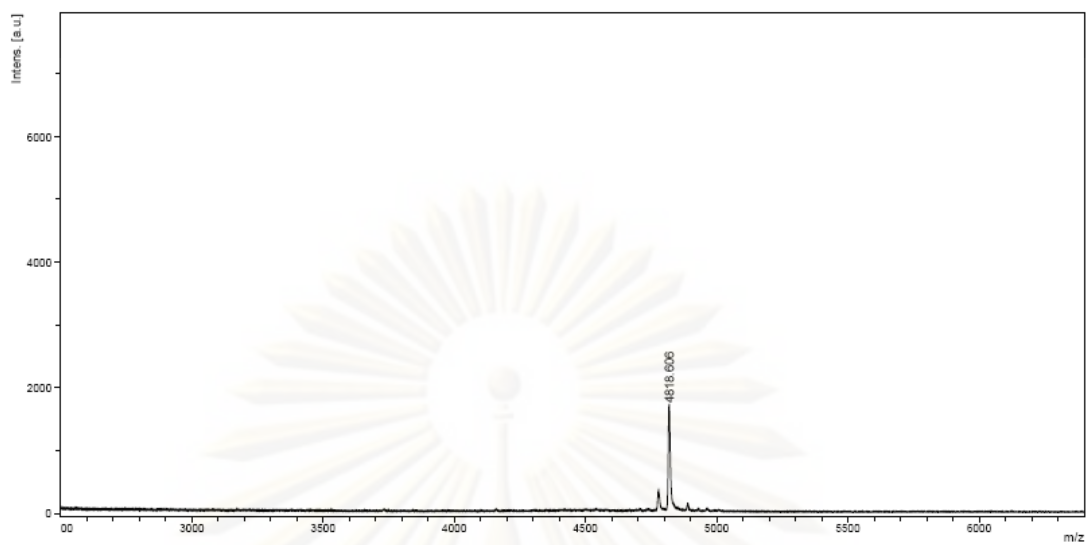


**Figure A.33** MALDI-TOF mass spectrum of P-GCCTGTACTGTAG-Ser-NH<sub>2</sub> (P13)

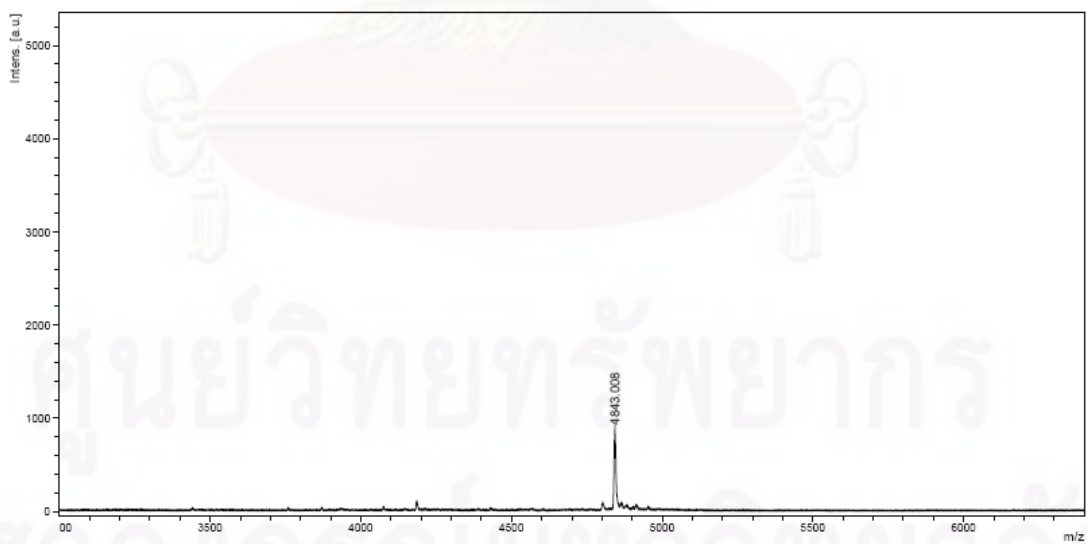


**Figure A.34** MALDI-TOF mass spectrum of P-GCCTGTCCTGTAG-Ser-NH<sub>2</sub> (P14)

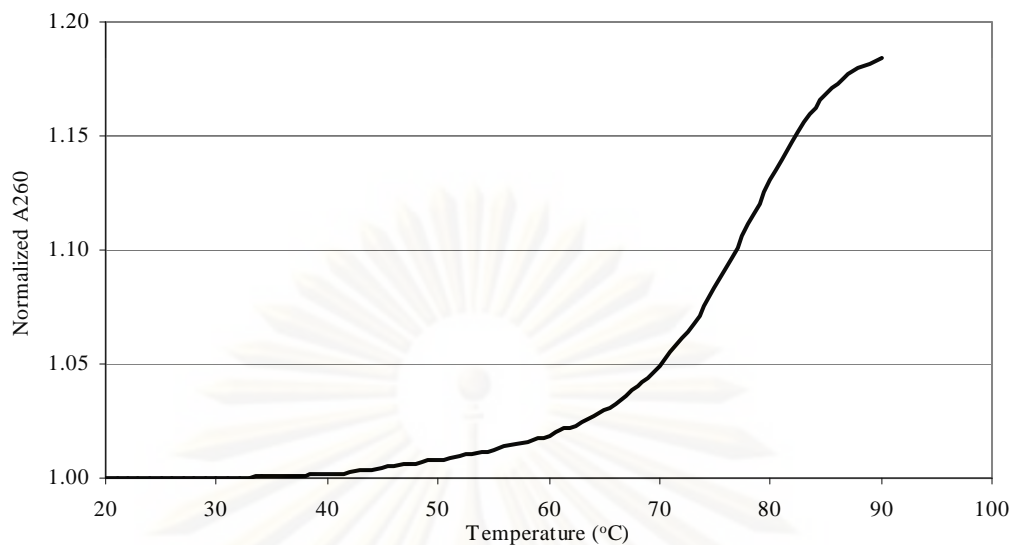


**Figure A.35** The melting curves of PNA **P1** with DNA **D1**. The  $T_m$  were measured at a ratio of PNA:DNA = 1:1, [PNA] = 1  $\mu$ M, 10 mM sodium phosphate buffer, pH 7.0, heating rate 1.0  $^{\circ}$ C/min.

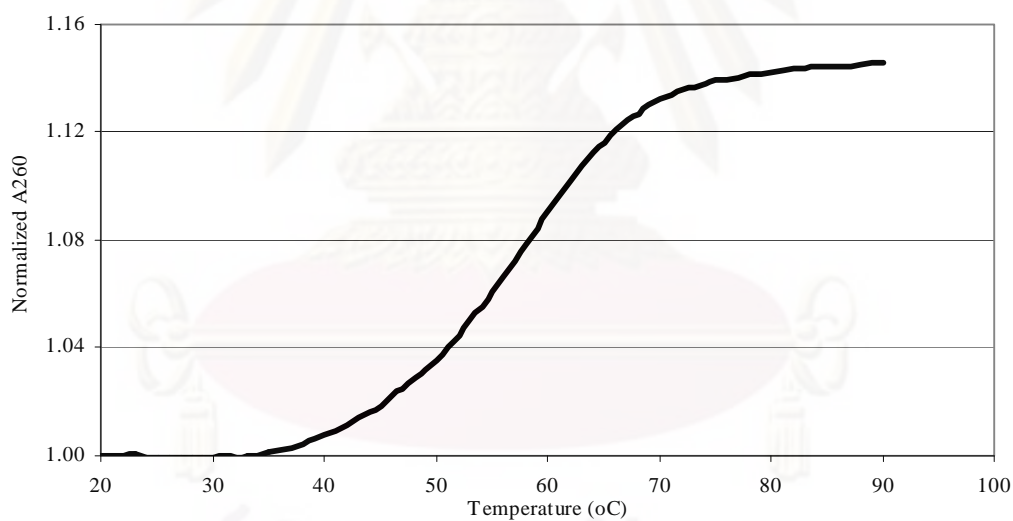


**Figure A.36** The melting curves of PNA **P2** with DNA **D2a**. The  $T_m$  were measured at a ratio of PNA: DNA = 1: 1, [PNA] = 1  $\mu$ M, 10 mM sodium phosphate buffer, pH 7.0, heating rate 1.0  $^{\circ}$ C/min.



## VITAE

Boonjira Boontha was born on June 29<sup>th</sup>, 1976 in Uttaradit, Thailand. She received Bachelor Degree of Science in Chemistry from Chaingmai University in 1998 and graduated with the Master Degree of Science in 1998 from Chulalongkorn University. Since 2005 she has become a student in Doctor of Philosophy of Chulalongkorn University studying in Department of Chemistry.



ศูนย์วิทยทรัพยากร  
จุฬาลงกรณ์มหาวิทยาลัย